

Evaluated kinetic and photochemical data for atmospheric chemistry: Volume V – heterogeneous reactions on solid substrates

J. N. Crowley¹, M. Ammann², R. A. Cox³, R. G. Hynes⁴, M. E. Jenkin⁵, A. Mellouki⁶, M. J. Rossi⁷, J. Troe⁸, and T. J. Wallington⁹

¹Max-Planck-Institut für Chemie, Division of Atmospheric Chemistry, Postfach 3060, 55020 Mainz, Germany

²Laboratory of Radiochemistry and Environmental Chemistry, OFLB 103, Paul Scherrer Institut, 5232 Villigen, Switzerland

³Centre for Atmospheric Science, Dept. of Chemistry, University of Cambridge, Lensfield Road Cambridge CB2 1EP, UK

⁴CSIRO Energy Technology, Lucas Heights Science and Technology Centre, Building 2, PMB7, Bangor, NSW 2234, Australia

⁵Atmospheric Chemistry Services, Okehampton, Devon EX20 1FB, UK

⁶ICARE (Institut de Combustion, Aérothermique, Réactivité et Environnement) CNRS (Centre National de la Recherche Scientifique) – UPR3021, 1C, Avenue de la recherche scientifique, 45071 Orleans cedex 02, France

⁷Laboratorium für Atmosphärenchemie, OFLA 008, Paul Scherrer Institut, 5232 Villigen, Switzerland

⁸Institute of Physical Chemistry, University of Göttingen, Tammannstr. 6, 37077 Göttingen, Germany

⁹Ford Motor Company, Research and Advanced Engineering, Mail Drop RIC-2122, Dearborn, Michigan 48121-2053, USA

*The IUPAC Subcommittee on Gas Kinetic Data Evaluation for Atmospheric Chemistry

Received: 14 December 2009 – Published in Atmos. Chem. Phys. Discuss.: 23 February 2010

Revised: 10 August 2010 – Accepted: 11 August 2010 – Published: 30 September 2010

Abstract. This article, the fifth in the ACP journal series, presents data evaluated by the IUPAC Subcommittee on Gas Kinetic Data Evaluation for Atmospheric Chemistry. It covers the heterogeneous processes on surfaces of solid particles present in the atmosphere, for which uptake coefficients and adsorption parameters have been presented on the IUPAC website in 2010. The article consists of an introduction and guide to the evaluation, giving a unifying framework for parameterisation of atmospheric heterogeneous processes. We provide summary sheets containing the recommended uptake parameters for the evaluated processes. Four substantial appendices contain detailed data sheets for each process considered for ice, mineral dust, sulfuric acid hydrate and nitric acid hydrate surfaces, which provide information upon which the recommendations are made.



Correspondence to: R. A. Cox
(rac26@cam.ac.uk)

1 Introduction

Since 2005 the IUPAC Subcommittee on Gas Kinetic Data Evaluation for Atmospheric Chemistry has extended its data evaluation work to produce recommendations for the uptake coefficients and adsorption parameters, which can be used to calculate the rates of heterogeneous reactions of trace gases in the atmosphere. The results of this work have been added to the IUPAC website in the last 2 years, alongside the updated kinetic data for gas phase reactions. Following our policy of publication of our updated evaluations in *Atmospheric Chemistry and Physics* journal, we now present in Volume V of the series, our work on the heterogeneous processes on surfaces of solid particles present in the atmosphere. This is done with a view to widening the dissemination and enhancing the accessibility of this evaluated material to the scientific community. This article will be followed by a second publication (Vol. VI), which will present evaluation of the heterogeneous processes in liquid particles present in the atmosphere.

The article consists of summary sheets containing the recommended values for the uptake coefficients and adsorption parameters for which sufficient experimental information exists to allow a recommendation. This is followed by a guide to the datasheets, which outlines the physico-chemical ba-

sis underlying the quantitative parameters describing atmospheric heterogeneous processes, and provides definitions of terms employed. Finally we present four appendices containing the data sheets for uptake of a range of O_x , HO_x , NO_x , SO_x , organic, and halogen-containing trace gases, on surfaces of ice (Appendix A1), mineral dust (Appendix A2), sulfuric acid hydrate (Appendix A4) and nitric acid hydrate (Appendix A5). Appendix A3 (uptake on soot surfaces) is omitted as this category has not yet been fully evaluated and we wished to keep the data-sheet numbering on the IUPAC website and the ACP publications consistent. The data sheets follow a similar format to those used for gas phase reactions, providing details of published experimental information upon which the recommendations are based, a table of preferred values and their reliability, and comments on the state of knowledge leading to the preferred values. The data sheets are concluded with a list of relevant references.

Summary sheets

Note: The parameter symbols and definitions in the Summary Tables are given in Tables 1 and 2 at the end of the introductory guide. Reliabilities are entered as $\pm\Delta$.

Preferred values for uptake on ice surfaces – Appendix A1

Ref. No	Species	α/γ	$\pm\Delta\alpha_s$	K_{linC} cm	N_{max} molecule cm ⁻²	$\Delta(E_{\text{ads}}/R)$ $\Delta\log N_{\text{max}}$	Temp. K
V.A1.1	O	$7 \times 10^{-6} + 2.6 \times 10^{-24} \exp(1370/T)[\text{O}_2]$	± 0.3				110–150
V.A1.2	O ₃	$< 1 \times 10^{-8}$	$0.7(\Delta\log\gamma)$				220–260
V.A1.3	OH	0.03	$0.5(\Delta\log\gamma)$				200–230
V.A1.4	HO ₂			No recommendation			
V.A1.5	H ₂ O ₂			$2.1 \times 10^{-5} \exp(3800/T)$	4.5×10^{14}	$0.5(\Delta\log K_{\text{linC}})$ $0.3(\Delta\log N_{\text{max}})$	200–240 200–240
V.A1.6	H ₂ O	$9.72 \times 10^{-2} \exp(232/T)$ $1.52 \times 10^{-3} \exp(1022/T)$	0.7 $0.7(\Delta\log\alpha)$				130–190 190–230 250–273
V.A1.7	NO	$\leq 5 \times 10^{-6}$	$1.0(\Delta\log\gamma)$				
V.A1.8	NO ₂			$3.07 \times 10^{-9} \exp(2646/T)$		± 100	190–250
V.A1.9	NO ₃	$< 1 \times 10^{-3}$	$0.5(\Delta\log\gamma)$				170–200
V.A1.10	NH ₃	4×10^{-4}	$0.5(\Delta\log\gamma)$	no recommendation			190–200
V.A1.11	HONO	0.02	$0.3(\Delta\log\alpha_s)$	$1.5 \times 10^{-8} \exp(5200/T)$	3×10^{14}	± 100	180–250
V.A1.12	HNO ₃	> 0.2	$0.3(\Delta\log\alpha)$	$7.5 \times 10^{-5} \exp(4585/T)$	2.7×10^{14}	± 700	190–240
V.A1.13	HO ₂ NO ₂			no recommendation			190–200
V.A1.14	N ₂ O ₅	0.02	$0.15(\Delta\log\gamma)$				190–200
V.A1.15	SO ₂			6.3 $7.3 \times 10^{-4} \exp(2065/T)$		± 0.3 ± 1000	228 190–250
V.A1.16	HCHO			0.7	2.7×10^{14}	$0.5(\Delta\log K_{\text{linC}})$ $0.2(\Delta\log N_{\text{max}})$	198–223
V.A1.17	HCOOH			$4.0 \times 10^{-12} \exp(7000/T)$	2.2×10^{14}	± 500 0.1	187–221
V.A1.18	CH ₃ CHO			$7 \times 10^{-8} \exp(3500/T)$	1.3×10^{14}	± 300 0.15	203–223
V.A1.19	CH ₃ COOH			$1.5 \times 10^{-14} \exp(8500/T)$	2.5×10^{14}	± 1000 0.1	195–240
V.A1.20	CH ₃ OH			$6.24 \times 10^{-12} \exp(6180/T)$	3.2×10^{14}	± 100 0.15	195–230
V.A1.21	C ₂ H ₅ OH			$5.0 \times 10^{-14} \exp(7500/T)$	2.8×10^{14}	± 200 0.15	210–250
V.A1.22	C ₃ H ₇ OH			25.6	3.1×10^{14}	$\pm 0.2(\Delta\log K_{\text{linC}})$ 0.15	228
V.A1.23	C ₄ H ₉ OH			$7.4 \times 10^{-16} \exp(9000/T)$	3.3×10^{14}	± 1000 0.15	210–250
V.A1.24	CH ₃ C(O)CH ₃			$1.0 \times 10^{-11} \exp(5850/T)$	2.7×10^{14}	± 100 0.1	195–230
V.A1.25	CH ₃ OOH	no recommendation					
V.A1.26	PAN			$1.49 \times 10^{-9} \exp(3608/T)$		± 100	160–180
V.A1.27	HCl	0.3	$0.5(\Delta\log\alpha_s)$	$0.0219 \exp(2858/T)$	3×10^{14}	$\Delta(E/R) = \pm 920$ K $\Delta\log K = \pm 0.2$	190–210 205–230
V.A1.28	HOCl	0.08	$0.3(\Delta\log\gamma)$	$3.6 \times 10^{-8} \exp(4760/T)$	3×10^{14}	$\Delta(E/R) = \pm 920$ K $\Delta\log K = \pm 0.2$	180–200 185–225
V.A1.29	ClO	$< 1 \times 10^{-4}$	undetermined				180–220
V.A1.30	HBr	$1 \times 10^{-5} \exp(840/T)$		4.14×10^5 (see data sheet)		$\Delta(E/R) = \pm 500$ K $\Delta\log K = \pm 0.3$	188 180–200
V.A1.31	HOBr	0.35 $3.8 \times 10^{-13} \exp(5130/T)$	$0.3(\Delta\log\gamma)$	no recommendation		$\Delta(E/R) = \pm 1000$ K	180–210
V.A1.32	HI	0.2	$0.3(\Delta\log\gamma)$	2.29×10^5 (see data sheet) 0.54×10^5		$\Delta\log K = \pm 0.3$	200–240 188 195
V.A1.33	HOI	no recommendation		no recommendation			
V.A1.34	ICI	$2.2 \times 10^{-6} \exp(2175/T)$	$0.3(\Delta\log\gamma)$			180–205	
V.A1.35	IBr	0.025	$0.3(\Delta\log\gamma)$	no recommendation			200
V.A1.36	BrCl	$< 1 \times 10^{-3}$	$0.3(\Delta\log\gamma)$	no recommendation			190–210
V.A1.37	BrO	$< 1 \times 10^{-4}$		no recommendation			200–220

Preferred values for reactions on ice surfaces – Appendix A1

Ref. No	Species	α_s / γ_{gs}	$\Delta\alpha_s$	$K_{\text{linC}}(\text{X})$ cm	k_s $\text{cm}^2 \text{s}^{-1}$	Δk_s $\text{cm}^2 \text{s}^{-1}$	$[\text{Y}]_s$ molecule cm^{-2}	Temp. K
V.A1.38	HONO+HCl	0.02	± 0.01	$1.5 \times 10^{-8} \exp(5200/T)$ (X=HONO)	4.0×10^{-19}	0.3 ($\Delta \log k_s$)	$K_{\text{linC}}(\text{HCl})=0.0219 \exp(2858/T)$ (Y=HCl)	180–220
V.A1.39	HONO+HBr	0.02	± 0.01	$1.5 \times 10^{-8} \exp(5200/T)$ (X=HONO)	5.0×10^{-18}	0.3 ($\Delta \log k_s$)	$3 \times 10^{14} (\text{Y}=\text{HBr})$	180–220
V.A1.40	HONO+HI	0.02	± 0.01	$1.5 \times 10^{-8} \exp(5200/T)$ (X=HONO)	8.0×10^{-19}	0.3 ($\Delta \log k_s$)	$3 \times 10^{14} (\text{Y}=\text{HI})$	180–220
V.A1.41	HOCl+HCl	0.22 $0.22 \times \theta_{\text{HCL}}$	± 0.2	E-R mechanism			$K_{\text{linC}}(\text{HCl})=0.0219 \exp(2858/T)$ (Y=HCl)	180–220
V.A1.42	HOCl+HBr	0.3	± 0.15	See data sheet	3.3×10^{-15}		$4.14 \times 10^5 [\text{HBr}]^{0.88}$	188
V.A1.43	ClONO ₂ +H ₂ O	0.5	± 0.3	1.2×10^4 (X=ClONO ₂)	5×10^{-17}		$10^{15} (1-0.81 \theta_{\text{HNO}_3})$	218
V.A1.44	ClONO ₂ +HCl	0.24	± 0.1	$1.04 \exp(2032/T)$ E-R mechanism	5×10^{-17}		θ_{HNO_3} Langmuir: see HONO ₂ uptake $K_{\text{linC}}(\text{HCl})=0.0219 \exp(2858/T)$	180-230 185–230
V.A1.45	ClONO ₂ +HBr	0.56	± 0.2	E-R mechanism			$4.14 \times 10^5 [\text{HBr}]^{0.88}$	188
V.A1.46	N ₂ O ₅ +HCl	no recommendation		no recommendation				
V.A1.47	N ₂ O ₅ +HBr			no recommendation				
V.A1.48	HOBr+HCl	0.25	± 0.05	no recommendation			$K_{\text{linC}}(\text{HCl})=0.0219 \exp(2858/T)$	188–230
V.A1.49	HOBr+HBr	4.8×10^{-4} $\exp(1240/T)$	0.15 ($\Delta \log \gamma$)					180–230
V.A1.50	BrONO ₂ +H ₂ O	5.3×10^{-4} $\exp(1100/T)$	$\Delta(\text{E/R})=$ $\pm 250 \text{ K}$					
V.A1.51	BrONO ₂ +HCl	0.3	± 0.3 ($\Delta \log \gamma$)					190–200
V.A1.52	BrONO ₂ +HBr	6.6×10^{-3} $\exp(700/T)$	$\Delta(\text{E/R})=$ $\pm 250 \text{ K}$					180–210
V.A1.53	SO ₂ +H ₂ O ₂			$5.3 \times 10^{-18} \exp(2065/T)/k_s$ X=SO ₂	7.3×10^{-15}	0.3 ($\Delta \log k_s$)	$K_{\text{linC}}(\text{H}_2\text{O}_2)=2.1 \times 10^{-5} \exp(3800/T)$ (Y=H ₂ O ₂)	200–230
V.A1.54	Cl ₂ O ₂ +HCl	no recommendation						
V.A1.55	Cl ₂ O ₂ +H ₂ O	5×10^{-4}	± 0.7 ($\Delta \log \gamma$)					226

Note: (X) = reactant from gas phase; (Y) = surface reactant

Preferred values of uptake coefficients on mineral dust surfaces – Appendix A2

Ref. No	Species	α_s/γ	$\pm \Delta\alpha_s$	K_{linC} cm	Temp. K
V.A2.1	O ₃	$1500[\text{O}_3]^{-0.7}$			298
V.A2.2	HO ₂	No recommendation			
V.A2.3	H ₂ O ₂	$6.24 \times 10^{-4} - 1.87 \times 10^{-6} \text{RH} + 9.37 \times 10^{-8} \text{RH}^2$ (15–70% RH)		0.5 ($\Delta \log \gamma$)	298
V.A2.4	NO ₂	1.2×10^{-8}		1.0 ($\Delta \log \gamma$)	298
V.A2.5	NO ₃	1.2×10^{-2}		0.5 ($\Delta \log \gamma$)	298
V.A2.6	NH ₃	No experimental data			
V.A2.7	HONO	No experimental data			298
V.A2.8	HNO ₃	1		L-H mechanism; see datasheet	298
V.A2.9	N ₂ O ₅	1.3×10^{-2}		0.5 ($\Delta \log \gamma$)	290–300
V.A2.10	SO ₂	4×10^{-5}		0.7 ($\Delta \log \gamma$)	260–300
V.A2.11	HC(O)OH	No recommendation		No recommendation	298
V.A2.12	CH ₃ C(O)CH ₃	No recommendation			

Preferred values for uptake on SAT/SAM surfaces – Appendix A4

Ref. No	Species	α_s/γ	$\pm\Delta\alpha_s/\gamma$	$K_{\text{linC}}(\text{X})$ cm	$[\text{Y}]_s$ molecule cm ⁻²	Temp. K
V.A4.1	HO ₂ (SAT)	no recommendation				
V.A4.2	N ₂ O ₅ (SAT)	6.5×10^{-3}				195–205
V.A4.3	HCl (SAT)	no recommendation				
			0.4($\Delta\log\gamma$)	6800	[HCl]×6800×(−2.47×10 ¹¹ +3.28×10 ¹¹ RH+3.27×10 ⁹ RH ² +2.43×10 ⁹ RH ³)/1.7×10 ¹⁴	190–199
				RH=79.4% only		190–199
V.A4.4	HBr (SAT)	0.18				190
V.A4.5	N ₂ O ₅ +HCl (SAT)	no recommendation				
V.A4.6	N ₂ O ₅ +HBr (SAT)	no recommendation				
V.A4.7	ClONO ₂ + H ₂ O (SAT)	$1 \times 10^{-4} + 4 \times 10^{-5}$ RH+4.7×10 ⁻⁷ RH ²				195–205
			0.3 ($\Delta\log\gamma$)			
V.A4.8	ClONO ₂ +HCl (SAT)	0.12	± 0.20	E-R mechanism	[HCl]×6800×(−2.47×10 ¹¹ +3.28×10 ¹¹ RH+3.27×10 ⁹ RH ² +2.43×10 ⁹ RH ³)/1.7×10 ¹⁴	190–200
V.A4.9	HNO ₃ (SAT)	>0.2	0.3($\Delta\log\alpha_s$)			190–240
V.A4.10	N ₂ O ₅ (SAM)	RH*4.63×10 ⁻⁴ +2.6×10 ⁻⁴	0.5 ($\Delta\log\gamma$)			200–225
V.A4.11	N ₂ O ₅ + HCl (SAM)	<10 ⁻⁴				200–220

Note: (X) = reactant from gas phase; (Y) = surface reactant; RH=p(H₂O)/p(ice)

Preferred values for uptake on NAT surfaces – Appendix A5

Ref. No	Species	α_s/γ	$\pm\Delta\alpha_s$	K_{linC} cm	N_{max} molecule cm ⁻²	$\Delta(E_{\text{ads}}/R)$ $\Delta\ln N_{\text{max}}$	Temp. K
V.A5.1	O ₃	<1 × 10 ⁻⁶	undetermined				
V.A5.2	H ₂ O (α -NAT)	0.32	0.3($\Delta\log\alpha_s$)				182
		0.38					192
		0.56					207
	H ₂ O (β -NAT)	0.15					182
		0.07					192
		0.017					207
V.A5.3	NO						
V.A5.4	NO ₂						
V.A5.5	N ₂ O ₅	6×10^{-3}	0.3($\Delta\log\gamma$)				190–200
V.A5.6	HNO ₃	0.2 (γ^{SS})	0.3 ($\Delta\log\alpha_s$)				190–200
V.A5.7	HCHO						
V.A5.8	HCl	0.3	0.3($\Delta\log\alpha_s$)	$9.5 \times 10^{-3} \exp(2858/T)$	3×10^{14}	$\pm 0.3(\Delta\log K_{\text{linC}})$	190–210
V.A5.9	ClO	<1 × 10 ⁻⁴	undetermined				180–200
V.A5.10	HBr	0.3	0.5($\Delta\log\alpha_s$)				190–200

Preferred values for reaction on NAT – Appendix A5

Ref. No	Species	$\alpha_s/\gamma_{\text{gs}}$	$\Delta\log\alpha_s/\gamma_s$	$K_{\text{linC}}(\text{X})$ cm	$[\text{Y}]_s$ molecule cm ⁻²	Temp. K
V.A5.12	HOCl+HCl	0.18	0.2	ER-mechanism	$K_{\text{linC}}(\text{HCl})=9.5 \times 10^{-3} \exp(2858/T)$	180–205
V.A5.13	ClONO ₂ +HCl	0.25	0.3	see data sheet		190–200
V.A5.14	ClONO ₂ +HBr	0.56	0.3	ER-mechanism	$4.14 \times 10^5 [\text{HBr}]^{0.88}$	180–200
V.A4.15	N ₂ O ₅ +HCl	4×10^{-3}	0.5		$7.3 \times 10^{-17} \exp(2858/T) [\text{HCl}]/$ $(7.3 \times 10^{-17} \exp(2858/T) [\text{HCl}]+1)$	190–210
V.A4.16	N ₂ O ₅ +HBr	2×10^{-2}	0.5		$4.14 \times 10^5 [\text{HBr}]^{0.88}$	200
V.A5.17	ClONO ₂ +H ₂ O	$7.1 \times 10^{-3} \exp(2940/T)$	0.20			185–210

Note: (X) = reactant from gas phase; (Y) = surface reactant

2 Guide to the data sheets

The heterogeneous processes considered in this evaluation involve chemical and/or physical interactions between trace gases and atmospheric condensed phase material. Broadly, this material falls into 3 categories: (i) large water droplets (diameter, $d > 1 \mu\text{m}$), (ii) fine liquid submicron ($d < 1 \mu\text{m}$) aerosol particles, and (iii) solid aerosol particles (coarse, fine, ultrafine mode). The interaction can be reversible (physisorption or dissolution), reactive, catalytic or a combination of all or some of these operating in parallel or sequentially, and can depend strongly on ambient conditions such as temperature or relative humidity.

This publication covers only interactions between gases and solid surfaces such as ice, acid hydrates and mineral dust, although the solid particles may be coated with aqueous films. Interaction with liquid surfaces including aqueous droplets, such as water, salt solutions (e.g., halide and sulphate), sulphuric acid, and semi volatile organics, will be covered in a following publication. The parameterisation of a heterogeneous process depends on the nature of the surface but here we present the general framework for reaction kinetics for both solid and liquid substrates.

A proper description of the interaction of a trace gas with a surface would include transport to and accommodation at the surface, followed by a number of competitive or parallel processes such as desorption back to the gas phase, reaction with the substrate surface or with other trace gases on the surface, and diffusion into and reaction in the particle bulk (important for liquid aerosol; less so for solid particles). The rates and efficiencies of these processes are controlled by surface and bulk-phase rate coefficients, local reactant concentrations, diffusion coefficients in the condensed phase, and solubilities. Each of these controlling factors may change with temperature and composition. The role of surface adsorbed H_2O is especially noteworthy as it can both accelerate and slow down rates of trace gas uptake and can be a rate determining parameter in some systems. When appropriate we prefer experimental results in which atmospherically relevant relative humidities prevailed, especially when dealing with non-ice surfaces (e.g. mineral dust). Atmospheric heterogeneous processes can be highly complex and only rarely are all the individual steps controlling reaction rates of heterogeneous processes known. A quasi steady state resistance model has frequently been used to describe the uptake of gas species to surfaces, and to relate the experimentally observable net probability of uptake (γ , see below) to the physical parameters that control it. In this model a linear combination of flux resistances (decoupled and normalized fluxes) by analogy to resistances in electric circuits, is used to describe the uptake process (Jayne et al., 1990; Hanson, 1997; Ammann et al., 2003; Pöschl et al., 2007), and we will refer to these formulations below where appropriate. Models involving solution of coupled differential rate equations of mass transport and chemical reactions using continuum flow for-

mulations (Winkler et al., 2004) and gas kinetic formulations (Flückiger and Rossi, 2003; Behr et al., 2004; Pöschl et al., 2007) have recently been described.

Experiments are usually carried out in regimes where the process of interest is limiting (i.e. the slowest step in the overall process). However, only a systematic variation of conditions will reveal the identity of this slowest elementary step.

3 Description of heterogeneous kinetics

3.1 Definition of the uptake coefficient

The most widely used approach to describe the kinetics of heterogeneous processes is to use the uptake coefficient, γ , which is the net probability that a molecule X undergoing a gas-kinetic collision with a surface is actually taken up at the surface. This approach links the processes at the interface and beyond with an apparent first order loss of X from the gas phase:

$$d[\text{X}]_{\text{g}}/dt = -k_{\text{r}}[\text{X}]_{\text{g}} = -\gamma \frac{\bar{c}}{4} [\text{SS}][\text{X}]_{\text{g}} \quad (1)$$

$[\text{X}]_{\text{g}}$ denotes the concentration of X in the gas phase (molecule cm^{-3}), $[\text{SS}]$ is the specific surface area of the condensed phase (cm^{-1}) (i.e., surface area of condensed phase per volume of gas phase), k_{r} is the first order rate coefficient for loss, and \bar{c} is the mean thermal velocity of X (cm s^{-1}). γ often depends on time, as uptake may be limited by adsorption equilibrium on the surface, by a limited number of reactants on the surface, by solubility, or by a limited number of reactants in the bulk of the particles. γ may also depend on the gas phase concentration of X. Therefore, γ is not a constant.

In many studies of trace gas uptake to surfaces evidence is obtained for surface saturation, usually observable as a decrease in the experimental uptake coefficient (γ). The rate of change of γ depends on a number of factors, depending on the type of interaction. For a purely reversible process this will depend on surface capacity and the concentration of the gas-phase species. For a reactive process it will depend on the number of reactive sites or the rate of delivery of a surface reactant as well as the gas-phase concentration of the trace-gas(es). γ may decline from near unity to near zero on time scales of minutes or hours, or, for the case of a reactive uptake with no consumption of reactive surface sites/species, will be time independent and equal to the initial uptake coefficient. The frequent use in laboratory studies of very large surface to volume ratios (use of bulk substrates) to force reactions to take place on reasonable time scales can also disguise the time dependence of a process (i.e. the onset of surface saturation), which in the atmosphere may be important.

3.2 Gas phase diffusion

If γ is large, $[X]_g$ may become depleted near the particle surface. In this case, a correction factor is commonly applied, such that Eq. (1) can still be used to relate the net flux into the particle phase with the overall loss from the gas phase. γ in Eq. (1) is then replaced by γ_{eff} , which is given by $\gamma_{\text{eff}} = C_{\text{diff}} \gamma$, where C_{diff} is a correction factor. Under appropriate steady state assumptions, this relation can also be expressed in the form of a resistor formulation (Schwartz, 1986; Hanson and Ravishankara, 1994; Finlayson-Pitts and Pitts, 2000):

$$\frac{1}{\gamma_{\text{eff}}} = \frac{1}{\Gamma_{\text{diff}}} + \frac{1}{\gamma} \quad (2)$$

Approximate formulas for C_{diff} or Γ_{diff} have been derived in the literature (Fuchs and Sutugin, 1970; Brown, 1978; Seinfeld and Pandis, 1998; Poeschl et al., 2007) for various geometries, such as suspended aerosol particles, but also cylindrical flow tubes. They are a function of the geometry (e.g., particle diameter, d_p) and the diffusion coefficient of X, D_g , and γ . Therefore, temperature and bath gas dependent diffusion coefficients for X are required. Diffusion control may also limit uptake rates to particles in the atmosphere, requiring a similar treatment for uptake kinetics.

3.3 Surface accommodation and kinetics of adsorption

A molecule colliding with the surface of solid or liquid condensed matter can undergo elastic or inelastic scattering processes that involve collisions with one or a few surface atoms or molecules on time scales of up to 10^{-12} s. Elastic and inelastic scattering result in reflection back to the gas phase. The molecule can also undergo adsorption, in which case it accommodates into a weakly bound state, which may involve hydrogen bonds, charge transfer, or Van der Waals interactions. Adsorbed molecules may leave the surface through thermally activated desorption, which results in lifetimes on the surface of typically between nanoseconds and seconds at atmospheric temperatures. Thermally desorbing or scattered molecules can be distinguished through molecular beam experiments (Nathanson et al., 1996; Morris et al., 2000). The adsorption state as defined above is usually referred to as physisorption in the surface science literature (Masel, 1996). Physisorption should be differentiated from chemisorption, which involves breaking of chemical bonds or significant distortion of electronic structure of adsorbate and substrate. As discussed below, chemisorption is considered to be a surface reaction. We recommend use of the term “surface accommodation coefficient”, α_s , for the probability of adsorption on a clean surface. Note that the symbol S and terms such as sticking probability or adsorption coefficient are found in the literature (Tabazadeh and Turco, 1993; Davidovits et al., 1995; Carslaw and Peter, 1997; Hanson, 1997; Ammann et al., 2003; Pöschl et al., 2007), however these terms often lack

an unequivocal definition. The term thermal accommodation coefficient, α_t , has been used to describe the probability that a molecule accommodates to the thermal energy of the substrate upon adsorption in a single collision model, when a molecule collides with the surface (Li et al., 2001; Worsnop et al., 2002). The concept of Langmuir type adsorption assumes that molecules can only adsorb on free surface sites, so that the rate of adsorption ($\text{cm}^{-2} \text{s}^{-1}$) is given by

$$J_{\text{ads}} = \frac{\alpha_s \bar{c}}{4(1-\theta)[X]_g} \quad (3)$$

θ denotes the fractional surface coverage, which is related to the surface concentration, $[X]_s$, via $[X]_s = \theta N_{\text{max}}$, where N_{max} is the maximum number of available surface sites per cm^2 . The reverse process, thermally activated desorption, is usually parameterised by a first order rate expression:

$$J_{\text{des}} = k_{\text{des}} [X]_s \quad (4)$$

k_{des} denotes the desorption rate constant (s^{-1}). In the absence of surface reaction or transfer to the bulk, the uptake coefficient as a function of time is given by

$$\gamma(t) = \alpha_s e^{-Bt} \quad (5)$$

with

$$B = \alpha_s \frac{\bar{c}[X]_g}{4N_{\text{max}}} + k_{\text{des}}$$

Equation (5) indicates that for low coverages, where $k_{\text{des}} \gg \alpha_s (\bar{c}[X]_g)/4N_{\text{max}}$, the characteristic time to reach equilibrium is given by $1/k_{\text{des}}$. After equilibrium has been established (see below), γ drops to zero. Therefore, at all concentrations, very high time resolution is necessary to observe an uptake coefficient equal to α_s , and laboratory experiments have to be carefully evaluated to judge whether initial uptake coefficients (reported as γ_0) may correspond to α_s or are lower limits to α_s . In the data sheets we tabulate reported values of γ_0 and provide a preferred value for α_s if appropriate and as discussed in the associated comments. Equation (5) may also be used to parameterise the temperature dependence of the uptake coefficient observed at a given time or averaged over a given time interval.

3.4 Adsorption equilibrium

The kinetics of adsorption may be relevant for extracting α_s from laboratory measurements, but only rarely represents a rate limiting step of loss of gas phase species under atmospheric conditions. Here, adsorption equilibrium is of wider importance as it may be used to estimate gas surface partitioning (e.g., in ice clouds) or because it defines the concentration of surface species available for surface reaction or for transfer to the bulk underneath (see below). Most of the relevant literature on adsorption equilibria covers trace gases interacting with ice and, to a lesser degree, mineral dust. However, adsorption of surface active gases on aqueous solutions

has been described using the same concept. Adsorption equilibrium is established when $J_{\text{ads}}=J_{\text{des}}$ and can be described in terms of the fractional coverage, θ , ($= [X]_s/N_{\text{max}}$) by:

$$\theta = \frac{[X]_s}{N_{\text{max}}} = \frac{K_{\text{LangC}}[X]_g}{1 + K_{\text{LangC}}[X]_g} \quad (6)$$

$$K_{\text{LangC}} = \frac{\alpha_s \bar{c}}{4k_{\text{des}} N_{\text{max}}} \quad (7)$$

Equation (6) is an isotherm commonly referred to as the Langmuir isotherm, which allows derivation of the partition coefficient, K_{LangC} , from measurements of surface coverage (molecule cm^{-2}) as a function of trace gas concentration or pressure. Equation (7) relates the partition coefficient to the kinetic parameters that determine the equilibrium on a molecular level. Therefore, measurement of K_{LangC} also provides constraints on α_s .

Note that the Langmuir isotherm only holds when the adsorbing species compete for fixed surface lattice sites and within the assumptions of the simple picture described above in the context of adsorption kinetics. However, it appears to be a reasonable approximation for adsorption characteristics on model surfaces used in laboratory studies of adsorption to solid surfaces (except on ice surfaces when adsorption of some trace gases leads to hydrate formation or surface melting) and of insoluble gases on liquid surfaces. We have adopted this formalism for representation of evaluated data, unless there is a gross departure from the simple picture. Note also that an expression similar to that of Eq. (6) can be used to express the equilibrium between the bulk of an aqueous solution and the surface for surface active solutes (Donaldson, 1999). From a thermodynamic point of view, the equilibrium between the gas and the surface can also be expressed using a dimensionless partition coefficient, K_p^o :

$$[X]_s/[X]_g \times A/V = \exp(-\Delta G_{\text{ads}}^0/RT) \equiv K_p^o \quad (8)$$

where A/V is the area-to-volume ratio (cm^{-1}) of an ideal gas adsorbed at the surface ($\sim 1.7 \times 10^7 \text{ cm}^{-1}$; Kemball, 1946; Kemball and Rideal, 1946) and ΔG_{ads}^0 is the free energy of adsorption. A/V defines the standard state for the adsorbed phase, which corresponds to a molar area of $3.74 \times 10^7 \text{ m}^2 \text{ mol}^{-1}$. ΔG_{ads}^0 is related as usual via the Gibbs equation to the enthalpy and entropy of adsorption:

$$-RT \ln K_p^o = \Delta H_{\text{ads}}^0 - T \Delta S_{\text{ads}}^0 \quad (9)$$

The relation between K_p^o and K_{LangC} (the ‘‘C’’ of LangC refers to the fact that units of concentration in molecules cm^{-3} are used) is equivalent to

$$K_{\text{LangC}} = K_p^o \cdot V/A \cdot \frac{1}{N_{\text{max}}} \text{ in units of } \text{cm}^3 \text{ molecule}^{-1} \quad (10)$$

The use of gas pressures results in:

$$K_{\text{LangP}} = K_p^o \cdot V/A \cdot \frac{1}{k_B T N_{\text{max}}} \quad (11)$$

in units of Pa^{-1} or atm^{-1} or Torr^{-1} or mbar^{-1}

A modified analysis using only the linear regime of the adsorption isotherm is sometimes possible. The partition coefficient (K_{linC}) once again has different units:

$$K_{\text{linC}} = K_p^o \cdot V/A \quad (12)$$

K_{linC} has units of molecule $\text{cm}^{-2}/\text{molecule cm}^{-3}$ (or cm) if concentrations (in molecule cm^{-3}) are used, and units of molecule $\text{cm}^{-2} \text{ Pa}^{-1}$ or molecule $\text{cm}^{-2} \text{ Torr}^{-1}$ if pressure is used, then denoted as K_{linP} .

Fractional surface coverages can be calculated from each different form of the partition coefficient via:

$$\begin{aligned} \theta_X &= K_p^o \frac{V}{A} \frac{P_x}{k_B T N_{\text{max}}} = K_p^o \frac{V}{A} \frac{[X]_g}{N_{\text{max}}} = K_{\text{linC}} \frac{[X]_g}{N_{\text{max}}} \\ &= K_{\text{linP}} \frac{P_x}{N_{\text{max}}} = K_{\text{LangC}} [X]_g = K_{\text{LangP}} P_x \end{aligned} \quad (13)$$

For the purpose of comparing partition coefficients and deriving preferred expressions for calculating equilibrium surface coverages, a single form of the partition coefficient is required. In principle, K_p^o would be the best choice; the disadvantage is that it is difficult to extract from the various studies if experimental surface to volume ratios ($S_{\text{exp}}/V_{\text{exp}}$) are not known, or if N_{max} has to be chosen arbitrarily and not from the experiment itself. Therefore, for practical purposes (e.g., using the constants to calculate coverages) reporting consistently in the form of K_{linC} has the advantage that no inherent assumption about N_{max} has to be made to derive partitioning from the experiments at low trace gas pressures. The tabulated values of partition coefficients are therefore presented as K_{linC} . The accompanying notes in each data sheet provide the original expressions and the values of N_{max} and V/A used to calculate K_{linC} . K_{linC} can be calculated from other forms of the partitioning coefficient as shown below:

Convert from	To	Multiply by
$K_{\text{LangC}} (\text{cm}^3 \text{ molecule}^{-1})$ or $K_{\text{LangP}} (1/\text{Pressure})$	$K_{\text{linC}} (\text{cm})$ $K_{\text{linP}} (1/\text{Pressure})$	$N_{\text{max}} (\text{molecule cm}^{-2})$
$K_{\text{LangP}} (\text{Pa}^{-1})$ or $K_{\text{linP}} (\text{cm}^{-2} \text{ Pa}^{-1})$	$K_{\text{LangC}} (\text{cm}^3)$ $K_{\text{linC}} (\text{cm}^2/\text{cm}^{-3})$	$1.381 \times 10^{-17} T$
$K_{\text{LangP}} (\text{mbar}^{-1})$ or $K_{\text{linP}} (\text{cm}^{-2} \text{ mbar}^{-1})$	$K_{\text{LangC}} (\text{cm}^3)$ $K_{\text{linC}} (\text{cm}^{-2}/\text{cm}^{-3})$	$1.381 \times 10^{-19} T$
$K_{\text{LangP}} (\text{bar}^{-1})$ or $K_{\text{linP}} (\text{cm}^{-2} \text{ bar}^{-1})$	$K_{\text{LangC}} (\text{cm}^3)$ $K_{\text{linC}} (\text{cm}^{-2}/\text{cm}^{-3})$	$1.381 \times 10^{-22} T^a$

^a Note that in some cases a pressure referenced to STP (1 atm) is reported. In this case the multiplication factor is 3.717×10^{-20} , independent of temperature.

Convert from	To	Multiply by
K_{LangP} (Torr ⁻¹) or K_{linP} (cm ⁻² Torr ⁻¹)	K_{LangC} (cm ³) K_{linC} (cm ⁻² /cm ⁻³)	 $1.036 \times 10^{-19} T$
K_p^o	K_{linC} (cm ⁻² /cm ⁻³)	V/A

If data are available from the low coverage (linear) part of the isotherm, these are used preferably as the influence of lateral interactions is reduced, and N_{max} , which is often difficult to obtain experimentally due to adsorbate-adsorbate interactions (Jedlovsky et al., 2006), is not required. The Van't Hoff equation (i.e., the differential form of the Gibbs equation):

$$\frac{d(\ln K)}{d(1/T)} = \frac{-\Delta H^0}{R} \quad (14)$$

describes the temperature dependence of K , but the entropy and enthalpy of adsorption derived from this analysis can be coverage dependent and this needs to be considered when comparing results from different experiments. In cases where a non-acidic adsorbing molecule dissociates upon adsorption the Langmuir isotherm takes a modified form:

$$\theta = \frac{N}{N_{\text{max}}} = \frac{\sqrt{K_{\text{Lang}}[\text{X}]_{\text{g}}}}{1 + \sqrt{K_{\text{Lang}}[\text{X}]_{\text{g}}}} \quad (15)$$

The occupancy of two adjacent surface sites for accommodation leads to a square root dependence of surface coverage at low $[\text{X}]$, which can be used as a diagnostic for dissociative adsorption. This is however rarely unambiguously observed experimentally for atmospheric surfaces.

3.5 Surface reactions

Parameterisation of uptake resulting from reaction of trace gases on a surface (reactive uptake) requires knowledge of the mechanism of the reaction. Generally there are two types of reaction. First, those in which the molecule arriving at the surface reacts with a constituent of the bulk phase to form either involatile products (e.g. stable hydrates) or volatile products which partition back to the gas phase. Second, those in which the molecule arriving at the surface reacts with a second species, which is present on the surface in the adsorbed state to form either involatile or volatile products. In both types the kinetics depends on the surface concentration of the second reactant, which must be included in any parameterisation of the reactive uptake coefficient. The two mechanisms, which are commonly used to describe the kinetics of surface reactions, are often referred to as Langmuir-Hinshelwood (LH) and Eley-Rideal mechanisms (ER). It should be noted that some reports in the literature use the term Langmuir-Rideal for the latter and that the reverse abbreviation RE has also been used (see also IUPAC Gold Book). They differ in that the former involves adsorption of the arriving molecule at available surface sites prior to a bimolecular reaction. The

latter involves direct collision induced reaction of the arriving gaseous molecule with a reactant molecule on the surface. The LH mechanism thus may involve competition of both reactant molecules for available surface sites. Note that in practice, it is very difficult to experimentally differentiate between LH and ER surface mechanisms. For parameterisation of the uptake coefficients we adopt the approach presented by Ammann et al. (2003), which builds on earlier studies (Elliott et al., 1991; Mozurkewich, 1993; Tabazadeh and Turco, 1993; Carslaw and Peter, 1997).

3.5.1 Bimolecular reaction between two surface species

The parameterisation for the reactive uptake coefficient, γ , for gas phase species X reacting with surface species, Y, after adsorption on the surface (LH type mechanism) is given by:

$$\frac{1}{\gamma} = \frac{1}{\alpha_s} + \frac{1}{\Gamma_s}$$

with

$$\Gamma_s = \frac{4k_s[\text{Y}]_s K_{\text{LangC}}(\text{X}) N_{\text{max}}}{\bar{c}(1 + K_{\text{LangC}}(\text{X})[\text{X}]_g)} \quad (16)$$

Here $[\text{Y}]_s$ is the surface concentration (molecules cm⁻²) of species Y and k_s is the surface reaction rate coefficient (units of cm² molecule⁻¹ s⁻¹). $K_{\text{LangC}}(\text{X})$ is the partition constant for species X. $1/\Gamma_s$ can be considered the resistance for the surface reaction. Note that Γ_s represents a normalized rate and is therefore not restricted to values smaller than one. If Y is a volatile molecule also present in the gas phase, its equilibrium surface concentration, $[\text{Y}]_s$ can be calculated using an appropriate adsorption isotherm. Values of $k_s K_{\text{LangC}}(\text{X})$ can be determined experimentally from measurements of γ as a function of surface coverage $[\text{Y}]_s$. Equation (16) demonstrates that γ depends on the gas phase concentration of X, if $K_{\text{LangC}}(\text{X})[\text{X}]_g$ is similar to or larger than 1 (i.e., at high coverage). This is especially important when interpreting data from laboratory experiments performed using gas-phase reactant concentrations, which lead to significant surface coverage. In the data sheets, we provide preferred values for α_s and k_s .

3.5.2 Direct gas surface reaction

Parameterisation for the reactive uptake coefficient, γ , for gas phase species X directly reacting with surface species, Y, upon collision (ER type mechanism) is given by:

$$\gamma = \frac{\gamma_{\text{gs}}(\text{X})[\text{Y}]_s}{N_{\text{max}}(\text{Y})} = \gamma_{\text{gs}}(\text{X})\theta(\text{Y}) \quad (17)$$

Here $\gamma_{\text{gs}}(\text{X})$ is the elementary reaction probability that a gas phase molecule X colliding with surface component Y reacts with it. $N_{\text{max}}(\text{Y})$ denotes the maximum coverage of Y for a volatile species Y in equilibrium with the gas phase. γ can be calculated for a given gas phase concentration of Y, if values of $K_{\text{LangC}}(\text{Y})$ and γ_{gs} are available. In the absence

of other rate limiting reactions, values of γ_{gs} can be determined experimentally from measurements of γ as a function of surface coverage near saturation, or by extrapolation using an appropriate adsorption isotherm. In the ER type mechanism, γ does not depend on the gas phase concentration of X, whereas in the LH type mechanism (at high $[\text{X}]_{\text{g}}$), it does. Also the temperature dependence, driven by the temperature dependence of $K_{\text{LangC}}(\text{X})$ in the LH case, is substantially different (Pöschl et al., 2007; Ammann and Pöschl, 2007).

3.6 Exchange with the bulk and bulk accommodation

Previously, the process of transfer of a gas molecule from the gas phase into the bulk has been considered a quasi-elementary process, and the mass accommodation coefficient has been defined as the probability that a molecule colliding with the surface is actually taken up into the bulk, mostly in relation with liquids. However, in many cases it is necessary to decouple this process into adsorption on the surface and surface to bulk transfer, i.e., dissolution (Davidovits et al., 1995; Hanson, 1997).

With the aim to clearly differentiate uptake into the bulk from surface accommodation, the term bulk accommodation is recommended, and the corresponding coefficient as bulk accommodation coefficient, α_{b} . In the absence of surface reactions,

$$\alpha_{\text{b}} = \alpha_{\text{s}} \frac{k_{\text{sb}}}{k_{\text{sb}} + k_{\text{des}}} \quad (18)$$

In Eq. (18), k_{sb} denotes the surface to bulk transfer rate coefficient in units of s^{-1} . If the adsorption equilibrium is established much faster than transfer to the bulk, the two processes can be expressed in the form of separated resistances:

$$\frac{1}{\alpha_{\text{b}}} = \frac{1}{\alpha_{\text{s}}} + \frac{1}{\Gamma_{\text{sb}}} \quad \text{with} \quad \Gamma_{\text{sb}} = \frac{\alpha_{\text{s}} k_{\text{sb}}}{k_{\text{des}}} \quad (19)$$

Equations (18) and (19) also allow parameterization of the temperature dependence of α_{b} , which has been used as a proof of the nature of bulk accommodation as a coupled process (Davidovits et al., 1995).

3.7 Solubility limited uptake into the bulk

In the absence of surface or bulk reactions, uptake into the bulk of liquid particles proceeds until the solubility equilibrium is reached. Under quasi-steady state conditions, the uptake coefficient can be described by

$$\frac{1}{\gamma} = \frac{1}{\alpha_{\text{b}}} + \frac{1}{\Gamma_{\text{sol}}} \quad \text{with} \quad \Gamma_{\text{sol}} = \frac{4HRT}{c \cdot \sqrt{\pi}} \cdot \sqrt{\frac{D_l}{t}} \quad (20)$$

H denotes the Henry's Law coefficient (M atm^{-1}), R the gas constant ($1 \text{ atm mol}^{-1} \text{ K}^{-1}$) and D_l the liquid phase diffusion coefficient ($\text{cm}^2 \text{ s}^{-1}$) (Schwartz, 1986). Solubility limited uptake can be used to measure the product $H(D_l)^{0.5}$, through the time dependence of the observed γ .

3.8 Reactive uptake into the bulk

For trace gas reactive uptake to the bulk of liquid (usually aqueous) particles,

$$\frac{1}{\gamma} = \frac{1}{\alpha_{\text{b}}} + \frac{1}{\Gamma_{\text{b}}} \quad \text{with} \quad \Gamma_{\text{b}} = \frac{4HRT}{\bar{c}} \sqrt{D_l \cdot k'_{\text{b}}} \quad (21)$$

k'_{b} is the pseudo first order rate coefficient for reaction of species taken up into the bulk. For small droplets the concept of the diffusive-reactive length is important. This is the average distance beyond the surface of the particle in which reactions take place and is given by:

$$l = \sqrt{\frac{D_l}{k'_{\text{b}}}} \quad (22)$$

For spherical particles of radius r , Eq. (21) can be modified to account for this with:

$$\frac{1}{\gamma} = \frac{1}{\alpha_{\text{b}}} + \frac{\bar{c}}{4HRT \sqrt{D_l \cdot k'_{\text{b}}} [\coth(r/l) - (l/r)]} \quad (23)$$

This is the basis of the ‘‘Framework’’ paper (Hanson et al., 1994) for modelling uptake rates to stratospheric aerosol. Note that for acidic species that can dissociate in the aqueous phase, an effective solubility, H^* , is used whereby:

$$H^* = H \times \left(\frac{1 + K_{\text{diss}}[\text{H}^+]_{\text{e}}}{K_{\text{w}}} \right) \quad (24)$$

K_{w} is the autoprotolysis constant of H_2O , K_{diss} is the acid dissociation constant of the trace gas in water and $[\text{H}^+]_{\text{e}}$ is the equilibrium hydrogen ion concentration in the droplet bulk.

3.9 Coupled processes on the surface and in the bulk

When processes occur on both the surface and in the bulk, adsorption and transfer to the bulk have to be separated. Following previous derivations (Jayne et al., 1990; Davidovits et al., 1995; Hanson, 1997; Shi et al., 1999; Ammann et al., 2003; Pöschl et al., 2007), coupling a Langmuir-Hinshelwood type surface reaction with a reaction in the bulk leads to:

$$\frac{1}{\gamma} = \frac{1}{\alpha_{\text{s}}} + \frac{1}{\Gamma_{\text{s}} + (\frac{1}{\Gamma_{\text{sb}}} + \frac{1}{\Gamma_{\text{b}}})^{-1}} \quad (25)$$

In the case of an Eley-Rideal reaction which occurs without prior adsorption or surface to bulk transfer, the resistance acts in parallel to adsorption, leading to an expression proposed by (Pöschl et al., 2007):

$$\frac{1}{\gamma} = \frac{1}{\gamma_{\text{gs}} + (\frac{1}{\alpha_{\text{s}}} + \frac{1}{\Gamma_{\text{sb}}} + \frac{1}{\Gamma_{\text{b}}})^{-1}} \quad (26)$$

Note that while Eq. (26) is consistent with the resistor diagram suggested by Hu et al. (1995), it is not consistent with

their suggested expression for $1/\gamma$. While they mentioned a Eley-Rideal mechanism, their parameterisation is not consistent with either of the two expressions. In follow-up papers (e.g., Shi et al., 1999) they used Eq. (25) as well.

4 Surface types considered

4.1 Ice

Experimental ice films are either single crystal or polycrystalline and can vary greatly in surface morphology, depending on the mode of formation (vapour deposition versus frozen solutions) and number of grain boundaries/triple points, which may contain supercooled water. This leads to significant uncertainty in the effective surface area of the ice films. There has also been much discussion about the role of pore diffusion (Keyser et al., 1991; Hanson and Ravishankara, 1993; Keyser and Leu, 1993; Leu et al., 1997) in vapour deposited ice films (see also below). Its importance depends on both the properties of the adsorbing species as well as on the condensed phase. For these reasons, when evaluating measurements of trace gas uptake to ice films we always cite the mode of formation of the ice film and any relevant information regarding surface morphology (e.g. BET surface areas).

In addition, many experimental studies of trace gas-ice interactions were carried out under experimental conditions (temperature and trace gas partial pressure) that correspond to stability regions of the phase diagram for either hydrate formation or supercooled aqueous solutions, so that the surface cannot be considered as “ice”. It has been found that the interaction of a trace gas with an ice film made from slowly freezing an aqueous sample can, to a good approximation, be described by the geometric surface area. Evidence is provided by BET surface measurements and by the fact that many molecules that react weakly have similar values of N_{\max} , and that these values are very close to theoretical calculations (Abbatt, 2003).

4.2 NAT (nitric acid trihydrate), NAD (nitric acid dihydrate) and SAT (sulfuric acid tetrahydrate)

Conditions in the stratosphere can be thermodynamically favourable for the existence of solid particles consisting of stable hydrates of nitric, hydrochloric and sulphuric acid. Uptake studies have mainly concentrated on nitric acid-trihydrate (NAT), and sulphuric acid monohydrate (SAM) and tetrahydrate (SAT). Films or particles of these substrates are prepared in a similar fashion to ice films by freezing mixtures or co-deposition of acid and water from the vapour phase. The films have similar physical properties to pure ice films but the surface character depends on RH in a different way to ice as a result of differences in water vapour pressure. For each stoichiometric crystalline acid hydrate there is a water-rich and a water-poor region on each side of the

solidus/liquidus curve. The characterization of the water activity in the neighboring regions on the solidus/liquidus curve is important in view of the dependence of many hydrolysis reactions on water activity.

4.3 Mineral Oxides

Investigations of trace gas uptake to mineral oxide surfaces include naturally occurring “dust” from e.g. Saharan or Asian source regions and surrogate materials including CaCO_3 , Al_2O_3 , Fe_2O_3 , MgO and clay minerals such as kaolinite, illite etc., which are components of atmospheric dust. The mineral oxides are often present as bulk, porous samples in laboratory experiments, which require careful analysis to take into account interstitial surface areas. The comparison of results from different studies is often difficult due to the use of different substrates (e.g. mineralogically distinct “natural dust” samples) and different modes of sample presentation and models for surface area calculation (see Sect. 4.2). Recognizing that synthetic oxides do not necessarily mimic the reactivity of natural dust, where possible our preferred values are presently based on experiments using Saharan or Asian dust samples, preferably presented in aerosol not bulk form. For some trace gases, both the uptake coefficient and adsorption capacity of some dust surfaces are found to have a strong dependence on humidity.

5 Surface areas

γ is usually obtained from observed loss rates of gas-phase species and calculated collision rates with the surface. For the latter the surface area available for uptake/reaction (A) is required. For liquid surfaces this poses no problems as the surface is “smooth” at the molecular level and the geometric surface area (A_{geom}) is generally applicable and readily defined. For solid surfaces (ice, soot, dust etc.) there is a finite probability that the impinging trace gas can collide with internal surface within the time scale of determination of the uptake coefficient. This issue is especially relevant for bulk samples, such as coatings or powders, but may also apply for aerosol particles. The geometric surface area represents a lower limit to A , and an upper limit to γ is obtained. The other extreme is the use of the total sample surface area (e.g. the N_2 -BET surface area, A_{BET}), which is the maximum available surface area, including internal pore volume and bulk surface area of granular material. This is usually expressed as surface area per unit weight of solid sample, which must also be known. Use of A_{BET} yields a lower limit for γ . The surface area available to the trace gas will be determined by parameters such as its surface accommodation coefficient and its desorption lifetime, which limit the rate of diffusion into the interstitial space of a porous sample. Pore diffusion corrections have frequently been applied, both for ice and mineral dust substrates (Keyser et al., 1991; Keyser

and Leu, 1993; Fenter et al., 1995; Leu et al., 1997; Michel et al., 2002; Carlos-Cuellar et al., 2003), and yield uptake coefficients, γ_{PD} that lie between γ_{geom} and γ_{BET} . The application of the geometric, or BET surface area or pore diffusion corrections leads to values of γ that deviate sometimes by orders of magnitude, and has been the subject of much debate (Leu et al., 1997; Hanson and Ravishankara, 1993). Sample preparation and presentation may also have a significant effect on the sample surface area and hence the derived uptake coefficients. For example, ice films created by freezing liquid water may have a smaller surface area than those made by vapour deposition, and single crystal mineral oxides are often less reactive than powdered samples of the same material. The use of aerosol particles rather than bulk surfaces in principle provides a better mimic of atmospheric conditions for experimental surface area.

6 Organisation of the datasheets

The basic structure of the heterogeneous datasheets is similar to the well established datasheets on homogeneous gas-phase reactions. For each heterogeneous interaction on a particular substrate we give a list of experimentally measured values of the uptake coefficients and partition coefficients where appropriate for physical uptake. The parameters are distinguished according to the definitions given above (e.g. γ , γ_{ss} , K_{linC} , etc.). Also given are references and pertinent information about the technique, reactant concentration, substrate and other conditions in linked comments. Reflecting the strong influence of the choice of surface area and sample preparation on γ (see Sect. 3) such information is, when available, also given.

Recommended values for the uptake coefficient, γ and for parameters needed for its calculation (e.g. α_{s} , k_{s} , K_{linC} , N_{max} , γ_{gs} and α_{b}) are provided. Recommended temperature dependencies are given in Arrhenius form when appropriate, together with our estimate of the uncertainties in the parameters. Comments on the state of the data set and justification of the recommendations are then presented, followed by a list of references cited. The reaction ordering of reacting species within each surface category follows that adopted for gas phase reactions, i.e. O_x , HO_x , NO_x , SO_x , organics, and halogenated species.

7 Citation

The citation for recommendations in the data sheets and summary tables is: ACP journal reference + website address: i.e. Crowley, J. N., Ammann, M., Cox, R. A., Hynes, R. G., Jenkin, M. E., Mellouki, A., Rossi, M. J., Troe, J., and Wallington, T. J., IUPAC Subcommittee: Evaluated kinetic and photochemical data for atmospheric chemistry: Volume V – heterogeneous reactions on solid substrates, Atmos. Chem. Phys., 10, 9059–9224, doi:10.5194/acp-10-

9059–2010, 2010 and IUPAC Subcommittee for Gas Kinetic Data Evaluation, <http://www.iupac-kinetic.ch.cam.ac.uk>.

Table 2: Methods used in the study of heterogeneous processes

A number of experimental techniques have been developed for the study of heterogeneous processes. Most methods rely on the determination of loss rates or time dependent concentration changes of gas-phase species in contact with a surface. These include low pressure coated surface laminar flow tube reactors and Knudsen cells for bulk surfaces and films, and droplet train reactors, aerosol flow tubes and static aerosol chambers for dispersed surfaces. Surface adsorbed reactants and products have frequently been observed using surface-sensitive techniques, such as reflectance infrared spectroscopy (DRIFTS, RAIRS), and these have in a few cases been applied to kinetics studies. A list of the related abbreviations used in the data sheets is given below.

Acknowledgements. The Chairman and members of the Subcommittee wish to express their appreciation to I.U.P.A.C. for the financial help which facilitated the preparation of this evaluation. We also acknowledge financial support from the following organisations: EU Framework Program 6, ACCENT network of excellence; the European Science Foundation (INTROP program), the UK Natural Environmental Research Council; the Swiss National Science Foundation, and the Deutsche Forschungsgemeinschaft (SFB 357). We also thank Barbara Cox for her work in preparing and editing the manuscript.

Edited by: R. Cohen

The service charges for this open access publication have been covered by the Max Planck Society.

References

- Abbatt, J. P. D.: Interactions of atmospheric trace gases with ice surfaces: Adsorption and reaction, Chem. Rev., 103, 4783–4800, 2003.
- Ammann, M., Pöschl, U., and Rudich, Y.: Effects of reversible adsorption and Langmuir-Hinshelwood surface reactions on gas uptake by atmospheric particles, Phys. Chem. Chem. Phys., 5, 351–356, 2003.
- Ammann, M. and Pöschl, U.: Kinetic model framework for aerosol and cloud surface chemistry and gas-particle interactions – Part 2: Exemplary practical applications and numerical simulations, Atmos. Chem. Phys., 7, 6025–6045, doi:10.5194/acp-7-6025-2007, 2007.
- Behr, P., Terziyski, A., and Zellner, R.: Reversible gas adsorption in coated wall flow tube reactors. Model simulations for Langmuir kinetics, Zeitschr. Phys. Chem., 218, 1307–1327, 2004.
- Brown, R. L.: Tubular flow reactor with first-order kinetics, J. Res. Nat. B. Stand., 83, 1978.
- Carlos-Cuellar, S., Li, P., Christensen, A. P., Krueger, B. J., Burrichter, C., and Grassian, V. H.: Heterogeneous uptake kinetics

- of volatile organic compounds on oxide surfaces using a Knudsen cell reactor: Adsorption of acetic acid, formaldehyde, and methanol on α -Fe₂O₃, α -Al₂O₃ and SiO₂, *J. Phys. Chem. A.*, 107, 4250–4261, 2003.
- Carlsaw, K. S. and Peter, T.: Uncertainties in reactive uptake coefficients for solid stratospheric particles. I. Surface chemistry, *Geophys. Res. Lett.*, 24, 1743–1746, 1997.
- Davidovits, P., Hu, J. H., Worsnop, D. R., Zahniser, M. S., and Kolb, C. E.: Entry of gas molecules into liquids, *Faraday Disc.*, 65–81, 1995.
- Donaldson, D. J.: Adsorption of atmospheric gases at the air-water interface. I: NH₃, *J. Phys. Chem. A.*, 103, 62–70, 1999.
- Elliott, S., Turco, R. P., Toon, O. B., and Hamill, P.: Application of physical adsorption thermodynamics to heterogeneous chemistry on polar stratospheric clouds, *J. Atmos. Chem.*, 13, 211–224, 1991.
- Fenter, F. F., Caloz, F., and Rossi, M. J.: Experimental evidence for the efficient dry deposition of nitric-acid on calcite, *Atmos. Environ.*, 29, 3365–3372, 1995.
- Finlayson-Pitts, B. J. and Pitts Jr., J. N.: *Chemistry of the upper and lower atmosphere*, Academic Press, San Diego, CA, 2000.
- Flückiger, B. and Rossi, M. J.: Common precursor mechanism for the heterogeneous reaction of D₂O, HCl, HBr, and HOBr with water ice in the range 170–230 K: Mass accommodation coefficients on ice, *J. Phys. Chem. A.*, 107, 4103–4115, 2003.
- Fuchs, N. A. and Sutugin, A. G.: *Highly dispersed aerosols*, Ann Arbor Science Publishers, Inc., Ann Arbor London, 1970.
- Hanson, D. R. and Ravishankara, A. R.: Comment on porosities of ice films used to simulate stratospheric cloud surfaces – response, *J. Phys. Chem.*, 97, 2802–2803, 1993.
- Hanson, D. R. and Ravishankara, A. R.: Reactive uptake of ClONO₂ onto sulfuric acid due to reaction with HCl and H₂O, *J. Phys. Chem.*, 98, 5728–5735, 1994.
- Hanson, D. R., Ravishankara, A. R., and Solomon, S.: Heterogeneous reactions in sulfuric-acid aerosols – A framework for model-calculations, *J. Geophys. Res.*, 99, 3615–3629, 1994.
- Hanson, D. R.: Surface specific reactions on liquids, *J. Phys. Chem. B*, 101, 4998–5001, 1997.
- Hu, J. H., Shi Q., Davidovits, P., Worsnop, D. R., Zahniser, M. S., and Kolb, C. E.: Reactive uptake of Cl₂(g) and Br₂(g) by Aqueous Surfaces as a Function of Br- and I- ion concentration: the effect of chemical reaction at the interface, *J. Phys. Chem.*, 99, 8768–8776, 1995.
- Jayne, J. T., Davidovits, P., Worsnop, D. R., Zahniser, M. S., and Kolb, C. E.: Uptake of SO₂(g) by Aqueous Surfaces as a Function of pH – the Effect of Chemical-Reaction at the Interface, *J. Phys. Chem.*, 94, 6041–6048, 1990.
- Jedlovsky, P., Partay, L., Hoang, P. N. M., Picauud, S., von Hessberg, P., and Crowley, J. N.: Determination of the adsorption isotherm on the surface of ice. An experimental and Grand Canonical Monte Carlo simulation study, *J. Am. Chem. Soc.*, 128, 15300–15309, 2006.
- Kemball, C.: The adsorption of vapours on mercury. II. The entropy and heat of adsorption of non-polar substances, *Proc. Royal Soc. Lond. A Math. Phys.*, 187, 73–87, 1946.
- Kemball, C. and Rideal, E. K.: The adsorption of vapours on mercury. I. Non-polar substances, *Proc. Royal Soc. Lond. A Math. Phys.*, 187, 53–73, 1946.
- Keyser, L. F., Moore, S. B., and Leu, M.-T.: Surface reaction and pore diffusion in flow-tube reactors, *J. Phys. Chem.*, 95, 5496–5502, 1991.
- Keyser, L. F. and Leu, M.-T.: Surface areas and porosities of ices used to simulate stratospheric clouds, *J. Colloid Interf. Sci.*, 155, 137–145, 1993.
- Leu, M. T., Keyser, L. F., and Timonen, R. S.: Morphology and surface areas of thin ice films, *J. Phys. Chem. B*, 101, 6259–6262, 1997.
- Li, Y. Q., Davidovits, P., Shi, Q., Jayne, J. T., Kolb, C. E., and Worsnop, D. R.: Mass and thermal accommodation coefficients of H₂O(g) on liquid water as a function of temperature, *J. Phys. Chem. A.*, 105, 10627–10634, 2001.
- Masel, R. I.: *Principles of adsorption and reaction on solid surfaces*, 1st ed., John Wiley & Sons, New York, 804 pp., 1996.
- Michel, A. E., Usher, C. R., and Grassian, V. H.: Heterogeneous and catalytic uptake of ozone on mineral oxides and dusts: A Knudsen cell investigation, *Geophys. Res. Lett.*, 29, 1665, 2002.
- Morris, J. R., Behr, P., Antman, M. D., Ringeisen, B. R., Splan, J., and Nathanson, G. M.: Molecular beam scattering from supercooled sulfuric acid: Collisions of HCl, HBr, and HNO₃ with 70 wt % D₂SO₄, *J. Phys. Chem. A.*, 104, 6738–6751, 2000.
- Mozurkewich, M.: Effect of competitive adsorption on polar stratospheric cloud reactions, *Geophys. Res. Lett.*, 20, 355–358, 1993.
- Nathanson, G. M., Davidovits, P., Worsnop, D. R., and Kolb, C. E.: Dynamics and kinetics at the gas-liquid interface, *J. Phys. Chem.*, 100, 13007–13020, 1996.
- Pöschl, U., Rudich, Y., and Ammann, M.: Kinetic model framework for aerosol and cloud surface chemistry and gas-particle interactions – Part I: General equations, parameters, and terminology, *Atmos. Chem. Phys.*, 7, 5989–6023, doi:10.5194/acp-7-5989-2007, 2007.
- Schwartz, S. E.: Mass transport considerations pertinent to aqueous phase reactions of gases in liquid water clouds, in: *NATO ASI Ser.*, edited by: Jaeschke, W., Springer-Verlag, New York, 415–471, 1986.
- Seinfeld, J. H. and Pandis, S. N.: *Atmospheric chemistry and physics: From air pollution to climate change*, John Wiley & Sons, Inc., New York, Chichester, Weinheim, Brisbane, Singapore, Toronto, 1998.
- Shi, Q., Davidovits, P., Jayne, J. T., Worsnop, D. R., and Kolb, C. E.: Uptake of gas-phase ammonia. 1. Uptake by aqueous surfaces as a function of pH, *J. Phys. Chem. A.*, 103, 8812–8823, 1999.
- Tabazadeh, A. and Turco, R. P.: A model for heterogeneous chemical processes on the surfaces of ice and nitric-acid trihydrate particles, *J. Geophys. Res. Atmos.*, 98, 12727–12740, 1993.
- Winkler, P. M., Vrtala, A., Wagner, P. E., Kulmala, M., Lehtinen, K. E. J., and Vesala, T.: Mass and thermal accommodation during gas-liquid condensation of water, *Phys. Rev. Lett.*, 93, 2004.
- Worsnop, D. R., Morris, J. W., Shi, Q., Davidovits, P., and Kolb, C. E.: A chemical kinetic model for reactive transformations of aerosol particles, *Geophys. Res. Lett.*, 29, 1996, 2002.

Table 1. Parameters used to describe heterogeneous reactions.

Parameter	Description	Units	notes
γ (γ_{ss}, γ_0)	Net uptake coefficient	–	a
Γ_b	Limiting uptake coefficient for bulk reaction (liquid)	–	
Γ_{sol}	Limiting uptake coefficient for dissolution (liquid)	–	
Γ_{diff}	Limiting uptake coefficient for gas-phase diffusion	–	
Γ_{sb}	Limiting uptake coefficient for surface to bulk transfer	–	
α_s	Surface accommodation coefficient	–	b
α_b	Bulk accommodation coefficient	–	c
γ_{gs}	Elementary gas-surface reactive uptake coefficient (or γ_{ER})	–	
k_s	Surface reaction rate coefficient	$\text{cm}^2 \text{ molecule}^{-1} \text{ s}^{-1}$	
K_{linC}	Gas-Surface partition coefficient (solid surfaces)	$\text{cm}^{-2}/\text{cm}^{-3}$	d
K_v	Gas-Volume partition coefficient (solid surfaces)	$\text{cm}^{-3}/\text{cm}^{-3}$	e
H	Solubility (Henry)	mol/l.atm	
D_l	Liquid phase diffusion coefficient	$\text{cm}^2 \text{ s}^{-1}$	
D_g	Gas phase diffusion coefficient	$\text{cm}^2 \text{ s}^{-1}$	
N or $[X]_s$	Number density of surface adsorbed species	molecules cm^{-2}	
N_{max}	Number density of surface adsorbed species at saturation	molecules cm^{-2}	

a: As γ can be time dependent, subdivisions are necessary, whereby γ_0 is the experimentally observed initial (frequently maximum) uptake coefficient, and γ_{ss} is the experimentally observed steady-state uptake coefficient.

b: The probability (per collision) that a gas phase molecule impinging on the solid surface resides on the surface for a finite time (non-elastic collision $> 10^{-12} \text{ s}^{-1}$).

c: The probability (per collision) that a gas phase molecule impinging on the liquid surface enters the liquid.

d: The partition coefficient that describes the gas-surface partitioning at equilibrium. As described above, the Langmuir isotherm is most commonly used in various units. We report the partition coefficient in the limit of low coverage (linear dependence of coverage on gas concentration) where the units are as given above.

e: The partition coefficient that describes the distribution of trace gas between the gas phase and condensed phase volumes. For a liquid particle this is the solubility, for a solid particle it will include the gas molecules that are associated both with the surface and with the volume of the particle.

Table 2. Techniques used to study heterogeneous reactions.

Methods	
AFT	Aerosol Flow Tube
BC	Bubble Column
CRFT	Coated Rod Flow Tube
CWFT	Coated Wall Flow Tube
DT	Droplet Train
Knudsen (Kn)	Knudsen Reactor
LJ	Liquid Jet
PBFT	Packed Bed Flow Tube
SR	Static Reactor
Detection	
AMS	Aerosol Mass Spectrometry
APS	Aerosol Particle Sizer
ATR	Attenuated Total Reflectance spectroscopy
DMA	Differential Mobility Analyser
DRIFTS	Diffuse Reflectance Infra-red Fourier Transform Spectroscopy
CL	Chemi-Luminescence
CIMS	Chemical Ionisation Mass Spectrometry
GC	Gas Chromatography
LOPAP	Long Path Liquid Phase Absorption
MS	Mass Spectrometry
MBMS	Molecular Beam Sampling MS
RF	Resonance Fluorescence
RC	Counting of decays of radioactive isotopes
SMPS	Scanning Mobility Particle Sizer
TIR	Transmission Infra red spectroscopy
TEM	Transmission Electron Microscopy
UV-Vis	Ultra-Violet-Visible Spectroscopy

DATASHEETS**Appendix A1****Uptake on ice****V.A1.1****O(³P) + ice****Experimental data**

Parameter	Temp./K	Reference	Technique/Comments
γ, γ_0 $\gamma_0 = 7 \times 10^{-6}$ for $[\text{O}_2] = 0$ $\gamma = 7 \times 10^{-6} + 2.6 \times 10^{-24} \exp(1372 \pm 72/T)$ for $[\text{O}_2]$ up to $1 \times 10^{15} \text{ cm}^{-3}$	112–151 112–151	Murray and Plane, 2003	CWFT-RF (a)

Comments

- (a) Cubic ice formed by vapour deposition at 90 K and annealed to 160 K. Uptake experiments performed using a fast flow reactor equipped with resonance fluorescence detection of O atoms at 130 nm. The BET surface area was used in the calculation of the uptake coefficients. A pulsed version of the O atom uptake experiment in the same flow tube was also performed and a chromatographic analysis of the pulse shape showed that O atom uptake was relatively strongly bound to some ice sites.

Preferred values

Parameter	Value	T/K
γ	$7 \times 10^{-6} + 2.6 \times 10^{-24} \exp(1370/T)$ $[\text{O}_2]$	110–150
<i>Reliability</i>		
$\Delta \log(\gamma)$	± 0.3	
$\Delta(E/R)/\text{K}$	± 200	

Comments on preferred values

Kinetic modelling indicated two mechanisms for O atom uptake: one that was independent of temperature and $[\text{O}_2]$ between 112–151 K, and one that was dependent on $[\text{O}_2]$ and had a negative temperature dependence. The preferred values are those reported in the single study of Murray and Plane (2003), with expanded errors. An Eley-Rideal mechanism was suggested as the mechanism by which adsorbed O atoms are removed from the ice surface by collisions with gas-phase O atoms or O_2 to form O_2 or O_3 , respectively. Quantum chemical calculations showed that O atoms bind to either a single dangling hydrogen on a perfectly crystalline ice surface or to two dangling hydrogens in a disordered ice structure.

References

Murray, B. J. and Plane, J. M. C.: Phys. Chem. Chem. Phys., 5, 4129, 2003.

V.A1.2**O₃ + ice****Experimental data**

Parameter	Temp./K	Reference	Technique/Comments
γ			
$<1 \times 10^{-4}$	195	Leu, 1988	CWFT-MS (a)
$<1 \times 10^{-6}$	195–262	Dlugokencky and Ravishankara, 1992	CWFT-CL (b)
$<6 \times 10^{-5}$	183	Kenner et al., 1993	CWFT-MS (c)
$2 \times 10^{-8} - 4 \times 10^{-10}$	223, 258	Langenberg and Schurath, 1999	(d)

Comments

- (a) Ice film made by vapour deposition. No uptake of O₃ on pure ice detected.
- (b) Low pressure flow tube (1.33 mbar He). A 2 mm thick ice film formed by freezing liquid water. The O₃ concentration was varied between 10⁸ and 10¹² molecule cm⁻³. No detectable O₃ loss on pure ice surfaces. Addition of e.g. sulphite or nitric acid prior to freezing induced temporary uptake.
- (c) 4–7 μm thick ice film made by vapour deposition. No uptake of O₃ on pure ice detected.
- (d) A fused silica gas chromatographic column was used as a flow tube. Ice films were prepared by vapour deposition and were 6.8–8.1 μm thick. O₃ (20–1000 nbar) was detected using chemiluminescence. The O₃ uptake coefficient was found to be dependent on [O₃], with higher values obtained at lower [O₃]. Data at 223 K could be parameterised using $\gamma = A / [(1+B)C]$, with $A = 5.5 \times 10^{-8}$, $B = 0.08$ and $C =$ the O₃ concentration in mbar.

Preferred values

Parameter	Value	T/K
γ	$<1 \times 10^{-8}$	220–260
<i>Reliability</i>		
$\Delta \log(\gamma)$	0.7	

Comments on preferred values

The four studies of the uptake on ozone to ice surfaces show the interaction of O₃ with ice surfaces is quite weak. Only the experiments of Langenberg and Schurath (1999), designed to measure weak interactions, were able to detect uptake of ozone and their data provide the basis of the recommendation. Langenberg and Schurath provided a parameterisation of the [O₃] dependent uptake coefficient at 223 K (see note (d) above), but were unable to treat data at 258 K in a similar fashion. For this reason, and also because the true surface area of the ice film could not be determined, an upper limit of 1×10^{-8} is preferred.

References

- Dlugokencky, E. J. and Ravishankara, A. R.: Geophys. Res. Lett., 19, 41–44, 1992.
- Langenberg, S. and Schurath, U.: Geophys. Res. Lett., 26, 1695–1698, 1999.
- Leu, M. T.: Geophys. Res. Lett., 15, 851–854, 1988.
- Kenner, R. D., Plumb, I. C., and Ryan, K. R.: Geophys. Res. Lett., 20, 193–196, 1993.

V.A1.3**HO + ice****Experimental data**

Parameter	Temp./K	Reference	Technique/Comments
γ, γ_0 $\gamma_0=0.1$ $\gamma_{ss}=0.03\pm 0.02$	205–230	Cooper and Abbatt, 1996	CWFT-RF (a)

Comments

(a) HO radicals generated by the reactions $F+H_2O \rightarrow HF+HO$ and $H+NO_2 \rightarrow HO+NO$. The total flow tube pressure was generally 1 Torr (1.33 mbar) with a total flow velocity of 1500–2200 cm s⁻¹.

Preferred values

Parameter	Value	T/K
γ_{ss}	0.03	200–230
<i>Reliability</i>		
$\Delta \log(\gamma)$	± 0.5	

Comments on preferred values

Cooper and Abbatt (1996) observed that HO radicals were irreversibly adsorbed on the ice surface. Initial uptake coefficients were large (~ 0.1) on fresh ice surfaces, but after 20 mins of OH uptake, surfaces became deactivated and uptake coefficients were reduced to a steady-state value of ~ 0.03 . The irreversible loss of HO may then be due to reaction of HO with an activated S-OH site formed from reaction of HO with a surface site, S. Cooper and Abbatt (1996) argue that this mechanism is consistent with the observed first-order loss of HO from the gas-phase if the rate limiting step is transfer of HO from the gas-phase to the activated surface (i.e. to an S-OH site). The uptake coefficient could be significantly increased (to ~ 0.2) by adsorbing HNO₃ to the surface (whilst remaining in the ice stability regime of the ice-HNO₃ phase diagram), or by melting the surface by adding a sufficient partial pressure of HCl. It should be stressed that the preferred value is representative of uptake to a clean ice surface and that in an atmospheric, chemically complex environment, the uptake coefficient could be larger (if the surface is contaminated with e.g. reactive organics) or smaller if S-OH is deactivated by trace gases other than HO.

References

Cooper, P. L. and Abbatt, J. P. D.: J. Phys. Chem., 100, 2249, 1996.

V.A1.4**HO₂ + ice****Experimental data**

Parameter	Temp./K	Reference	Technique/Comments
γ 0.025±0.005	223	Cooper and Abbatt, 1996	CWFT-RF (a)

Comments

- (a) Flow tube operated at ~ 1.3 mbar pressure of He. Ice film made by freezing water. HO₂ ($\leq 5 \times 10^{10}$ molecule cm⁻³) was generated by the reaction of H₂O₂ with F atoms and was detected as HO following reaction with NO. HO₂ decays were exponential, and loss of HO₂ at the surface was irreversible, so that $\gamma = \gamma_0 = \gamma_{ss}$.

Preferred values

No recommendation.

Reliability

$\Delta \log \gamma$ is undefined.

Comments on preferred values

There is only one measurement of the uptake of HO₂ to an ice surface, which was conducted at a single temperature (Cooper and Abbatt, 1996). The limited dataset suggests that the uptake is irreversible (i.e. the surface does not saturate) at concentrations of HO₂ that far exceed those in the atmosphere. As information on the temperature and concentration dependence of the HO₂ uptake coefficient is not available, no recommendation is given. Analogous work on HO uptake by the same authors has shown that HO uptake is in part driven by self-reaction on the surface. Further experimental work is required to test whether the same applies to HO₂, and to extend the database to other temperatures.

References

Cooper, P. L. and Abbatt, J. P. D.: J. Phys. Chem., 100, 2249–2254, 1996.

V.A1.5

H₂O₂ + ice

Experimental data

Parameter	Temp./K	Reference	Technique/Comments
γ			
0.02	228–270	Conklin et al., 1993	PBFT (a)
$K_{\text{linC}}/\text{cm}, K_v$			
$K_{\text{linC}}=1.56$	228	Clegg and Abbatt, 2001	CWFT-MS (b)
$K_v=8.3 \times 10^4$	270	Conklin et al., 1993	PC (a)
$K_v=1.24 \times 10^5$	262		
$K_v=5.78 \times 10^5$	243		
$K_v=1.07 \times 10^7$	228		

Comments

- (a) Column packed with $\approx 200 \mu\text{m}$ ice spheres. H₂O₂ ($\approx 10^{10}$ – 10^{12} molecule cm⁻³) detected using liquid phase enzymatic fluorometry. As a result of the long duration of the experiments (up to 20 h), some of the uptake observed (exceeding 1 monolayer at the lowest temperatures) is due to bulk dissolution of H₂O₂. Equilibrium gas-to-ice volume partitioning coefficients were extracted from experimental data when the net uptake was zero, or by using an advection-dispersion model of H₂O₂ transport in the column (at 228 K). The coefficient K_v includes both surface and bulk H₂O₂.
- (b) Ice films were made by freezing water. The uptake of H₂O₂ was observed to be totally reversible. The geometric surface area was used to calculate the coverage. The value of K_{linC} presented in the Table was determined from data presented in a plot and uses the observed linear relationship between N (surface coverage in molecule cm⁻² of ice) and [H₂O₂]. No significant dependence of K_{linC} on temperature was observed.

Preferred values

Parameter	Value	T/K
$K_{\text{linC}}/\text{cm}$	$2.1 \times 10^{-5} \exp(3800/T)$	200–240
$N_{\text{max}}/\text{molecule cm}^{-2}$	4.5×10^{14}	200–240
<i>Reliability</i>		
$\Delta \log K_{\text{linC}}$	0.5	200–240
$\Delta \log N_{\text{max}}$	0.3	200–240

Comments on preferred values

The experimental data show that the interaction of H₂O₂ with ice is reversible, and that, at long exposure times, both surface and volume uptake are observed. The solubility in ice appears to be a factor of ≈ 200 smaller than in liquid water, extrapolated to the same temperature (Conklin et al., 1993). Partitioning to the surface is surprisingly weak, and no temperature dependence was detected in the one study of this parameter (Clegg and Abbatt, 2001). A further value of $K_{\text{linC}} = 2.1 \times 10^{-5} \exp(3800/T)$ has been reported by Marecal et al. (2010) in a modelling study. This value is based on unpublished experimental work (Pouvesle et al., from the MPI-Mainz group) using a coated wall flow tube, though no experimental details are given. This parameterisation results in values of K_{linC} which are orders of magnitude larger than reported by Clegg and Abbatt (2001). The larger partition coefficient measured by Pouvesle et al. is more consistent with the emerging picture of the interaction of hydrogen bonding trace gases with ice surfaces in which a distinct inverse relationship between the vapour pressure of the trace gas and the partition coefficient is observed (Sokolov and Abbatt, 2002). For this reason we prefer the value reported by Marecal et al. (2010) but with expanded error limits to reflect the divergence in the available studies and the fact that it has not yet been published. We also adopt the value of N_{max} reported by Marecal et al.

References

- Clegg, S. M. and Abbatt, J. P. D.: *J. Phys. Chem. A*, 105, 6630–6636, 2001.
- Conklin, M. H., Sigg, A., Neftel, A., and Bales, R. C.: *J. Geophys. Res.*, 98, 18367–18376, 1993.
- Marecal, V., Pirre, M., Riviere, E. D., Pouvesle, N., Crowley, J. N., Freitas, S. R., and Longo, K. M.: *Atmos. Chem. Phys.* 10, 4977–5000, 2010.
- Sokolov, O. and Abbatt, J. P. D.: *J. Phys. Chem. A*, 106, 775–782, 2002.

V.A1.6

H₂O + ice

Experimental data

Parameter	Temp./K	Reference	Technique/Comments
γ_{ss}, α			
0.37–0.94 (α)	133–158	Koros et al., 1966	gravimetric (a)
6.0×10^{-2} (α)	193–223	Isono and Iwai, 1969	micro photographs (b)
1.0 (α)	≤ 193	Davy and Somorjai, 1971	gravimetric (c)
0.8 \pm 0.08	208		
0.5 \pm 0.05	228		
0.55 \pm 0.05(α)	268 \pm 2	Bonacci et al., 1976	total pressure (d)
$\gamma_{ss} > 0.3$	195	Leu, 1988	CWFT (e)
0.65 \pm 0.08 (α)	185	Haynes et al., 1992	UHV interferometry (f)
1.0 \pm 0.01 (α)	160	Speedy et al., 1996	UHV-MB (g)
0.97 \pm 0.10 (α)	80–220	Brown et al., 1996	UHV-MB (h)
0.14 (single crystal D ₂ O ice) (α)	140	Chaix et al., 1998	Knudsen (i)
0.13	170		
0.11	190		
0.27 (frozen liquid D ₂ O ice) (α)	170		
0.25	190		
0.17	200		
0.19 (vapor deposited D ₂ O ice) (α)	170		
0.17	190		
0.11	210		
0.60 (cubic ice D ₂ O) (α)	140		
0.15 (artificial D ₂ O snow) (α)	170		
0.15	190		
0.07	210		
1.0–0.45 (α)	130–170	Fraser et al., 2001	TPD in UHV reactor (j)
0.19–0.085 (α)	170–230	Delval and Rossi, 2003; 2005	SFR/FTIR (k)
0.15 \pm 0.05 (α)	175	Smith et al., 2003	HeNe
0.18 \pm 0.07	180		interferometry (l)
0.26 \pm 0.08	190		
0.7 \pm 0.3 (average value of α)	251–273	Sadtchenko et al., 2004	evaporation (m)
0.48	251		
0.42 \pm 0.05 (α)	173–193	Delval and Rossi, 2004	SFR/QCMB (n)
0.42 \pm 0.18	193–223		
0.25 \pm 0.05 (bulk=frozen liquid H ₂ O ice)(α)	180	Pratte et al., 2006	Knudsen (o)
0.35 \pm 0.10 (vapor-condensed ice)			
0.30 \pm 0.05 (artificial snow)			
0.15 \pm 0.05 (single crystal ice film)			
0.58 \pm 0.08 (cubic ice film)	130		
(6 \pm 2) $\times 10^{-3}$ (single ice particles of 5.3 to 7.8 μ m diameter) (α)	223	Magee et al., 2006	Electrostatic levitation (p)
0.88 \pm 0.10 (single crystal ice) (α)	258–273	Lu et al., 2006	Filament evaporation (q)

Comments

- (a) Gravimetric measurements of targets impinged by a supersonic molecular H₂O beam as a function of time. Direct measurement of α after correction for the loss of H₂O from the multiple collision target. Values of α in the range 133 to 233 K lie between 0.37 and 0.94 which represent averages of individual measurements.
- (b) Evaporation in vacuum and deposition of spherical H₂O ice crystals onto tipped Cu-substrate in the range 193 to 223 K. From the linear increase in ice crystal radius with time the mass change of each ice crystal was determined from photomicrographs at a measured H₂O supersaturation ratio. Below 193 K, α increases with decreasing temperature.
- (c) Kinetics of vacuum sublimation of single ice crystals monitored by gravimetric measurement using an electromicrobalance in the temperature range 183 to 233 K resulted in a negative T-dependence of the evaporation coefficient, and by microscopic reversibility, of the condensation coefficient α . The sublimation rates of the different samples were reproducible to within $\pm 10\%$, and were independent of crystal orientation and crystallinity (single crystal vs. polycrystalline). Dopants such as NH₄OH, NaOH, HF, HNO₃ and NH₄F significantly lowered the sublimation rate when ice is either grown from 0.01 to 0.1 M solutions or exposed to the dopant gas in the range 1.3 to 13 mbar.
- (d) Measurement of both condensation and evaporation coefficient of liquid water (278 \pm 3 K) and ice in a static chamber by recording the total pressure and the liquid or solid temperature transient upon perturbation of the gas-condensed phase equilibrium by pumping or adding H₂O vapour to the liquid or solid sample. α for ice was time invariant in contrast to liquid water, which depended on the observation period 0.2 to 10 s. However, the instantaneous value for liquid water and the steady-state value for ice were indistinguishable within experimental uncertainty.
- (e) Fast flow tube reactor with MS detection. A diffusion correction was applied to γ , using the measured diffusion coefficient of H₂O in He scaled to 195 K.
- (f) Interferometric observation of the growth and evaporation of H₂O from a vapor-deposited ice film. No barrier for the adsorption of H₂O onto ice was found because the desorption activation energy was equal to the enthalpy of sublimation $\Delta H_{\text{sub}}=(49.4\pm 0.8)$ kJ mol⁻¹ within experimental uncertainty. No dependence of the kinetic parameters on the various ice morphologies were observed.
- (g) Measurement of the free molecular evaporation, J_{ev} , of a recrystallized cubic ice film, (1 μm thick, deposited on Ru(001) from the vapor) using mass spectrometry under UHV conditions. The ice film was deposited as amorphous film at 85 K and was annealed in situ up to 162 K. The rate of evaporation for D₂O was also measured and resulted in J_{ev} being smaller by a factor of two.
- (h) Molecular beam and optical interference techniques at 632.8 nm were both used to measure the H₂O condensation coefficient on ice multilayers grown on Ru(001). α was measured from 80 to 220 K and was consistent with a value α of unity. The H₂O desorption flux follows zero-order kinetics and is expressed as $J_{\text{des}}=(4.0\pm 1.0)\times 10^{15}\exp((-5805\pm 96)/T)$ monolayers s⁻¹. Earlier results on α obtained by optical interference measurements obtained by Haynes et al. (1992) (see (f)) were reinterpreted using temperature dependent values of ρ_{ice} and n_{ice} to result in $\alpha=1.0$, independent of temperature.
- (i) Time-resolved uptake measurement in a Knudsen flow reactor using D₂¹⁸O as a probe interacting with D₂¹⁶O ice. Using reaction vessels of different gas phase residence times the kinetics of adsorption and desorption could be separated leading to condensation and evaporation coefficients (α). Different types of ice substrates led to different α values which were all significantly smaller than unity and show a significant negative temperature dependence implying a precursor-mediated reaction mechanism.
- (j) TPD using m/e 18 of H₂O using line-of-sight residual gas MS in the range 130–170 K. The ice sample was deposited on a Au substrate at 10 K and corresponded to a high-density amorphous phase. However, a phase change (120 to 140 K) from amorphous to the crystalline hexagonal form preceded the evaporation so that the parameters given correspond to the I_h crystalline phase. The desorption was found to obey a zero-order rate law and was expressed as J_{ev} (molecule cm⁻² s⁻¹)= $10^{30\pm 2}\exp((-5773\pm 60)/T)$. J_{ev} measured at 130 K corresponds to $\alpha=1.0$ beyond which it significantly deviates from unity.

- (k) Uptake experiment of H₂O vapor on temperature-controlled Si window monitored by FTIR in transmission, HeNe interferometry and residual gas MS inside a stirred flow reactor (SFR) that also could be used as a static reactor. Ice was generated from vapor phase condensation at 190 K. Thermochemical closure between evaporation and condensation was checked by the measurement of the vapor pressure in the static reactor. The following Arrhenius expressions for the evaporation flux and the condensation rate constant k_c in the range 200–230 K were obtained for pure ice: $J_{ev}=1.6\times 10^{(28\pm 1)}\exp(-(5184\pm 604)/T)\text{ molec cm}^{-2}\text{ s}^{-1}$, $k_c=1.7\times 10^{-(2\pm 1)}\exp((805\pm 755)/T)\text{ s}^{-1}$.
- (l) Study of the evaporation rate of 6 μm thick crystalline hexagonal ice deposited on a thermostatted Ru(001) single crystal at 160 K using HeNe interferometry at 594 nm with a temperature-independent refractive index of ice $n=1.31$. The evaporation rates of H₂¹⁸O and D₂O are smaller by 9% and by a factor of two, respectively. A transition state model was used to explain these results which, however, predicts only 50% of the rate decrease in going from H₂O to D₂O.
- (m) Transient evaporation of H₂O and D₂O from thin ice film deposited on a 10 μm tungsten filament. Measurement of transient voltage and resistance across the filament and ion current (ion gauge and TOF MS). These observables enabled the rate of evaporation and the temperature of the evaporating H₂O molecules in the range 251–273 K to be determined. The vaporization rate follows Arrhenius behaviour and results in an activation energy of $50\pm 4\text{ kJ/mol}$ which corresponds to the low-temperature enthalpy of evaporation of pure ice at <200 K. The extrapolation of the low-temperature molecular precursor model of Davy and Somorjai (1971) (see (c)) to 273 K greatly underpredicts α relative to this measurement. However, the α at 251 K seems to be smaller than the given average value of $\alpha=0.7$.
- (n) Same experiment as in (k) except that the mass loss of ice using a quartz crystal microbalance (QCMB) was recorded as a function of time in the stated temperature range. The rate constant for H₂O condensation, k_c , was measured in two series of experiments from the net rate of evaporation, once under stirred flow conditions and once under fast pumping conditions where no condensation occurred. A break of the Arrhenius plot at $T=193\pm 2\text{ K}$ separates evaporation and condensation into two regimes with $J_{ev}=2.2\times 10^{30}\exp(-(6040\pm 235)/T)$ for $173<T/\text{K}<193$, and $J_{ev}=1.6\times 10^{28}\exp(-(5137\pm 253)/T)$ for $193<T/\text{K}<223$.
- (o) Knudsen flow reactor study using pulsed valve admission of H₂O, which was monitored using MS. Except for artificial snow a negative temperature dependence in the range 140 to 210 K was observed, consistent with a precursor-mediated adsorption mechanism. Both rate (flux) of evaporation and α are significantly different for different types of ice whereas the enthalpy of sublimation is the same, namely $(50.2\pm 5.9)\text{ kJ/mol}$. Thermochemical closure of the kinetic parameters of the rates of evaporation and condensation (activation energies) is achieved resulting in the known thermochemistry (ΔH_{subl}^0).
- (p) Observation of the mass change of single frozen H₂O droplets in a electrodynamic levitation cell at temperatures between 213 and 233 K during several evaporation and condensation cycles. Variable H₂O saturation ratios are determined at an accuracy of 5% using a calibration technique based on growth of H₂SO₄ droplets as a function of RH. No significant temperature dependence of α was observed over the given range. The typical uncertainty for α is in the range 4.5 to 7.5×10^{-3} using a standard growth model. Total pressure is not reported.
- (q) Filament evaporation in high vacuum chamber (see (m)) using MS. Vapor-deposited H₂¹⁸O tracing layers of typically 50–100 nm thickness were sandwiched between two polycrystalline H₂¹⁶O layers of total thickness of typically 3 μm at 150 K. From the tracing layer position and the time of appearance of H₂¹⁸O absolute H₂O evaporation rates were measured in the range 258–273 K. Evaporation rates as a function of time revealed two processes, one from single crystallites and the other from disordered H₂O trapped inside grain boundaries. In comparison to polycrystalline samples (see (m)) single crystal evaporation rates are on average slower by a factor of two.

Preferred values

Parameter	Value	T/K
α	$9.72 \times 10^{-2} \exp(232/T)$	130–190
α	$1.52 \times 10^{-3} \exp(1022/T)$	190–230
α	0.7	250–273
<i>Reliability</i>		
$\Delta \log(\alpha)$	0.3	
$\Delta \alpha$	± 0.3	250–273

Comments on preferred values

Results on both evaporation (sublimation, desorption) and condensation (adsorption) rates have been used to derive the mass accommodation coefficient α , assuming that the principle of microscopic reversibility applies under identical experimental conditions, which has been verified experimentally (Haynes et al., 1992) despite certain reports to the contrary (Marek and Straub, 2001).

Gas kinetic theory provides a maximum rate R or flux F of evaporation and condensation for the simple process $\text{H}_2\text{O}(\text{g}) \leftrightarrow \text{H}_2\text{O}(\text{s})$ (k_c , R_{ev}), with $\text{H}_2\text{O}(\text{s})$ corresponding to ice. The maximum rate of evaporation (and condensation) is given by the Hertz-Knudsen equation $J_{ev}^{\max} = (2\pi MRT)^{-0.5} P_{eq}$, where P_{eq} corresponds to the equilibrium vapor pressure of H_2O over ice; rate and flux are related through $V \cdot R = J \cdot A$, with V and A being the volume and geometric surface area of the system. The condensation and evaporation coefficients are given by the following expressions:

For H_2O condensation experiments: $\alpha = k_c / \omega$

where k_c is the measured first order rate constant for condensation and ω is the calculated gas-kinetic collision frequency ($\omega = \langle c \rangle / 4V$) / A with $\langle c \rangle$ being the average molecular velocity).

For evaporation experiments $\alpha = J_{ev} / J_{ev}^{\max}$ or R_{ev} / R_{ev}^{\max} .

Representative kinetic results are displayed in the Table above in terms of α (and γ_{ss}). Those that are expressed as J_{ev} and J_{ev}^{\max} as a function of temperature in the range 140 to 230 K have been converted to α using the vapor pressure data of Marti and Mauersberger (1993) and of Mauersberger and Krankowsky (2003). Apart from a few exceptions the consensus obtained from recent experiments seems to be that α for H_2O on ice is significantly less than unity for $T > 160$ K. Moreover, α decreases to 0.13 at 230 K, after which it increases again towards 273 K to attain $\alpha = 0.8 \pm 0.2$ at 260 K (Sadtschenko et al., 2004; Lu et al., 2006). The low temperature data of Sack and Baragiola (1993) seem to be out of line as their measured evaporation fluxes J_{ev} consistently exceed J_{ev}^{\max} by a factor of up to ten at 140 K and by a factor of two at 160 K for no obvious reason thus leading to α exceeding unity.

In general, the preferred values for α pertain to those for vapor-condensed ice. According to the measured temperature dependence of α we have split it into three ranges, namely 130–190, 190–230 and 230–260 K, each with its own temperature dependence.

The preferred values for α over the range 130–190 K are given by the Arrhenius fit to the weighted average data of Haynes et al. (1992), Chaix et al. (1998), Fraser et al. (2001), Delval and Rossi (2004) and Pratte et al. (2006). Although less relevant for the atmosphere, the low temperature data have been considered here as a benchmark as α must converge towards unity at $T \leq 130$ K according to most experimental results.

For the range 190–230 K the data of Chaix et al. (1998), Delval et al. (2003, 2004) and Pratte et al. (2006) have been used to determine the preferred value of α . The data of Davy and Somorjai (1971) have the same temperature dependence in this range although the absolute value of α is larger by a factor of 3.5.

The preferred value of α in the third temperature range (230–260 K) is based on the work of Bonacci et al. (1976), Sadtschenko et al. (2004) and Lu et al. (2006). In this range α has a positive temperature dependence that is possibly associated with the known presence of a significant quasi-liquid layer on pure ice for $T \geq 233$ K. It is likely that α is unity at $T = 273$ K although it has not yet been measured at this temperature.

From a plot of α vs. T of the data (not shown) displayed in the table one concludes that out of 13 independent measurement of α over varying T-ranges all except one (Smith et al., 2003) show a negative temperature dependence. Haynes et al. (1992) do not observe a temperature dependence and prefer to state a T-independent value of α in the range 172 to 205 K. However, the condensation coefficient of Haynes et al. (1992) steadily decreases from $\alpha=1.06$ at 20 K to 0.68 at 185 K as do the α values of Fraser et al. (2001) in the range 130 to 170 K. Brown et al. (1996) reanalyse the data of Haynes et al. (1992) in the framework of their combination of molecular beam and interferometric experiments and come to the conclusion that $\alpha=0.97\pm 0.10$ for all investigated temperatures in the range 90 to 145 K when allowing both the density of ice and its index of refraction to linearly vary over the given T-range. Tolbert and Middlebrook (1990) agree with this proposal for the growth of thin films of ice at $T < 145$ K. Later interferometric work by the same group (Smith et al., 2003) relaxes this restrictive condition and obtains an α value that is smaller than unity over the narrow range 175 to 190 K, albeit with a positive temperature dependence.

Support for the negative temperature dependence comes from the work of Davy and Somorjai (1971), Chaix et al. (1998) (for D₂O condensation and evaporation kinetics), Delval and Rossi (2003, 2004) and Pratte et al. (2006) using a vacuum microbalance technique, a Knudsen reactor or a stirred flow reactor, the latter equipped with both gas and condensed phase diagnostics, respectively. The separation of condensation and evaporation kinetics (k_c and R_{ev}) is performed using multiple data sets as well as steady-state and transient experimental techniques. The incorrectly used term uptake coefficient used by Chaix et al. (1998), Delval and Rossi (2003, 2004) and Pratte et al. (2006) corresponds to mass accommodation in terms of either the condensation or evaporation coefficient, because the condensation rate was taken into account when studying the evaporation rate, and vice versa. The corrected uptake coefficient therefore corresponds to α .

The direct measurement of k_c in transient supersaturation experiments has been validated by Pratte et al. (2006) using two steady state techniques, namely the CFM (Compensated Flow Method) and TASSM (Two Aperture Steady State Method). Pratte et al. (2006) also examined the condensation/evaporation kinetics of different types of ice and found significant differences ranging from $\alpha=0.67$ for cubic ice at 130 K to $\alpha=0.19$ for single crystal ice at $T=145$ K as did Chaix et al. (1998). However, the equilibrium vapor pressure P_{eq} is invariant from one type of ice to another when evaluated according to $[H_2O]_{ss}=P_{eq}/RT=R_{ev}/k_c$ and is consistent with the heat of sublimation $\Delta H_{sub}^0=51.5\pm 6.7$ kJ mol⁻¹. Thermochemical closure is only afforded when considering negative activation energies for H₂O condensation (k_c) because activation energies for evaporation (R_{ev}) by themselves significantly fall short of the accepted thermochemistry for H₂O sublimation (Pratte et al., 2006). The Arrhenius plot for k_c in the range 130 to 210 K shows a discontinuity equal to a break or change in slope of the straight line at 193 ± 2 K with a concomitant change in the corresponding plot of J_{ev} (Delval and Rossi, 2004; Pratte et al., 2006) which is the temperature at which the T-dependence of α changes (see preferred values). This observation has been made in both the Knudsen as well as the stirred flow reactor, the latter of which used both the gas phase (MS) as well as the mass loss of the thin ice film (QCMB) as a function of time. The data beyond 230 K of the stirred flow reactor (Delval and Rossi, 2004) have not been taken into account in the evaluation because of possible systematic errors owing to heating/cooling effects of the ice surface due to excessive rates of condensation/evaporation at these higher partial pressures of H₂O.

The results of Bonacci et al. (1976), obtained in the high-temperature range, are similar, albeit a bit lower than Sadtchenko et al. (2004). The α values reported for single crystal ice by Lu et al. (2006) seems to be larger than for vapor-phase polycrystalline ice (Sadtchenko et al., 2004) at 260 K which is unexpected in light of results obtained at lower temperatures (Chaix et al., 1998; Pratte et al., 2006), and considering the fact that the same technique was used in both cases.

In conclusion, the H₂O/ice system presents several puzzles despite the number of experimental investigations.

References

- Bonacci, J. C., Myers, A. L., Nongbri, G., and Eagleton, L. C.: Chem. Eng. Sci. 31, 609, 1976.
Brown, D. E., George, S. M., Huang, C., Wong, E. K. L., Rider, K. B., Scott Smith, R., and Kay, B. D.: J. Phys. Chem., 100, 4988, 1996.
Chaix, L., van den Bergh, H., and Rossi, M. J.: J. Phys. Chem. A., 102, 10300, 1998.
Davy, J. G. and Somorjai, G. A.: J. Chem. Phys., 55, 3624, 1971.
Delval, C. and Rossi, M. J.: Atmos. Chem. Phys., 3, 1131, 2003.
Delval, C. and Rossi, M. J.: Phys. Chem. Chem. Phys., 6, 4665, 2004.
Delval, C. and Rossi, M. J.: J. Phys. Chem. A., 109, 7151, 2005.
Flückiger, B. and Rossi, M. J.: J. Phys. Chem. A., 107, 4103, 2003.
Fraser, H. J., Collings, M. P., McCoustra, M. R. S., and Williams, D. A.: Mon. Not. R. Astron. Soc., 327, 1165, 2001.
Haynes, D. R., Tro, N. J., and George, S. M.: J. Phys. Chem., 96, 8504, 1992.
Isono, K. and Iwai, K.: Nature, 223, 1149, 1969.
Koros, R. M., Deckers, J. M., Andres, R. P., and Boudart, M.: Chem. Eng. Sci., 21, 941, 1966.

- Leu, M.-T.: *Geophys. Res. Lett.*, 15, 17, 1988.
- Lu, H., McCartney, S. A., Chonde, M., Smyla, D., and Sadtchenko, V.: *J. Chem. Phys.*, 125, 044709, 2006.
- Magee, N., Moyle, A. M., and Lamb, D.: *J. Geophys. Res.*, 33(17), L17813, 2006.
- Marek, R. and Straub, J.: *Int. J. Heat Mass Transf.*, 44, 39, 2001.
- Marti, J. and Mauersberger, K.: *Geophys. Res. Lett.*, 20, 363, 1993.
- Mauersberger, K. and Krankowsky, D.: *Geophys. Res. Lett.*, 30(3), 2003.
- Pratte, P., van den Bergh, H., and Rossi, M. J.: *J. Phys. Chem. A.*, 110, 3042, 2006.
- Sack, N. J. and Baragiola, R. A.: *Phys. Rev. B*, 48, 9973, 1993.
- Sadtchenko, V., Brindza, M., Chonde, M., Palmore, B., and Eom, R.: *J. Chem. Phys.*, 121, 11980, 2004.
- Smith, J. A., Livingston, F. E., and George, S. M.: *J. Phys. Chem. B*, 107, 3871, 2003.
- Speedy, R. J., Debenedetti, P. G., Smith, R. S., Huang, C., and Kay, B. D.: *J. Chem. Phys.*, 105, 240, 1996.
- Tolbert, M. A. and Middlebrook, A. M.: *J. Geophys. Res.*, 95, 22433, 1990.

V.A1.7**NO + ice****Experimental data**

Parameter	Temp./K	Reference	Technique/Comments
γ_{ss}, γ_0			
$\gamma_{ss} \leq 1.0 \times 10^{-4}$	195	Leu, 1988a	CWFT-MS (a)
$\gamma_0 \leq 5.0 \times 10^{-6}$	193-243	Saastad et al., 1993	Knudsen-MS

Comments

- (a) water ice film formed by vapour-deposition at 200 K as described in Leu (1988b).
- (b) Measurement of the total pressure drop in a static system over bulk ice and frozen 70% H₂SO₄-H₂O monitored by MS. NO partial pressures were 10⁻⁵–10⁻² mbar.

Preferred values

Parameter	Value	T/K
γ	$\leq 5 \times 10^{-6}$	190–250
<i>Reliability</i>		
$\Delta \log(\gamma)$	± 1.0	190–250

Comments on preferred values

There is no measurable uptake on ice surfaces or frozen sulfuric acid solutions at 195–243 K. Bartels-Rausch et al. (2002) used a chromatographic retention technique to measure the adsorption enthalpies of various NO_x species onto ice spheres. Thermo-chromatography theory was used to extract the enthalpies of adsorption from the data. The adsorption enthalpy for NO was –20 kJ/mol. This small adsorption enthalpy is consistent with the experiments of Saastad et al. (1993) in which no measurable loss of NO to the ice surface was observed. Adsorption entropies were also estimated using two different standard states.

References

- Bartels-Rausch, T., Eichler, B., Zimmermann, P., Gäggler, H. W., and Ammann, M.: Atmos. Chem. Phys., 2, 235, 2002.
- Leu, M.-T.: Geophys. Res. Lett., 15, 851, 1988a.
- Leu, M.-T.: Geophys. Res. Lett., 15, 17, 1988b.
- Saastad, O. W., Ellermann, T., and Nielsen, C. J.: Geophys. Res. Lett., 20, 1191, 1993.

V.A1.8

NO₂ + ice

Experimental data

Parameter	Temp./K	Reference	Technique/Comments
γ_{ss}			
$\gamma_{ss} < 1.0 \times 10^{-4}$	195	Leu, 1988	CWFT-MS (a)
$\gamma_{ss} < 5.0 \times 10^{-6}$	193-243	Saastad et al., 1993	Static-MS (b)
K_{linC} (cm)			
$3.07 \times 10^{-9} \exp(2646/T)$	140–150 K	Bartels-Rausch et al., 2002	PBFT-RC (c)

Comments

- (a) Uptake experiment in an ice-coated flow tube coupled to electron-impact MS. The ice film was deposited from water vapor.
- (b) Measurement of the total pressure drop in a static system over bulk ice and frozen 70% H₂SO₄-H₂O monitored by MS.
- (c) NO₂-ice partitioning coefficients derived from packed ice bed (PC) experiments using radioactively labelled NO₂ at concentrations of 3 ppbv and below. Ice prepared from freezing water drops in liquid N₂ and then annealing at 258 K for 12 h. The technique involves observing the migration of radioactively labelled NO₂ molecules along the temperature gradient established along the flow tube. The adsorption enthalpy of -22 ± 1 kJ mol⁻¹ was derived by solving a migration model of linear gas chromatography and assuming a value of the adsorption entropy of -39 J K⁻¹ mol⁻¹ (based on $A_0 = 6.7 \times 10^6$ m²) based on theoretical arguments. The tabulated K_{linC} was derived from these values. Due to the very low partitioning coefficient of NO₂, adsorption could only be observed at very low temperature, i.e. between 140 and 150 K. From the absence of a concentration dependence, the authors conclude that N₂O₄ was not involved in the adsorption process that governed partitioning.

Preferred values

Parameter	Value	T/K
K_{linC}/cm	$3.07 \times 10^{-9} \exp(2646/T)$	190–250
<i>Reliability</i>		
$\Delta \log(\gamma)$	± 1.0	190–250
$\Delta(E/R) = \pm 100$ K		

Comments on preferred values

Due to the low interaction energy, the adsorption kinetics or equilibrium of NO₂ can not be observed at relevant temperatures. The partitioning derived from Bartels-Rausch et al. (2002) is tied to the observation at 144 K. Therefore the extrapolation to higher temperature is somewhat problematic and should be treated with caution as the properties of the ice surface may change towards higher temperatures. The low interaction energy has been confirmed using surface spectroscopy techniques (Ozensoy et al., 2006; Wang and Koel, 1999; Rieley et al., 1996). NO₂ presumably undergoes surface hydrolysis (self reaction) to form nitrite and nitrate or HONO and HNO₃, respectively, as confirmed by the latter studies. However, the kinetics and its extent have not been quantified so far, even less so under atmospheric conditions.

References

- Leu, M.-T.: *Geophys. Res. Lett.*, 15, 851, 1988.
- Saastad, O. W., Ellermann, T., and Nielsen, C. J.: *Geophys. Res. Lett.*, 20, 1191, 1993.
- Wang, J. and Koel, B. E.: *Surf. Science*, 436, 15–28, 1999.
- Rieley, H., McMurray, D. P., and Haq, S.: *J. Chem. Soc. Faraday Trans*, 92, 933–939, 1996.
- Ozensoy, E., Peden, C. H. F., and Szanyi, J.: *J. Phys. Chem. B.*, 110, 8025–8034, 2006.
- Bartels-Rausch, T., Eichler, B., Zimmermann, P., Gäggeler, H. W., and Ammann, M.: *Atmos. Chem. Phys.*, 2, 235–247, 2002.

V.A1.9**NO₃ + ice****Experimental data**

Parameter	Temp./K	Reference	Technique/Comments
γ <1.0×10 ⁻³	170–200	Fenter and Rossi, 1997	Knudsen-LIF (a)

Comments

- (a) Ice surface prepared by vapour deposition or freezing a liquid sample. The geometric surface area was used to calculate the uptake coefficient, γ . NO₃ was generated by thermal decomposition of N₂O₅ and detected following excitation at 662 nm. After correction for loss of NO₃ to the walls of the Knudsen reactor, no residual uptake to the ice surface was detectable, hence the upper limit to γ .

Preferred values

Parameter	Value	T/K
γ	<1×10 ⁻³	170–200
<i>Reliability</i>		
$\Delta\log(\gamma)$	±0.5	170–200

Comments on preferred values

There is only one study of the interaction of NO₃ with ice surfaces, (Fenter and Rossi, 1997) which reported an upper limit to the uptake coefficient. This result is the basis of the recommendation.

References

Fenter, F. F. and Rossi, M. J.: J. Phys. Chem. A., 101, 4110–4113, 1997.

V.A1.10**NH₃ + ice****Experimental data**

Parameter	Temp./K	Reference	Technique/Comments
γ_{ss} (3.8 ± 1.4) $\times 10^{-4}$	189.9 \pm 0.5	Jin and Chu, 2007	CWFT-MS (a)

Comments

- (a) The ice film ($\approx 3.5 \mu\text{m}$ thick) was condensed from the vapour phase at the experimental temperature. Uptake of NH₃ ($p(\text{NH}_3) = 5.3 \times 10^{-7} - 2.9 \times 10^{-6}$ mbar) was continuous, irreversible and independent of the NH₃ partial pressure. The uptake coefficients varied with ice film thickness and were corrected for pore diffusion.

Preferred values

Parameter	Value	T/K
γ	4×10^{-4}	190–200
<i>Reliability</i>		
$\Delta \log(\gamma)$	± 0.5	190–200

Comments on preferred values

Jin and Chu (2007) report continuous and irreversible uptake of NH₃ onto ice films, with the amount taken up exceeding monolayer coverage by more than a factor of 10, thus indicating possible formation of stable hydrates or solid-liquid phase change under the conditions employed. Based on an estimated diffusion coefficient on ice, Jin and Chu (2007) suggest that diffusion into their ice cannot account for the continuous uptake. This contrasts with the conclusions of Hoog et al. (2007), who analysed the NH₄⁺ content (by ion chromatography subsequent to melting) of ice crystals that had been exposed to NH₃ at significantly higher concentrations ($\approx 6 - 100 \times 10^{-4}$ mbar).

Theoretical work suggests that NH₃ molecules remaining in the gas-phase are energetically more favourable than incorporation into the bulk ice for single NH₃ at infinite dilution. An adsorption free energy of 11 kJ mol⁻¹ has been calculated (Pártay et al., 2007). Spectroscopic evidence for hydrogen bonded NH₃ on ice has been obtained at 38 K, with no evidence for thermal desorption up to ≈ 140 K. Evidence for ionisation of NH₃ to NH₄⁺ and subsequent transfer to the bulk of the ice surface was however obtained at these temperatures (Ogasawara et al., 2000) and would presumably also take place at higher temperatures.

References

- Hoog, I., Mitra, S. K., Diehl, K., and Borrmann, S.: J. Atmos. Chem. 57, 73–84, 2007.
 Jin, R. and Chu, L. T.: J. Phys. Chem. A., 111, 7833, 2007.
 Ogasawara, H., Horimoto, N., and Kawai, M.: J. Chem. Phys., 112, 8229–8232, 2000.
 Pártay, L. B., Jedlovsky, P., Hoang, P. N. M., Picaud, S., and Mezei, M.: J. Phys. Chem. C., 111, 9407–9416, 2007.

V.A1.11

HONO + ice → products

Experimental data

Parameter	Temp./K	Reference	Technique/Comments
γ_0, γ_{ss}			
$\gamma_0=1 \times 10^{-3}$	180–200	Fenter and Rossi, 1996	Kn-MS (a)
$\gamma_{ss}=1 \times 10^{-3}$	190	Seisel and Rossi, 1997	Kn-MS (a)
$\gamma_0=3.7 \times 10^{-3}$	178	Chu et al., 2000	CWFT-MS (b)
$\gamma_0=1.6 \times 10^{-3}$	192		
$\gamma_0=6.4 \times 10^{-4}$	200		
K_{linC} (cm)			
$1.0 \times 10^{-5} \exp(3843/T)$	170–205	Chu et al., 2000	CWFT-MS (b)
$2.1 \times 10^{-9} \exp(3849/T)$	170–200	Bartels-Rausch et al., 2002	PBFT-RC (c)
$7.4 \times 10^{-9} \exp(5400/T)$	213–253	Kerbrat et al., 2010	PBFT-RC (d)

Comments

- (a) Ice prepared both by vapour-phase deposition and by cooling of a sample of distilled water. HONO prepared from use of acidified NaNO_2 solution, with NO and NO_2 as major contaminants. Saturation of the uptake takes place after deposition of 3% of a monolayer (3×10^{14} molecule cm^{-2}) at a HONO concentration of about 10^{12} molecule cm^{-3} in the reactor. The uptake appears to be reversible.
- (b) Uptake experiment using a laminar flow tube equipped with mass spectrometric detection at 0.5 Torr of He. The ice film (about 30 μm thick) was prepared by vapour deposition. The HONO concentration was measured using IR absorption spectroscopy upstream of the flow tube and was roughly 10% of the total associated NO_x inflow. The tabulated γ_0 values refer to the geometric surface area of the ice film. The correction using pore diffusion theory would reduce them by a factor of 20 to 50. The initial uptake coefficient shows a pronounced negative temperature dependence with a $\Delta E/R$ value of 27.2 kJ mol^{-1} , which was ascribed to a precursor mediated uptake process. The surface coverages reported at equilibrium range from 10^{13} to 3×10^{14} molecule cm^{-2} (geometric surface area) in the range from 205 to 174 K at a HONO pressure of 2.5×10^{-7} mbar. No pressure dependence given. An adsorption enthalpy of $-33.9 \pm 8.8 \text{ kJ mol}^{-1}$ was derived. The tabulated K_{linC} was derived from the reported surface coverages divided by the gas phase pressure and fitted versus $1/T$. The intercept leads to a standard adsorption entropy of 80.7 $\text{J mol}^{-1} \text{ K}^{-1}$.
- (c) HONO-ice partitioning coefficients derived from packed ice bed (PB) experiments at atmospheric pressure using radioactively labelled HONO at concentrations of 3 ppbv and below. Ice prepared from freezing water drops 0.5 mm in diameter in liquid N_2 and then annealing at 258 K during at least 12 h. HONO was prepared by converting NO_2 quantitatively to HONO on a solid organic reductant. NO was the main contaminant (in similar amounts). The adsorption enthalpy of $-32 \pm 2 \text{ kJ/mol}$ was derived by solving a migration model of linear gas chromatography and assuming a value of the adsorption entropy of 42 $\text{J K}^{-1} \text{ mol}^{-1}$ (based on $A_0=6.7 \times 10^{-6} \text{ m}^2$) based on theoretical arguments. The tabulated K_{linC} was derived from these values.
- (d) Experiments were performed in an atmospheric pressure flow tube filled with 0.5mm diameter ice spheres. The ice was prepared by freezing water in liquid N_2 and then annealing at 258 K. Ice spheres were sieved. No effect of changing ice particle diameter to 0.8mm was observed. HONO was produced from NO_2 partially labelled with the radioactive isotope ^{13}N by reaction with a solid organic reductant. Migration profiles of labelled HONO molecules along the flow tube were measured using gamma detectors, non-labelled HONO was detected downstream of the flow tube. The HONO breakthrough curves showed strong tailing, i.e., the HONO signal never reached the initial concentration again, interpreted as a slow diffusive uptake into the interior of the polycrystalline ice spheres. Breakthrough curves were used to extract a value for $H(D)^{1/2}=1.6 \times 10^{-2} \text{ m s}^{-1/2}$ that allows parameterization of this diffusive uptake. This was then used to correct the steady state partition coefficient derived from the migration profiles of the labelled molecules to obtain the values for K_{linC} presented in the table in parameterized form.

Preferred values

Parameter	Value	T/K
α_s	0.02	180–220
$K_{\text{linC}}/\text{cm}$	$1.5 \times 10^{-8} \exp(5200/T)$	180–250
$N_{\text{max}}/\text{cm}^{-2}$	3×10^{14}	180–220
<i>Reliability</i>		
$\Delta \log \alpha_s$	± 0.3	180–220
$\Delta(E/R)/\text{K}$	± 100	180–220
$\Delta \log N_{\text{max}}/\text{cm}^{-2}$	± 0.1	180–220

Comments on preferred values

At low temperature, the rate of uptake of HONO is strongly time dependent and rapidly drops to zero, indicating saturation of the surface. The study by Fenter and Rossi (1996) was performed on frozen aqueous solutions, while that by Chu et al. (2000) was performed on vapour deposited ice. When referred to the geometric ice surface area, the initial uptake coefficients derived in both studies agree, while in case of correction for pore diffusion the values by Chu et al. (2000) are an order of magnitude lower. The times needed to saturate the surface observed in both studies are consistent with a value of $\alpha_s=0.02$. Then, the initial uptake kinetics may be described by:

$$\alpha_s e^{-Bt}$$

with

$$B = \frac{\alpha_s \bar{c}}{4} \left(\frac{[\text{HONO}]_g}{N_{\text{max}}} + \frac{1}{K_{\text{linC}}^{\text{HONO}}} \right)$$

It is likely that the effective time resolution was not sufficient to resolve α_s by the initial uptake coefficient due to adsorption equilibrium as has been shown for other flow tube studies, which may also have an effect on the temperature dependence.

At higher temperature, Kerbrat et al. (2010) report a significant longterm contribution to uptake suggested to be driven by slow diffusion into the interior of the polycrystalline ice matrix used in their experiment. They corrected the data to obtain a surface partition coefficient and an effective solubility in the bulk condensed phase. However, the relevance of bulk uptake remains uncertain as long as the reservoirs into which diffusion occurs are neither identified nor quantified for ice of direct atmospheric relevance. We therefore only recommend parameters for partitioning of HONO to the ice surface. Chu et al. (2000) report surface coverage as a function of temperature that is consistent with the higher temperature data by Kerbrat et al. (2010). The data indicate saturation at about 3×10^{14} molecules cm^{-2} . We therefore neglect the two lowest temperature data points of Chu et al. and combine the others with those by Kerbrat et al. (2010) to obtain the temperature dependence of K_{linC} . The partitioning coefficients reported by Bartels-Rausch et al. (2002) heavily rely on an estimate for the adsorption entropy, which is highly uncertain as it strongly depends on an assumed adsorption mechanism. We therefore do not include these data in the recommendation for K_{linC} . The adsorption enthalpy related to the recommended parameterization is 43 kJ/mol, which is close to the enthalpy of solvation of HONO in water of 41 kJ/mol, as reported by Park and Lee (1988), indicating hydration of the HONO molecule at the ice surface.

References

- Bartels-Rausch, T., Eichler, B., Zimmermann, P., Gäggeler, H. W., and Ammann, M.: *Atmos. Chem., Phys.* 2, 235–247, 2002.
 Chu, L., Diao, G., and Chu, L. T.: *J. Phys. Chem. A.*, 104, 3150, 2000.
 Fenter, F. F. and Rossi, M. J.: *J. Phys. Chem.*, 100, 13765, 1996.
 Kerbrat, M., Huthwelker, T., Gaeggeler, H. W., and Ammann, M.: *J. Phys. Chem. C*, 114, 2208–2219, 2010.
 Park, J. Y. and Lee, Y. N.: *J. Phys. Chem.* 92, 6294–6302, 1988.

V.A1.12

HNO₃ + ice

Experimental data

Parameter	Temp./K	Reference	Technique/Comments
γ_0, γ_{ss}			
$\gamma_0 > 0.2$	197	Leu, 1988	CWFT-MS (a)
$\gamma_0 > 0.3$	191–200	Hanson, 1992	CWFT-MS (b)
$\gamma_0 > 0.2$	208–248	Abatt, 1997	CWFT-MS (c)
$\gamma_0 > 5 \times 10^{-3}$	220–223	Zondlo et al., 1997	Knudsen (d)
$\gamma_{ss} = (2 \pm 1) \times 10^{-4}$			
$\gamma = 0.3$	200	Seisel et al., 1998	Knudsen (e)
$\gamma = 0.27 \pm 0.08$	180	Aguzzi and Rossi, 2001	Knudsen (f)
0.25 ± 0.08	190		
0.17 ± 0.08	200		
0.09 ± 0.03	210		
$\gamma = (3.3 \pm 0.6) \times 10^{-2}$	214	Hynes et al., 2002	CWFT-MS (g)
1.2×10^{-2}	218		
6.0×10^{-3}	235		
$\gamma_0 = 7 \times 10^{-3}$	209	Hudson et al., 2002	Knudsen (h)
$\gamma_0 = 3 \times 10^{-3}$	220		
K_{inC}/cm			
4.64×10^4 *	218	Abbatt, 1997	CWFT-MS (c)
2.00×10^4 *	228		
0.83×10^4 *	238		
0.32×10^4 *	248		
$(1.06 \pm 0.16) \times 10^3$ (2 site model)	218	Hynes et al., 2002	CWFT-MS (g)
$(0.48 \pm 0.072) \times 10^3$ (2 site model)	228		
$(10.05 \pm 3.22) \times 10^4$	214	Ullerstam et al., 2005	CWFT-MS (i)
$(5.53 \pm 1.93) \times 10^4$	229		
$(1.74 \pm 0.51) \times 10^4$	239		
10.26×10^4	214	Cox et al., 2005	CWFT-MS (j)
3.91×10^{-10}	229		
1.75×10^{-10}	239		

*calculated in this evaluation; see comments

Comments

- (a) Fast flow tube reactor with MS detection. Ice condensed from the vapour phase onto the cold flow tube. γ corrected for gas diffusion using estimated diffusion coefficients.
- (b) Fast flow tube reactor with CIMS detection of HNO₃ at $p(\text{HNO}_3) = (1-4) \times 10^{-7}$ mbar. Ice condensed from the vapour phase onto the cold flow tube. γ corrected for gas diffusion using estimated diffusion coefficients. Evidence for time-dependent uptake due to surface saturation.
- (c) Coated-wall flow tube with MS detection. Flow tube pressure=1.3 mbar, He carrier gas. The ice surfaces were prepared by wetting the inner wall of a tube which was inserted into the cooled flow tube resulting in a smooth ice film. Initially, HNO₃ is taken up rapidly independent of the HNO₃ partial pressure with γ as cited. Uptake then saturates at a surface coverage of $N_{\text{max}} \sim 0.2$ to 0.3 monolayers. Subsequently, small rates of uptake following a $T^{0.5}$ rate law were observed corresponding to diffusional loss processes on the ice. The heterogeneous interaction is nearly irreversible as only about 25% of the quantity of HNO₃ was recovered after the HNO₃ flow was halted. The formation of an amorphous albeit stable

surface layer of $\text{HNO}_3\text{-H}_2\text{O}$ is postulated as the HNO_3 partial pressures are well below those for formation of stable hydrates. The integrated amount of HNO_3 adsorbed was weakly dependent on $p(\text{HNO}_3)$ in the range $(1.7\text{--}41)\times 10^{-7}$ mbar at 218 K, and increased with decreasing temperature at approximately constant $p(\text{HNO}_3)$ (6.5 to 9.0×10^{-7} mbar). The cited Langmuir equilibrium constants were calculated from the reported equilibrium surface coverages using a single site model with N_{max} assumed $=2.7\times 10^{14}$ molecule cm^{-2} .

- (d) Two-chamber flow reactor equipped with FTIR reflection-absorption as well as MS detection. The flow reactor configuration only allowed uptake coefficients lower than 5×10^{-3} to be measured. At low $p(\text{HNO}_3)$, uptake partially saturates after deposition of approximately one monolayer and reaches steady state. Above $\sim 2.7\times 10^{-5}$ mbar of HNO_3 uptake occurs continually at γ_0 without signs of saturation. The former uptake regime is interpreted as leading to an amorphous mixture of $\text{HNO}_3\text{-H}_2\text{O}$, whereas the continuous uptake leads to a supercooled liquid mixture of a typical composition of 3:1 to 4:1 $\text{H}_2\text{O-HNO}_3$.
- (e) Uptake experiment in a Knudsen flow reactor equipped with a residual gas MS and simultaneous grazing-incidence FTIR reflection-absorption spectrometry.
- (f) Uptake experiment in a Knudsen flow reactor on ice films condensed from the vapour phase and on frozen bulk H_2O . Pulsed valve and steady state uptake experiments resulted in identical values for γ after correction for the interaction of HNO_3 with the Teflon coating. γ shows a strong negative temperature dependence for $T\geq 195$ K with $E_a=-28\pm 4$ kJ mol^{-1} and a constant value of 0.3 below 195 K.
- (g) Coated wall flow tube study at 2.3 mbar He using MS detection of HNO_3 . $p(\text{HNO}_3)$ was in the range $(0.4\text{--}2.7)\times 10^{-6}$ mbar and led to time-dependent uptake converging to steady-state conditions after typically 200 s of uptake. γ for HNO_3 uptake was unaffected by the presence of HCl in comparable quantities at 218 K. Surface coverages were determined from integrated uptake prior to saturation. They showed little variation with $p(\text{HNO}_3)$ over the range studied and maximum surface coverage was 3×10^{14} molecule cm^{-2} at 218 K and 228 K. Partition coefficient was determined using 2-site Langmuir isotherm fit to experimental data at 218 and 228 K, with $N_{\text{max}}=10^{15}$ molecule cm^{-2} . The enthalpy of HNO_3 adsorption onto ice was $-(54.0\pm 2.6)$ kJ/mol, evaluated using the Van't Hoff equation and the values of K_{linC} cited.
- (h) Uptake experiment in a Knudsen flow reactor equipped with simultaneous reflection-I.R. absorption spectroscopy and MS. Surface area of vapour deposited ice, measured by BET method using butane adsorbent gas, was a factor of 2.27 larger than the geometric area of the base surface. γ values were time dependent in the ice stability region at low $p(\text{HNO}_3)$. Initial values cited for $p(\text{HNO}_3)\sim 1\times 10^{-6}$ mbar. Surface coverages were determined from integrated uptake prior to saturation, and showed a strong T dependence below 214 K.
- (i) Coated wall flow tube with $p(\text{HNO}_3)$ in range $10^{-8}\text{--}10^{-6}$ hPa detected using CIMS. Ice films formed by freezing liquid water. At $T>214$ K surface coverages measured in both unsaturated regime at low partial pressure and close to saturation. Maximum surface coverage was $(2.1\text{--}2.7)\times 10^{14}$ molecule cm^{-2} independent of temperature. The uptake is nearly irreversible as only 10–40% of the quantity of HNO_3 desorbed after the HNO_3 exposure was halted. At 200 K continuous uptakes were observed without saturation and little desorption. Partition coefficients were determined using single-site Langmuir isotherm fit to experimental data at 214, 229 and 239 K, giving the expression: $K_{\text{LangP}}(\text{hPa}^{-1})=-(5.1\pm 0.4)\times 10^5 T+(12.3\pm 0.9)\times 10^7$. The enthalpy of HNO_3 adsorption onto ice was $-(30.3\pm 6)$ kJ/mol, evaluated using the Van't Hoff equation, and similar values were obtained from T -dependence of integrated desorption.
- (j) Model of gas flow and surface exchange in CWFT with a single site Langmuir mechanism. The model was used to reanalyse experimental results from Ullerstam et al. (see note (i)). The experimental time-dependent uptake profiles were best fitted with an additional process involving diffusion of the adsorbed molecules into the ice film. The model allowed true surface coverages to be distinguished from total uptake including transfer to the bulk, leading to more accurate estimates of the Langmuir constant, K_{eq} , for surface adsorption. At $T\geq 229$ K, K_{eq} decreased by up to 30% as $p(\text{HNO}_3)$ decreased from the saturated region; the cited values are midrange.

Preferred values

Parameter	Value	<i>T</i> /K
α_s	0.2	190–240
N_{\max} /molecule cm ⁻²	2.7×10^{14}	214–240
K_{linC} /cm	$7.5 \times 10^{-5} \exp(4585/T)$	214–240
<i>Reliability</i>		
$\Delta \log \alpha_s$	± 0.3	190–240
$\Delta \log K_{\text{linC}}$ /cm	± 0.3	228
$\Delta(E/R)/K$	± 700	

Comments on preferred values

There have been many experimental studies of nitric acid–ice interaction but mostly at temperatures and concentrations corresponding to stability regions for either hydrate or supercooled HNO₃/H₂O solutions. Under these conditions at $T < 210$ K uptake is continuous and irreversible. At higher temperatures in the “ice stability” region, uptake rate is time dependent, declining from an initial rapid uptake ($\gamma > 0.2$) to very slow uptake when the surface is saturated at $N_{\max} \sim 3.0 \times 10^{14}$ molecules cm⁻². Surface coverages at low $p(\text{HNO}_3)$ on ice films in the temperature range 210–240 K have been quoted in a number of studies (Abbatt, 1997; Hudson et al., 2002; Hynes et al., 2002; Ullerstam et al., 2005; Cox et al., 2005; Arora et al., 1999), who measured HNO₃ uptake on ice particles. There is good agreement in the measured uptakes near saturation in the CWFT studies. For example, for a temperature of 228 K, a gas-phase concentration of 3×10^{10} molecule cm⁻³ of HNO₃ results in equilibrium surface coverages (N_{\max}) of 1.9×10^{14} molecule cm⁻² (Abbatt, 1997), 1.6×10^{14} molecules cm⁻² (Hynes et al., 2002), 2.4×10^{14} molecules cm⁻² (Ullerstam et al., 2005). The Knudsen cell study of Hudson et al. (2002) shows much lower saturated coverages at 220 K and a huge increase with decreasing temperature.

Values of the maximum surface coverage, N_{\max} , vary between $1.2 \pm 0.2 \times 10^{14}$ molecules cm⁻² (230 K, Arora et al., 1999), $(2.1\text{--}2.7) \times 10^{14}$ molecule cm⁻² (214–239 K, Ullerstam et al., 2005), and 3×10^{14} molecule cm⁻² (Hynes et al., 2002). These values are consistent with values for other traces gases on similar ice surfaces, and with molecular dynamics calculations (Abbatt, 2003).

Partition coefficients in the table were derived using a single site Langmuir model for the data reported by the Abbatt group and a 2-site model for the Hynes data, who also used a high value of $N_{\max} = 10^{15}$ cm⁻² in their fit. Ullerstam et al. showed that the 2-site model failed when tested against data at low $p(\text{HNO}_3)$. Variable values of the derived equilibrium partition coefficients and adsorption enthalpy, ΔH_{ads} , result from different models used to interpret the results. Bartels-Rausch et al. reported $\Delta H_{\text{ads}} = -44$ kJ mol⁻¹ from chromatographic measurements of HNO₃ retention in a packed ice column, which lies midway between the other reported values.

The preferred partitioning coefficient is based on the data of Ullerstam et al., 2005, using the refined analysis given in the study of Cox et al., 2005. This may be used in the full form of the single site Langmuir isotherm:

$$\theta = \frac{N_{\max} K_{\text{LangC}}[\text{HNO}_3]}{1 + K_{\text{LangC}}[\text{HNO}_3]}$$

together with the recommended N_{\max} value, based on the values given by Ullerstam, 2005, to provide a simple parameterisation appropriate for equilibrium surface coverages at concentrations up to $\sim 5 \times 10^{-7}$ mbar in the given temperature range. At lower temperatures and higher $p(\text{HNO}_3)$, near the phase boundary for thermodynamic stability of hydrates or supercooled HNO₃/H₂O solutions, uptake is continuous with no saturation and the Langmuir model cannot be used. Note however that all flow tube studies report that the adsorption of HNO₃ to ice is not completely reversible, even in the HNO₃/ice stability regime. Surface spectroscopic investigations (Zondlo et al., 1997; Hudson et al., 2002) suggest that adsorbed HNO₃ is solvated to form nitrate ions, suggesting that adsorbed molecules enter the surface layer of the ice film.

Measurements of the uptake coefficient are problematic in CWFT experiments, due to the difficulty in separating adsorption and desorption kinetics and to diffusion limitations, which will result in determination of a lower limit. Knudsen cell measurements of γ_0 indicate a surface accommodation coefficient of ~ 0.3 at $T < 200$ K. The uptake coefficient decreases with time as increasing amounts of HNO₃ are adsorbed in the ice film, and most measurements are affected by this. The recommended value for α_s is based on the measurements of Abbatt (1997), Hanson (1992) and Agussi and Rossi (2001).

Ullerstam and Abbatt (2005) showed that on growing ice, the long term uptake of nitric acid is significantly enhanced compared to an experiment performed at equilibrium, i.e. at 100% relative humidity (RH) with respect to ice. The fraction of HNO_3 that is deposited onto the growing ice surface is independent of the growth rate and may be driven by the solubility of the nitric acid in the growing ice film rather than by condensation kinetics alone.

References

- Abbatt, J. P. D.: *Geophys. Res. Lett.*, 24, 1479, 1997.
- Abbatt, J. P. D.: *Chem. Rev.*, 103, 4783, 2003.
- Aguzzi, A. and Rossi, M. J.: *Phys. Chem. Chem. Phys.*, 3, 3707, 2001.
- Bartels-Rausch, T., Eichler, B., Zimmermann, P., Gäggeler, H. W., and Ammann, M.: *Atm. Chem. Phys.*, 2, 235, 2002.
- Cox, R. A., Fernandez, M. A., Symington, A., Ullerstam, M., and Abbatt, J. P. D.: *Phys. Chem. Chem. Phys.*, 7, 3434, 2005.
- Hanson, D. R.: *J. Geophys. Res. Lett.*, 19, 2063, 1992.
- Hudson, P. K., Shilling, J. E., Tolbert, M. A., and Toon, O. B.: *J. Phys. Chem. A*, 106, 9874–9882, 2002.
- Hynes, R. G., Fernandez, M. A., and Cox, R. A.: *J. Geophys. Res.*, 107, 4797, doi:10.1029/2001JD001557, 2002.
- Leu, M.-T.: *Geophys. Res. Lett.*, 15, 17, 1988.
- Picaud, S., Toubin, C., and Girardet, C.: *Surface Science*, 454, 178–182, 2000.
- Seisel, S., Flückiger, B., and Rossi, M. J.: *Ber. Bunsenges. Phys. Chem. A*, 102, 811, 1998.
- Ullerstam, M., Thornberry, T., and Abbatt, J. P. D.: *Faraday Discuss.*, 130, 211, 2005.
- Ullerstam, M. and Abbatt, J. P. D.: *Phys. Chem. Chem. Phys.*, 7, 3596, 2005.
- Zondlo, M. A., Barone, S. B., and Tolbert, M. A.: *Geophys. Res. Lett.*, 24, 1391, 1997.

V.A1.13**HO₂NO₂ + ice****Experimental data**

Parameter	Temp./K	Reference	Technique/Comments
γ_{ss} 0.15±0.10	193	Li et al., 1996	CWFT-MS (a)

Comments

- (a) The ice was prepared by vapour deposition, resulting in films between 13 and 160 μm thick. $p(\text{HNO}_4)$ was varied between 1.6×10^{-5} mbar and 6×10^{-4} mbar. HNO_4 was produced by mixing NO_2BF_4 with H_2O_2 at 273 K. H_2O_2 , the main impurity, was partially retained in a cold trap at 258 K. During the experiments, H_2O_2 , HNO_3 and NO_2 were less than 20% of HNO_4 . The HNO_3 impurity was quantitatively adsorbed onto the ice film and therefore did not interfere with PNA detection. Saturation of the uptake on ice was observed at >100 monolayers. Evaporation of PNA and HNO_3 was observed in temperature programmed desorption experiments. HNO_3 was obviously originating from uptake of HNO_3 as an impurity from the PNA source. It was concluded that no decomposition of PNA occurs on ice.

Preferred values

Parameter	Value	<i>T/K</i>
γ	no recommendation	
<i>Reliability</i>		
$\Delta \log(\gamma)$	undetermined	

Comments on preferred values

The interaction of PNA with ice seems to be irreversible in the pressure range above 10^{-5} mbar used in the single study by Li et al. (1996). The uptake curves show strong tailing, and the MS signal does not return to the original value observed in absence of ice, even after uptake of more than 100 formal monolayers. The authors argue that under these conditions, PNA hydrates may form (crystalline or amorphous solid), but that the temperature was well below the hydrate/ice/liquid eutectic. However the substantial amounts of HNO_3 impurity which partitioned to the ice surface would undoubtedly have led to surface melting, which accounts for the non-reversible uptake. The observed uptake is not likely to be representative of atmospheric conditions, where PNA levels are orders of magnitude lower. We therefore do not recommend a partitioning coefficient or an uptake coefficient.

References

Li, Z., Friedl, R. R., Moore, S. B., and Sander, S. P.: J. Geophys. Res., 101, 6795, 1996.

V.A1.14

N₂O₅ + ice

Experimental data

Parameter	Temp./K	Reference	Technique/Comments
γ, γ_{ss}			
$\gamma=0.028 \pm 0.011$	195	Leu, 1988	CWFT-MS (a)
$\gamma > 7 \times 10^{-3}$	185	Tolbert et al., 1988	Knudsen-MS (b)
$\gamma = 0.034 \pm 0.008$	188	Quinlan et al., 1990	Knudsen-MS (c)
$\gamma = 0.023 \pm 0.008$			
$\gamma = 0.024 \pm 0.007$	201	Hanson and Ravishankara, 1991	CWFT-CIMS (d)
$\gamma = 0.01-0.02$	191	Hanson and Ravishankara, 1992, 1993	CWFT-CIMS (e)
$\gamma = 0.02 \pm 0.002$	200	Seisel et al., 1998	Knudsen-MS (f)
$\gamma_{ss} = (7 \pm 3) \times 10^{-4}$	185	Zondlo et al., 1998	MS/FTIR (g)

Comments

- (a) Flow reactor at 0.36–0.67 mbar. The ice film was made by vapour deposition. N₂O₅ (initial concentration $\approx 1 \times 10^{13}$ molecule cm⁻³) detected as its NO₂⁺ ion-fragment. HNO₃ found to build up on the surface. γ calculated using geometric ice surface area.
- (b) N₂O₅ (initial concentration $\approx 1 \times 10^{13}$ molecule cm⁻³) detected as its NO⁺ and NO₂⁺ ion-fragments. Surface adsorbed HNO₃ (reaction product) was detected by thermal desorption spectrometry. Coincidence of fragment ions from HNO₃ (reaction product) and N₂O₅ enabled only an upper limit to the uptake coefficient (calculated using geometric ice surface area) to be determined.
- (c) N₂O₅ (initial concentration $\approx 1 \times 10^{13}$ molecule cm⁻³) detected as its NO⁺ and NO₂⁺ ion-fragments. Gas-phase HNO₃ reaction product was detected following thermal desorption, TD, as its HNO₃⁺, NO⁺ and NO₂⁺ ion-fragments. γ (calculated using geometric ice surface area) showed a pronounced time dependence, maximising after several seconds of exposure, and then decreasing again. The value of γ quoted in the Table is the maximum value observed. The two values quoted represent results obtained on ice made from freezing a bulk solution (0.034 ± 0.008) or vapour deposited ice (0.023 ± 0.008). The TD yield of HNO₃ was found to match the amount of N₂O₅ lost to the surface ($3-7 \times 10^{16}$ cm⁻²), suggesting that the uptake is purely reactive.
- (d) Low initial N₂O₅ concentration (10⁹–10¹⁰ molecule cm⁻³) measured using I⁻ chemi-ionisation. The 7–15 μm thick ice film was made by vapour deposition. Deactivation of the surface was seen to take place during exposures of several minutes duration. γ was calculated from first-order decay constants at low exposure times, using the geometric surface area of the ice.
- (e) Same experimental procedure as (d), but with the ice film thickness varied between ≈ 1 and 40 μm. γ was found to vary between ≈ 0.01 and 0.02.
- (f) The ice surface was formed by either vapour deposition or by freezing liquid water. The N₂O₅ concentration was 1.5×10^{11} molecule cm⁻³.
- (g) The ice surface was formed by vapour deposition, [N₂O₅] was varied between $\approx 2 \times 10^{10}$ and 3×10^{11} molecule cm⁻³. The uptake coefficient reported represents a steady-state value, presumably for an HNO₃ contaminated ice surface. Surface analysis was performed using reflection-absorption infra-red spectroscopy and revealed the presence of H₃O⁺ and NO₃⁻ ions in an H₂O/HNO₃ amorphous solution at 185 K and the loss of crystalline structure of the ice.

Preferred values

Parameter	Value	T/K
γ	0.02	190–200
<i>Reliability</i>		
$\Delta\log\gamma$	± 0.15	190–200

Comments on preferred values

The preferred value of γ is taken from Hanson and Ravishankara (1991, 1992, 1993) who used very low N_2O_5 concentrations, and applies to a pure (i.e. non passivated) ice surface. The less detailed study of Seisel et al. (1998) at 200 K is in accord with this recommendation. Hanson and Ravishankara (1991) observed deactivation of the surface after a few minutes of exposure to N_2O_5 , whereas Quinlan et al. (1990) observed increasing reactivity with time. This is most likely due to the use by Quinlan et al. (1990) of high concentrations of N_2O_5 at the surface, causing surface melting by HNO_3 .

Evidence for an efficient hydrolysis of N_2O_5 to HNO_3 (probably present mainly in ionised form at the surface) is provided by the observation of surface deactivation for N_2O_5 uptake (Hanson and Ravishankara, 1991), thermal desorption experiments (Quinlan et al., 1990) and infrared surface analysis of ions such as NO_3^- and H_3O^+ (Zondlo et al., 1998; Horn et al., 1994; Koch et al., 1997). At appropriate combinations of N_2O_5 concentration and temperature, NAT is formed (Hanson and Ravishankara, 1991).

References

- Hanson, D. R. and Ravishankara, A. R.: J. Geophys. Res., 96, 5081–5090, 1991.
Hanson, D. R. and Ravishankara, A. R.: J. Phys. Chem., 96, 2682–2691, 1992.
Hanson, D. R. and Ravishankara, A. R.: J. Phys. Chem., 97, 2802–2803, 1993.
Horn, A. B., Koch, T., Chesters, M. A., McCoustra, M. R. S., and Sodeau, J. R. S.: J. Phys. Chem., 98, 946–951, 1994.
Koch, T. G., Banham, S. F., Sodeau, J. R., Horn, A. B., McCoustra, M. R. S., and Chesters, M. A.: J. Geophys. Res., 102, 1513–1522, 1997.
Leu, M. T.: Geophys. Res. Lett., 15, 851–854, 1988.
Seisel, S., Flückiger, B., and Rossi, M. J.: Ber. Bunsenges. Phys. Chem., 102, 811–820, 1998.
Tolbert, M. A., Rossi, M. J., and Golden, D. M.: Science, 240, 1018–1021, 1988.
Quinlan, M. A., Reihls, C. M., Golden, D. M., and Tolbert, M. A.: J. Phys. Chem., 94, 3255–3260, 1990.
Zondlo, M. A., Barone, S. B., and Tolbert, M. A.: J. Phys. Chem. A., 102, 5735–5748, 1993.

V.A1.15

SO₂ + ice

Experimental data

Parameter	Temp./K	Reference	Technique/Comments
γ, γ_0			
$\gamma_0=(0.8-3.0)\times 10^{-5}$	191	Chu et al., 2000	CWFT-MS (a)
$\gamma=(0.4-1.4)\times 10^{-6}$	213-238	Clegg and Abbatt, 2001	CWFT-MS (b)
$K_{\text{linC/cm}}$			
36.5 ([SO ₂]= 6.6×10^{10} cm ⁻³)	191	Chu et al., 2000 (a)	CWFT-MS (a)
5.5 (pH=9; [SO ₂]= 1.3×10^{10} cm ⁻³)	228	Clegg and Abbatt, 2001 (b)	CWFT-MS (b)
7.1 (pH=6; [SO ₂]= 4.2×10^{10} cm ⁻³)			
1.2 (pH=6; [SO ₂]= 4.2×10^{12} cm ⁻³)			
0.47 (pH=4.1; [SO ₂]= 4.2×10^{10} cm ⁻³)			
333 (pH=10.4; [SO ₂]= 2.1×10^{10} cm ⁻³)			

Comments

- (a) Ice films were formed by vapour-deposition at 190–211 K with a thickness of ~ 2.5 – 3.0 μm . The SO₂ partial pressure ranged from 1.0×10^{-6} to 2.3×10^{-5} mbar. The initial uptake coefficients, γ_0 , were corrected for axial and laminar diffusion. Corrections for surface roughness were performed using a layered pore diffusion model giving the “true” value for the uptake coefficient, γ . The variability in the reported γ_0 values is due to a three-fold change in the SO₂ partial pressure and variability in the surface area and roughness of the vapour-deposited water-ice films. On exposure the surfaces were rapidly saturated, and a single measurement reported a surface coverage of $\theta=2.4\times 10^{12}$ molecules/cm² for p(SO₂)= 1.0×10^{-6} mbar at 191 K. These data were used to evaluate the cited value of K_{linC} .
- (b) Ice films made by freezing a water-coated pyrex sleeve within the flow tube. The SO₂ partial pressure ranged from 3×10^{-7} to 1.7×10^{-4} mbar. The uptake saturated rapidly at a given SO₂ partial pressure and surface coverage on pure ice over the whole range varies approximately with $P_{\text{SO}_2}^{0.5}$. The coverage, θ , was much less than a monolayer (N_{max} was estimated to be 5×10^{14} molecules/cm² for the ice surfaces prepared in this way) and shows a strong decrease with decreasing pH. The number of molecules desorbed from the ice surface was about equal to the number of molecules adsorbed, indicating that the adsorption process is fully reversible. The partition constants cited in the table were evaluated from surface coverages at selected p(SO₂) given in Figure 4 of Clegg and Abbatt’s paper, with emphasis on the lower concentrations ($<1.3\times 10^{-6}$ mbar) where θ was approximately proportional to p(SO₂).

Preferred values

Parameter	Value	T/K
$K_{\text{linC/cm}}$	$7.3\times 10^{-4}\exp(2065/T)$	190–250
Reliability		
$\Delta(E/R)/K$	± 1000	190–250

Comments on preferred values

Chu et al. (2000) determined the initial SO₂ uptake coefficient to be $\sim 1\times 10^{-5}$ on water-ice films at 191 K but they did not observe the reversible uptake reported by Clegg and Abbatt (2001). The weak reversible adsorption does not allow accurate determination of uptake coefficients and no recommendation is made for γ .

Clegg and Abbatt (2001) suggest that their observed dependence of the uptake on $[\text{SO}_2]^{0.5}$ is due to dissociation of the hydrated form of SO_2 to HSO_3^- on the ice surface. This was tested by raising and lowering the pH of their ice surfaces. It was found that SO_2 uptake was enhanced at higher pH and was inhibited at lower pH (due to surface protons inhibiting the dissociation of adsorbed SO_2). A simple precursor model was developed by Clegg and Abbatt (2001) to explain the observed SO_2 uptake behaviour. The total adsorbed $\text{S(IV)}^{\text{tot}} = [\text{SO}_2]_{\text{ads}} + [\text{HSO}_3^-]_{\text{ads}}$ at equilibrium is given as a function of $[\text{SO}_2]_{\text{g}}$ by the expression: $[\text{S(IV)}^{\text{tot}}]_{\text{ads}} = K_1[\text{SO}_2] + (K_1 K_2 [\text{SO}_2])^{0.5}$. For ice at natural pH (~ 6) the experimental data at 228 K for $[\text{SO}_2]$ in the range 10^{11} – 10^{13} molecule cm^{-3} were approximated by the expression: $[\text{S(IV)}^{\text{tot}}]_{\text{ads}} = K [\text{SO}_2]^{0.5}$, where $K = 1.2 \times 10^6$ molecule $^{1/2}$ $\text{cm}^{-1/2}$, indicating $[\text{HSO}_3^-]$ is the predominant adsorbed species. This model is also consistent with a linear dependence on $[\text{SO}_2]$ at low concentrations and K_{linC} can be identified with $K_1[\text{SO}_2]$. The recommended partition coefficient at 228 K was evaluated from data of Clegg and Abbatt for SO_2 on ice at low partial pressures ($[\text{SO}_2] \leq 1.3 \times 10^{-6}$ mbar or $\leq 1 \times 10^{13}$ molecule cm^{-3}).

Chu et al. reported a single measurement of partitioning to pure ice at 191 K, from which a value of $K_{\text{linC}} = 36.5$ cm can be derived, assuming this reflects linear dependence on $[\text{SO}_2]$. This is substantially higher than the value at 228 K, which suggests a negative T dependence as expected for reversible adsorption. An Arrhenius fit to the data points at 191 and 228 K yields the recommended expression for the temperature dependence of K_{linC} .

Some support for the negative temperature dependence comes from the thesis work of Langenberg (1997) who derived $\Delta H_{\text{ads}} = -21 \pm 3$ kJmol $^{-1}$ and $\Delta S_{\text{ads}} = 39 \pm 10$ J K^{-1} mol $^{-1}$ from uptake of SO_2 on a packed column over the temperature range 207–267 K. These results yield an expression for $K_{\text{linC}} = 6.4 \times 10^{-6} \exp(2527/T)$ cm, and a value of 0.42 cm at 228 K, somewhat lower than the preferred value obtained by Clegg and Abbatt on ice at pH=6. Clegg and Abbatt (2001) observed an *increase* in the surface coverage as the temperature was increased from 213 K to 228 K at a constant $p(\text{SO}_2)$ of 4×10^{-5} mbar (corresponding to a surface coverage of 1.5×10^{12} molecule cm^{-2} at 228 K). An Arrhenius fit to these data is consistent with earlier partitioning data for SO_2 to ice (Clapsaddle and Lamb, 1989) and gives the expression: $[\text{S(IV)}^{\text{tot}}]_{\text{ads}} = \{5.6 \times 10^{12} \exp(-4425/T)\} \times [\text{SO}_2]^{0.5}$ molecule $^{1/2}$ $\text{cm}^{-1/2}$. It was suggested that the increase in surface coverage with temperature is due to the existence of a quasi-liquid layer on the ice surface, which increases in thickness and facilitates the dissociation of SO_2 or can accommodate more S(IV) species, as temperature increases. However Huthwelker et al. (2001) showed, on the basis of a detailed analysis of uptake amounts and temperature dependence reported from earlier experimental data (Clapsaddle and Lamb, 1989; Conklin et al., 1993), that SO_2 dissociates and diffuses into an internal reservoir for example comprised of veins and nodes, but not into a quasi-liquid layer on the ice surface.

References

- Chu, L., Diao, G., and Chu, L. T.: J. Phys. Chem. A., 104, 7565, 2000.
 Clegg, S. M. and Abbatt, J. P. D.: J. Phys. Chem. A., 105, 6630, 2001.
 Clapsaddle, C. and Lamb, D.: Geophys. Res. Lett., 16, 1173, 1989.
 Conklin, M. H., Laird, K., Sommerfeld, R. A., and Villinski, J. E.: Atmos. Environ. A, 27, 159–166, 1993.
 Huthwelker, Th., Lamb, D., Baker, M., Swanson, B., and Peter, T., J. Colloid and Interface Science, 238, 147–159, 2001.
 Langenberg, S., PhD thesis: Anwendung de Kapillar-Gaschromatographie zur Untersuchung von Spurengas-Aerosolwechselwirkungen, University of Bonn, Germany, 1997.

V.A1.16**HCHO + ice****Experimental data**

Parameter	Temp./K	Reference	Technique/Comments
$K_{\text{linC/cm}}$ 0.7 ± 0.3	198–223	Winkler et al., 2002	CWFT-MS (a)

Comments

- (a) Ice surface formed by freezing water. The geometric surface area was used to calculate the coverage. The formaldehyde uptake data showed neither a dependence on temperature nor an approach to saturation, thus precluding an analysis using Langmuir isotherms. K_{linC} ($\text{cm}^{-2}/\text{cm}^{-3}$) was determined from a linear relationship between N (surface coverage in molecule cm^{-2} of ice) and $[\text{HCHO}]$ (units of molecule cm^{-3}) at low coverage where $N < 1 \times 10^{13}$ molecule cm^{-2} .

Preferred values

Parameter	Value	T/K
$K_{\text{linC/cm}}$	0.7	198–223
$N_{\text{max/molecule cm}^{-2}}$	2.7×10^{14}	
<i>Reliability</i>		
$\Delta \log K_{\text{linC}}$	0.5	189–233
$\Delta \log N_{\text{max}}$	0.2	198–233

Comments on preferred values

The sole experimental study of the formaldehyde-ice interaction by Winkler et al. (2002) shows that the adsorption of formaldehyde to ice is completely reversible, and that the interaction is quite weak. This is consistent with a theoretical study (Hantal et al., 2007), which found a much lower heat of adsorption for formaldehyde ($\approx -30 \text{ kJ mol}^{-1}$) compared to methanol although in both cases the thermodynamic driving force was the formation of hydrogen-bonds.

References

- Hantal, G., Jedlovzky, P., Hoang, P. N. M., and Picaud, S.: J. Phys. Chem. C, 111, 14170, 2007.
Winkler, A. K., Holmes, N. S., and Crowley, J. N.: Phys. Chem. Chem. Phys., 4, 5270, 2002.

V.A1.17

HC(O)OH + ice

Experimental data

Parameter	Temp./K	Reference	Technique/Comments
$K_{\text{linC}}/\text{cm}$			
72600	187	von Hessberg et al., 2008	CWFT-CIMS (a)
11000	197		
1980	209		
418	221		
$5.8 \times 10^{-11} \exp(6500/T)$	187–221		
681	208	Symington et al., 2009	CWFT-MS (b)
137	218		
82	228		

Comments

- (a) Ice film made by freezing distilled water. Uptake was found to be reversible and equilibrium surface coverages were calculated using the geometric ice surface area. Values of $N_{\text{max}}=2.2 \times 10^{14}$ molecule cm^{-2} (independent of temperature) and $\Delta H_{\text{ads}}=-51 \pm 6 \text{ kJ mol}^{-1}$ were reported. The HC(O)OH concentration was varied between 2×10^9 and 2×10^{11} molecule cm^{-3} with the fraction of dimer present calculated to be less than 10% for all temperatures and concentrations except for 187 K and $[\text{HC(O)OH}] > 2 \times 10^{10}$ molecule cm^{-3} .
- (b) Ice film made by freezing distilled water. Uptake was found to be reversible and equilibrium surface coverages were calculated using the geometric ice surface area. Equilibrium uptake of HC(O)OH to ice at various temperatures was analysed using the Langmuir isotherm. The table uses the reported values of $K_{\text{LangP}}(T)$ and $N_{\text{max}}(T)$. The temperature dependent expression of K_{linC} was derived by fitting to these three data points. A value of $\Delta H_{\text{ads}}=-44 \text{ kJ mol}^{-1}$, was reported. The HC(O)OH concentration was varied between $\approx 2 \times 10^{10}$ and 2×10^{14} molecule cm^{-3} and was corrected for the presence of dimers.

Preferred values

Parameter	Value	T/K
$K_{\text{linC}}/\text{cm}$	$4.0 \times 10^{-12} \exp(7000/T)$	187–221 K
$N_{\text{max}}/\text{molecules cm}^{-2}$	2.2×10^{14}	
<i>Reliability</i>		
$\Delta(E/R)/\text{K}$	± 500	
$\Delta \log N_{\text{max}}$	0.1	

Comments on preferred values

There are two experimental studies of the reversible uptake of HC(O)OH to pure ice surfaces. Both studies used the same experimental approach and the values of the equilibrium partitioning coefficients and N_{max} are in reasonable agreement. The preferred value therefore takes both datasets into account. Reported values of N_{max} are consistent with other oxidized organics (Abbatt, 2003). Other experimental studies have provided evidence for strong (hydrogen bonding) interaction between HC(O)OH and H_2O molecules at the surface of ice films, which does not lead to spontaneous ionization (Souda 2003; Bahr et al., 2005). These observations are supported by theoretical studies (Compoin et al., 2002), which show that HC(O)OH is hydrogen bound to two neighbouring H_2O molecules.

References

- Abbatt, J. P. D.: *Chem. Rev.* 103, 4783–4800, 2003.
- Bahr, S., Borodin, A., Hofft, O., Kempter, V., and Allouche, A.: *J. Chem. Phys.*, 122, 2005.
- Compoint, M., Toubin, C., Picaud, S., Hoang, P. N. M., and Girardet, C.: *Chem. Phys. Lett.*, 365, 1–7, 2002.
- Souda, R.: *J. Chem. Phys.*, 119, 2774–2779, 2003.
- Symington, A., Cox, R. A., and Fernandez, M. A.: *Z. Phys. Chem.* 224, 1219–1245, 2010.
- von Hessberg, P., Pouvesle, N., Winkler, A. K., Schuster, G., and Crowley, J. N.: *Phys. Chem. Chem. Phys.*, 10, 2345–2355, 2008.

V.A1.18

CH₃CHO + ice

Experimental data

Parameter	Temp./K	Reference	Technique/Comments
γ_0			
>0.1	120–145	Hudson et al., 2002	Knudsen (a)
>0.04	150		
>0.01	155		
$>5 \times 10^{-3}$	160		
$K_{\text{linC/cm}}$			
$3.8 \times 10^{-10} \exp(4174/T)$	140–170	Hudson et al., 2002	Knudsen (b)
2.08 ± 0.19	203	Petitjean et al., 2009	CWFT-MS (c)
0.95 ± 0.09	213		
0.46 ± 0.04	223		

Comments

- (a) Vapour deposited ice film of geometric area $\approx 5 \text{ cm}^2$. γ_0 values taken from a γ . The geometric surface area of the vapour deposited ice film was used to calculate the uptake coefficient, γ_0 , which is a lower limit as, especially at the higher temperatures, adsorption and desorption were not separated in time.
- (b) Equilibrium uptake of $\sim 4 \times 10^{-7}$ mbar acetaldehyde ($\approx 10^{10}$ molecule cm^{-3}) to ice at various temperatures was analysed using the Langmuir isotherm. The expression for K_{linC} uses the reported value of ΔS_{ads} (via Trouton's rule) $= -87.9 \text{ J mol}^{-1} \text{ K}^{-1}$ and $\Delta H_{\text{ads}} = -34.7 \text{ kJ mol}^{-1}$ and is derived from $K_{\text{LangP}} (\text{atm}^{-1}) = \exp\{-(T^*87.9 - 34700)/8.314 * T\}$ using $N_{\text{max}} = 4 \times 10^{14}$ molecules cm^{-2} .
- (c) Ice film (40–100 μm thick) made from freezing liquid water at 263 K. Adsorption isotherms were measured with CH₃CHO concentrations between 5.7×10^{11} and 8.35×10^{14} molecule cm^3 . The data analysed using full Langmuir isotherms and the linear dependence of surface coverage on concentration to derive the partition coefficients listed in the table.

Preferred values

Parameter	Value	T/K
$K_{\text{linC/cm}}$	$7.0 \times 10^{-8} \exp(3500/T)$	203–223 K
$N_{\text{max}}/\text{molecules cm}^{-2}$	1.3×10^{14}	
<i>Reliability</i>		
$\Delta(E/R)/\text{K}$	± 300	
$\Delta \log N_{\text{max}}$	0.15	

Comments on preferred values

Petitjean et al. (2009) found the uptake of CH₃CHO to ice surfaces to be completely reversible. They report partition coefficients and also derive an adsorption enthalpy of $16 (\pm 3) \text{ kJ mol}^{-1}$ by an unconstrained Vant Hoff-type analysis of data at 203, 213 and 223 K only. In a second approach the analysis was constrained with adsorption entropy of $87.3 \text{ J mol}^{-1} \text{ K}^{-1}$ to derive an adsorption enthalpy of 42 kJ mol^{-1} . The preferred values for K_{linC} above were obtained by fitting to the data of Petitjean et al. (2009) obtained in the linear coverage regime between 203 and 223 K. The adsorption enthalpy is $\sim -29 \text{ kJ mol}^{-1}$. Hudson et al. (2002) found that the interaction of CH₃CHO with ice was too weak to detect close to atmospherically relevant temperatures. Extrapolation of their data to the temperatures covered by Petitjean et al. (2009) results in discrepancies

of a factor of 5-10. The value of N_{\max} given was that obtained by Petitjean et al. (2009). Petitjean also found the uptake of CH_3CHO to ice surfaces that contained HNO_3 was enhanced by 1–2 orders of magnitude at their temperatures, presumably due to dissolution in super-cooled $\text{HNO}_3 / \text{H}_2\text{O}$ mixtures. In contrast, Hudson et al. (2002) observed no uptake of CH_3CHO on super-cooled $\text{HNO}_3 / \text{H}_2\text{O}$ surfaces at 200 K.

References

- Hudson, P. K., Zondlo, M. A., and Tolbert, M. A.: J. Phys. Chem. A., 106, 2882–2888, 2002.
Petitjean, M., Mirabel, Ph., and Le Calv, S.: J. Phys. Chem. A 113, 5091–5098, 2009.

V.A1.19

CH₃C(O)OH + ice

Experimental data

Parameter	Temp./K	Reference	Technique/Comments
$K_{\text{linC}} / \text{cm}$			
$1.9 \times 10^{-11} \exp(6800/T)$	220–245	Sokolov and Abbatt, 2002	CWFT-MS (a)
320	193	Picaud et al., 2005	CWFT-MS (b)
258	203		
153	213		
73	223		
$2.3 \times 10^{-10} \exp(6530/T)$	197–227	von Hessberg et al., 2008	CWFT-MS (c)
$1.9 \times 10^{-12} \exp(7400/T)$	213–243	Kerbrat et al., 2010	PBFT-CIMS (d)
$5.5 \times 10^{-9} \exp(5703/T)$	197–227	Symington et al., 2010	CWFT-MS (e)

Comments

- (a) Ice film made by freezing distilled water. Uptake was found to be reversible and equilibrium surface coverages were calculated using the geometric ice surface area. Equilibrium uptake of CH₃C(O)OH to ice at various temperatures was analysed using the Langmuir isotherm. The values for K_{linC} at individual temperatures given in the Table uses the reported values of $K_{\text{LangP}}(T)$ and $N_{\text{max}}(T)$. No errors were reported. The temperature dependent expression of K_{linC} was derived by fitting to these five data points. A value of $\Delta H_{\text{ads}} = -73 \pm 12 \text{ kJ mol}^{-1}$ was reported. CH₃C(O)OH concentration varied between $\approx 4 \times 10^{10}$ and 2×10^{13} molecule cm⁻³ with between 2 and 20% present as dimers.
- (b) Ice film, 30–80 μm thick was made by freezing distilled water. Uptake was found to be reversible and equilibrium surface coverages were calculated using the geometric ice surface area. Equilibrium uptake of CH₃C(O)OH to ice at various temperatures was analysed using the BET isotherm to derive a value of $\Delta H_{\text{ads}} = -33.5 \pm 4.2 \text{ kJ mol}^{-1}$. The parameterised BET isotherms were used to calculate values of K_{linC} at the four temperatures where reversible uptake was observed. The authors suggest that most of the acetic acid was in the form of dimers in their experiments.
- (c) Ice film made by freezing distilled water. Uptake was found to be reversible and equilibrium surface coverages were calculated using the geometric ice surface area. Values of $N_{\text{max}} = 2.4 \times 10^{14}$ molecule cm⁻² (independent of temperature) and $\Delta H_{\text{ads}} = -55 \pm 9 \text{ kJ mol}^{-1}$ were reported. CH₃C(O)OH concentration varied between 3×10^9 and 2×10^{11} molecule cm⁻³ and the fraction of dimers present was calculated to be less than 15% for all temperatures and concentrations except for 197 K and $[\text{HC(O)OH}] > 2 \times 10^{10}$ molecule cm⁻³.
- (d) Packed ice bed flow tube at atmospheric pressure. Partition coefficients derived from analysis of breakthrough curves and using the geometric ice surface area.
- (e) Ice film made by freezing distilled water. CH₃C(O)OH concentration varied between $\sim 3 \times 10^{10}$ and 4×10^{12} molecule cm⁻³. Uptake was found to be reversible and equilibrium surface coverages were calculated using the geometric ice surface area. Equilibrium uptake of CH₃C(O)OH to ice at various temperatures was analysed using the Langmuir isotherm and N_{max} was found to be 2.4×10^{14} . Linear least squares fit of selected data for concentrations less than 2×10^{12} was used to determine the optimum values for K_{linC} . A value of $\Delta H_{\text{ads}} = -49 (\pm 8) \text{ kJ mol}^{-1}$, was reported.

Preferred values

Parameter	Value	<i>T</i> /K
$K_{\text{linC/cm}}$	$1.5 \times 10^{-14} \exp(8500/T)$	195–240 K
$N_{\text{max/molecules cm}^{-2}}$	2.5×10^{14}	
<i>Reliability</i>		
$\Delta(E/R)/K$	± 1000	195–240
$\Delta \log N_{\text{max}}$	0.1	

Comments on preferred values

There are five experimental studies of the reversible uptake of $\text{CH}_3\text{C}(\text{O})\text{OH}$ to pure ice surfaces, the results differing somewhat, possibly due to the presence of varying amounts of the acetic acid dimer. Sokolov and Abbatt (2002), von Hessberg et al. (2007), Kerbrat et al. (2010), and Symington et al. (2010) suggest that the fraction of dimers present in their samples was of the order of a few percent, whereas Picaud et al. (2005) calculated that almost 100% of their sample was dimerised. It is not clear if this assumption was partially responsible for the much lower partitioning coefficients found by Picaud et al. (2005). The published data of Sokolov and Abbatt (2002), von Hessberg et al. (2007), Kerbrat et al. (2010) and Symington et al. (2010), are in good agreement and were used to derive the preferred expression, which indicates an enthalpy of adsorption of $70 (\pm 10)$ kJ mol^{-1} . The values of N_{max} returned by the various studies is variable, probably due to extrapolations from low coverages and also due to lateral interactions at high coverages, which make this parameter generally difficult to access experimentally (Jedlovsky et al., 2006). Theoretical investigations (Compoint et al., 2002; Picaud et al., 2005) have showed that the hydroxyl and carbonyl groups of acetic acid are bound to two surface water molecules, with the CH_3 group directed away from the ice surface. This would tend to suggest that acetic acid dimers, for which OH and CO bonds are no longer available, would undergo significantly weaker interaction with the ice surface.

References

- Compoint, M., Toubin, C., Picaud, S., Hoang, P. N. M., and Girardet, C.: Chem. Phys. Lett., 365, 1–7, 2002.
- Jedlovsky, P., Partay, L., Hoang, P. N. M., Picaud, S., von Hessberg, P., and Crowley, J. N.: J. Am. Chem. Soc., 128, 15300–15309, 2006.
- Kerbrat, M., Huthwelker, T., Bartels-Rausch, T., Gäggeler, H. W., and Ammann, M., Phys. Chem. Chem. Phys., 12, 7194–7202, 2010.
- Picaud, S., Hoang, P. N. M., Peybernes, N., Le Calve, S., and Mirabel, P.: J. Chem. Phys. 122, article 194707, 2005.
- Sokolov, O. and Abbatt, J. P. D.: J. Phys. Chem., 106, 775–782, 2002.
- Symington, A., Cox, R. A. and Fernandez, M. A.: Z. Phys. Chem. 224, 1219–1245, 2010.
- von Hessberg, P., Pouvesle, N., and Crowley, J. N.: Phys. Chem. Chem. Phys., 10, 2345–2355, 2008.

V.A1.20

CH₃OH + ice

Experimental data

Parameter	Temp./K	Reference	Technique/Comments
γ_0			
>0.02	198	Winkler et al., 2002	CWFT-MS (a)
>0.1	150–160	Hudson et al., 2002	Knudsen (b)
>0.04	170		
$K_{\text{linC}}/\text{cm}$			
$6.24 \times 10^{-12} \exp(6178/T)$	198–223	Winkler et al., 2002	CWFT-MS (c)
$3.82 \times 10^{-10} \exp(4980/T)$	140–170	Hudson et al., 2002	Knudsen (d)

Comments

- (a) 50–100 μm thick ice film (geometric area $\approx 100 \text{ cm}^2$) made by freezing water. γ_0 (calculated from the geometric ice surface area) is a lower limit as adsorption and desorption were not separated in time.
- (b) Vapour deposited ice film of geometric area $\approx 5 \text{ cm}^2$. γ_0 values taken from a figure in Hudson et al., 2002. γ_0 is a lower limit as adsorption and desorption were not separated in time.
- (c) K_{linC} determined from linear relationship between N (surface coverage in molecule cm^{-2} of ice) and [methanol] (units of molecule cm^{-3}) at low coverage where $N < 1 \times 10^{13}$ molecule cm^{-2} . The geometric surface area was used to calculate the coverage. Analysis of datasets including measurements at higher coverage using a Langmuir isotherm resulted in lower values of the partitioning coefficient, potentially a result of adsorbate-adsorbate interactions. $N_{\text{max}} = (3.2 \pm 1.0) \times 10^{14} \text{ cm}^{-2}$. Enthalpy of adsorption derived as $\Delta H_{\text{ads}} = (-51 \pm 10) \text{ kJ mol}^{-1}$.
- (d) The geometric surface area of the vapour deposited ice film was used to calculate the coverage. Equilibrium uptake of methanol ($\approx 10^{10}$ molecule cm^{-3}) to ice at various temperatures was analysed using the Langmuir isotherm, with N_{max} assumed to be 4×10^{14} molecules cm^{-2} . The expression given in the Table uses the reported values of ΔS_{ads} (via Trouton's rule) of $-87.9 \text{ J mol}^{-1} \text{ K}^{-1}$ and an experimental value of $\Delta H_{\text{ads}} = -41.4 \text{ kJ mol}^{-1}$.

Preferred values

Parameter	Value	T/K
$K_{\text{linC}}/\text{cm}$	$6.24 \times 10^{-12} \exp(6180/T)$	195–230
$N_{\text{max}}/\text{molecules cm}^{-2}$	3.2×10^{14}	
<i>Reliability</i>		
$\Delta(E/R)/\text{K}$	$\pm 100 \text{ K}$	195–230
$\Delta \log N_{\text{max}}$	0.15	

Comments on preferred values

The two experimental studies of the methanol-ice interaction show that, at low methanol concentrations, the adsorption of methanol to ice is completely reversible. The data of Winkler et al. (2002) show significantly higher coverage at 200 K than those calculated from the parameterisation of Hudson et al. (2002), who were unable to observe methanol adsorption at this temperature. Bearing in mind that the same experiments of Hudson et al. (2002) provided the only outliers in several datasets measuring acetone adsorption to ice, the data of Winkler et al. are preferred, and form the basis of the recommendation. Equilibrium surface coverages at higher concentrations can be calculated using the full form of the Langmuir isotherm (Winkler et al., 2002). No evidence was found for enhanced uptake or product formation with films containing 1 monolayer of HNO₃ (Hudson et al., 2002) or films which were in equilibrium with $\approx 10^{12}$ molecule cm^{-3} of gas phase O₃ at 198 K (Winkler et al., 2002).

Measurements of the experimental uptake coefficient are problematic due to the simultaneous desorption of methanol from the surface, which, apart from data at the lowest temperatures, will result in determination of a lower limit. No recommendation is given for γ or α_s .

Theoretical investigations (Picaud et al., 2000; Collignon and Picaud, 2004) suggest that the OH group of methanol is associated with the ice surface and predict a maximum coverage of $\approx 4 \times 10^{14}$ molecule cm^{-2} at 210 K, consistent with the observations. At low surface coverages, methanol is bound to either one or two H_2O molecules, whereas at high surface coverages, adsorbate-adsorbate interactions become important such that the Langmuir analysis breaks down and the N_{max} is difficult to access (Jedlovsky et al., 2006).

References

- Collignon, B. and Picaud, S.: Chem. Phys. Lett., 393, 457–463, 2004.
- Hudson, P. K., Zondlo, M. A., and Tolbert, M. A.: J. Phys. Chem. A., 106, 2882–2888, 2002.
- Jedlovsky, P., Partay, L., Hoang, P. N. M., Picaud, S., von Hessberg, P., and Crowley, J. N.: J. Am. Chem. Soc., 128, 15300–15309, 2006.
- Picaud, S., Toubin, C., and Girardet, C.: Surface Science 454, 178–182, 2000.
- Winkler, A. K., Holmes, N. S., and Crowley, J. N.: Phys. Chem. Chem. Phys., 4, 5270–5275, 2002.

V.A1.21

C₂H₅OH + ice

Experimental data

Parameter	Temp./K	Reference	Technique/Comments
$K_{\text{linC}} / \text{cm}$			
8.36	228	Sokolov and Abbatt, 2002	CWFT-MS (a)
$(7.5 \pm 3.0) \times 10^{-14} \exp\{(7445 \pm 200)/T\}$	218–233		
197	203	Peybernès et al., 2004	CWFT-MS (b)
85	213		
23	223		
106 ± 21	213	Kerbrat et al., 2007	CWFT-MS (c)
26.1 ± 10	223		
2.94 ± 0.23	233		
1.11 ± 0.09	243		

Comments

- (a) Ice film made by freezing distilled water. Uptake was found to be reversible and equilibrium surface coverages were calculated using the geometric ice surface area. Equilibrium uptake of C₂H₅OH to ice at various temperatures was analysed using the Langmuir isotherm. The value for K_{linC} at 228 K given in the Table uses the reported values of $K_{\text{LangP}} = 1.22 \times 10^3 \text{ Torr}^{-1}$ and $N_{\text{max}} = 2.9 \times 10^{14} \text{ molecule cm}^{-2}$ (no error limits were reported). The temperature dependent expression was derived from their quoted values of $\Delta H_{\text{ads}} = (-61.9 \pm 1.7) \text{ kJ mol}^{-1}$, $\Delta S_{\text{ads}} = (-113 \pm 4) \text{ J mol}^{-1} \text{ K}^{-1}$, so that $K_p^0 = \exp\{-(T^*113 - 61\,900)/8.314^*T\}$, and $V/A = 6.0 \times 10^{-8} \text{ cm}$ (also quoted by the authors). The error in the pre-exponential factor stems from the error in ΔS_{ads} .
- (b) Ice film (30–100 μm thick) made by freezing distilled water at 253 K. Uptake of ethanol was found to be reversible for T between 203 and 223 K, equilibrium surface coverages were calculated using the geometric ice surface area. Values of $\Delta H_{\text{ads}} = (-57 \pm 8) \text{ kJ mol}^{-1}$, $N_{\text{max}} = (2.8 \pm 0.8) \times 10^{14} \text{ molecule cm}^{-2}$ obtained using BET analysis of adsorption isotherms. The parameterised BET isotherms were used to calculate values of K_{linC} at the three temperatures where reversible uptake was observed.
- (c) Method as described in note (b). Values of K_{linC} at 213 and 223 K were converted from values of N_{max} of $(2.37 \pm 0.27) \text{ molecule cm}^{-2}$ at 213 K and $(2.58 \pm 0.62) \text{ molecule cm}^{-2}$ at 223 K and values of K_{LangC} of $(4.48 \pm 0.72) \times 10^{-13}$ and $(1.01 \pm 0.32) \times 10^{-13} \text{ cm}^3 \text{ molecule}^{-1}$ at 213 and 223 K, respectively. Values of K_{linC} at 233 and 243 K were obtained from linear relationship between N (surface coverage in molecule cm⁻² of ice) and [C₂H₅OH] (units of molecule cm⁻³). Enthalpy of adsorption derived as $\Delta H_{\text{ads}} = (-68 \pm 15) \text{ kJ mol}^{-1}$.

Preferred values

Parameter	Value	T/K
$K_{\text{linC}}/\text{cm}$	$5.0 \times 10^{-14} \exp(7500/T)$	210–250
$N_{\text{max}}/\text{molecule cm}^{-2}$	2.8×10^{14}	
Reliability		
$\Delta(E/R)$	± 200 K	210–250
$\Delta \log N_{\text{max}}$	0.15	

Comments on preferred values

The three experimental investigations (all using the same method) of the reversible uptake of C₂H₅OH to pure ice surfaces at $T > 200 \text{ K}$ are in good agreement and the preferred value of K_{linC} is derived from a non weighted fit to all data sets. Good agreement is also obtained for the values of N_{max} derived from Langmuir or BET isotherm analyses.

Kerbrat et al. (2007) have observed that by generating ice from 0.63 or 2.49 wt% solutions of HNO₃, the uptake of C₂H₅OH is increased drastically (up to a factor of 60), but remains reversible. This phenomenon is attributed to the presence of super-cooled liquid on the ice surface.

Molecular dynamics simulations of the C₂H₅OH – ice interaction (Peybernès et al., 2004) predict values of N_{\max} and adsorption energy which are in accord with the experimental data. C₂H₅OH is predicted to hydrogen bond to the ice surface with the alkyl group directed away from the ice surface.

References

- Kerbrat, M., Le Calvé, S., and Mirabel, P.: J. Phys. Chem. A., 111, 925–931, 2007.
Peybernès, N., Le Calvé, S., Mirabel, P., Picaud, S., and Hoang, P. N. M.: J. Phys. Chem. B, 108, 17425–17432, 2004.
Sokolov, O. and Abbatt, J. P. D.: J. Phys. Chem., 106, 775–782, 2002.

V.A1.22**1 – C₃H₇OH + ice****Experimental data**

Parameter	Temp./K	Reference	Technique/Comments
$K_{\text{linC}}/\text{cm}$			
25.6	228	Sokolov and Abbatt, 2002	CWFT-MS (a)

Comments

- (a) Ice film made by freezing distilled water. Uptake was found to be reversible and equilibrium surface coverages were calculated using the geometric ice surface area. The equilibrium uptake of C₃H₇OH to ice at 228 K was analysed using the Langmuir isotherm. The value of K_{linC} reported in the Table was derived from values of $K_{\text{LangP}}=3.5 \times 10^3 \text{ Torr}^{-1}$ and $N_{\text{max}}=3.1 \times 10^{14} \text{ molecule cm}^{-2}$ at 228 K.

Preferred values

Parameter	Value	T/K
$K_{\text{linC}}/\text{cm}$	25.6	228
$N_{\text{max}}/\text{molecule cm}^{-2}$	3.1×10^{14}	
<i>Reliability</i>		
$\Delta \log K_{\text{linC}}$ (228 K)	0.2	228
$\Delta \log N_{\text{max}}$	0.15	

Comments on preferred values

There is only one study of the reversible uptake of C₃H₇OH to pure ice surfaces. The value of N_{max} derived from Langmuir analyses is consistent with other straight chain alcohols (Sokolov and Abbatt, 2002). The uncertainty on the preferred values of K_{linC} and N_{max} are increased to reflect that this is the sole study to date. A rough guide to the temperature dependence of K_{linC} is: $K_{\text{linC}}=3.6 \times 10^{-14} \exp(7800/T)$, which was estimated from the observed, similar temperature dependencies for C₂H₅OH and C₄H₉OH and the single value at 228 K given above. In the absence of validating experimental data, this expression should be used with caution.

References

Sokolov, O. and Abbatt, J. P. D.: J. Phys. Chem., 106, 775–782, 2002.

V.A1.23**1 – C₄H₉OH + ice****Experimental data**

Parameter	Temp./K	Reference	Technique/Comments
$K_{\text{linC}} / \text{cm}$			
358	221	Sokolov and Abbatt, 2002	CWFT-MS (a)
101	228		
42.7	233		
$7.4 \times 10^{-16} \exp(9000/T)$	221–233		

Comments

(a) Ice film made by freezing distilled water. Uptake was found to be reversible and equilibrium surface coverages were calculated using the geometric ice surface area. Equilibrium uptake of C₄H₉OH to ice at various temperatures was analysed using the Langmuir isotherm. The values for K_{linC} at individual temperatures given in the Table uses the reported values of K_{LangP} (221 K)= 4.6×10^4 , K_{LangP} (228 K)= 1.34×10^4 , K_{LangP} (233 K)= 5.2×10^3 (units of Torr⁻¹) and N_{max} (221 K)= 3.4×10^{14} , N_{max} (228 K)= 3.2×10^{14} and N_{max} (233 K)= 3.4×10^{14} (units of molecule cm⁻²). No errors were reported. The temperature dependent expression of K_{linC} was derived by fitting to these three data points.

Preferred values

Parameter	Value	T/K
$K_{\text{linC}}/\text{cm}$	$7.4 \times 10^{-16} \exp(9000/T)$	210–250
$N_{\text{max}}/\text{molecule cm}^{-2}$	3.3×10^{14}	
<i>Reliability</i>		
$\Delta(E/R)$	± 1000	210–250
$\Delta \log N_{\text{max}}$	0.15	

Comments on preferred values

There is only one study of the reversible uptake of 1-C₄H₉OH to pure ice surfaces. The value of N_{max} derived from Langmuir analyses is consistent with other straight chain alcohols (Sokolov and Abbatt, 2002). The uncertainty on the preferred value of K_{linC} is increased to reflect that this is the sole study to date.

References

Sokolov, O. and Abbatt, J. P. D.: J. Phys. Chem., 106, 775–782, 2002.

V.A1.24

CH₃C(O)CH₃ + ice

Experimental data

Parameter	Temp./K	Reference	Technique/ Comments
γ_0			
>0.02	198	Winkler et al., 2002	CWFT-MS (a)
>0.1	<165	Hudson et al., 2002	KNUD (b)
>0.2	<150		
0.009	200	Behr et al., 2004	CWFT-MS (c)
0.006	193–218	Behr et al., 2006	CWFT-MS (d)
α_s			
0.004–0.043		Bartels-Rausch et al., 2005	CWFT-CIMS (e)
$K_{\text{linC}}/\text{cm}$			
$1.25 \times 10^{-10} \exp(5375/T)$	198–223	Winkler et al., 2002	CWFT-MS (f)
$3.8 \times 10^{-10} \exp(4727/T)$	140–170	Hudson et al., 2002	KNUD (g)
$1.25 \times 10^{-15} T^* \exp(6610/T)$	193–213	Dominé and Rey-Hanot, 2002	MS (h)
$1.32 \times 10^{-11} \exp(5795/T)$	193–223	Peybernès et al., 2004	CWFT-MS (i)
$3.21 \times 10^{-13} \exp(6255/T)$	198–228	Bartels-Rausch et al., 2004	CC-CIMS (j)
$1.73 \times 10^{-12} \exp(6134/T)$	203–223	Bartels-Rausch et al., 2005	CWFT-CIMS (e)
$3.0 \times 10^{-7} \exp(3849/T)$	193–218	Behr et al., 2006	CWFT-MS (k)

Comments

- (a) 50–100 μm thick ice film (geometric area $\approx 100 \text{ cm}^2$) made by freezing water. γ_0 (calculated from the geometric ice surface area) is a lower limit as adsorption and desorption were not separated in time.
- (b) Vapour deposited ice film of geometric area $\approx 5 \text{ cm}^2$. γ_0 values taken from a figure in Hudson et al., 2002. γ_0 is a lower limit as adsorption and desorption were not separated in time.
- (c) Vapour deposited ice film. Uptake coefficient extracted from experimental data by numerical analysis of the flow tube, taking adsorption and desorption processes into account.
- (d) Vapour deposited ice film. Uptake coefficient extracted from experimental data by numerical analysis of the flow tube, taking adsorption and desorption processes into account. Evidence for two types of adsorption sites was found, the uptake coefficient refers to “aged” ice which the authors suggest is hexagonal (I_h) ice. A value of 0.008 was obtained for fresh cubic (I_c) ice.
- (e) Atmospheric pressure flow tube. Gas-transport modelling enabled S_0 and partitioning coefficients to be extracted from experimental data based on the assumption that $\Delta S_{\text{ads}} = (-101 \pm 16) \text{ J mol}^{-1} \text{ K}^{-1}$ taken from Bartels-Rausch et al. (2004). The Enthalpy of adsorption was derived as $\Delta H_{\text{ads}} = (-46 \pm 2) \text{ kJ mol}^{-1}$. The surface partitioning coefficient, K_{linC} , reported here is determined from a Van’t Hoff analysis of the raw coverage data, which corresponded to $\Delta S_{\text{ads}} = -87 \text{ J mol}^{-1} \text{ K}^{-1}$ and $\Delta H_{\text{ads}} = -51 \text{ kJ mol}^{-1}$ as reported in Bartels-Rausch et al. (2005) on p. 4537.
- (f) K_{linC} ($\text{cm}^{-2}/\text{cm}^{-3}$) determined from linear relationship between N (surface coverage in molecule cm^{-2} of ice) and [acetone] (units of molecule cm^{-3}) at low coverage where $N < 1 \times 10^{13}$ molecule cm^{-2} ($K_{\text{linC}} = N / [\text{acetone}]$). The geometric surface area was used to calculate the coverage. Analysis of datasets including measurements at higher coverage using a Langmuir isotherm resulted in somewhat lower values of the partition coefficient, potentially a result of adsorbate-adsorbate interactions. $N_{\text{max}} = (2.7 \pm 0.7) \times 10^{14}$ molecule cm^{-2} . Heat of adsorption derived as $\Delta H_{\text{ads}} = (-46 \pm 7) \text{ kJ mol}^{-1}$.

- (g) The geometric surface area of the vapour deposited ice film was used to calculate the coverage. Equilibrium uptake of $\approx 4 \times 10^{-7}$ mbar acetone ($\approx 10^{10}$ molecule cm^{-3}) to ice at various temperatures was analysed using the Langmuir isotherm. The expression for K_{linC} uses the reported value of ΔS_{ads} (via Trouton's rule) $= -87.9 \text{ J mol}^{-1} \text{ K}^{-1}$ and $\Delta H_{\text{ads}} = -39.3 \text{ kJ mol}^{-1}$ and is derived from $K_{\text{LangP}} (\text{atm}^{-1}) = \exp\{-(T^* 87.9 - 39300)/8.314 * T\}$ using $N_{\text{max}} = 4 \times 10^{14}$ molecules cm^{-2} .
- (h) The geometric surface area of the ≈ 1 mm thick ice film (made by freezing water) was used to calculate the coverage. The partitioning coefficient, $K_{\text{linP}} = 90.53 \exp(6610/T) \text{ cm}^{-2} \text{ Pa}^{-1}$, was determined from linear relationship between N (surface coverage in molecule cm^{-2} of ice) and acetone pressure in Pa. Enthalpy of adsorption derived as $\Delta H_{\text{ads}} = (-46 \pm 7) \text{ kJ mol}^{-1}$.
- (i) Partitioning coefficient, K_{langC} reported as $9.61 \times 10^{-26} \exp(5795/T) \text{ molecule}^{-1} \text{ cm}^3$. The geometric surface area of the ice film (made by freezing water) was used to calculate the coverage. $N_{\text{max}} = (1.37 \pm 0.13) \times 10^{14}$ molecule cm^{-2} . Enthalpy of adsorption derived as $\Delta H_{\text{ads}} = (-48.1 \pm 3.1) \text{ kJ mol}^{-1}$. Analysis using a BET isotherm resulted in a value of $\Delta H_{\text{ads}} = (-50.3 \pm 2.5) \text{ kJ mol}^{-1}$. The corresponding value of N_{max} was $(1.30 \pm 0.18) \times 10^{14}$ molecule cm^{-2} .
- (j) Measurement of retention times of acetone in a chromatographic column packed with ice crystals or spheres. Ice surface area derived by BET analysis of methane adsorption isotherms. Crystallinity of ice surfaces had no influence on the coverage. Enthalpy and entropy of adsorption derived as $\Delta H_{\text{ads}} = (-52 \pm 2) \text{ kJ mol}^{-1}$ and $\Delta S_{\text{ads}} = (-101 \pm 16) \text{ J mol}^{-1} \text{ K}^{-1}$, respectively, so that $K_p^0 = \exp\{-(T^* 101 - 52000)/8.314 * T\}$. The expression for K_{linC} was calculated using $V/A = 6.05 \times 10^{-8} \text{ cm}$. This work is considered to supersede the previous determination from this group using the same method (Guimbaud et al., 2003).
- (k) Vapour deposited ice film. The partitioning coefficient, K_{langC} , determined from experimental data by numerical analysis of the flow tube, was reported as $5.0 \times 10^{-22} \exp(3849/T) \text{ molecule}^{-1} \text{ cm}^3$. K_{linC} was calculated using the reported value of $N_{\text{max}} = 6.0 \times 10^{14}$ molecule cm^{-2} . Enthalpy of adsorption (for aged or hexagonal I_h ice) derived as $\Delta H_{\text{ads}} = (-32 \pm 6) \text{ kJ mol}^{-1}$. A higher value of $\Delta H_{\text{ads}} = (-49 \pm 3) \text{ kJ mol}^{-1}$ was obtained for freshly deposited ice, which the authors suggest may correspond to a cubic ice phase (I_c).

Preferred values

Parameter	Value	T/K
$K_{\text{linC}}/\text{cm}$	$1.0 \times 10^{-11} \exp(5850/T)$	195–230
$N_{\text{max}}/\text{molecules cm}^{-2}$	2.7×10^{14}	
<i>Reliability</i>		
$\Delta(E/R)$	± 100	210–250
$\Delta \log N_{\text{max}}$	0.1	

Comments on preferred values

The experimental studies of the acetone–ice interaction are in reasonable agreement and show that the adsorption of acetone to ice is completely reversible. Consistent values of the adsorption enthalpy, ΔH_{ads} and equilibrium partitioning have been obtained. To explain ice-age dependent surface coverages, Behr et al. (2006) suggest that their vapour deposited ice initially was a mixture of cubic (I_c) and hexagonal ice (I_h), with $I_c \rightarrow I_h$ interconversion taking place over a period of hours after deposition.

Values of the maximum surface coverage on ice films made from freezing liquid water, N_{max} , vary between 1.3×10^{14} molecules cm^{-2} (Peybernès et al., 2002) and 2.7×10^{14} molecule cm^{-2} (Winkler et al., 2002). The latter value is consistent with values for other trace gases on similar ice surfaces, and with molecular dynamics calculations (Picaud et al., 2000).

The preferred partitioning coefficient, K_{linC} , is based on the CWFT data of Winkler et al. (2002), Dominé and Reyhanot (2002), Peybernès et al. (2004) and Bartels-Rausch et al. (2005) and provides a simple parameterisation appropriate for low acetone concentrations, whereby $N = K_{\text{linC}}[\text{acetone}]$ with the acetone concentration in units of molecule cm^{-3} and N in units of molecule cm^{-2} . Equilibrium surface coverages at higher concentrations can be calculated using the full form of the Langmuir isotherm (Winkler et al., 2002; Peybernès 2004).

The data of Hudson et al., 2002 and Behr et al., 2006 were obtained using vapor deposited ice and represent the lowest and highest partitioning coefficients, respectively at e.g. 210 K. The data of Bartels et al., 2004 were obtained using packed ice/snow

and the differences in coverage may reflect a different surface type. Journet et al. (2005) showed that vapour deposited ice could, for a given geometric surface area, accommodate 3–4 times as much acetone as ice formed from freezing liquid water.

No evidence was found for enhanced uptake on ice films containing 1 monolayer of HNO_3 (Hudson et al., 2002). Whereas frozen $\text{HNO}_3/\text{H}_2\text{O}$ solutions (0.2–3 N) resulted in greatly enhanced, reversible uptake of acetone and a change in shape of the adsorption isotherm, with values of N_{max} approaching > 100 monolayers (Journet et al., 2005). In contrast, frozen H_2SO_4 solutions (0.2 N) yielded results similar to pure ice.

Theoretical and surface spectroscopic investigations suggest that the carbonyl oxygen atom of acetone is hydrogen bonded to the ice surface via dangling OH groups (Schaff and Roberts, 1996; Schaff and Roberts, 1998; Mitlin and Leung, 2002; Marinelli and Allouche, 2001).

Measurements of the experimental uptake coefficient are problematic due to the simultaneous desorption of acetone from the surface, which, apart from at the lowest temperatures, will result in determination of a lower limit. As the experimental uptake coefficient should be smaller than the surface accommodation coefficient, the value of α_s derived by Bartels-Rausch et al. (2005) appears to be rather low. Similarly, the uptake coefficients extracted using a flow tube model by Behr et al. are much lower than the lower limits presented by Hudson et al. (2002) and Winkler et al. (2002). No recommendation is given for γ or α_s .

References

- Bartels-Rausch, T., Guimbaud, C., Gäggeler, H. W., and Ammann, M.: *Geophys. Res. Lett.*, 31, L16110, doi:10.1029/2004/GL020070, 2004, (erratum reported in *Geophys. Res. Lett.*, 31, L23106, doi:10.1029/2004/GL021838, 2004.)
- Behr, P., Terziyski, A., and Zellner, R.: *Z. Phys. Chem.*, 218, 1307–1327, 2004.
- Behr, P., Terziyski, A., and Zellner, R.: *J. Phys. Chem. A.*, 110, 8098–8107, 2006.
- Dominé, F. and Rey-Hanot, L.: *Geophys. Res. Lett.*, 29(18), 2021–2024, 2002.
- Guimbaud, C., Bartels-Rausch, T., and Ammann, M.: *Int. J. Mass Spec.*, 226, 279–290, 2003.
- Hudson, P. K., Zondlo, M. A., and Tolbert, M. A.: *J. Phys. Chem. A.*, 106, 2882–2888, 2002.
- Journet, E., Le Calvé, S., and Mirabel, P.: *J. Phys. Chem. B.*, 109, 14112–14117, 2005.
- Marinelli, F. and Allouche, A.: *Chem. Phys.*, 272, 137–147, 2001.
- Mitlin, S. and Leung, K. T.: *Surface Science*, 505, L227–L236, 2002.
- Peybernès, N., Marchand, C., Le Calvé, S., and Mirabel, P.: *Phys. Chem. Chem. Phys.*, 6, 1277–1284, 2004.
- Picaud, S., Toubin, C., and Girardet, C.: *Surface Science*, 454, 178–182, 2000.
- Schaff, J. E. and Roberts, J. T.: *J. Phys. Chem.*, 100, 14151–14160, 1996.
- Schaff, J. E. and Roberts, J. T.: *Langmuir*, 14, 1478–1486, 1998.
- Winkler, A. K., Holmes, N. S., and Crowley, J. N.: *Phys. Chem. Chem. Phys.*, 4, 5270–5275, 2002.

V.A1.25**CH₃OOH + ice**

No Experimental data.

V.A1.26**CH₃C(O)OONO₂ + ice****Experimental data**

Parameter	Temp./K	Reference	Technique/Comments
$K_{\text{linC}}/\text{cm}$ $1.49 \times 10^{-9} \exp(3608/T)$	160–180 K	Bartels-Rausch et al., 2002	PBFT-RC (a)

Comments

- (a) Peroxyacetylnitrate (PAN) – ice partitioning coefficients derived from packed ice bed (PBFT) experiments using radioactively labelled PAN at concentrations of 3 ppbv and below. PAN was produced from NO₂ through photolysis of acetone. Ice was prepared from freezing water drops in liquid N₂ and then annealing at 258 K during at least 12 h. The technique involves observation of migration of the radioactively labelled PAN molecules along the temperature gradient established along the flow tube. The adsorption enthalpy of $-30 \pm 7 \text{ kJ mol}^{-1}$ was derived by solving a migration model of linear gas chromatography, and assuming a value of the adsorption entropy of $-45 \text{ J mol}^{-1} \text{ K}^{-1}$ (based on $A_0 = 6.7 \times 10^6 \text{ m}^2$) based on theoretical arguments. The tabulated K_{linC} was derived from these values. Due to the low partitioning coefficient of PAN, adsorption could only be observed at temperatures below 180 K. No decomposition products (NO₂ or NO) were observed).

Preferred values

Parameter	Value	T/K
$K_{\text{linC}}/\text{cm}$	$1.49 \times 10^{-9} \exp(3608/T)$	160–180
<i>Reliability</i>		
$\Delta(E/R) = \pm 100$	180–220	

Comments on preferred values

Due to the low interaction energy, the adsorption kinetics or equilibrium of PAN can only be observed at very low temperature. The partitioning derived from Bartels-Rausch et al. (2002) is tied to the observation at about 170 K. Therefore the extrapolation to higher temperature is somewhat problematic and should be treated with caution as the properties of the ice surface may change towards higher temperatures.

References

Bartels-Rausch, T., Eichler, B., Zimmermann, P., Gaggeler, H. W., and Ammann, M.: Atmos. Chem. Phys., 2, 235–247, 2002.

V.A1.27

HCl + ice

Experimental data

Parameter	Temp./K	Reference	Technique/Comments
γ			
>0.2	197	Leu, 1988	CWFT-MS (a)
$(4.0\pm 2.0)\times 10^{-4}$	196	Leu et al., 1991	CWFT-MS (b)
>0.2	191–200	Hanson and Ravishankara, 1992	CWFT-MS (c)
>0.2	188–193	Chu et al., 1993	CWFT-MS (d)
0.34 ± 0.03	190	Flückiger et al., 1998	Knudsen-MS (e)
0.26 ± 0.02	200		
0.22 ± 0.02	210		
$(7\pm 3)\times 10^{-2}$	205	Hynes et al., 2001	CWFT-MS (f)
$(1\pm 0.3)\times 10^{-2}$	215		
$(5\pm 2)\times 10^{-3}$	230		
parameterisation	188	Huthwelker et al., 2004	Knudsen-MS (g)
	203		
$K_{\text{linC}}/\text{cm}$		(* calculated in this evaluation :see comments)	
$2.5\times 10^4*$	208	Abbatt, 1997	CWFT-MS (h)
$3.6\times 10^4*$	201	Lee et al., 1999	CWFT-MS (i)
$3.18\times 10^4*$	205	Hynes et al., 2001	CWFT-MS (j)
$1.2\times 10^4*$	213		
$0.63\times 10^4*$	223		
$0.43\times 10^4*$	230		
$1.08\times 10^4*$	228	Sokolov and Abbatt, 2002	CWFT-MS (k)
$(9.9\pm 3.3)\times 10^4 *$	218	Hynes et al., 2002	CWFT-MS (l)
6.0×10^3	230	Cox et al., 2005	CWFT-MS (m)
$(5.4\pm 0.3)\times 10^4$	208	Fernandez et al., 2005	CWFT-MS (n)
$(1.68\pm 0.12)\times 10^4$	218		
$(0.78\pm 0.6)\times 10^4$	228		
1.02×10^4	213	McNeill et al., 2006	CWFT-MS (o)
2.6×10^4	203		
1.14×10^4	195		

Comments

- (a) Fast flow tube reactor with MS detection. Ice condensed from the vapor phase onto the cold flow tube. γ corrected for gas diffusion using estimated diffusion coefficients. The amount taken up by ice increased with $p(\text{HCl})$ and decreasing temperature, and with ice thickness.
- (b) Flow tube reactor with MS detection. Ice was condensed from the vapor phase onto the cold wall of the flow tube, and corrected for diffusion using estimated diffusion coefficients scaled to 197 K.
- (c) Ice-coated flow tube with MS detection. The substrates were prepared by condensing H_2O at 196 K resulting in a film of thickness 10 μm . The geometric surface area was used to calculate γ from the uptake rate corrected for gas diffusion. γ values declined after a few minutes of exposure due to reversible adsorption of HCl; $p(\text{HCl})$ was $\sim 10^{-2}$ mbar to 10^{-4} mbar range.

- (d) Ice-coated flow tube with CIMS detection. Significant corrections for diffusion were made using calculated diffusion coefficients for the reactants in He. At low HCl concentrations (10^{10} molecule cm^{-3}) rapid saturation of the pure ice surface is observed within one minute and γ decreases from >0.3 to <0.01 . At high HCl concentrations (2×10^{12} molecule cm^{-3}) there was unlimited uptake at $\gamma > 0.3$ due to formation of a new phase.
- (e) Knudsen cell reactor with MS detection. Both transient supersaturation (pulsed valve) as well as steady-state experiments were performed with $p(\text{HCl})$ in the range of 6.7×10^{-7} mbar to 2.7×10^{-4} mbar, respectively. γ values were obtained at HCl doses leading to a quasi-liquid layer of HCl-H₂O on the surface.
- (f) Uptake experiment using a fast flow reactor at 2.3–2.7 mbar He equipped with electron-impact quadrupole mass spectrometry. The uptake coefficient γ has a negative temperature dependence. The calculated coverage of HCl on ice is only weakly dependent on temperature and pressure $p(\text{HCl})$ in the range $(0.5\text{--}2.7) \times 10^{-6}$ mbar. It leads to an average saturation coverage of HCl on ice of $(2.0 \pm 0.7) \times 10^{14}$ molecules cm^{-2} at 205 K using the geometric surface area.
- (g) Uptake experiment in a Knudsen flow reactor on typical time scales of 30 min or so. The emphasis is placed on the measurement of the total amount of HCl, N_{HCl} , taken up in the partial pressure range 4×10^{-8} to 2.3×10^{-5} mbar. N_{HCl} is divided into a diffusive and a non-diffusive component, with the former becoming important at later times, typically after the first 300s of uptake. The diffusive component has a $t^{0.5}$ dependence and is proportional to $p_{\text{HCl}}^{-0.5}$. A parametrization scheme of N_{HCl} is proposed as a function of time, temperature, HCl acidity constant on ice, Henry's law constant for physical solubility of HCl and the diffusion constant of HCl in the diffusion layer.
- (h) Coated wall flow tube study of HNO₃ uptake on frozen-film ice surface using MS detection. Surface coverages determined from integrated uptake prior to saturation. Data for surface coverage of HCl is reported for conditions where adsorption partially reversible and close to saturation. HCl surface coverage was 2.5×10^{14} molecule cm^{-2} at $p(\text{HCl}) = 1.3 \times 10^{-6}$ Torr (6.03×10^{10} molecule cm^{-3} at 208 K). Partition coefficient calculated in this evaluation using 1-site Langmuir model assuming maximum surface coverage of 3×10^{14} molecule cm^{-2} .
- (i) HCl uptake on frozen-film and vapour deposited ice surface at 201 K, using MS detection. $p(\text{HCl}) = (0.1\text{--}3.0) \times 10^{-6}$ Torr. Adsorption of HCl partially reversible, but continuous uptake observed when $p(\text{HCl})$ increased above 2×10^{-6} Torr, postulated to be due to HCl induced melting of surface film. Larger uptakes were observed on vapour deposited ice, assumed to be due to the surface "roughness". HCl surface coverage was $(1.1 \pm 0.6) \times 10^{14}$ molecule cm^{-2} at $p(\text{HCl}) = (1 \text{ to } 15) \times 10^{-7}$ Torr ($(4.8 \text{ to } 72) \times 10^9$ molecule cm^{-3} at 201 K). Cited upper limit partition coefficient calculated in this evaluation using 1-site Langmuir model assuming maximum surface coverage of 3×10^{14} molecule cm^{-2} .
- (j) HCl uptake on frozen-film ice surface using MS detection. $p(\text{HCl}) = (0.5\text{--}3.0) \times 10^{-6}$ Torr and $T = 205\text{--}235$ K. Surface coverages determined from integrated uptake prior to saturation. Adsorption of HCl was partially reversible and close to saturation in this pressure range since coverage increased only weakly with increased $p(\text{HCl})$. HCl surface coverage declined from $(2.0 \pm 0.7) \times 10^{14}$ molecule cm^{-2} to $(1.3 \pm 0.7) \times 10^{14}$ molecule cm^{-2} at $p(\text{HCl}) = 1.1 \times 10^{-6}$ Torr over temperature range. Mean partition coefficients over this range calculated in this evaluation using 1-site Langmuir model assuming maximum surface coverage of 3×10^{14} molecule cm^{-2} . Partition coefficients cited by authors were obtained using analysis with a 2-site Langmuir model were much lower and did not reproduce the T dependence of θ .
- (k) Study of competitive uptake of HNO₃ and HCl on frozen-film ice surface using MS detection. In simultaneous adsorption, HCl adsorbs less strongly than HNO₃ (estimated $K_{\text{linC}}(\text{HNO}_3)/K_{\text{linC}}(\text{HCl}) = 2 \pm 1$). In absence of HNO₃, HCl surface coverage was $(1.3 \pm 0.2) \times 10^{14}$ molecule cm^{-2} at $p(\text{HCl}) = 0.5 \times 10^{-6}$ Torr (2.1×10^{10} molecule cm^{-3} at 228 K). Partition coefficient calculated in this evaluation using 1-site Langmuir model assuming maximum surface coverage of 3×10^{14} molecule cm^{-2} .
- (l) Study of competitive uptake of HNO₃ and HCl on frozen-film ice surface at 218 K using same system as in Comment (j). In the presence of HNO₃, HCl adsorbs less strongly than on bare ice and is completely reversible. On bare ice, HCl surface coverage was $(1.3 \pm 0.2) \times 10^{14}$ molecule cm^{-2} at $p(\text{HCl}) = (0.4 \text{ to } 2.0) \times 10^{-6}$ Torr ($(1.8 \text{ to } 8.8) \times 10^{10}$ molecule cm^{-3} at 218 K). Mean partition coefficient over this range in this evaluation using 1-site Langmuir model assuming maximum surface coverage of 3×10^{14} molecule cm^{-2} .

- (m) Model of gas flow and surface exchange in CWFT with a single site Langmuir mechanism. The model was used to re-analyse experimental results from Hynes et al. (see comment (l)). The experimental time-dependent uptake profiles were best fitted with an additional process involving diffusion of the adsorbed molecules into the ice film. The model allowed true surface coverages to be distinguished from total uptake including transfer to the bulk. The reported Langmuir constant, K_{eq} , was obtained by fitting uptake profiles close to saturation, $p(\text{HCl})=1.3 \times 10^{-6}$ Torr (4.8×10^{10} molecule cm^{-3} at 230 K), with a diffusion term included.
- (n) Flow tube study at 2.3 mbar He using MS detection. Co-adsorption of HCl and HNO_3 on frozen film ice at 208–228 K. The surface was doped with a constant $p(\text{HNO}_3)$ (1.0×10^{-6} Torr) and HCl uptake saturated after typically 200 s and was completely reversible. The surface coverage increased with $p(\text{HCl})$ ($(0.2 \text{ to } 3.6) \times 10^{-6}$ Torr) up to a maximum of 3×10^{14} molecule cm^{-2} at both 218 K and 228 K. Partition coefficients cited were determined using 1-site, 2-component Langmuir model fit to experimental data, using partition coefficients for HNO_3 fixed at the values given in Cox et al. (2005) (see note (m)), which are adopted in this evaluation.
- (o) Study of interaction of HCl on zone-refined solid ice tube, frozen film ice, and vapour deposited ice at 186–243 K, using ellipsometry to monitor ice surface and CIMS detection of gas uptake. HCl induces a disordered region (i.e. quasi-liquid layer) ~ 100 nm thick near the ice/HCl-hydrate phase boundary, leading to diffusion of surface HCl into bulk ice. In the “core” of the ice stability region uptake is reversible, although there is evidence for 2 different binding sites on films. Cited data obtained by Langmuir model fit in this region.

Preferred values

Parameter	Value	T/K
α_s	0.3	190–210
$N_{\text{max}}/\text{molecules cm}^{-2}$	3×10^{14}	190–230
$K_{\text{linC}}/\text{cm}$	$0.0219 \exp(2858/T)$	205–230
<i>Reliability</i>		
$\Delta \log(\alpha_s)$	± 0.3	190–210
$\Delta(K_{\text{linC}})/\text{cm}$	± 0.2	205–230
$\Delta(E/R)/K$	± 920	

Comments on preferred values

There have been many experimental studies of HCl – ice interactions but most earlier studies were at temperatures < 200 K and concentrations corresponding to stability regions of the phase diagram for either hydrate or supercooled HCl/ H_2O solutions. Under these conditions uptake is continuous and irreversible, especially at high $p(\text{HCl})$. At higher temperatures in the ‘ice stability’ region, uptake rate is time dependent, declining from an initial rapid uptake ($\gamma \sim 0.1$) to very slow uptake when the surface is saturated at a surface coverage, θ of about 3.0×10^{14} molecules cm^{-2} on smooth ice films; adsorption is partially reversible and can be described quite well using a Langmuir model. The slow uptake has been shown to be diffusive in character (Huthwelker et al., 2004; Cox et al., 2005) and to increase in rate near the boundary of the ice stability region. Recent ellipsometric observations of ice films exposed to HCl (McNeil et al., 2006) show that surface melting to form a quasi-liquid layer up to $100 \mu\text{m}$ thick results from adsorption of HCl in this region, which is consistent with the observed uptake behaviour. The Langmuir model ultimately fails under these conditions, and uptakes in excess of 1 monolayer are achieved at high $p(\text{HCl})$.

Surface coverages at low $p(\text{HCl})$ on ice films in the temperature range 200–240 K have been reported in a number of CWFT studies (Abbatt, 1997; Lee et al., 1999; Hynes et al., 2001; 2002; Sokolov and Abbatt, 2002; and Fernandez et al., 2005). There is reasonable agreement in the measured uptakes. For example, a gas-phase concentration of 2 to 6×10^{10} molecule cm^{-3} of HCl results in sub-monolayer equilibrium surface coverages (N) of $(1.3 \pm 0.2) \times 10^{14}$ molecules cm^{-2} for a temperature of 228 K (Hynes et al., 2001; Sokolov and Abbatt, 2002), of 2.0×10^{14} molecules cm^{-2} at 218 K (Fernandez et al., 2005), and 2.5×10^{14} molecules cm^{-2} at 208 K (Abbatt, 1997). All studies report a weak dependence of θ on $p(\text{HCl})$, but none of the studies investigated $p(\text{HCl})$ dependence of uptake in the unsaturated region of the Langmuir isotherm. Values of the maximum surface coverage, $N_{\text{max}} \sim 3 \times 10^{14}$ molecule cm^{-2} , reported by Hynes et al. (2001, 2002), and Lee et al. (1999) are consistent with values for other trace gases on similar ice surfaces, and with molecular dynamics calculations (Abbatt, 2003).

Hynes et al. (2001) used a 2-site model to derive Langmuir equilibrium constants from data close to saturation, but the evidence for 2-site kinetics is not compelling. Fernandez et al. (2005), McNeil et al. (2006) and Cox et al. (2005) report Langmuir partition coefficients using a 1-site model. For this evaluation we have calculated K_{eq} values from reported surface coverages, using the full form of the single site Langmuir isotherm ($\theta = [\text{HCl}]_{\text{ads}}/N_{\text{max}} = [\text{HCl}]_{\text{g}} \cdot K_{eq} / (1 + [\text{HCl}]_{\text{g}} \cdot K_{eq})$) and assuming maximum surface coverage, $N_{\text{max}} \sim 3 \times 10^{14}$ molecule cm^{-2} , independent of temperature. Average $p(\text{HCl})$ were taken when a range was reported. The values of K_{eq} plotted in Van't Hoff form give the recommended parameterisation of K_{eq} , which with N_{max} gives equilibrium surface coverages at concentrations up to $\sim 1 \times 10^{-6}$ mbar in the given temperature range. At lower temperatures and higher pressures, corresponding either to hydrate or surfaces with a quasi-liquid layer, uptake can be continuous with no surface saturation. Diffusion rate of adsorbed molecules into the bulk can be approximated using $(Dt)^{1/2}/L$ with $D = 1 \times 10^{-12}$ $\text{cm}^2 \text{s}^{-1}$ and $L = 100$ nm as used by Cox et al. (2005).

Measurements of the uptake coefficient are problematic in CWFT experiments, due to the difficulty in separating adsorption and desorption kinetics and to diffusion limitations, which will result in determination of a lower limit. Knudsen cell measurements of γ_0 indicate a surface accommodation coefficient of ~ 0.3 at $T < 200$ K. At higher temperatures γ decreases with time as increasing amounts of HCl are adsorbed in the ice film, and measurements in the ice-stability region are affected by this. The recommended values for γ_0 are based on the measurements of Flückiger et al. (1998).

References

- Abbatt, J. P. D.: *Geophys. Res. Lett.*, 24, 1479, 1997.
Abbatt, J. P. D.: *Chem. Rev.*, 103, 4783, 2003.
Cox, R. A., Fernandez, M. A., Symington, A., Ullerstam, M., and Abbatt, J. P. D.: *Phys. Chem. Chem. Phys.*, 7, 3434, 2005.
Chu, L.T., Leu, M.-T., and Keyser, L. F.: *J. Phys. Chem.*, 97, 7779, 1993.
Fernandez, M. A., Hynes, R. G., and Cox, R. A.: *J. Phys. Chem. A.*, 109, 9986, 2005.
Flückiger, B., Thielmann, A., Gutzwiller, L., and Rossi, M. J.: *Ber. Bunsenges. Phys. Chem.*, 102, 915, 1998.
Huthwelker, T., Malmström, M. E., Helleis, F., Moortgat, G. K., and Peter, T.: *J. Phys. Chem. A.*, 108, 6302, 2004.
Hanson, D. R. and Ravishankara, A. R.: *J. Phys. Chem.*, 96, 2682, 1992.
Hynes, R. G., Mössinger, J., and Cox, R. A.: *Geophys. Res. Lett.*, 28, 2827, 2001.
Hynes, R. G., Fernandez, M. A., and Cox, R. A.: *J. Geophys. Res.*, 107, 4797, doi:10.1029/2001JD001557, 2002.
Lee, S-H., Leard, D. C., Zhang, R., Molina, L. T., and Molina, M. J.: *Chem. Phys. Lett.*, 315, 7, 1999.
Leu, M.-T.: *Geophys. Res. Lett.*, 15, 17, 1988.
Leu, M.-T., Moore, S. B., and Keyser, L. F.: *J. Phys. Chem.*, 95, 7763, 1991.
McNeill, V. F.: *Studies of heterogeneous ice chemistry relevant to the atmosphere*, PhD Thesis, Massachusetts Ins. Technol., 2005 (<http://hdl.handle.net/1721.1/28841>).
McNeill, V. F., Loerting, T., Geiger, F. M., Trout, B. L., and Molina, M. J.: *Proc. Nat. Acad. Sci.(US)*, 103, 9422, 2006.
Sokolov, O. and Abbatt, J. P. D.: *Geophys. Res. Lett.*, 29, 1851, 2002.

V.A1.28

HOCl + ice

Experimental data

Parameter	Temp./K	Reference	Technique/Comments
γ_0			
8.5×10^{-2}	180	Oppliger et al., 1997	Knudsen (a)
	200		
$K_{\text{linC}}/\text{cm}$			
5×10^3	191	Hanson and Ravishankara, 1992	CWFT-CIMS (b)
216	195	Abbatt and Molina, 1992	CWFT-MS (c)
3.27×10^3	189	Chu and Chu, 1999	CWFT (d)
513	198		
215	208		
161	221		

Comments

- (a) Knudsen cell reactor using pulsed admission of HOCl and MS detection. The ice samples were generated from vapour phase deposition and resulted typically in a 20 μm thick film. A balancing H_2O flow was set in order to keep the composition of the interface constant. Uptake rate constants for HOCl have been measured for doses $<2.5 \times 10^{14}$ molecule corresponding to $<2.5\%$ of a monolayer. At higher doses and in steady-state uptake experiments, strong saturation effects were found.
- (b) HOCl was generated from the reaction $\text{HCl} + \text{Ca}(\text{ClO})_2$ and also in-situ by the reaction of ClONO_2 with the ice surface. Uptake of gaseous HOCl (concentration $\sim 2 \times 10^9$ molecule cm^{-3}) on pure ice was reversible at 191 K, the surface saturating within a few seconds, followed by rapid desorption when exposure ceased. The fractional surface coverage in all the reported experiments did not exceed 0.01. The cited K_{linC} value is based on $\theta=0.01$ for the given [HOCl]. A value of $\sim 10^7$ atm^{-1} ($K_{\text{linC}}=53$ cm) was estimated for the Langmuir constant at 191 K from experiments in which HOCl was produced in-situ by the reaction of ClONO_2 with ice. These experiments also gave values of ΔH_{ads} and ΔS_{ads} of -58 ± 8 kJ mol^{-1} and -167 ± 41.8 $\text{J mol}^{-1} \text{K}^{-1}$ respectively in the range 191–211 K. HOCl did not adsorb on HNO_3 doped ice.
- (c) Ice film deposited from vapour. The thickness ranged from 2 to 10 μm . Uptake of HOCl was fully reversible at 195 K. The uptake of HOCl was 3.2×10^{13} molecule cm^{-2} at $[\text{HOCl}] = 1.5 \times 10^{11}$ molecule cm^{-3} . The cited K_{linC} was calculated from these quantities. Measurement of coverage at fixed $p(\text{HOCl})$ over the temperature range 195–208 yielded a value of $\Delta H_{\text{ads}} = 43.9 \pm 8$ kJ mol^{-1} .
- (d) Uptake of $[\text{HOCl}] \sim 3 \times 10^{10}$ molecule cm^{-3} on vapour deposited ice was reversible at 189 K, the surface saturating with a coverage of $\sim 1 \times 10^{14}$ molecule cm^{-2} within a few seconds. The uptake was followed by complete desorption when exposure ceased. Cited data for temperature dependence of partition coefficient at constant $p(\text{HOCl}) = 8 \times 10^{-7}$ mbar are taken from Chu and Chu (1999). A value of ΔH_{ads} of -34 ± 8 kJ mol^{-1} was estimated from the data.

Preferred values

Parameter	Value	T/K
α_s	0.08	180–200
$N_{\max}/\text{molecule cm}^{-2}$	3×10^{14}	
$K_{\text{linC}}/\text{cm}$	$3.6 \times 10^{-8} \exp(4760/T)$	185–225
<i>Reliability</i>		
$\Delta \log(\alpha_s)$	± 0.3	180–200
$\Delta(K_{\text{linC}})/\text{cm}$	± 0.2	205
$\Delta(E/R)/K$	± 1200	

Comments on preferred values

The available data show that the uptake rate of HOCl on ice is time dependent and absorption is reversible and rather weak. Under these conditions uptake coefficients are difficult to measure and only one study, that of Oppliger et al. (1997) using a Knudsen cell at very low doses, reports a value for γ , which is adopted for this recommendation.

Partition coefficients were calculated from the three studies reporting surface coverages at specified [HOCl], assuming $N_{\max}=3 \times 10^{14}$ molecule cm^{-3} . The results of Hanson and Ravishankara (1992) and Chu and Chu (1999) are in fair agreement near 190 K and 208 K, but K_{linC} values derived from Abbatt and Molina are significantly lower in this range. It is probable that at the much higher [HOCl] used in this study, the assumption of linear dependence of coverage on [HOCl] was not valid, leading to underestimation of the true K_{linC} . Hanson and Ravishankara derive Langmuir constants indirectly from release of HOCl following its production in the $\text{ClONO}_2 + \text{H}_2\text{O}$ reaction, but the values expressed as partition coefficients are considerably lower, probably due to the presence of the co-product HNO_3 which is likely to compete strongly with HOCl for adsorption sites. The enthalpies of adsorption reported in the 3 studies cover a wide range ($\Delta H_{\text{ads}} = -34$ to -58.8 kJ mol^{-1}) and the temperature dependence observed by Chu and Chu (1999) gives a curved Van't Hoff plot and the derived adsorption enthalpy cannot be considered reliable. The preferred expression for K_{linC} was obtained from a fit to a plot of $\log(K_{\text{linC}})$ vs. $1/T$ for the data of Hanson and Ravishankara (1992) and Chu and Chu (1999). The preferred value of $N_{\max}=3 \times 10^{14}$ molecule cm^{-3} is based on typical saturation coverage on ice.

References

- Abbatt, J. P. D and Molina, M., *Geophys. Res. Lett.*, 19, 461–464, 1992.
 Chu, L. and Chu, L. T.: *J. Chem. Phys. A.*, 103, 691–699, 1999.
 Hanson, D. R. and Ravishankara, A. R.: *J. Phys. Chem.*, 96, 2682, 1992.
 Oppliger, R., Allanic, A., and Rossi, M. J.: *J. Phys. Chem. A.*, 101, 1903, 1997.

V.A1.29

ClO + ice → products

Experimental data

Parameter	Temp./K	Reference	Technique/Comments
γ, γ_{ss}			
$\gamma > 1.0 \times 10^{-2}$	190	Leu, 1988	CWFT-MS (a)
$\gamma_{ss} = (8 \pm 2) \times 10^{-5}$	183	Kenner et al., 1993	CWFT-MS (b)
$\gamma < 1.0 \times 10^{-4}$	213	Abbatt, 1996	CWFT-RF (c)
$\gamma > 1.0 \times 10^{-3}$	225	McKeachie et al., 2004	CWFT-UV/MS (d)

Comments

- (a) Flow tube reactor using electron-impact MS. The ice was condensed from the vapour phase onto the wall of the flow tube. ClO was produced by reacting Cl atoms with an excess of OClO or Cl₂O. The value given in the table is a lower limit. Cl₂ was not detected. The ClO concentration is not reported.
- (b) Fast flow reactor with electron-impact MS. A 4–7 μm thick ice film was deposited from water vapour. ClO was passed through the flow tube either continuously or in pulses. ClO was produced by microwave discharge of O₂ and Cl₂ in He or by first producing Cl atoms by microwave discharge of Cl₂ in He and reacting Cl with O₃. Both methods led to consistent observations of ClO uptake. The ClO pressure was about 6.3×10^{-6} mbar. Cl₂ could not be measured as product because of excess of Cl₂ present from the source. HCl could also not be measured due to a large background in the MS.
- (c) Coated wall flow tube at 1.3 mbar total pressure of He coupled to a resonance fluorescence (RF) detector. The ice film was prepared by coating a Pyrex tube with water followed by freezing. ClO was generated from the reaction Cl+O₃. Cl atoms were produced by microwave discharge of Cl₂ in He. For detection, ClO was reacted with NO, and Cl atoms detected by resonance fluorescence. The ClO concentrations used in this work were of the order of 4×10^{-6} mbar.
- (d) Coated wall flow tube coupled to either a UV-VIS absorption cell, EI-MS or resonance enhanced multiphoton time-of-flight MS (REMPI-TOF-MS). ClO was produced either via Cl+O₃, or via OClO+O to allow checking for interference of excess Cl₂, O₃, or OClO, separately. The ClO pressure was about 2×10^{-4} mbar. The ice film on a pyrex flow tube was prepared by spraying a mist into the precooled flow tube, or by vapour deposition from either He saturated with water or from laboratory air. The preparation of the film had no effect on the results. ClOOCl was the main target of this study, and uptake of ClO to ice was inferred from the suppression of ClOOCl formation in the presence of an ice film. ClClO₂ and OClO were detected as products when the ice film was evaporated after exposure to ClO. Separate experiments showed that ClOOCl was not measurably taken up by ice. The uptake coefficient reported in the table was estimated from the amount of OClO recovered after different exposure times. The uptake coefficient seemed to increase with increasing ClO exposure time.

Preferred values

Parameter	Value	T/K
γ	$< 1 \times 10^{-4}$	180–220
<i>Reliability</i>		
$\Delta \log (\gamma_0)$	undetermined	

Comments on preferred values

There is substantial disagreement between the Kenner et al. (1993) and Abbatt (1996) studies on one hand, and the Leu (1988) and McKeachie et al. (2004) studies on the other hand. One of the reasons could simply lie in the ice preparation method leading to highly porous films in case of vapour deposition from the gas phase. However, Abbatt (1996) used a film frozen from solution and found low reactivity consistent with Kenner et al. (1993). The Leu (1988) study involved excess amounts of OClO and Cl₂O present in the reactant mixture that, if they are reactive towards ice, could interfere with the ClO measurement using electron impact ionization MS, as noted by all three other authors. McKeachie et al. (2004) used the most selective detection scheme allowing for unequivocal detection of all involved species. They suggest that a complex in the gas phase (Francisco and Sander, 1995) initiates a disproportionation reaction at the ice surface leading to OClO and ClCl(O)O that remain on the ice. This would explain the induction behaviour observed in their experiment and the discrepancy with the Kenner et al. (1993) and Abbatt (1996) studies, which were both performed at nearly two orders of magnitude lower partial pressures. McKeachie et al. also argue that the higher water vapour pressure at higher temperature promotes the abundance of the ClO·H₂O complexes. A significant retention of ClO on ice was excluded by Kenner et al. (1993) by measuring the arrival times of ClO pulses applied to the ice films, indicating that at low pressures the ClO surface coverage is low enough to prevent the secondary chemistry proposed by McKeachie et al. (2004). We therefore recommend the lower observed uptake coefficients as upper limits for ClO uptake at atmospherically relevant pressures.

References

- Abbatt, J. P. D.: *Geophys. Res. Lett.*, 23, 1681–1684, 1996.
Francisco, J. S. and Sander, S. P.: *J. Am. Chem. Soc.*, 117, 9917–9918, 1995.
Kenner, R. D., Plumb, I. C., and Ryan, K. R.: *Geophys. Res. Lett.*, 20, 193–196, 1993.
Leu, M. T.: *Geophys. Res. Lett.*, 15, 851–854, 1988.
McKeachie, J. R., Appel, M. F., Kirchner, U., Schindler, R. N., and Benter, T.: *J. Phys. Chem. B*, 108, 16786–16797, 2004.

V.A1.30

HBr + ice

Experimental data

Parameter	Temp./K	Reference	Technique/Comments
γ_0, γ_{ss}			
$\gamma_{ss}=0.3-1.0$	201	Hanson and Ravishankara, 1992	CWFT-CIMS (a)
$\gamma_{ss}=0.4\pm 0.15$	180	Seisel and Rossi, 1997	Knudsen-MS (b)
$\gamma_{ss}=0.30\pm 0.11$	190		
$\gamma_{ss}=0.25\pm 0.6$	200		
$\gamma_0, \gamma_{ss}=0.33\pm 0.02$	190	Flückiger et al., 1998	Knudsen-MS (c)
$\gamma_0, \gamma_{ss}=0.27\pm 0.03$	200		
$\gamma_0, \gamma_{ss}=0.22\pm 0.02$	210		
$\gamma_0, \gamma_{ss}=0.03\pm 0.005$	212-233	Percival et al., 1999	CWFT-MS (d)
$\gamma_0, \gamma_{ss}>0.1$	<212		
$\gamma_0=0.18\pm 0.065$	181	Chu et al., 2000	CWFT-MS (f)
$\gamma_0=0.07\pm 0.02$	200		
$\gamma_0=0.04\pm 0.01$	227		
$\gamma_0=0.24\pm 0.05$	100	Hudson et al., 2001	(f)
$\gamma_0=0.61\pm 0.06$	140		
$K_{\text{linC}}/\text{cm}$			
4.15×10^5	188	Chu and Chu, 1999	CWFT-MS (g)

Comments

- (a) Ice layers 2–10 μm thick were condensed from the vapour phase onto the cold flow tube wall and doped with HNO_3 for NAT studies. The uptake of HBr on pure ice is very efficient with no signs of saturation. It is thought that a new fluid binary phase: $\text{HBr-H}_2\text{O}$, forms.
- (b) Uptake of pure HBr on vapour-condensed ice films and on bulk aqueous solutions of H_2SO_4 . $[\text{HBr}]=(2-8)\times 10^{11}$ molecule cm^{-3} . No saturation effects observed.
- (c) $[\text{HBr}]=(2-8)\times 10^{11}$ molecule cm^{-3} ; vapour condensed ice. Transient pulsed-dose as well as steady-state experiments with HBr at molecular densities of $(5.6-560)\times 10^{10}$ molecule cm^{-3} . The temperature dependence confirmed the strong negative effect observed by Seisel and Rossi (1997). However, the formation of stoichiometric hydrates could not be confirmed.
- (d) Frozen film ice. The HBr concentrations were in the range $(1-30)\times 10^{12}$ molecule cm^{-3} and the γ values were independent of concentration. No evidence for saturation.
- (e) Uptake experiment using a laminar flow tube equipped with mass spectrometric detection. $p(\text{HBr})$ was 1×10^{-6} Torr in 0.5 Torr of He. The tabulated values are taken from Fig. 7 of the cited paper and have not been corrected using pore diffusion theory.
- (f) The uptake coefficient of HBr on ice was determined using single-shot laser-induced thermal desorption by IR laser radiation from HBr/ H_2O multilayer films of 14 nm thickness deposited on an Al_2O_3 substrate monitored by residual gas MS. HBr pressure between 3×10^{-8} to 1.4×10^{-7} Torr led to low HBr coverages. Absolute HBr coverages were obtained using HeNe interferometric techniques.
- (g) Uptake of HBr into vapour deposited ice films measured as a function of $p(\text{HBr})$ over the range $(0.44-51)\times 10^{-7}$ Torr in 0.5 Torr of He, without compensating water flow. Continuous uptake was observed until film became saturated and desorption of HBr was observed; the film evaporated at this point. Integrated uptake was represented as a function of HBr pressure by a power function: $p(\text{HBr})=K\theta^f$, with $f=0.83\pm 0.05$ and $K=(5.1\pm 4.7)\times 10^{-20}$ cm^{-2} molecule $^{-1}$. Uptake amount also increased with film thickness. Thickness dependence of the amount of HBr taken up into 0.5 - 10 μm films was fitted with an ice micro-granule model (Keyser et al., 1993) to obtain “true” surface coverage θ_0 of 1.1×10^{15} ,

6.1×10^{14} , and 2.9×10^{14} molecules cm^{-2} for $p(\text{HBr})=1.0 \times 10^{-6}$, 5.2×10^{-7} , and 2.2×10^{-7} Torr, respectively. HCl-HBr co-adsorption experiments showed that uptake of both acids was reduced by competition for surface sites.

Preferred values

Parameter	Value	T/K
γ	$1 \times 10^{-5} \exp(840/T)$	180–240
K/cm	4.14×10^5	188
f	0.88	188
<i>Reliability</i>		
$\Delta \log(\gamma)$	± 0.2	298
$\Delta \log(K)$	± 0.3	188
$\Delta(f)$	± 0.01	188
$\Delta(E/R)/K$	± 500	200–240

Comments on preferred values

Several groups have measured the uptake coefficient for HBr on ice films over a range of temperature. All studies report continuous uptake with no apparent saturation of the ice surface and this is attributed to formation of HBr hydrates, $\text{HBr} \cdot n\text{H}_2\text{O}$ ($n=2$ or 3), which are incorporated into the surface layers of the ice film. The values of the uptake coefficient and the temperature dependence are in poor agreement, the differences probably resulting partly from the differences in the morphology of the ice films. Nevertheless we recommend an Arrhenius expression for the temperature dependence of γ , obtained by fitting the data of Hanson and Ravishankara (1992), Seisel and Rossi (1997), Flückiger, et al. (1998), Percival, et al. (1999), and Chu et al. (2000). The uncertainty on the E/R is estimated.

Chu and Chu (1999) have reported comprehensive measurements of HBr uptake at 188 K. No evidence was found for reversible uptake, the uptake amounts increasing monotonically with $p(\text{HBr})$ and greatly exceeding single monolayer (ML) coverage for geometric surface area. This is attributed to pore diffusion and hydrate formation. Uptake amounts at the thin film limit cited in comment (f) were obtained after correction using a pore diffusion model and are still up to a factor of 5 larger than the typical maximum surface coverages for monolayer adsorption on an ice surface at temperatures around 200 K. Thus uptake amounts cannot be described by the Langmuir model, and are best described by an isotherm of the form:

$$N_{ads}(\text{molecule cm}^{-2}) = K [\text{HBr}]^f$$

The recommended partition coefficient for HBr, K , on ice was obtained by fitting the corrected surface coverages at 188 K reported by Chu and Chu (1999) to this isotherm.

References

- Chu, L., Diao, G., and Chu, L. T.: J. Phys. Chem. A., 104, 3150, 2000.
 Chu, L. T. and Chu, L.: J. Phys. Chem. A., 103, 384, 1999.
 Flückiger, B., Thielmann, A., Gutzwiller, L., and Rossi, M. J.: Ber. Bunsenges. Phys. Chem., 102, 915, 1998.
 Hanson, D. R. and Ravishankara, A. R.: J. Phys. Chem., 96, 9441, 1992.
 Hudson, P. K., Foster, K. L., Tolbert, M. A., George, S. M., Carlo, S. R., and Grassian, V. H.: J. Phys. Chem. A., 105, 694, 2001.
 Keyser, L. F., Moore, S. B., and Leu, M.-T. J.: Phys. Chem., 97, 2800, 1993.
 Percival, C. J., Mössinger, J. C., and Cox, R. A.: Phys. Chem. Chem. Phys., 1, 4565, 1999.
 Seisel, S. and Rossi, M. J.: Ber. Bunsenges. Phys. Chem., 101, 943, 1997.

V.A1.31

HOBr + ice

Experimental data

Parameter	Temp./K	Reference	Technique/Comments
γ_0, γ_{ss}			
$\gamma_{ss}=(2.0\pm 1.0)\times 10^{-3}$	228	Abbatt, 1994	CWFT-MS (a)
$\gamma_0=0.27\pm 0.04$	190	Allanic et al., 1997	Knudsen (b)
$\gamma_0=0.15\pm 0.03$	200		
$\gamma_{ss}=0.11\pm 0.03$	190.5	Chu and Chu, 1999	CWFT-MS (c)
$(2\pm 1)\times 10^{-2}$	210.1		
$(2.1\pm 0.5)\times 10^{-3}$	222.9		
$(5.8\pm 3.4)\times 10^{-4}$	238.6		
$\gamma_{ss}=0.37$	175	Chaix et al., 2000	Knudsen (d)
0.30 ± 0.03	185		
0.20 ± 0.04	190		
$(4.7\pm 2)\times 10^{-2}$	200		
$(2\pm 0.1)\times 10^{-2}$	210		
$\gamma_{ss}=(4.0\pm 0.7)\times 10^{-2}$	205	Mössinger et al., 2002	CWFT-MS (e)
$\gamma_{ss}=(3.0\pm 0.1)\times 10^{-3}$	227		
K_{linC}/cm			
5.9×10^5	198	Chu and Chu, 1999	CWFT-MS (f)
4.2×10^5	204		
0.34×10^5	209		

Comments

- (a) Frozen film ice surface. HOBr (5×10^{11} molecule cm^{-3}) was generated in situ in the flow tube injector, by reaction of Br₂ with OH. No evidence for reversible adsorption of HOBr on ice, and no gas-phase products observed. For concentrations exceeding 10^{12} molecule cm^{-3} second-order kinetics for HOBr disappearance was observed.
- (b) Ice films (20 μm thick) were generated from vapor phase deposition. Both steady-state and real-time pulsed admission of HOBr gave identical γ values.
- (c) Vapour deposited ice films. [HOBr] in range $2\text{--}22\times 10^{11}$ molecule cm^{-3} . The uptake coefficient has a strong negative temperature dependence. Correction applied using a pore diffusion model, but the uncorrected values of γ are given in the table.
- (d) Continuous flow and pulsed exposure. The uptake coefficient has a strong negative temperature dependence with an activation energy $E_a=-40.5\pm 4.2$ kJ mol^{-1} over the range 185 to 228 K.
- (e) Frozen film ice surface; γ independent of [HOBr] in range $(2\text{--}22)\times 10^{11}$ molecule cm^{-3} .
- (f) Experimental conditions as in (c). HOBr uptake measured as function of p(HOBr). Uptake saturated after about 250 min exposure and integrated uptake amounts at 198, 204 and 209 K (in molecules cm^{-2}) were fitted to the isotherm $\theta=K_p/p(\text{HOBr})$.

Preferred values

Parameter	Value	<i>T</i> /K
$\alpha_s = 0.35$	180–210	
$\gamma = 3.8 \times 10^{-13} \exp(5130/T)$	200–240	
<i>Reliability</i>		
$\Delta \log(\alpha_s)$	± 0.3	180–210
$\Delta \log(\gamma)$	± 0.3	200–240
$\Delta(E/R)/K$	± 1000	200–240

Comments on preferred values

The results of experimental studies of the uptake kinetics of HOBr onto ice films show very good agreement. All studies show that initial uptake is irreversible and at low concentration ($<10^{12}$ molecule cm^{-3}) is first order in [HOBr]. At higher concentrations second order uptake kinetics are observed. After initial exposure γ is essentially time-independent showing little saturation at modest exposure times, although at very long exposure times Chu and Chu (1999) achieved saturation of the residual ice film under conditions of an evaporating film. No gas phase products have been observed following HOBr uptake. The results are interpreted in terms of formation of stable hydrates of HOBr after adsorption on ice films, although the thermodynamic equilibrium properties of the HOBr-ice system are unknown.

γ is weakly temperature dependent at $T < 190$ K, which is attributed to surface accommodation and is the basis of the preferred value for α_s . Above 200 K γ is strongly temperature dependent, decreasing from 0.3 at 190 K to <0.0005 at 240 K. Chu and Chu (1999) and Mössinger et al. (2002) were unable to fit the temperature dependence of γ over the whole range using a simple precursor-adsorption kinetic model with a single set of parameters, noting a discontinuity in the temperature trend between 210 and 230 K. This was attributed to a change to a more mobile ice surface in this region, but other mechanistic factors could be responsible. The recommended values for the steady-state uptake coefficient over the range 190–240 K are given by an Arrhenius fit to the data in this range.

The adsorption studies of Chu and Chu show that continued exposure of ice films to HOBr eventually lead to saturation. However the adsorbed amounts far exceeded 1 monolayer and could not therefore be described using a Langmuir model. The parameters reported by Chu and Chu did not describe the adsorption process well and no recommendation is given for HOBr partitioning.

References

- Abbatt, J. P. D.: Geophys. Res. Lett., 21, 665, 1994.
 Allanic, A., Oppliger, R., and Rossi, M. J.: J. Geophys. Res., 102, 23529, 1997.
 Chaix, L., Allanic, A., and Rossi, M. J.: J. Phys. Chem. A., 104, 7268, 2000.
 Chu, L. and Chu, L. T.: J. Phys. Chem. A., 103, 8640, 1999.
 Mössinger, J. C., Hynes, R. G., and Cox, R. A.: J. Geophys. Res., 107, 4740, 2002.

V.A1.32

HI + ice

Experimental data

Parameter	Temp./K	Reference	Technique/Comments
γ			
$\gamma_0, \gamma_{ss} > 0.27$	190	Flückiger et al., 1998	Knud-MS (a)
$\gamma_0, \gamma_{ss} = 0.26 \pm 0.02$	200		
$\gamma_0, \gamma_{ss} = 0.20 \pm 0.03$	210		
$\gamma_0, \gamma_{ss} = 0.02 \pm 0.004$	212–233	Percival et al., 1999	CWFT-MS (b)
$\gamma_0 = > 0.1$	<212		
K (cm; Isotherm of the form $\theta = K[\text{HI}]^f$ (molecule cm^{-2})			
2.29×10^5	188	Chu and Chu, 1997	CWFT-MS (c)
0.54×10^5	195		

Comments

- (a) Both transient (pulsed valve) and steady-state experiments have been performed in the HI dose range of 10^{14} molecule per pulse to 10^{16} molecules per pulse, leading to peak molecular densities of $(5.6\text{--}560) \times 10^{10}$ molecule cm^{-3} .
- (b) Frozen film ice. The HI concentrations were in the range $(1\text{--}30) \times 10^{12}$ molecule cm^{-3} and the γ values were independent of concentration. No evidence for saturation.
- (c) Uptake of HI into vapour deposited ice films, thickness 1.8 ± 0.4 μm , measured as a function of $p(\text{HI})$ over range $(0.24\text{--}25) \times 10^{-7}$ Torr in 0.4 Torr of He. No added water vapour, allowing film to evaporate after ~ 1 h. Continuous uptake was observed until film evaporated and total desorption of HI was observed at this point. Integrated uptake was approximately a linear function of HI pressure at $p(\text{HI}) < \sim 10^{-7}$ Torr, but uptake amount increased more rapidly at higher $p(\text{HI})$, suggesting surface melting. Uptake amount also increased with film thickness at higher $p(\text{HI})$. The results are interpreted in terms of formation of HI \cdot 2H $_2$ O hydrates, within the ice film. The data were fitted to the equation: $\log p(\text{HI}) = \log K + f \log \theta$, giving $f = 0.80 \pm 0.05$ (average value for 188 and 195 K), but a value of K was not reported. The uptake is strongly temperature dependent and an adsorption enthalpy of -72.3 kJ mol^{-1} is reported from their analysis. The quoted K values were obtained in this evaluation from a linear fit to the data below $[\text{HI}] \sim 1 \times 10^{10}$ molecule cm^{-3} .

Preferred values

Parameter	Value	T/K
γ	0.2	190–210
K/cm	2.29×10^5	188
K/cm	0.54×10^5	195
f	1.0	190
<i>Reliability</i>		
$\Delta \log(\gamma)$	± 0.3	200
$\Delta \log(K)$	± 0.3	190

Comments on preferred values

Only two groups have reported the uptake coefficient for HI on ice films over a range of temperature. All studies report continuous uptake with no saturation of the ice surface and this is attributed to formation of HI hydrates which are incorporated into the surface layers of the ice film. The values of the uptake coefficient and the temperature dependence are in poor agreement, the differences probably resulting partly from the differences in the morphology of the ice films.

Chu and Chu (1997) report comprehensive measurements of HI uptake at 188 and 195 K. The uptake amounts increased with $p(\text{HBr})$ and greatly exceeded ML coverage for geometric surface area, even at low $[\text{HI}]$. This is attributed to hydrate formation. Thus uptake amounts cannot be described by the Langmuir model, and are best described by an isotherm of the form:

$$N_{ads}(\text{molecule cm}^{-2}) = K [\text{HI}]^f$$

However at low $[\text{HI}]$ coverage is approximately linear and the recommended partition coefficient for HBr on ice is obtained from a linear fit to the data below $[\text{HI}] \sim 1 \times 10^{10} \text{ molecule cm}^{-3}$, i.e. $f = 1.0$.

References

- Chu, L. T. and Chu, L.: J. Phys. Chem. B., 103, 6271, 1997.
Flückiger, B., Thielmann, A., Gutzwiller, L., and Rossi, M. J.: Ber. Bunsenges. Phys. Chem., 102, 915, 1998.
Percival, C. J., Mössinger, J. C., and Cox, R. A.: Phys. Chem. Chem. Phys., 1, 4565, 1999.

V.A1.33**HOI + ice****Experimental data**

Parameter	Temp./K	Reference	Technique/Comments
γ, γ_0			
3.2×10^{-2}	180	Allanic and Rossi, 1999	Knud-MS (a)
4.9×10^{-2}	190		
5.7×10^{-2}	200		
$\gamma_0 > 10^{-2}$	243	Holmes et al., 2001	CWFT-MS (b)

Comments

- (a) HOI (at concentrations of $\sim 1 \times 10^{10}$ molecule cm^{-3}) was formed in the reaction of $\text{O}(^3\text{P})$ with $\text{C}_2\text{H}_5\text{I}$. The ice film was formed by vapour deposition. The uptake did not saturate (time independent) under these conditions and displayed a negative temperature dependence. It was found to be independent of HOI concentration (varied over a factor of four). The values of γ listed are averages from 3-5 datasets. Individual values scatter by a factor of up to two for unchanged conditions. The only gas-phase product detected was I_2 with no recoverable HOI after the evaporation of the 20 μm thick ice film.
- (b) HOI (at concentrations of $< \sim 1 \times 10^{10}$ molecule cm^{-3}) was formed in the reaction of $\text{O}(^3\text{P})$ with $\text{C}_2\text{H}_7\text{I}$. The ice film was formed by freezing liquid water at 258 K. The uptake coefficient decreased with exposure time and HOI was observed to desorb from the ice film after exposure stopped, indicating a (partially) reversible process. Diffusion limitation prevented precise measurement of the initial uptake coefficient.

Preferred values

no recommendation

Comments on preferred values

The results of Allanic and Rossi (1999) and Holmes et al. (2001) were obtained in different temperature ranges and concur that the uptake coefficient is large. A parameterisation, $\gamma = 7 \times 10^{-5} \exp(1300/T)$ generates uptake coefficients that are consistent with both datasets. At the lower temperatures covered by Allanic and Rossi (1999), the uptake is observed to be irreversible, whereas Holmes et al. (2001) observe partially reversible adsorption at 243 K. From the experimental datasets it is not obvious how HOI reacts with the ice surface. Both studies observed I_2 as product and Holmes et al. (2001) suggest that this may arise from self-reaction of HOI (or reaction of HOI with IONO_2 impurity) on the ice surface. It is possible that on a pure ice surface, HOI will adsorb reversibly unless high concentrations and low temperatures result in formation of a thermodynamically stable phase (e.g. formation of hydrates). For this reason we make no recommendation for the uptake coefficient or the Langmuir constant to pure ice, whilst noting that HOI reacts readily on ice surfaces containing reactive species (Allanic and Rossi, 1999; Holmes et al., 2001).

References

- Allanic, A. and Rossi, M. J.: *J. Geophys. Res.* 104, 18689–18696, 1999.
 Holmes, N. S., Adams, J. W., and Crowley, J. N.: *Phys. Chem. Chem. Phys.* 3, 1679–1686, 2001.

V.A1.34**ICI + ice****Experimental data**

Parameter	Temp./K	Reference	Technique/Comments
γ_0			
0.09 ± 0.023	200	Allanic et al., 2000	Knudsen-MS (a)
$2.2 \times 10^{-6} \exp(2175/T)$	180-205		
0.30 ± 0.05 (HCl doped ice)	200		
0.30 ± 0.02 (HBr doped ice)	200		
0.32 ± 0.02 (HI doped ice)	200		

Comments

- (a) Vapour deposited ice film, approx. 75 nm thick. Uptake on pure ice saturated and was reversible. Expression for γ_0 obtained from data taken from figure in Allanic et al. over range given. Enhanced uptake was observed on ice doped with $\sim 3 \times 10^{15} \text{ cm}^{-2}$ HCl, HBr and HI: with HBr, HCl production was observed, and with HI, HCl and I_2 observed.

Preferred values

Parameter	Value	T/K
γ_0	$2.2 \times 10^{-6} \exp(2175/T)$	180–205
<i>Reliability</i>		
$\Delta \log(\gamma_0)$	± 0.3	180–205

Comments on preferred values

The results of the only reported study are accepted for the recommendation. They suggest a physical adsorption of ICl on the ice surface, driven by dipole-dipole interaction. There is insufficient information to establish the partition coefficient. In experiments conducted with HCl, HBr and HI-doped ice, fast uptake was observed with reaction to form HCl. The proposed uptake mechanism involves initial formation X-BrCl intermediate (X=Cl⁻, Br⁻ or I⁻).

References

Allanic, A., Oppliger, R., Van den Bergh, H., and Rossi, M. J.: Z. Phys. Chem., 214(11), 1479, 2000.

V.A1.35**IBr + ice****Experimental data**

Parameter	Temp./K	Reference	Technique/Comments
γ_0			
0.025±0.010	200	Allanic et al., 2000	Knudsen-MS (a)
0.20±0.05 (HCl doped ice)	200		
0.30±0.05 (HBr doped ice)	200		
0.50±0.02 (HI doped ice)	200		

Comments

- (a) Vapour deposited ice film, approx. 75 nm thick. Uptake on pure ice instantly saturated and was reversible. Enhanced uptake was observed on ice doped with $\sim 3 \times 10^{15} \text{ cm}^{-2}$ HCl, HBr and HI. Gas phase products observed only with HI, when HBr and I_2 was observed.

Preferred values

Parameter	Value	T/K
γ_0	0.025	200
<i>Reliability</i>		
$\Delta \log(\gamma_0)$	±0.3	

Comments on preferred values

The results of the only reported study are accepted for the recommendation. They suggest a physical adsorption of IBr on the ice surface, driven by dipole-dipole interaction. There is insufficient information to establish the partition coefficient. In experiments conducted with HCl, HBr and HI doped ice, fast uptake was observed. The proposed uptake mechanism involves initial formation of the X-IBr intermediate ($X=\text{Cl}^- \text{ Br}^-$ or I^-).

References

Allanic, A., Oppliger, R., Van den Bergh, H., and Rossi, M. J.: Z.Phys.Chem., 214(11) 1479–1500. 2000.

V.A1.36**BrCl + ice****Experimental data**

Parameter	Temp./K	Reference	Technique/Comments
γ_0			
$\ll 0.01$	190-205	Allanic et al., 1997	Knudsen-MS (a)
0.045 (HCl doped ice)	200		
0.35 (HBr doped ice)	200		
0.60 (HBr doped ice)	190		

Comments

- (a) Vapour deposited ice film, approx. 75 mm thick. No measurable uptake observed on pure ice. Uptake was observed on ice doped with $\sim 3 \times 10^{15} \text{ cm}^{-2}$ HCl and HBr, and in the latter case Br_2 production was observed.

Preferred values

Parameter	Value	T/K
γ_0	$< 1 \times 10^{-3}$	190–210
<i>Reliability</i>		
$\Delta \log(\gamma_0)$	± 0.3	190–210

Comments on preferred values

The recommended value of the uptake coefficient is based on results of the only reported study. They suggest a very weak interaction between BrCl and ice surface, but there is insufficient information to establish partition coefficient. In experiments conducted with HCl and HBr doped ice, uptake was observed with reaction to form Br_2 with adsorbed HBr. The proposed uptake mechanism involves initial formation X-BrCl intermediate ($X = \text{Cl}^-$ or Br^-).

References

Allanic, A., Oppliger, R., Van den Bergh, H., and Rossi, M. J.: Z. Phys. Chem., 214(11), 1479, 2000.

V.A1.37**BrO + ice → products****Experimental data**

Parameter	Temp./K	Reference	Technique/Comments
γ <(1.0±0.4)×10 ⁻⁴	213	Abbatt, 1996	CWFT-RF (c)

Comments

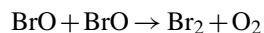
- (a) Coated wall flow tube at 1.3 mbar total pressure of He coupled to a resonance fluorescence (RF) detector. The ice film was prepared by coating a Pyrex tube with water followed by freezing. BrO was generated from the reaction Br+O₃. Br atoms were produced by microwave discharge of Br₂ in He. For detection, BrO was reacted with NO and Br atoms detected by resonance fluorescence. The BrO pressures used in this work were in the range of 9×10⁻⁸ to 9×10⁻⁷ mbar, and the uptake coefficient reported in the table did not vary within this pressure range. Br₂ was observed as product in amounts consistent with the BrO loss.

Preferred values

Parameter	Value	T/K
γ	<1×10 ⁻⁴	200–220
<i>Reliability</i>		
$\Delta\log(\gamma)$	undetermined	

Comments on preferred values

In absence of scavengers, such as sulphite, the main fate of BrO on the ice surface is likely to be the surface recombination reaction:



The absence of a BrO concentration dependence in the only available study is suggested by the author to be due to a saturating surface coverage of BrO, even at the relatively low pressures of the experiments, which is the reason for recommending the γ value obtained under these conditions as an upper limit. In the absence of a measured value for K_{linC} , no surface reaction rate constant can be recommended.

References

Abbatt, J. P. D.: Geophys. Res. Lett., 23, 1681–1684, 1996.

V.A1.38

HONO + HCl (ice) → ClNO + H₂O

Uptake coefficient data

Parameter	Temp./K	Reference	Technique/ Comments
γ_{ss}			
$\gamma_{ss}(\text{HONO})=(6\pm 2)\times 10^{-2}$	180	Fenter and Rossi, 1996	CWFT-MS (a)
$\gamma_{ss}(\text{HONO})=(4.5\pm 1.5)\times 10^{-2}$	190		
$\gamma_{ss}(\text{HONO})=(3.0\pm 0.5)\times 10^{-2}$	200		
$\gamma_{ss}(\text{HONO})=(1.7\pm 0.6)\times 10^{-4}$ (p(HCl)= 2.3×10^{-6} mbar)	191	Diao and Chu, 2005	CWFT-MS (b)
$\gamma_{ss}(\text{HONO})=(1.4\pm 0.4)\times 10^{-2}$ (p(HCl)= 2.3×10^{-5} mbar)	191		

Comments

- (a) Ice prepared both by vapour-phase deposition and by cooling of a sample of distilled water. HONO prepared from use of acidified NaNO₂ solution, with NO and NO₂ as major contaminants. HONO concentration was about 10¹² molecule cm⁻³ in the reactor. Under conditions of excess HONO ranging from 50% up to tenfold, the rate of uptake of HONO is controlled by the rate of HCl uptake on ice, and vice versa. Both the uptake of HONO and HCl converge to steady state after several tens of seconds, after which there is quantitative conversion of HCl and HONO to ClNO.
- (b) 30 μm thick vapor-deposited ice film doped with HCl in the range 6.5×10⁻⁷ to 1.7×10⁻⁴ mbar prior to exposure to HONO. Cited values for γ are corrected for gas phase diffusion but not for pore diffusion, which reduced the value of γ by a factor of 8 to 50. At HCl pressures below 5×10⁻⁶ mbar, to which the ice was exposed, $\gamma_{ss}(\text{HONO})$ slightly decreased with pressure. At higher HCl pressures, $\gamma_{ss}(\text{HONO})$ scales with p(HCl) and coverage. An Eley Rideal type mechanism is suggested for the high pressure range, where the uptake coefficient scales with the surface coverage to the power of 1.67. NOCl has been observed as a product and using this product as observable leads to identical $\gamma_{ss}(\text{HONO})$ within experimental uncertainty. Correlation of relative rates with the reactions of HONO with HBr and HI confirm the nucleophilic character of the reaction.

Preferred values

Parameter	Value	T/K
α_s	0.02	180–220
k_s	4×10^{-19}	180–220
/cm ² molecule s ⁻¹		
<i>Reliability</i>		
$\Delta\log(\alpha_s)$	±0.3	180–220
$\Delta\log k_s$	±0.3	180–220

Comments on preferred values

Both studies report rapid uptake of HONO to ice doped with HCl. The conditions of these experiments all corresponded to near maximum coverage of HCl in the ice or HCl hydrate stability region. Surface melting was also a likely occurrence under these conditions (McNeill et al., 2006). The kinetic data by Fenter and Rossi (1996) agree well with those of Diao and Chu (2000) at the highest pressures used, given that different ice surfaces and different HCl exposures were used.

The Eley Rideal type mechanism suggested by Diao and Chu (2000) is not supported as no HONO pressure dependence is reported. Fenter and Rossi note that the rate of loss of one of the reactants is limited by the amount of the other reactant adsorbed on the surface. We therefore rather suggest using a Langmuir-Hinshelwood type mechanism with the following expression for the uptake coefficient:

$$\frac{1}{\gamma} = \frac{1}{\alpha_s} + \frac{1}{\Gamma_s}$$

with

$$\Gamma_s = \frac{4k_s[\text{HCl}]_s K_{\text{LangC}}(\text{HONO}) N_{\text{max}}(\text{HONO})}{\bar{c}(1 + K_{\text{LangC}}(\text{HONO})[\text{HONO}]_g)}$$

The surface coverage of HCl should be taken as

$$[\text{HCl}]_s = N_{\text{max}} \frac{K_{\text{LangC}}(\text{HCl})[\text{HCl}]}{1 + K_{\text{LangC}}(\text{HCl})[\text{HCl}]}$$

with $K_{\text{LangC}}(\text{HCl}) = 7.3 \times 10^{-17} \times \exp(2858/T) \text{ cm}^3 \text{ molecule}^{-1}$ (see data sheet V.A1.27).

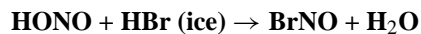
Similarly $K_{\text{LangC}}(\text{HONO}) = 5 \times 10^{-28} \exp(5200/T) \text{ cm}^3$ and $N_{\text{max}}(\text{HONO}) = 3.0 \times 10^{14} \text{ molecule cm}^{-2}$ (see data sheet V.A1.11).

This parameterisation gives a reasonable agreement with the Diao and Chu (2000) data. The same parameterization also fits well the high pressure data, when surface coverages as reported by Diao and Chu (2000) are used at pressures 10^{-5} mbar and above. The recommended parameterization also reproduces the temperature dependence of the uptake coefficient, which was observed to decrease by a factor of two between 180 and 200 K (Fenter and Rossi, 1996).

References

- Diao, G. and Chu, L. T.: J. Phys. Chem. A., 109, 1364, 2005.
 Fenter, F. F. and Rossi, M. J.: J. Phys. Chem., 100, 13765, 1996.
 McNeill, V. F., Loerting, T., Geiger, F. M., Trout, B. L., and Molina, M. J.: Proc. Nat. Acad. Sci.(US), 103, 9422, 2006.

V.A1.39



Uptake coefficient data

Parameter	Temp./K	Reference	Technique/ Comments
$\gamma_{\text{ss}}(\text{HONO})$			
2×10^{-2} (HBr doped ice)	180	Seisel and Rossi, 1997	Knud-MS (a)
2.5×10^{-2} (concurrent HONO and HBr excess)	200		
$(2.3 \pm 0.3) \times 10^{-2}$ (Frozen HBr solution)	190		
$(1.6 \pm 0.2) \times 10^{-3}$ (p(HBr)= 3.9×10^{-8} mbar)	191	Chu et al., 2000	CWFT-MS (b)
$(1.7 \pm 0.8) \times 10^{-2}$ (p(HBr)= 8.7×10^{-5} mbar)	191		
$(5.7 \pm 4.0) \times 10^{-4}$ (p(HBr)= 3.3×10^{-8} mbar)	200		
$(1.6 \pm 0.7) \times 10^{-2}$ (p(HBr)= 8.7×10^{-5} mbar)	200		
$(8.7 \pm 1.6) \times 10^{-4}$ (p(HBr)= 6.8×10^{-7} mbar)	230		
$(4.5 \pm 1.1) \times 10^{-3}$ (p(HBr)= 4.5×10^{-5} mbar)	230		
$(3.1 \pm 1.0) \times 10^{-4}$ (p(HBr)= 6.5×10^{-7} mbar)	191	Diao and Chu, 2005	CWFT-MS (c)
$(2.1 \pm 0.3) \times 10^{-2}$ (p(HBr)= 6.8×10^{-5} mbar)	191		

Comments

- (a) Uptake of HBr (2×10^{11} to 8×10^{12} molecule cm^{-3}) and HONO (1×10^{11} to 8×10^{13} molecule cm^{-3}) on vapor-deposited ice films and on frozen aqueous solutions. HONO was prepared from use of acidified NaNO_2 solution, with NO and NO_2 as major contaminants. The rate law for HONO uptake is first order. Pulsed valve admission of HONO resulted in γ values consistent with the steady-state experiments. The uptake of HONO on HBr-doped ice is first order in HONO. No temperature dependence of γ_0 is observed in the range 180 to 210 K. Less than 20% of the HBr taken up on the ice reacts with HONO. Continuous uptake of HONO was observed for concurrent exposure of HONO and HBr to ice. HONO is quantitatively converted to BrNO.
- (b) 30 μm thick vapor-condensed H_2O ice film doped with HBr in the range 10^{-8} mbar to 10^{-4} mbar prior to exposure to HONO. The tabulated γ values are based on the geometric surface area of the film. Correction for pore diffusion into the ice substrate decreased the γ value by a factor of 8 to 50. Pseudo-first order conditions apply as the amount of (pre)adsorbed HBr was always larger than HONO. Starting at an HBr uptake of 10^{15} molecules cm^{-2} $\gamma_{\text{ss}}(\text{HONO})$ scales with p(HBr), while the uptake coefficients remains more or less constant at pressures below 10^{-6} mbar. γ_{HONO} decreases with temperature. An Eley Rideal type mechanism is suggested for the high pressure range. BrNO has been observed as a product, and using this product as observable leads to identical $\gamma_{\text{ss}}(\text{HONO})$ within experimental uncertainty.
- (c) 30 μm thick vapor-condensed H_2O ice film doped with HBr in the range 10^{-6} mbar to 10^{-4} mbar prior to exposure to HONO. The tabulated γ values are based on the geometric surface area of the film. Correction for pore diffusion into the ice substrate decreased the γ value by a factor of 8 to 50. The lower γ values compared to those reported by Chu et al. (2000) are attributed to a lower exposure of the films to HBr prior to reaction with HONO. Correlation of relative rates with the reactions of HONO with HBr and HI confirm the nucleophilic character of the reaction.

Preferred values

Parameter	Value	T/K
α_s (HONO)	0.02	180–220
k_s /cm ² molecule ⁻¹ s ⁻¹	5.0×10^{-18}	180–220
<i>Reliability</i>		
$\Delta \log(\alpha_s)$	± 0.3	180–220
$\Delta \log(k_s)$ /cm ² molecule ⁻¹ s ⁻¹	± 0.3	180–220

Comments on preferred values

All three studies report rapid uptake of HONO to ice doped with HBr. The conditions of these experiments were such that the HBr-ice phase was not well defined for HBr pressures above 10^{-6} mbar. The kinetic data by Seisel and Rossi (1996) seem to converge with those of Chu et al. (2000) and Diao and Chu (2005) at the highest pressures used. The uptake coefficient for a frozen HBr solution was also similar to that at the maximum pressures. The absence of a temperature dependence reported by Seisel and Rossi (1997) contrasts with the temperature dependence reported by Chu et al. (2000). This may be due to the significantly higher HONO pressures used by Seisel and Rossi (1997), which could have led to saturating HONO coverages based on the recommended partition coefficient for HONO. This may have been the reason why the time to reach steady state uptake was indeed temperature dependent. The Eley Rideal type mechanism suggested by Diao and Chu (2000) is not supported as no HONO pressure dependence was reported. Seisel and Rossi (1997) also did not observe a further increase of the BrNO formation with HONO pressure at the highest pressures. We therefore suggest using the following expression describing a Langmuir-Hinshelwood type mechanism with adsorbed HBr reacting with adsorbed HONO:

$$\frac{1}{\gamma} = \frac{1}{\alpha_s} + \frac{1}{\Gamma_s}$$

with

$$\Gamma_s = \frac{4k_s[\text{HBr}]_s K_{\text{LangC}}(\text{HONO}) N_{\text{max}}(\text{HONO})}{\bar{c}(1 + K_{\text{LangC}}(\text{HONO})[\text{HONO}]_g)}$$

We recommend using $[\text{HBr}]_s = 3 \times 10^{14}$ cm² at HBr pressures between 10^{-8} and 10^{-7} mbar and the expression $[\text{HBr}]_s = 414\,000 [\text{HBr}]^{0.88}$ cm⁻² at pressures above 10^{-7} mbar (see data sheet V.A1.30).

From the recommendations presented for uptake of HONO on ice in V.A1.11, we use $K_{\text{LangC}}(\text{HONO}) = 5.0 \times 10^{-23} \exp(5200/T)$ cm³ molecule⁻¹ and $N_{\text{max}}(\text{HONO}) = 3.0 \times 10^{14}$ molecule cm⁻². Taking the recommended pressure dependence of HBr surface coverage and the recommended surface reaction rate constant gives good agreement with the Chu et al. (2000) data at pressures above 10^{-6} mbar, and notably also reproduces the temperature dependence. However, at atmospherically relevant low pressures, where the conditions presumably fall into the ice stability regime, the same parameterization only fits, when a saturating surface coverage of 3×10^{14} cm⁻² is assumed similar to the HCl case. This indicates that the interfacial concentration accessible to HONO is similar to HCl at similar pressures in the ice stability regime. The data by Diao and Chu (2005) are somewhat lower than those of Chu et al. (2000). This may be due to the different internal surface areas or depths into bulk ice HBr has diffused, which then leads to different effective reactant concentrations exposed to HONO. We therefore recommend a large uncertainty associated with the surface reaction rate constant. The recommended equation also nicely explains the difference between the Seisel and Rossi (1997) and the Chu et al. (2000) data, the difference being driven by the HONO pressure dependence.

References

- Chu, L., Diao, G., and Chu, L. T.: J. Phys. Chem. A., 104, 3150, 2000.
 Diao, G. and Chu, L. T.: J. Phys. Chem. A., 109, 1364, 2005.
 Seisel, S. and Rossi, M.: Ber. Bunsenges. Phys. Chem., 101, 943–955, 1997.

V.A1.40**HONO + HI (ice) → INO + H₂O****Uptake coefficient data**

Parameter	Temp./K	Reference	Technique/ Comments
$\gamma_{ss}(\text{HONO})$			
$(2.9 \pm 0.9) \times 10^{-4}$ (p(HI) = 1.1×10^{-7} mbar)	191	Diao and Chu, 2005	CWFT-MS (a)
$(3.0 \pm 0.8) \times 10^{-2}$ (p(HI) = 8.9×10^{-5} mbar)	191		

Comments

- (a) 30 μm thick vapor-condensed H₂O ice film doped with HI in the range 10^{-7} mbar to 10^{-5} mbar prior to exposure to HONO. The tabulated γ values are based on the geometric surface area of the film. Correction for pore diffusion into the ice substrate decreased the γ value by a factor of 6 to 50. INO could not be directly observed. It was suspected that INO formed on the ice film would react with I(ad) on the stainless steel surfaces between the ice film and the mass spectrometer to form I₂ that was detected. I(ad) would form from dissociative adsorption of HI. Correlation of relative rates with the reactions of HONO with HBr and HCl indicate the nucleophilic character of the reaction.

Preferred values

Parameter	Value	T/K
α_s (HONO)	0.02	180–220
k_s /cm ² molecule ⁻¹ s ⁻¹	8×10^{-19}	180–220
<i>Reliability</i>		
$\Delta \log(\alpha_s)$	± 0.3	180–220
$\Delta \log(k_s)$ /cm ² molecule ⁻¹ s ⁻¹	± 0.3	180–220

Comments on preferred values

The single study by Diao and Chu (2005) reports rapid uptake of HONO to ice doped with HI. The conditions of these experiments were such that the HI-ice phase was not well defined above HI pressures above 10^{-6} mbar. The Eley Rideal type mechanism suggested by Diao and Chu (2000) is not supported as no HONO pressure dependence was reported. We therefore rather suggest the following expression for the uptake coefficient, describing a Langmuir-Hinshelwood type mechanism:

$$\frac{1}{\gamma} = \frac{1}{\alpha_s} + \frac{1}{\Gamma_s}$$

with

$$\Gamma_s = \frac{4k_s[\text{HI}]_s K_{\text{LangC}}(\text{HONO}) N_{\text{max}}(\text{HONO})}{\bar{c}(1 + K_{\text{LangC}}(\text{HONO})[\text{HONO}]_g)}$$

The surface coverage of HI should be taken as $[\text{HI}]_s = 3.0 \times 10^{14} \text{ cm}^{-2}$ at HI pressures between 10^{-8} and 10^{-7} mbar and as $[\text{HI}]_s = 8.0 \times 10^{20} \text{ cm}^{-2} [\text{HI}] \text{ cm}^{-2}$ at HI pressures above 10^{-7} mbar (see data sheet V.A1.32).

With k_s and α_S as recommended above, and $K_{\text{LangC}}(\text{HONO}) = 5.0 \times 10^{-23} \exp(5200/T) \text{ cm}^3 \text{ molecule}^{-1}$ based on the value for $N_{\text{max}}(\text{HONO}) = 3.0 \times 10^{14} \text{ molecule cm}^{-2}$ reported in the data sheet V.A1.11, a nice agreement with the data at pressures above 10^{-6} mbar is obtained. As is evident, at atmospherically relevant low pressures, where the conditions presumably fall into the ice stability regime, only the saturating surface coverage of $3 \times 10^{14} \text{ cm}^{-2}$ leads to agreement with experimental data, similar to the HCl case. This indicates that the interfacial concentration accessible to HONO is similar to the case of HCl and HBr at similar pressures. Given that the surface area may not be well characterized in the experiments, we recommend a large uncertainty associated with the surface reaction rate constant.

References

Diao, G. and Chu, L. T.: J. Phys. Chem. A., 109, 1364, 2005.

V.A1.41



Uptake coefficient data

Parameter	Temp./K	Reference	Technique/ Comments
$\gamma_{\text{ss}}(\text{HOCl})$			
$\geq 0.3 (+0.7, -0.1)$	191	Hanson and Ravishankara, 1992	CWFT-CIMS (a)
0.16 ± 0.1	202	Abbatt and Molina, 1992	CWFT-MS (b)
$\geq 0.24 (+0.5, -0.15)$	195		
0.34 ± 0.20	188	Chu et al., 1993	CWFT-MS (c)
0.15	160	Oppliger et al., 1997	Knudsen (d)
	200		
0.15	188	Chu and Chu, 1999	CWFT-MS (e)
	200		

Comments

- (a) Kinetic study on vapor deposited ice film. The initial $[\text{HOCl}]$ was 2×10^9 molecule cm^{-3} . The decay rate of HOCl was identical for $[\text{HCl}] = 2 \times 10^9$ or 2×10^{10} molecule cm^{-3} , indicating surface saturation of HCl. Cl_2 product was rapidly released from ice surface.
- (b) The uptake of HOCl in the presence of excess HCl is time-independent. Uptake rate shows a negative temperature dependence: γ increases from 0.16 to 0.24 when the temperature drops from 202 to 195 K.
- (c) The ice film was deposited from water vapor saturated He and consisted of μm -sized granules. The thickness ranged from 3.7 to 34.7 μm which were calculated and calibrated gravimetrically. The internal surface was measured using BET gas adsorption measurements. $p(\text{HOCl})$ ranged from $(1.7 \text{ to } 24) \times 10^{-7}$ mbar and P_{HCl} from $(1.2 \text{ to } 10.6) \times 10^{-6}$ mbar. Taking into account a structural model for the ice substrate a lower limit value of $\gamma_{\text{ss}} = 0.134 \pm 0.08$ was obtained.
- (d) Uptake experiment performed in a Knudsen flow reactor with MS detection using both steady-state and real-time pulsed valve admission of HOCl and HCl with a balancing H_2O flow. The ice samples were generated from vapor phase deposition of approximately 2×10^5 monolayers of H_2O (20 μm thick). Mass balance studies indicate that HOCl reacts with all HCl taken up by the ice sample even though the rate of formation of Cl_2 decreases towards the end of the reaction. The rate of Cl_2 formation upon HOCl exposure to HCl-doped ice slows down in the presence of HNO_3 hydrates.
- (e) The ice was condensed from the vapor phase at 188.5 K and flow tube pressure was 0.37 mbar. Cited values for γ are not corrected for pore diffusion. Uptake of HOCl mbar ($p(\text{HOCl}) = 9.7 \times 10^{-7}$ mbar) was continuous and $\gamma_{\text{ss}}(\text{HOCl})$ was independent of $[\text{HCl}]$ over range $(1.9\text{--}11.0) \times 10^{-6}$ mbar; at lower $[\text{HCl}]$ ($p(\text{HOCl}) \approx p(\text{HCl})$), γ decreased, presumably due to depletion of the surface HCl. An Eley-Rideal mechanism was proposed for the surface reaction, but no supporting evidence was presented.

Preferred values

Parameter	Value	T/K
$\gamma_{\text{gs}}(\text{HOCl})$	0.22	180–220
$N_{\text{max}}(\text{HCl})/\text{molecule cm}^{-2}$	3×10^{14}	180–220
<i>Reliability</i>		
$\Delta \log(\gamma_{\text{gs}})$	± 0.2	298

Comments on preferred values

All studies report rapid uptake of HOCl onto ice films doped with HCl. Cl₂ is the sole product with a yield of 100%. The conditions of these experiments all corresponded to near maximum coverage of HCl in the ice or HCl hydrate stability region. Surface melting was also a likely occurrence under these conditions (McNeill et al., 2006). The reported γ values are in reasonably good agreement and there is a suggestion of a negative temperature dependence. However, considering the small temperature range and the cited experimental errors, which arise substantially from the large corrections necessary to account for the effect of gas phase diffusion on the measured rate constants in the CWFT studies, we recommend a temperature independent value of γ_{gs} . The preferred value is a mean of the values obtained from all studies cited and the T range is extended to 220 K.

Only the study of Chu and Chu (1999) observed an [HCl] dependence of the uptake coefficient on pure ice surfaces, although Abbatt and Molina (1992) noted that uptake of HOCl on HNO₃-doped ice was much slower and exhibited [HCl] dependence. A plot of the uptake coefficient calculated as a function of $p(\text{HCl})$ at 188 K, assuming both Eley-Rideal and Langmuir Hinshelwood mechanisms, showed that neither model captures the observed fall-off in γ at low $p(\text{HCl})$ observed by Chu and Chu, which almost certainly results from reagent depletion as ($p(\text{HCl}) \leq p(\text{HOCl})$).

The recommended reactive uptake coefficient for HOCl as a function of [HCl]_g is given by the Ely -Rideal parameterisation:

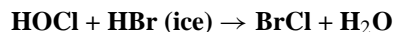
$$\gamma = \gamma_{\text{gs}} \times \theta(\text{HCl})$$

with $\theta(\text{HCl})$ calculated using the recommended value of K_{linC} for HCl on ice (see data sheet V.A1.27) with $N_{\text{max}} = 3 \times 10^{14}$ molecule cm⁻². In the presence of HNO₃ a competitive Langmuir isotherm can be used to obtain θ_{HCl} .

References

- Abbatt, J. P. D. and Molina, M. J.: Geophys. Res. Lett., 19, 461, 1992.
Chu, L. and Chu, L. T.: J. Phys. Chem., 103A, 691, 1999.
Chu, L. T., Leu, M.-T., and Keyser, L. F.: J. Phys. Chem., 97, 12798, 1993.
Hanson, D. R. and Ravishankara, A. R.: J. Phys. Chem., 96, 2682, 1992.
Hanson, D. R. and Ravishankara, A. R.: J. Phys. Chem., 97, 12309, 1993.
McNeill, V. F., Loerting, T., Geiger, F. M., Trout, B. L., and Mario Molina, M. J.: Proc. Nat. Acad. Sci.(US), 103, 9422, 2006.
Oppliger, R., Allanic, A., and Rossi, M. J.: J. Phys. Chem. A., 101, 1903, 1997.
Zhang, R., Leu, M.-T., and Keyser, L. F.: J. Phys. Chem., 98, 13563, 1994.

V.A1.42



Uptake coefficient data

Parameter	Temp./K	Reference	Technique/Comments
γ_{ss}			
0.06–0.38	189	Chu and Chu, 1999	CWFT-MS (a)
0.01–0.07	220		

Comments

- (a) The ice was condensed from the vapor phase at the experimental temperature. Ice film thickness was $2.4 \pm 0.2 \mu\text{m}$ at 189 K and $42 \pm 4 \mu\text{m}$ at 220 K; flow tube pressure was 0.37 mbar. Cited values for γ_{ss} are not corrected for pore diffusion which reduced the value of γ by a factor of 2 to 10. Uptake of HOCl ($p(\text{HOCl}) = 9.7 \times 10^{-7}$ mbar) was continuous, and $\gamma_{\text{ss}}(\text{HOCl})$ increased with $[\text{HBr}]_{\text{g}}$. The range of values given in the table at 188 K were obtained with $p(\text{HBr})$ over range $(1.5\text{--}88.0) \times 10^{-7}$ mbar, and at 220 K the values cited in the table were obtained with p_{HBr} over range $(1.1\text{--}15.9) \times 10^{-6}$ mbar. These trends were deduced to be consistent with an Eley-Rideal mechanism for the surface reaction, but the parameterisation of surface $[\text{HBr}]$ in terms of $p(\text{HBr})$ was not given.

Preferred values

Parameter	Value	T/K
$\alpha_{\text{s}}(\text{HOCl})$	0.3	180–220
$N_{\text{max}}(\text{HOCl})/\text{molecule cm}^{-2}$	3×10^{14}	180–220
$k_{\text{s}}/\text{cm}^2 \text{ molecule}^{-1} \text{ s}^{-1}$	3.3×10^{-15}	180–220
<i>Reliability</i>		
$\Delta(\alpha_{\text{s}})$	± 0.15	180–220
$\Delta \log(k_{\text{s}})$	0.3	180–220

Comments on preferred values

The single study by Chu and Chu (1999) reports rapid irreversible uptake of HOCl onto ice films doped with HBr, in contrast to the uptake of HOCl on pure ice films. Products BrCl and Br₂ were observed but their yield was $\leq 100\%$. The uptake coefficient increased with $p(\text{HBr})$ at both 188 K and 220 K but was much lower for equivalent $p(\text{HBr})$ at 220 K. However this may reflect an effect of ice film thickness ($2.4 \pm 0.2 \mu\text{m}$ at 189 K and $42 \pm 4 \mu\text{m}$ at 220 K); the conditions of these experiments corresponded to the HBr hydrate stability region (Chu and Chu, 1999), where *surface* $[\text{HBr}]$ may be lower on a thicker film due to transfer into the bulk. The preferred value of α_{s} for the range 188–220 K is the value obtained at high p_{HBr} on the thinner film at 188 K.

The evidence for Eley-Rideal kinetics suggested by Chu and Chu (1999) is not convincing and HBr adsorption doesn't follow a Langmuir model under the laboratory experimental conditions used (see data sheet for HBr+ice). Nevertheless, a reasonable fit to the data from Chu and Chu (1999) is obtained using a Langmuir-Hinshelwood model for the uptake, which gives the expression:

$$\frac{1}{\gamma} = \frac{1}{\alpha_{\text{s}}} + \frac{1}{\Gamma_{\text{s}}}$$

with

$$\Gamma_{\text{s}} = \frac{4k_{\text{s}}[\text{HBr}]_{\text{s}}K_{\text{LangC}}(\text{HOCl})N_{\text{max}}(\text{HOCl})}{\bar{c}(1 + K_{\text{LangC}}(\text{HOCl})[\text{HOCl}]_{\text{g}})}$$

We recommend using $[\text{HBr}]_s = 3 \times 10^{14} \text{ cm}^{-2}$ at HBr pressures between 10^{-8} and 10^{-7} mbar and the expression: $[\text{HBr}]_s = 4.14 \times 10^5 \times [\text{HBr}]^{0.88} \text{ cm}^{-2}$ at pressures above 10^{-7} mbar (see data sheet V.A1.30), $N_{\text{max}} = 3 \times 10^{14} \text{ molecule cm}^{-2}$, $\alpha_s = 0.3$ and $k_s = 3.3 \times 10^{-15} \text{ cm}^2 \text{ molecule}^{-1}$. These parameters give the recommended expression for γ at 188 K, but this model cannot be used at other temperatures in the absence of an HBr adsorption isotherm at those temperatures.

References

Chu, L. and Chu, L. T.: J. Phys. Chem., 103A, 691, 1999.

V.A1.43

ClONO₂ + H₂O (ice surfaces) → HNO₃ + HOCl

Uptake coefficient data

Parameter	Temp./K	Reference	Technique/ Comments
$\gamma_0, \gamma_{ss}(\text{ClONO}_2)$			
$\gamma_{ss}=(9.0\pm 2.0)\times 10^{-3}$	185	Tolbert et al., 1987	Knud-MS (a)
$\gamma_{ss}=(6.0\pm 3.0)\times 10^{-2}$	200	Leu, 1988	CWFT (b)
$\gamma_{ss}=0.3(+0.7, -0.1)$	201	Hanson and Ravishankara, 1991	CWFT (c)
$\gamma_{ss}=(5.0\pm 4.0)\times 10^{-3}$	196	Leu et al., 1991	CWFT (d)
$\gamma_0=0.8(+0.2, -0.3)$	191	Hanson and Ravishankara, 1992	CWFT (e)
$\gamma_{ss}=0.30\pm 0.10$	191	Hanson and Ravishankara, 1993a	CWFT (f)
$\gamma_{ss}>3.0\times 10^{-2}$	188	Chu et al., 1993	CWFT (g)
$\gamma_{ss}=0.13$			
$\gamma_{ss}=(8.0\pm 2.0)\times 10^{-2}$	195	Zhang et al., 1994	CWFT (h)
$\gamma_0=0.2\pm 0.05$	180–200	Oppliger et al., 1997	Knud-MS (i)
$\gamma_{ss}=(3.0\pm 0.5)\times 10^{-2}$			
$\gamma_0=(9.0\pm 2.5)\times 10^{-2}$	218	Fernandez et al., 2005	CWFT-MS (j)
$\gamma_{ss}=(2.0\pm 0.5)\times 10^{-2}$			
$K_{\text{linC}}/\text{cm}$			
1.2×10^{-4}	218–228	Fernandez et al., 2005	CWFT-MS (j)

Comments

- (a) γ for reactive uptake ClONO₂ on pure ice prepared in situ by vapor deposition was measured at typical pressures $p(\text{ClONO}_2)=2.7\times 10^{-5}$ and $p(\text{H}_2\text{O})=1.9\times 10^{-3}$ mbar.
- (b) Vapour deposited ice. Significant diffusion corrections had to be made using calculated diffusion coefficients for ClONO₂ in He; cited standard deviation of γ includes the uncertainty in the estimation of the diffusion coefficient of ClONO₂ in He at 200 K.
- (c) Vapour deposited ice with CIMS detection. At high uptake coefficient ($\gamma\geq 0.1$) required corrections for gas-phase diffusion using calculated diffusion coefficients for ClONO₂ in He. Rapid saturation of the ice surface for ClONO₂ uptake was observed at concentrations as low as 2×10^9 molecule cm⁻³.
- (d) The substrates were prepared in situ from the gas phase by condensation at 196K resulting in film thicknesses of 70 μm . The surface areas and bulk densities of condensed films were measured ex situ in addition to the measurement of their FTIR absorption spectra.
- (e) Details under (c). Ice films (thickness 15–25 μm) were deposited from the vapor phase at 195K. No dependence of γ on thickness.
- (f) Details under (e). This study was undertaken to supplement the original work on ice and HNO₃-doped (NAT) surfaces to further confirm the independence of γ on the substrate thickness.
- (g) Details under (d). Vapour deposited ice film 3.7 to 34.7 μm thick, calibrated gravimetrically. The morphology of the ice films were layers of μm -sized granules whose internal surface was measured using BET gas adsorption measurements. Minimum $p(\text{ClONO}_2)=1.9\times 10^{-7}$ mbar.
- (h) Fast flow reactor coupled to a differentially pumped beam-sampling MS. Nucleation and growth of hexagonal water ice on top of the reactant NAT film was observed for saturation ratios of H₂O ≥ 1.5 . Under these conditions the reaction efficiency increased significantly.

- (i) Knudsen flow reactor using both steady-state and pulsed admission of ClONO₂ onto ice film (20 μm thick) generated from vapor phase deposition. γ is extremely prone to saturation of the ice.
- (j) Frozen film ice. Uptake monitored by following ClONO₂ loss and HOCl formation. HOCl partitioned rapidly to gas-phase. γ decreased with exposure time until surface HNO₃ product saturated according to Langmuir equilibrium surface coverage for HNO₃. The observed kinetics were best described by a Langmuir-Hinshelwood mechanism, with values of k_s and K_{linC} at 218 K obtained by fitting to the experimental data using a numerical model. The cited value of K_{linC} was obtained using $N_{\text{max}}=3 \times 10^{14}$ molecule cm⁻².

Preferred values

Parameter	Value	T/K
$\alpha_s(\text{ClONO}_2)$	0.5	180–230
$k_s K_{\text{linC}}/\text{cm}^3 \text{ molecule s}^{-1}$	$5.2 \times 10^{-17} \exp(2032/T)$	180–230
$k_s/\text{cm}^2 \text{ molecule}^{-1} \text{ s}^{-1}$	5×10^{-17}	218
<i>Reliability</i>		
$\Delta(\alpha_s)$	± 0.3	180–230

Comments on preferred values

Uptake of ClONO₂ on ice films is followed by rapid reaction with H₂O to form HOCl and HNO₃ in a surface reaction. At stratospheric temperatures HOCl mainly partitions into the gas phase, but HNO₃ remains at the surface until the surface layer saturates either by physical adsorption of nitric acid molecules or by formation of ions or hydrates (NAT). The presence of HNO₃ on the surface inhibits the rate of reactive uptake leading to a strongly time dependent uptake coefficient of ClONO₂ decreasing from $\gamma > 0.1$ on a clean ice surface to a steady state uptake coefficient of < 0.02 or less when HNO₃ product has built up to saturation. The uptake coefficients on NAD and NAT substrates at < 200 K are even lower and show a strong decline with decreasing relative humidity, confirming the inhibiting effect of surface HNO₃.

The preferred value for the surface accommodation coefficient is an average of the initial uptake coefficient measured at low $p(\text{ClONO}_2)$ in the studies of Hanson and Ravishankara (1992) and Oppliger et al. (1997), using different techniques. These measurements agree reasonably well, considering the uncertainties arising from gas phase diffusion effects in the flow tube study and unavoidable inhibition by surface HNO₃ in the static Knudsen cell study.

For uptake on surfaces with HNO₃ present in the ice stability region a parameterisation for γ using a Langmuir-Hinshelwood model is recommended, based on the analysis and results of Fernandez et al. (2005):

$$\gamma(\text{ClONO}_2) = 1/(1/\alpha_s + c/4k_s K_{\text{linC}}[\text{H}_2\text{O}]_s)$$

The recommended values of K_{linC} (ClONO₂) and the surface reaction rate coefficient of k_s at 218 K are those derived by Fernandez et al. (2005).

The surface concentration of water molecules $[\text{H}_2\text{O}]_s$ can be estimated assuming that the surface sites are blocked by adsorbed HNO₃ with an effective area of $1.23 \times 10^{-15} \text{ cm}^2 \text{ molecule}^{-1}$. Thus: $[\text{H}_2\text{O}]_s/\text{molecule cm}^{-2} = 1 \times 10^{15} - 3 \times N_{\text{max}} \times \theta \text{ molecule m}^{-2}$, where θ is the fractional surface coverage of nitric acid and $N_{\text{max}}=2.7 \times 10^{14} \text{ molecule cm}^{-2}$ for $[\text{HNO}_3]_s$ at saturation, taken from the present evaluation.

The temperature dependence of the product $k_s K_{\text{linC}}$ was obtained by fitting to experimental γ_0 values in the range 218–190 K using the Langmuir Hinshelwood expression. Uptake coefficients for different $[\text{HNO}_3]$ can be calculated using the recommended Langmuir expression for θ_{HNO_3} (see data sheet V.A1.12). The parameterisation gives a reasonable representation at $T \geq 200$ K but overestimates the uptake coefficient in the NAT stability region.

References

- Abbatt, J. P. D. and Molina, M. J.: J. Phys. Chem., 96, 7674, 1992.
- Barone, S. B., Zondlo, M. A., and Tolbert, M. A.: J. Phys. Chem. A., 101, 8643, 1997.
- Chu, L. T., Leu, M.-T., and Keyser, L. F.: J. Phys. Chem., 97, 12798, 1993.
- Fernandez, M. A., Hynes, R. G., and Cox, R. A.: J. Phys. Chem. A., 109, 9986, 2005.
- Hanson, D. R. and Ravishankara, A. R.: J. Geophys. Res., 96, 5081, 1991.

- Hanson, D. R. and Ravishankara, A. R.: *J. Geophys. Res.*, 98, 22931, 1993.
Hanson, D. R. and Ravishankara, A. R.: *J. Phys. Chem.*, 96, 2682, 1992.
Hanson, D. R. and Ravishankara, A. R.: *J. Phys. Chem.*, 97, 2802, 1993a.
Leu, M.-T.: *Geophys. Res. Lett.*, 15, 17, 1988.
Leu, M.-T., Moore, S. B., and Keyser, L. F.: *J. Phys. Chem.*, 95, 7763, 1991.
Oppliger, R., Allan, A., and Rossi, M. J.: *J. Phys. Chem. A.*, 101, 1903, 1997.
Tolbert, M. A., Rossi, M. J., Malhotra, R., and Golden, D. M.: *Science*, 238, 1258, 1987.
Zhang, R., Jayne, J. T., and Molina, M. J.: *Phys. Chem.*, 98, 867, 1994.
Zondlo, M. A., Barone, S. B., and Tolbert, M. A.: *J. Phys. Chem. A.*, 102, 5735, 1998.

V.A1.44



Uptake coefficient data

Parameter	Temp./K	Reference	Technique/ Comments
$\gamma_0, \gamma_{ss}(\text{ClONO}_2)$			
$\gamma_{ss}=0.27(+0.73, -0.13)$	200	Leu, 1988	CWFT-MS (a)
$\gamma_{ss}=0.3(+0.7, -0.1)$	191	Hanson and Ravishankara, 1992	CWFT-CIMS (b)
$\gamma_{ss}=0.27\pm 0.19$	188	Chu et al., 1993	CWFT-MS (c)
$\gamma_0=0.64\pm 0.07$	180	Oppliger et al., 1997	Knud-MS (d)
$\gamma_0=0.27\pm 0.07$	200		
$\gamma_0 > 0.3$ ($p(\text{HCl})=(0.26-10.6)\times 10^{-6}$ mbar)	201	Lee et al., 1999	CWFT-CIMS (e)
$\gamma_0 > 0.1$ ($p(\text{HCl})=(1.3-2.6)\times 10^{-6}$ mbar)	201	Lee et al., 1999	Aerosol FT-CIMS (f)
$\gamma_{ss} > 0.1$ ($p(\text{HCl})=1.33\times 10^{-6}$ mbar)	218, 228	Fernandez et al., 2005	CWFT-MS (g)
$\gamma_{ss}=0.023\pm 0.012$ ($p(\text{HCl})=1.33\times 10^{-7}$ mbar)*	218		
$\gamma_{ss}=0.078\pm 0.025$ ($p(\text{HCl})=8.11\times 10^{-7}$ mbar)*	218		
$\gamma_{ss}=0.020\pm 0.004$ ($p(\text{HCl})=5.85\times 10^{-7}$ mbar)*	228		
$\gamma_{ss}=0.040\pm 0.007$ ($p(\text{HCl})=1.46\times 10^{-6}$ mbar)*	228		
*ice doped with 1.33×10^{-6} mbar HNO_3			
$\gamma_{ss} > 0.1$ ($p(\text{HCl})=1.33\times 10^{-6}$ mbar)	196	McNeil et al., 2006	CWFT-CIMS (h)
$\gamma_{ss}=0.014\pm 0.0051$ ($p(\text{HCl})=1.33\times 10^{-6}$ mbar)	218		

Comments

- (a) Ice was condensed from the vapor phase onto the cold wall of the flow tube (1 gr total) together with HCl vapor to obtain mole fractions X_{HCl} in the range 0.37 to 7.1% relative to H_2O . The reaction probability γ increased from 0.06, the value obtained for the reaction $\text{ClONO}_2 + \text{H}_2\text{O} \rightarrow \text{HNO}_3 + \text{HOCl}$, to a constant value of 0.27 independent of X_{HCl} for the range 1.5 to 7.1% (see Table). Significant diffusion corrections had to be made using calculated diffusion coefficients for ClONO_2 in He.
- (b) Vapour deposited ice with CIMS detection. The uptake of ClONO_2 , HCl and the formation of the reaction product Cl_2 , were studied at constant $[\text{HCl}]$ (2×10^{10} molecule cm^{-3}) with ClONO_2 concentration ranging from 6×10^9 to 3×10^{10} molecule cm^{-3} . The authors argue in favor of a direct reaction between ClONO_2 and HCl rather than a reaction via the intermediate HOCl in view of the high value for γ . The high uptake coefficient ($\gamma \geq 0.1$) required corrections for gas-phase diffusion using calculated diffusion coefficients for ClONO_2 in He.
- (c) Ice film deposited He- H_2O vapor mixture to thicknesses ranging from 3.7 to 34.7 μm which were both calculated and calibrated gravimetrically. The morphology of the ice films were layers of μm -sized granules whose internal surface was measured using BET gas adsorption measurements. $p(\text{ClONO}_2)$ ranged from 8.6×10^{-8} to $\sim 1.3\times 10^{-6}$ mbar and $p(\text{HCl})$ from 2.1×10^{-7} to 3.1×10^{-6} mbar. The diffusion correction amounted to a factor exceeding ten in some cases.
- (d) Both steady-state and real-time pulsed valve admission of ClONO_2 to Knudsen flow reactor coupled to MS detector. The ice samples were generated from vapor phase deposition of approximately 2×10^6 monolayers of H_2O (20 μm thickness). Pulses of 10^{14} molecules interacting with HCl-doped ice at excess HCl conditions resulted in prompt formation of Cl_2 thus pointing to a direct mechanism of product formation. γ has a negative temperature dependence that parallels the change in solubility of HCl in ice with temperature.

- (e) Uptake experiment in a laminar flow tube with both vapour-deposited and frozen film ice. Comparable amounts of HCl were taken up on smooth as well as on rough ice films on the order of 1 to 4×10^{14} molecules cm^{-2} for HCl ranging from 1.3×10^{-7} to 5×10^{-6} mbar, with only a weak dependence on p_{HCl} for these conditions. The measured uptake coefficient of ClONO_2 is only a lower limit because of diffusion limitations but this showed practically no dependence on $p(\text{HCl})$. An ionic reaction mechanism was proposed, which assumes significant mobility of the reactants close to the surface of the condensed phase in a liquid-like layer of $\text{HCl}/\text{H}_2\text{O}$.
- (f) Uptake experiment conducted at 1 bar in an aerosol flow tube equipped with CIMS detection for reactant and product. Aerosols consisted of 1 – $5 \mu\text{m}$ single ice crystals. Similar conditions to (e) and similar results were obtained, i.e. no dependence of γ on $p(\text{HCl})$, within experimental error.
- (g) Uptake of chlorine nitrate in the presence of HCl was measured on a frozen-film of pure ice and ice doped with continuous flow of HNO_3 ($p(\text{HNO}_3)=1.33 \times 10^{-6}$ mbar) in the temperature range 208 – 228 K, with $p(\text{ClONO}_2) < 1 \times 10^{-6}$ mbar. On pure ice uptake was diffusion limited and gas phase Cl_2 was formed with a yield of 100% . On HNO_3 -doped ice at low $p(\text{HCl})$, γ_{max} was linearly dependent on surface coverage of HCl which was related to $p(\text{HCl})$ by a 2-species (HCl/HNO_3) Langmuir isotherm. At low $p(\text{HCl})$, HOCl was observed as a product in addition to Cl_2 , indicating competition between reaction of ClONO_2 with surface water and HCl. Kinetics of Cl_2 formation were consistent with an Eley-Rideal mechanism.
- (h) The ice surfaces were hollow cylinders of zone-refined ice prepared externally and inserted into the flow tube. The zone refining formed ice with few large crystals which were amenable to probing of surface phase change induced by HCl adsorption by ellipsometry. The uptake coefficient was measured at constant reactant conditions ($p(\text{HCl})=1.33 \times 10^{-6}$ mbar, $p(\text{ClONO}_2)=6 \times 10^7$ mbar) at two temperatures corresponding to surface disorder (196 K) and no surface disorder (218 K). Reactive uptake was found to be enhanced at the lower temperature and this is attributed to HCl being more readily available for reaction in the quasi liquid layer formed by HCl near its phase boundary.

Preferred values

Parameter	Value	T/K
$\gamma_{\text{gs}}(\text{ClONO}_2)$	0.24	185–230
$\gamma_{\text{s}}(\text{ClONO}_2)$	$\gamma_{\text{gs}} \times \theta_{\text{HCl}}$	185–230
<i>Reliability</i>		
$\Delta(\gamma_{\text{gs}})$	± 0.1	

Comments on preferred values

Heterogeneous reaction of ClONO_2 with HCl occurs rapidly on ice surfaces at all atmospherically relevant temperatures. Cl_2 is the sole product of this reaction, and is released promptly to the gas phase (Oppliger et al., 1997). Most earlier studies were at temperatures < 200 K and HCl concentrations corresponding to stability regions of the phase diagram for either HCl hydrate or supercooled $\text{HCl}/\text{H}_2\text{O}$ solutions, which McNeill et al. (2006) have shown can be formed by surface melting induced by exposure to HCl. All studies under these conditions with $p(\text{HCl}) > p(\text{ClONO}_2)$ gave a reactive uptake coefficient ≥ 0.3 , which was practically independent of $p(\text{HCl})$. The lower limit for γ results from the large correction needed for the influence of gas phase diffusion on the measured loss rate coefficients. The Knudsen cell results (Oppliger et al., 1997), which do not require correction for gas phase diffusion, are considered the most accurate and these data show a small negative temperature dependence. An Arrhenius fit to these data gives: $\gamma_{\text{gs}}=1.14 \times 10^{-4} \exp(1553/T)$, which provides values consistent with the upper limits from flow tube studies at comparable $p(\text{HCl})$ and temperature. However in view of the uncertainties and the spread of reported values, a temperature independent value is recommended for γ_{max} .

At higher temperatures, at low $p(\text{HCl})$ and at $p(\text{HCl}) \leq p(\text{ClONO}_2)$ uptake coefficients decline and depend on $p(\text{HCl})$ (Oppliger et al., 1997; Fernandez et al., 2005). Also it is established that the presence of HNO_3 in/on the surface layer of ice, either added or produced by surface reaction of ClONO_2 , reduces the uptake rate (Hanson and Ravishankara, 1992; Oppliger et al., 1997; Fernandez et al., 2005). Fernandez et al. (2005) showed that this is due to reduced HCl surface coverage in the presence of HNO_3 . The mechanism of the reaction has been discussed in several of the cited studies. Hanson and Ravishankara (1992) showed that formation of HOCl was not intermediate in the fast reaction forming Cl_2 , which occurred by a direct surface reaction. Oppliger et al. (1997) also concluded that reaction involved a direct surface reaction of ClONO_2 with Cl^- ions.

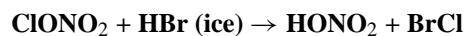
Carslaw and Peter (1997) described the reaction rate for ClONO₂+HCl and related stratospheric reactions on ice particles in terms of surface coverage of HCl, using a modified Langmuir-Hinshelwood model. This approach was used by Fernandez et al. (2005) to model their reactive uptake coefficients measured on HNO₃-doped ice, but their results were best described in terms of an Eley-Rideal mechanism without competitive adsorption of ClONO₂ prior to surface reaction. This forms the basis of the recommended parameterisation of the reactive uptake coefficient for ClONO₂ as a function of [HCl]_g given by the product of γ_{gs} and the dimensionless surface coverage θ_{HCl} . In the ice stability region ($T \geq 200$ K) this coverage can be calculated for a fresh ice surface and in the presence of co-adsorbed HNO₃ using a single site Langmuir model with the appropriate partition coefficients for HCl and HNO₃:

$$\theta_{\text{HCl}} = \frac{K_{\text{LangC}}[\text{HCl}]}{1 + K_{\text{LangC}}[\text{HCl}] + K_{\text{LangC}}[\text{HNO}_3]}$$

Calculated values of γ given by this parameterisation for $p(\text{HCl})=10^{-6}$ and 10^{-7} Torr reproduces experimental values of γ for reactive uptake of ClONO₂ as a function of $p(\text{HCl})$ on nitric acid doped ice at 218 and 228 K; θ_{HCl} can be calculated using the partition coefficient expression: $K_{\text{linC}}(\text{HCl})=1.3 \times 10^{-5} \exp(4600/T)$ cm with $N_{\text{max}}=3 \times 10^{14}$ molecule cm⁻² derived from the same experimental study (Fernandez et al., 2005). γ was assumed to have 2 components due to reaction of ClONO₂ with H₂O and HCl.

References

- Abbatt, J. P. D. and Molina, M. J.: *J. Phys. Chem.*, 96, 7674, 1992.
 Chu, L. T., Leu, M.-T., and Keyser, L. F.: *J. Phys. Chem.*, 97, 12798, 1993.
 Carslaw, K. S. and Peter, Th.: *Geophys. Res. Lett.*, 24, 1743, 1997.
 Fernandez, M. A., Hynes, R. G., and Cox, R. A.: *J. Phys. Chem. A.*, 109, 9986, 2005.
 Hanson, D. R. and Ravishankara, A. R.: *J. Geophys. Res.*, 98, 22931, 1993.
 Hanson, D. R. and Ravishankara, A. R.: *J. Phys. Chem.*, 96, 2682, 1992.
 Hanson, D. R. and Ravishankara, A. R.: *J. Phys. Chem.*, 98, 5728, 1994.
 Lee, S.-H., Leard, D. C., Zhang, R., Molina, L. T., and Molina, M. J.: *Chem. Phys. Lett.*, 315, 7, 1999.
 Leu, M.-T., Moore, S. B., and Keyser, L. F.: *J. Phys. Chem.*, 95, 7763, 1991.
 Leu, M.-T.: *Geophys. Res. Lett.*, 15, 17, 1988.
 McNeill, V. F., Loerting, T., Geiger, F. M., Trout, B. L., and Molina, M. J.: *Proc. Nat. Acad. Sci. (USA)*, 103, 9422–9427, 2006.
 Oppliger, R., Allan, A., and Rossi, M. J.: *J. Phys. Chem. A.*, 101, 1903, 1997.

V.A1.45**Uptake coefficient data**

Parameter	Temp./K	Reference	Technique/Comments
γ_{ss}			
≥ 0.3	201	Hanson and Ravishankara, 1992	CWFT-CIMS (a)
0.56 ± 0.11	180–200	Allanic et al., 2000	Knud-MS(b)

Comments

- (a) Ice layers 2–10 μm thick were condensed from the vapor phase. An efficient reaction with $\gamma_{ss} \geq 0.3$ was observed on pure ice, HNO₃-treated ice and on cold Pyrex at 50% r.h., where γ scales with the amount of adsorbed HBr. No difference in reactivity was found between pure ice and HNO₃-treated ice. Significant diffusion corrections had to be made using calculated diffusion coefficients for ClONO₂ in He.
- (b) The ice samples were generated from vapor phase deposition. Fast secondary interfacial reactions prevent the observation of the expected primary product BrCl.

Preferred values

Parameter	Value	T/K
$\gamma_{gs}(\text{ClONO}_2)$	0.56	180–200
$\gamma_s(\text{ClONO}_2)$	$\gamma_{gs}(\text{ClONO}_2) \times \theta_{\text{HBr}}$	180–200
θ_{HBr}	$4.14 \times 10^{-10} [\text{HBr}]^{0.88}$ at 188 K	180–200
<i>Reliability</i>		
$\Delta(\gamma_{gs})$	± 0.2	185–210

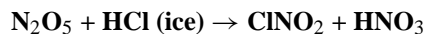
Comments on preferred values

Heterogeneous reaction of ClONO₂ with HBr occurs rapidly on ice surfaces at temperatures relevant for the UTLS. BrCl is a likely product of this reaction, but has not been observed in the gas phase due to secondary reactions (Allanic et al., 1997). Both cited studies were at temperatures and HBr concentrations corresponding to stability regions of the phase diagram for HBr hydrate (Chu and Chu, 1999). Under these conditions with $p_{\text{HBr}} > p_{\text{ClONO}_2}$, the reactive uptake coefficient was practically independent of temperature and p_{HBr} , except on Pyrex when γ increased with [HBr]. The Knudsen cell results (Oppliger et al., 1997) which do not require correction for gas phase diffusion form the basis of our recommendation for γ_0 .

Carslaw and Peter (1997) described the reaction rate for ClONO₂+HX and related stratospheric reactions on ice particles in terms of surface coverage of HX, using a modified Langmuir-Hinshelwood model. As for the ClONO₂+HCl reaction the reactive uptake coefficient of ClONO₂ as a function of [HBr]_g is given by the product of γ_0 and the dimensionless surface coverage of HBr, i.e. assuming an Eley-Rideal type mechanism. HBr adsorption doesn't follow a Langmuir model under the laboratory experimental conditions used (see data sheet for HBr+ice). The recommended expression for the reactive uptake coefficient at 188 K uses the current IUPAC recommended parameterisation for $\theta_{\text{HBr}} = 4.14 \times 10^{-10} [\text{HBr}]^{0.88}$ at this temperature. This is only valid for surface coverages up to $\theta_{\text{HBr}} = 1$, calculated with this isotherm.

References

- Allanic, A., Oppliger, R., van den Bergh, H., and Rossi, M. J.: Z. Phys. Chem., 214, 1479, 2000.
 Chu, L. T. and Chu, L.: J. Phys. Chem. A., 103, 384, 1999.
 Carslaw, K. S. and Peter, T.: Geophys. Res. Lett., 24, 1743, 1997.
 Hanson, D. R. and Ravishankara, A. R.: J. Phys. Chem., 96, 9441, 1992.

V.A1.46**Experimental data**

Parameter	Temp./K	Reference	Technique/Comments
γ			
0.028 (HCl mole fraction=0)	195	Leu, 1988	CWFT-MS (a)
0.037 (HCl mole fraction=0.015)			
0.063 (HCl mole fraction=0.04)			
$> 1 \times 10^{-3}$	185	Tolbert et al., 1988	Knudsen-MS (b)
0.0048–0.035	200	Seisel et al., 1998	Knudsen-MS (c)

Comments

- (a) Flow reactor at 0.36–0.67 mbar. The HCl containing ice film was made by vapour deposition of both gases simultaneously, resulting in HCl mole fractions of 0.015 and 0.04. N_2O_5 (initial concentration $\approx 1 \times 10^{-12}$ molecule cm^{-3}) detected as its NO_2^+ ion-fragment (electron impact ionisation). γ was calculated using the geometric ice surface area.
- (b) The HCl containing ice film was made by vapour deposition of both gases simultaneously, resulting in HCl mole fractions of 0.07 and 0.14. N_2O_5 (initial concentration $\approx 10^{-13}$ molecule cm^{-3}) detected as its NO^+ and NO_2^+ ion-fragments. The uptake coefficient (calculated using geometric ice surface area) is suggested to be a lower limit due to the non specific detection of N_2O_5 .
- (c) Uptake of N_2O_5 to ice made by vapour deposition or frozen solutions. HCl flows were varied, the concentrations were not reported by the authors. Calculations using Knudsen reactor parameters and escape rate for N_2O_5 show that the HCl concentrations were between 10^{11} and 10^{12} molecule cm^{-3} .

Preferred values

No Recommendation.

Comments on preferred values

Leu (1988) combined the two experimental values of γ on HCl-ice with his own data on a pure ice surface to show a distinct trend in γ with HCl mole fraction. As the surface concentration of HCl is unknown in these experiments, the dependence of γ on [HCl] (gas phase) cannot be extracted from the dataset. Despite the use of larger HCl mole fractions, the uptake coefficients quoted by Tolbert et al. (1988) are significantly lower than the values of Leu et al. Both Leu et al. (1988) and Tolbert et al. (1988) detected ClNO_2 as product, but did not quantify the yield. Seisel et al. (1998) found that small amounts of HCl increased the N_2O_5 uptake coefficient slightly, the results in qualitative agreement with those of Leu (1988). At high concentrations of HCl (which induced surface melting) the uptake coefficient increased as did the yield of ClNO_2 . The use in these studies of high concentrations of N_2O_5 and HCl and low temperatures, and the fact that N_2O_5 may hydrolyse to HNO_3 makes assessment of the true thermodynamic state of the surface difficult. However, it appears that atmospheric concentrations of HCl will not significantly affect the rate of uptake of N_2O_5 to an ice surface.

The production of ClNO_2 could not be confirmed in the studies of Sodeau et al. (2000), who co-deposited H_2O , N_2O_5 and HCl at 85 K and analysed the surface using RAIRS.

References

- Leu, M. T.: Geophys. Res. Lett., 15, 851–854, 1988.
- Seisel, S, Flueckiger, B., and Rossi, M. J.: Berichte der Bunsen-Gesellschaft 102, 811, 1998.
- Sodeau, J. R., Roddis, T. B., and Gane, M. P.: J. Phys. Chem. A., 104, 1890–1897, 2000.
- Tolbert, M. A., Rossi, M. J., and Golden, D. M.: Science, 240, 1018–1021, 1988.

V.A1.47**N₂O₅ + HBr (ice) → products****Experimental data**

Parameter	Temp./K	Reference	Technique/Comments
γ (0.02–0.15)	180–200	Seisel et al., 1998	Knudsen-MS/LIF (a)

Comments

- (a) Steady state and pulsed valve experiments, with the ice surface formed both by vapour deposition and freezing of liquid water. HBr was either present in the ice film during freezing (of a 0.1 M aqueous solution), or was introduced from the gas phase.

Preferred values

No Recommendation.

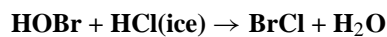
Comments on preferred values

The study of Seisel et al. (1998) is the only published study of the title reaction. They determined uptake coefficients for N₂O₅ on ice that were dependent on the amount of HBr (gas phase concentrations of $\approx 10^{10}$ – 10^{11} molecule cm⁻³) available for the reaction and which varied between 0.02 and 0.15. At the lower range of HBr concentrations the uptake coefficient approached that of N₂O₅ on pure ice. The same authors measured Br₂ and HONO as the major gas phase products of the title reaction, with yields of up to 80% (at high [HBr]) with the rest removed by hydrolysis. The non-observation of the expected BrNO₂ product and the formation Br₂ and HONO was attributed to the secondary reaction of BrNO₂ with HBr. The lack of knowledge of the thermodynamic state of the surface, and the fact that N₂O₅ was in excess of HBr makes this dataset unsuitable for parameterisation of the effect of adsorbed HBr on the uptake of N₂O₅ to an ice surface. Note however, that under normal atmospheric HBr concentrations, the title reaction will not compete with N₂O₅ hydrolysis.

References

Seisel, S., Flückiger, B., and Rossi, M. J.: Ber. Bunsen Ges. Phys. Chem., 102, 811–820, 1998.

V.A1.48



Uptake coefficient data

Parameter	Temp./K	Reference	Technique/Comments
$\gamma, \gamma_{\text{ss}}$ (HOBr)			
0.25(+0.10/−0.05)	228	Abbatt, 1994	CWFT-MS (a)
$(3.3 \pm 0.5) \times 10^{-1}$	190	Allanic et al., 1997	Knudsen-MS (b)
$(2.3 \pm 0.2) \times 10^{-1}$	200		
5×10^{-2} (pHCl= 1.8×10^{-7} mbar)	190	Chu and Chu, 1999	CWFT-MS (c)
0.23 (pHCl= 1.2×10^{-5} mbar)			
4×10^{-3} (pHCl= 5.6×10^{-7} mbar)	222		
0.19 (pHCl= 2×10^{-5} mbar)			
0.3±0.05	180–195	Chaix et al., 2000	Knudsen-MS (d)
>0.1; [HCl]= 8×10^{11}	205–227	Mössinger et al., 2002	CWFT-MS (e)
$\gamma_{\text{ss}}=0.005 \pm 0.002$; [HCl] ₀ = 5.8×10^{11}	227		

Comments

- (a) Frozen film ice surface; [HOBr]~ 10^{12} molecule cm^{-3} , generated in situ by reaction of Br₂ with OH. [HCl]₀=(1–2)× 10^{12} molecule cm^{-3} which corresponded to a fractional surface coverage of >0.95 at 228 K, based on the recommended K_{linC} (data sheet V.A1.27). Gas phase BrCl formation kinetics matched the HOBr decay.
- (b) ≈20 μm thick ice film made by vapour deposition and located in a Knudsen reactor operated in either continuous flow or pulsed mode. Uptake coefficients cited obtained at short (0.3 s) residence time avoiding saturation effects. p(HCl) used was sufficient to give at least 1 ML coverage and all HOBr taken up was converted to BrCl.
- (c) The ice film of typical thickness of 28 μm was grown from H₂O vapor condensation in the temperature range 190 to 240 K. Uptake coefficients were determined from HOBr loss and BrCl formation, giving comparable values. Both γ_{HOBr} and γ_{BrCl} decreased substantially with decreasing p(HCl) from 2×10^{-5} mbar down to 2×10^{-7} mbar.
- (d) Ice surfaces formed by vapour deposition (type C) freezing bulk solutions of distilled water either rapidly (type B) or slowly (type SC), the latter with the intention of forming single-crystalline ice. Water vapour was continuously added to maintain the ice films during experiments. Both pulsed-valve and continuous flow experiments were performed on the different types of HX-doped ice samples, using two sources of HOBr. Typical flow rates of HX used to dope the surface of ice ranged from 10^{14} to 10^{16} molecule s^{-1} leading to the deposition of 0.5 to 10 formal monolayers of HX onto ice depending on the deposition time. In all cases the uptake of HOBr led to rapid and quantitative production of BrCl with the cited uptake coefficient.
- (e) The ice coating was produced by freezing a liquid H₂O film and HOBr was stored as an aqueous solution at 273 K. [HOBr] and [HCl] varied between (2–22)× 10^{11} and (4–8)× 10^{11} molecule cm^{-3} , respectively. The lower limit of $\gamma > 0.1$ reflects diffusion limited uptake. For [HCl]<[HOBr] the HOBr uptake was time and concentration dependent owing to the changing HCl surface coverage. BrCl was observed as product. Evidence for an Ely Rideal mechanism was presented.

Preferred values

Parameter	Value	T/K
γ_{gs} (HOBr)	0.25	185–210
Reliability		
$\Delta(\gamma_{\text{gs}})$	±0.05	185–210

Comments on preferred values

All studies report rapid uptake of HOBr onto ice films doped with HCl. BrCl is the sole product with a yield of 100%. The conditions of these experiments mostly corresponded to near maximum coverage of HCl in the ice or HCl hydrate stability region. The reported maximum values of γ at high [HCl] in the temperature range 180–228 K are in reasonably good agreement, with a slight tendency to increase with decreasing temperature. We recommend a temperature independent value of γ_{\max} , which is a mean of the values obtained from all studies cited and the T range is extended to 220 K.

Chu and Chu (1999) observed a dependence of the uptake coefficient on initial [HCl] and Mössinger et al. (2002) found evidence for surface coverage dependence of the uptake coefficient when initial [HOBr] was in excess of [HCl], leading to significant HCl consumption. The kinetic dependence in both studies appears to be complex and the data are not well fitted by either an Eley-Rideal or Langmuir Hinshelwood mechanism. In particular neither model captures the observed fall-off in γ with initial p(HCl) assuming that surface coverage of HCl is given by the recommended IUPAC value of the [HCl] partition coefficient with $N_{\max}=3\times 10^{14}$ molecule cm^{-3} . This probably results from reagent depletion due to the surface reaction. Therefore we cannot recommend a reactive uptake coefficient for HOBr as a function of [HCl]_g.

References

- Abbatt, J. P. D.: Geophys. Res. Lett., 21, 665, 1994.
Allanic, A., Oppliger, R., and Rossi, M. J.: J. Geophys. Res., 102D, 23529, 1997.
Chaix, L., Allanic, A., and Rossi, M. J.: J. Phys. Chem. A., 104, 7268, 2000.
Chu, L. and Chu, L. T.: J. Phys. Chem. A., 103, 8640, 1999.
Mössinger, J. C., Hynes, R. G., and Cox, R. A.: J. Geophys. Res., 107, 4740, doi:10.1029/2002JD002151, 2002.

V.A1.49



Uptake coefficient data

Parameter	Temp./K	Reference	Technique/Comments
γ, γ_0			
0.12 ± 0.03	228	Abbatt, 1994	CWFT-MS (a)
≥ 1.5	230–240	Kirchner et al., 1997	CWFT-MS (b)
0.44	180	Chaix et al., 2000	Knudsen-MS (c)
0.39	185		
0.37	190		
0.305	195		
0.205	200		
0.16	205		

Comments

- (a) Frozen film ice surface; $[\text{HOBr}] \sim 10^{12}$ molecule cm^{-3} , generated in situ by reaction of Br_2 with OH. $[\text{HBr}]_0 = (1-2) \times 10^{12}$ molecule cm^{-3} which corresponded to a surface coverage of at least 10 formal ML at 188 K, based on the recommended K_{linC} (data sheet V.A1.27). Gas phase Br_2 formation kinetics matched the HOBr decay. Continuous steady state uptake rate observed.
- (b) Reflectron time-of-flight mass spectrometer used. The total pressure was in the range 5 to 20 mbar He. Ice films were produced by spraying water or aqueous solutions of HBr onto the interior walls of the cold flow tube. $[\text{HOBr}]$ was in the range 0.7 to 1.2×10^{13} molecule cm^{-3} .
- (c) Ice surfaces formed by vapour deposition (type C) freezing bulk solutions of distilled water either rapidly (type B) or slowly (type SC), the latter with the intention of forming single-crystalline ice. Water vapour was continuously added to maintain the ice films during experiments. Both pulsed-valve and continuous flow experiments were performed on the different types of HBr-doped ice samples, using two sources of HOBr. Typical flow rates of HBr used to dope the surface of ice ranged from 10^{14} to 10^{16} molecule s^{-1} leading to the deposition of 0.5 to 10 formal monolayers onto ice depending on the deposition time. In all cases the uptake of HOBr led to production of Br_2 . The cited uptake coefficients are the mean of values reported for type C and type B ice surfaces at each temperature, which were very similar.

Preferred values

Parameter	Value	T/K
$\gamma_{\text{gs}}(\text{HOBr})$	$4.8 \times 10^{-4} \exp(1240/T)$	180–230
Reliability		
$\Delta \log(\text{E/R})$	± 0.15	185–210

Comments on preferred values

All studies report rapid and continuous uptake of HOBr onto ice films doped with gaseous HBr. Under the conditions of these experiments both HBr and HOBr form stable hydrates on ice surfaces and no dependence of $\gamma(\text{HOBr})$ on $[\text{HBr}]$ was found. Br_2 is the sole product observed. The reported γ values in the temperature range 180–228 K are reasonably consistent and show a negative temperature dependence. The recommended expression for γ_{max} , is an Arrhenius fit to the data of Abbatt at 229 K and the mean of the values reported by Chaix et al. (2000) on vapour-deposited and frozen film ice at each temperature in the range 180–205 K. These values can be assumed to be independent of $[\text{HBr}]$ provided $[\text{HBr}]_0 > [\text{HOBr}]_0$.

References

Abbatt, J. P. D.: *Geophys. Res. Lett.*, 21, 665, 1994.

Chaix, L., Allanic, A., and Rossi, M. J.: *J. Phys. Chem. A.*, 104, 7268, 2000.

Kirchner, U., Benter, T., and Schindler, R. N.: *Ber. Bunsenges. Phys. Chem.*, 101, 975, 1997.

V.A1.50



Experimental data

Parameter	Temp./K	Reference	Technique/ Comments
γ			
>0.3	200±10	Hanson and Ravishankara, 1993	CWFT-CIMS (a)
0.25±0.07	190	Allanic et al., 1997	Knudsen-MS (b)
0.33±0.10	200		
$1.08 \times 10^{-3} \exp[(1040 \pm 130)/T]$ (ice type 1)	180-210	Aguzzi and Rossi, 2002	Knudsen-MS (c)
$5.32 \times 10^{-4} \exp[(1125 \pm 130)/T]$ (ice type 2)			
$1.16 \times 10^{-9} \exp[(3450 \pm 130)/T]$ (ice type 3)			

Comments

- (a) Ice surface prepared by vapour deposition and the geometric surface area was used to calculate the uptake coefficient. The formation of HOBr was observed as gas-phase product of the surface hydrolysis of BrONO₂ and displayed the same kinetics as BrONO₂ loss.
- (b) ≈20 μm thick ice film made by vapour deposition and located in a Knudsen reactor operated in either continuous flow or pulsed mode. Uptake coefficients reported were from pulsed experiments which suffered less from an interference by Br₂O (formed by the reaction of BrONO₂ with HOBr). At the prevailing BrONO₂ concentrations (≈1 × 10¹¹ molecule cm⁻³) and reaction times, no passivation of the ice surface was observed and HOBr formation was prompt.
- (c) Ice surfaces formed by vapour deposition (type 1) freezing bulk solutions of distilled water either rapidly (type 2) or slowly (type 3), the latter with the intention of forming single-crystalline ice. The temperature dependencies listed in the table were obtained by weighted, least squares fitting to tabulated data of Aguzzi and Rossi, 2002.

Preferred values

Parameter	Value	T/K
γ	$5.3 \times 10^{-4} \exp(1100/T)$	180–210
<i>Reliability</i>		
$\Delta(E/R)/\text{K}$	±250	210–250

Comments on preferred values

There is good agreement between the various groups (and different methods) on the uptake coefficient at 190 and 200 K. All studies agree that the reaction of BrONO₂ on an ice surface proceeds efficiently to form HOBr, which can be released into the gas-phase. The co-product, HNO₃, was not detected in these studies.

The most comprehensive dataset of Aguzzi et al. (2002) shows that the uptake coefficient on morphologically different ice surfaces displayed a negative dependence on temperature, indicative of a precursor mechanism in which a H₂OBr⁺·NO₃⁻ complex is formed (Gane et al., 2001; McNamara and Hillier, 2001) prior to dissociation to HOBr and HNO₃. The preferred expression for the temperature dependent uptake coefficient is that obtained by Aguzzi and Rossi (2002) using ice films of type 2 (presumably polycrystalline). The assumption that the geometric surface area is equal to that available for reaction should be good for this surface and the temperature dependence is rounded down slightly. The considerably steeper temperature dependence obtained using “single crystal” ice leads to a much lower value of the uptake coefficient at higher temperatures (factor of ≈5), though the agreement with the type 1 and type 2 ices at 190 K is satisfactory. The yield of HOBr released to the gas-phase was close to 100% at 200 and 210 K, decreasing to 10–20% at lower temperatures. The “lost” HOBr was released to the gas

phase when the ice film was subsequently warmed. The rate of HOBr release was reduced in the presence of nitric acid on the surface. This observation could be attributed to the reduction in surface H₂O or enhanced stabilisation of the complex when high levels of surface nitrate are present. The uptake coefficient was however found to be independent of HNO₃ adsorbed onto the ice, enabling a simple parameterisation .

References

- Aguzzi, A. and Rossi, M. J.: *J. Phys. Chem. A.*, 106, 5891–5901, 2002.
- Allanic, A., Oppliger, R., and Rossi, M. J.: *J. Geophys. Res.*, 102, 23529–23541, 1997.
- Gane, M. P., Williams, N. A., and Sodeau, J. R.: *J. Phys. Chem. A.*, 105, 4002–4009, 2001.
- Hanson, D. R. and Ravishankara, A. R.: Reactions of halogen species on ice surfaces, in: *The tropospheric chemistry of ozone in the polar regions*, edited by: Niki, H. and Becker, K. H., Springer-Verlag, Berlin-Heidelberg:, 1993.
- McNamara, J. P. and Hillier, I. H.: *J. Phys. Chem. A.*, 105, 7011–7024, 2001.

V.A1.51**Experimental data**

Parameter	Temp./K	Reference	Technique/Comments
γ			
0.32±0.1	190	Allanic et al., 1997	Knudsen-MS (a)
0.25±0.1	200		

Comments

- (a) $\approx 20 \mu\text{m}$ thick ice film made by vapour deposition and located in a Knudsen reactor operated in either continuous flow or pulsed mode. Ice surface was pre-treated with HCl before exposure to BrONO₂ (the flows of HCl and BrONO₂ were not concurrent). Values of the uptake coefficient listed in the Table are taken from pulsed valve experiments (which are in good agreement with continuous flow results). The amount of HCl on the surface was stated to be sufficient to result in phase change (surface melting).

Preferred values

Parameter	Value	T/K
γ	0.3	190–200
<i>Reliability</i>		
$\Delta\log\gamma$	0.3	190–200

Comments on preferred values

The preferred value of γ is taken from the single quantitative study of this parameter. At the experimental temperatures covered, the uptake coefficient for BrONO₂ on an ice surface containing HCl is essentially the same as that on pure ice (see BrONO₂+ice datasheet). When HCl is present, the uptake of BrONO₂ can form BrCl either directly from Reaction (R1) or via reaction of the HOBr product of Reaction (R2) with HCl (Reaction R3) (Hanson and Ravishankara, 1993; Allanic et al., 1997).



In their study of BrONO₂ uptake to ice/HCl surfaces, Allanic et al. (1997) observed prompt release of BrCl at short exposure time. HOBr appeared as a gas-phase product only when surface HCl had been depleted. The ratio of HOBr to BrCl released to the gas-phase thus depends on the surface concentration of HCl (and therefore on the gas-phase HCl concentration) and the surface residence time of HOBr. The experimental studies do not define the relative importance of release of HOBr versus BrCl under atmospheric conditions (e.g. HCl concentrations resulting in submonolayer coverages). As the formation of HOBr via hydrolysis is very efficient, it is possible that the direct formation of BrCl via Reaction (R1) will generally not take place in the atmosphere.

References

- Allanic, A., Oppliger, R., and Rossi, M. J.: J. Geophys. Res., 102, 23529–23541, 1997.
 Hanson, D. R. and Ravishankara, A. R.: Reactions of halogen species on ice surfaces, in: The tropospheric chemistry of ozone in the polar regions, edited by: Niki, H. and Becker, K. H., Springer-Verlag, Berlin-Heidelberg, 1993.

V.A1.52**Experimental data**

Parameter	Temp./K	Reference	Technique/Comments
γ $6.6 \times 10^{-3} \exp[(700 \pm 180)/T]$ (ice type 1, 2)	180–210	Aguzzi and Rossi, 2002	Knudsen-MS (a)

Comments

- (a) Ice surfaces formed by vapour deposition (type 1) freezing bulk solutions of distilled water either rapidly (type 2) or slowly (type 3), the latter with the intention of forming single-crystalline ice. The temperature dependence of γ listed in the table was obtained by weighted, least squares fitting to tabulated data of Aguzzi and Rossi, 2002.

Preferred values

Parameter	Value	T/K
γ	$6.6 \times 10^{-3} \exp(700/T)$	180–210
<i>Reliability</i>		
$\Delta(E/R)/K$	± 250	180–210

Comments on preferred values

There is only one study of the uptake of BrONO_2 to ice in the presence of HBr. At the high initial levels of HBr on the surface used in this study ($> 10^{16} \text{ cm}^{-2}$), the major product was Br_2 . As surface HBr was depleted, HOBr (formed by BrONO_2 hydrolysis) was also observed in the gas-phase. Note that the uptake coefficients in the presence of HBr are essentially the same as on pure ice so that no dependence of the overall uptake coefficient on HBr concentrations is anticipated. At low HBr concentrations (or surface coverages) as found in the atmosphere, it is likely that HOBr will be released into the gas phase before reacting with HBr to form Br_2 .

References

Aguzzi, A. and Rossi, M. J.: J. Phys. Chem. A., 106, 5891–5901, 2002.

V.A1.53

SO₂ + H₂O₂ – doped ice

Experimental data

Parameter	Temp./K	Reference	Technique/Comments
$\gamma(\text{SO}_2)$ (0.7–5.3) × 10 ⁻⁴ (3.0 wt % H ₂ O ₂ -ice film)	191	Chu et al., 2000	CWFT-MS (a)
~8.3 × 10 ⁻⁵ (3.0 wt % H ₂ O ₂ -ice film)	211		
(0.1–1.0) × 10 ⁻⁵ (0.8 wt % H ₂ O ₂ -ice film)	191		
(0.9–9.0) × 10 ⁻³ for $p(\text{SO}_2)$ fixed at 1.5 × 10 ⁻⁶ mbar and $p(\text{H}_2\text{O}_2)=2 \times 10^{-5}$ – 2.5×10^{-4} mbar	228	Clegg and Abbatt, 2001 (b)	CWFT-MS (b)
(30–1.0) × 10 ⁻³ for $p(\text{H}_2\text{O}_2)$ fixed at 8.7 × 10 ⁻⁵ mbar and $p(\text{SO}_2)=(0.3$ – $20) \times 10^{-6}$ mbar	228		

Comments

- (a) H₂O₂ doped ice surfaces were prepared by bubbling helium through H₂O₂ solutions (30 wt % or 3 wt %) into a flow tube at 190–211 K via a sliding injector. The resulting vapour deposited ice films were determined to contain 3 wt % and 0.8 wt % H₂O₂, respectively. The average film thickness was estimated to be ~2.5 μm. The SO₂ partial pressure ranged from 1.6 × 10⁻⁵ to 5.1 × 10⁻⁵ mbar for uptake experiments on water-ice. The initial uptake coefficients, γ_0 , were corrected for axial and laminar diffusion. Corrections for surface roughness were performed using a layered pore diffusion models, giving the "true" value for the uptake coefficient which are cited. These uptake coefficients decreased slightly with increasing SO₂ partial pressure at 191 K, and were constant at 211 K. The surface coverage of SO₂ on the 3.0 wt % H₂O₂ ice film ranged from 7 × 10¹³ to 4.7 × 10¹⁵ molecules/cm² as the temperature increased from 191 to 211 K at a constant SO₂ partial pressure of 1.7 × 10⁻⁶ mbar. It was shown by analysis of the exposed films by IC that SO₂ was converted to sulphate upon uptake into H₂O₂ – doped films.
- (b) Water-ice films were made by freezing a water-coated pyrex sleeve within the flow tube. Doped ice surfaces were prepared by flowing H₂O₂ over the ice film from the back of the flow tube until the entire length of the film surface was at equilibrium with the gaseous H₂O₂. A moveable sliding injector containing SO₂ was pulled back in stages over the ice film. The SO₂ and H₂O₂ partial pressure ranges are given in the table and in all cases, the H₂O₂ was the excess reagent. SO₂ uptake on H₂O₂-doped ice films was much larger than on pure ice and was irreversible. For a fixed SO₂ partial pressure of 1.5 × 10⁻⁶ mbar, the SO₂ reaction probability varied linearly with the H₂O₂ partial pressure up to 3 × 10⁻⁴ mbar. For a fixed H₂O₂ partial pressure of 8.7 × 10⁻⁵ mbar, the SO₂ reaction probability decreased with $p(\text{SO}_2)^{-0.7}$ in the range (0.27 to 17) × 10⁻⁵ mbar.

Preferred values

Parameter	Value	T/K
$k_s/\text{cm}^2 \text{ molecule}^{-1} \text{ s}^{-1}$	7.3×10^{-15}	228
$k_s K_{\text{linC}}(\text{SO}_2)/\text{cm}^3 \text{ molecule}^{-1} \text{ s}^{-1}$	$5.3 \times 10^{-18} \exp(2065/T)$	200–230
$K_{\text{linC}}(\text{H}_2\text{O}_2)/\text{cm}$	$2.1 \times 10^{-5} \exp(3800/T)$	200–240
$N_{\text{max}}/\text{molecule cm}^{-2}$	4.5×10^{14}	
<i>Reliability</i>		
$\Delta \log(k_s K_{\text{linC}}(\text{SO}_2))$	±0.3	228
$\Delta(E/R)/\text{K}$	±1000	200–298

Comments on preferred values

Both Chu et al. (2000) and Clegg and Abbatt (2001) observed that the SO₂ uptake is significantly enhanced by the presence of adsorbed H₂O₂. Unlike the reversible SO₂ uptake observed on pure water-ice, the uptake on H₂O₂-doped ice is irreversible. This is due to the reaction between H₂O₂ and SO₂ forming sulfates on the ice surface (Chu et al., 2000). However SO₂ loss rate was still time-dependent, declining as the surface was exposed. This was attributed to accumulation of H₂SO₄ products on the ice surface, which inhibits SO₂ uptake (see SO₂+ice data sheet). This is as observed in some of the Chu et al. (2000) experiments, but the dependence of γ on the SO₂ partial pressure is stronger and better defined in the experiments of Clegg and Abbatt (2001). Note that a direct comparison between the experimental results of Chu et al. (2000) and those of Clegg and Abbatt (2001) is difficult as H₂O₂ surface coverages were uncertain in the experiments of Chu et al. (2000) who used frozen solutions of H₂O₂.

Clegg and Abbatt (2001) suggested the following mechanism to explain their observations:



Equation (4) is considered to be the rate-determining step. The overall rate of reaction is then proportional to $p_{\text{SO}_2}^{0.5} \cdot p(\text{H}_2\text{O}_2)$, noting the square root dependence of the SO₂ surface coverage on the SO₂ partial pressure (see SO₂+ice data sheet), and the linear dependence on H₂O₂ coverage at low $p(\text{H}_2\text{O}_2)$. In terms of the reaction probability for SO₂, $\gamma(\text{SO}_2) \propto p_{\text{SO}_2}^{-0.5} p(\text{H}_2\text{O}_2)$.

However at low [SO₂], surface coverage of SO₂ on ice was approximately proportional to $p(\text{SO}_2)$, although the SO₂ reaction probability decreased with $p(\text{SO}_2)^{-0.7}$ at fixed H₂O₂ coverage, indicating complexity in the chemistry. For this evaluation we adopt a simple Langmuir-Hinshelwood formalism, with the uptake coefficient Γ_s given by:

$$\Gamma_{\text{sb}} = \frac{4k_s[\text{H}_2\text{O}_2]_s K_{\text{linC}}(\text{SO}_2)}{\bar{c}}$$

with

$$[\text{H}_2\text{O}_2]_s = N_{\text{max}} \frac{K_{\text{LangC}}(\text{H}_2\text{O}_2)[\text{H}_2\text{O}_2]}{1 + K_{\text{LangC}}(\text{H}_2\text{O}_2)[\text{H}_2\text{O}_2]}$$

An average value for the parameter $k_s = 7.3 \times 10^{-15} \text{ cm}^2 \text{ molecule}^{-1} \text{ s}^{-1}$ at 228 K was evaluated from the experimental [H₂O₂] dependence of γ measured by Clegg and Abbatt (2001) on neutral (pH=6) ice, together with the IUPAC recommended value of $K_{\text{linC}}(\text{SO}_2)$ (see SO₂+ice data sheet). This forms the basis of our recommendation, which should be applied only for SO₂ partial pressures below $\sim 1 \times 10^{-6}$ mbar. At higher SO₂ the following [SO₂] dependent expression for Γ_{sb} gives a better description of the uptake rates:

$$\Gamma_s = \frac{4k_s[\text{H}_2\text{O}_2]_s K(\text{SO}_2)}{\bar{c}([\text{SO}_2]_g^{0.5})}$$

where $K(\text{SO}_2)$ is given in the SO₂+ice data sheet (V.A1.15)

The strong influence of pH suggests that as H₂SO₄ builds up with each exposure of SO₂ to the H₂O₂-doped surfaces, the surface protons inhibit Reaction (R3), the dissociation of SO₂. This leads to less gas-phase SO₂ adsorbing to the ice surface and hence a lower reaction probability. Clegg and Abbatt (2001) estimate that about 10¹⁴–10¹⁵ molecules/cm² (i.e. approx 1 monolayer) of H₂SO₄ need to be formed before the SO₂+H₂O₂→H₂SO₄ reaction shuts off (i.e., before the surface becomes poisoned with protons).

References

- Chu, L., Diao, G., and Chu, L. T.: J. Phys. Chem. A., 104, 7565, 2000.
Clegg, S. M. and Abbatt, J. P. D.: Atmos Chem. Phys., 1, 73, 2001.

V.A1.54**ClOOCl + HCl (ice) → Cl₂ + products****Experimental data**

Parameter	Temp./K	Reference	Technique/Comments
γ ₀			
6 × 10 ⁻³ (0.026 Torr HCl)	226	De Haan and Birks, 1997	CWFT-MS (a)
2 × 10 ⁻⁴ (0.016 Torr HCl)			

Comments

- (a) Flow tube reactor using electron-impact MS. ClOOCl was generated in the self reaction of ClO at low temperatures and detected as Cl₂O₂⁺. The ice film (300–900 μm) was made by “brushing” water onto the cold flow tube surface and the geometric surface area was used to calculate the uptake coefficient. HCl was deposited from the gas-phase (0.004–0.06 Torr) to an existing ice surface. Thermodynamics suggests that the ice films were pre-melted by the large HCl concentrations. The uptake coefficient showed a strong dependence on the exposure time to HCl and also on the partial pressure of HCl. The values listed in the table are for long HCl exposure times when the entire ice surface was coated with HCl. Cl₂ was observed as the only gas-phase product. The initial uptake coefficients decreased within minutes of exposure to steady values (which were not reported).

Preferred values

No Recommendations.

Comments on preferred values

The single study (De Haan and Birks, 1997) which reports uptake coefficients for the ClOOCl/HCl system was conducted using HCl partial pressures that melted the ice surface. The uptake coefficients reported cannot therefore be reliably extrapolated to atmospheric HCl partial pressures (which typically are more than 3 orders of magnitude lower). McKeachie et al. (2004) report complete uptake of ClOOCl to ice films at 213 K made from 10 % aqueous solutions of HCl, though an uptake coefficient was not reported. Both De Haan and Birks (1997) and McKeachie et al. (2004) observed Cl₂ as product and De Haan and Birks (1997) speculate that the co-product would be HOOC1 (or surface bound ClOO⁻ and H₃O⁺).

References

- De Haan, D. O. and Birks, J. W.: *J. Phys. Chem.*, 101, 8026–8034, 1997.
 McKeachie, J. R., Appel, M. F., Kirchner, U., Schindler, R. N., and Benter, T.: *J. Phys. Chem. B.*, 108, 16786–16797, 2004.

V.A1.55**ClOOCl + ice → products****Experimental data**

Parameter	Temp./K	Reference	Technique/Comments
γ $5.1 \pm 3.9 \times 10^{-4}$	226	De Haan and Birks, 1997	CWFT-MS (a)

Comments

- (a) Flow tube reactor using electron-impact MS. ClOOCl was generated in the self reaction of ClO at low temperatures and detected as Cl_2O_2^+ . The ice film (300–900 μm) was made by “brushing water” onto the cold flow tube surface and the geometric surface area was used to calculate the uptake coefficient. The value of γ presented is an average value from several experiments (results varied between <3 to 11×10^{-4}), though it is not clear that these were all conducted at the same temperature and ClOOCl partial pressure (which was reported to have been varied between 10^{11} and 10^{13} molecule cm^{-3} for a variety of substrates including pure ice).

Preferred values

Parameter	Value	T/K
γ	5×10^{-4}	226
<i>Reliability</i>		
$\Delta \log(\gamma)$	0.7	226

Comments on preferred values

The study of De Haan and Birks (1997) reports an uptake coefficient that is close to the detection limit of the apparatus. The uptake appears to be irreversible, and De Haan and Birks (1997) suggest that a hydrolysis reaction forming H_2OCl^+ and ClOO^- ions may take place. McKeachie et al. (2004) report insignificant interaction of ClOOCl to an ice surface at 213 K, but do not report an uptake coefficient. Considering that there is only one study reporting an uptake coefficient, the use of large concentrations of ClOOCl, the possible reaction of impurity reactants and the unusual mode of making the ice film, the uncertainty is considerable.

References

- De Haan, D. O. and Birks, J. W.: J. Phys. Chem., 101, 8026–8034, 1997.
 McKeachie, J. R., Appel, M. F., Kirchner, U., Schindler, R. N., and Benter, T.: J. Phys. Chem. B., 108, 16786–16797, 2004.

Appendix A2

Uptake on mineral dust surfaces

V.A2.1

O₃ + mineral oxide (dust) surfaces

Experimental data

Parameter	Temp./K	Reference	Technique/Comments
γ_0, γ_{ss}			
$\gamma_{ss}^{BET} = (1.4 \pm 0.35) \times 10^{-6}$ (SiO ₂)	295	Il'in et al., 1992	SR-UV (a)
$\gamma_0^{BET} = (8 \pm 5) \times 10^{-5}$ (α -Al ₂ O ₃ powder)	296	Michel et al., 2002	Knudsen-MS (b)
$\gamma_0^{BET} = (1.8 \pm 0.7) \times 10^{-4}$ (α -Fe ₂ O ₃ powder)			
$\gamma_0^{BET} = (5 \pm 3) \times 10^{-5}$ (SiO ₂ powder)			
$\gamma_0^{BET} = (2.7 \pm 0.9) \times 10^{-5}$ (China loess)			
$\gamma_0^{BET} = (6 \pm 3) \times 10^{-5}$ (Saharan Dust, ground)			
$\gamma_0^{BET} = (4 \pm 2) \times 10^{-6}$ (Saharan Dust, sieved, <50 μ m)			
$\gamma_0^{BET} = (1.4 \pm 0.3) \times 10^{-4}$ (α -Al ₂ O ₃ powder, 25 μ m)	295	Michel et al., 2003	Knudsen-MS (c)
$\gamma_0^{BET} = 7.6 \times 10^{-6}$ (α -Al ₂ O ₃ powder, 25 μ m)			
$\gamma_0^{BET} = (9 \pm 3) \times 10^{-5}$ (α -Al ₂ O ₃ powder, 1 μ m)			
$\gamma_0^{BET} = (2.0 \pm 0.3) \times 10^{-4}$ (α -Fe ₂ O ₃ powder)			
$\gamma_{ss}^{BET} = 2.2 \pm 10^{-5}$ (α -Fe ₂ O ₃ powder)			
$\gamma_0^{BET} = (6.3 \pm 0.9) \times 10^{-5}$ (SiO ₂ powder)			
$\gamma_0^{BET} = (3 \pm 1) \times 10^{-5}$ (kaolinite)			
$\gamma_0^{BET} = (2.7 \pm 0.8) \times 10^{-5}$ (China loess sand)			
$\gamma_0^{BET} = (6 \pm 2) \times 10^{-5}$ (Saharan Dust, ground)			
$\gamma_{ss}^{BET} = 6 \times 10^{-6}$ (Saharan Dust, ground)			
$\gamma_0^{BET} = (2.7 \pm 0.9) \times 10^{-6}$ (Saharan Dust, sieved, <50 μ m)			
γ_0, γ_{ss}			
$\gamma_0^{pd} = (5.5 \pm 3.5) \times 10^{-6}$ (Saharan Dust, unheated, 8.4 $\times 10^{12}$ cm ⁻³ O ₃)	296	Hanisch and Crowley, 2003	Knudsen-MS (d)
$\gamma_0^{pd} = (3.5 \pm 3.0) \times 10^{-4}$ (Saharan Dust, unheated, 5.4 $\times 10^{10}$ cm ⁻³ O ₃)			
$\gamma_{ss}^{pd} = (2.2 \pm 1.3) \times 10^{-6}$ (Saharan Dust, unheated, 8.4 $\times 10^{12}$ cm ⁻³ O ₃)			
$\gamma_{ss}^{pd} = (4.8 \pm 2.8) \times 10^{-5}$ (Saharan Dust, unheated, 5.4 $\times 10^{10}$ cm ⁻³ O ₃)			
$\gamma_0^{BET} = 1.0 \times 10^{-5}$ (α -Al ₂ O ₃ , [O ₃] = 10 ¹³ cm ⁻³)	298	Sullivan et al., 2004	SR-UV (e)
$\gamma_0^{BET} = 1.0 \times 10^{-6}$ (α -Al ₂ O ₃ , [O ₃] = 10 ¹⁴ cm ⁻³)			
$\gamma_0^{BET} = 6 \times 10^{-6}$ (Saharan dust, [O ₃] = 2 $\times 10^{12}$ cm ⁻³)	298	Chang et al., 2005	SR-UV (e)
$\gamma_0^{BET} = 2 \times 10^{-7}$ (Saharan dust, [O ₃] = 10 ¹⁴ cm ⁻³)			
$\gamma_{ss}^{pd} = (2.7 \pm 0.3) \times 10^{-6}$ (Kaolinite powder)	298	Karagulian and Rossi, 2006	Knudsen-MS (f)
$\gamma_{ss}^{pd} = (7.8 \pm 0.7) \times 10^{-7}$ (CaCO ₃ powder)	298		
$\gamma_{ss}^{BET} = (3.5 \pm 0.9) \times 10^{-8}$ (α -Al ₂ O ₃ , dry, [O ₃] = 9.8 $\times 10^{14}$ cm ⁻³)	298	Mogili et al., 2006	SR-UV/FTIR aerosol chamber (g)
$\gamma_{ss}^{BET} = (4.5 \pm 0.9) \times 10^{-9}$ (α -Al ₂ O ₃ , 19% RH, [O ₃] = 1.1 $\times 10^{15}$ cm ⁻³)			
$\gamma_{ss}^{BET} = (1.0 \pm 0.3) \times 10^{-7}$ (α -Fe ₂ O ₃ , dry, [O ₃] = 6.8 $\times 10^{14}$ cm ⁻³ , dry)			
$\gamma_{ss}^{BET} = (5.0 \pm 1.2) \times 10^{-8}$ (α -Fe ₂ O ₃ , dry, [O ₃] = 1.9 $\times 10^{14}$ cm ⁻³ , dry)			
$\gamma_{ss}^{BET} = (4.4 \pm 1.1) \times 10^{-9}$ (α -Fe ₂ O ₃ , 41% RH, [O ₃] = 8.5 $\times 10^{14}$ cm ⁻³ , dry)			
$\gamma_{ss}^{BET} = (9.0 \pm 2.3) \times 10^{-9}$ (α -Fe ₂ O ₃ , 43% RH, [O ₃] = 7.5 $\times 10^{13}$ cm ⁻³ , dry)			
K_{linC} /cm			
1.6 $\times 10^3$ (Saharan dust)	296	Hanisch and Crowley, 2003	Knudsen-MS (h)

Comments

- (a) Observation of O₃ in reaction vessels using optical absorption at 254 nm in the presence of Ar. Typical ozone and Ar pressures were 1.3–13 and 2.6 mbar, respectively. Mechanistic information and the temperature dependence of the decay rate constants were given for quartz, glass and water surfaces.
- (b) Bulk powder samples generated by gently heating an aqueous slurry of the powder on the sample support. The ozone concentration was $1.9 \times 10^{11} \text{ cm}^{-3}$. The initial and steady state γ values shown in the table have been calculated using the BET surface area in the linear mass dependent regime.
- (c) Bulk powder samples generated by gently heating an aqueous slurry of the powder on the heated sample support. The ozone concentration was varied from 10^{11} cm^{-3} to 10^{12} cm^{-3} . The initial and steady state γ values shown in the table have been calculated using the BET surface area in the linear mass dependent regime. The uptake coefficients were independent of the ozone concentration within the range given. A small temperature dependence of γ was observed, leading to an activation energy of $7 \pm 4 \text{ kJmol}^{-1}$. The steady state uptake coefficients were reported for an interaction time of 4.5 h. Owing to the fact that the amount of consumed O₃ is always of the order of 1 to 2 monolayers regardless of the duration of the interaction leads the authors to the conclusion that the O₃/mineral dust interaction is catalytic in nature.
- (d) Powder samples were prepared by dispersing an aqueous or methanol based paste onto the sample holder and evacuating overnight. Some samples were heated to 450 K prior to use. Steady state uptake coefficients were calculated (extrapolated) based on a bi-exponential fit to the observed uptake curves. The tabulated initial and steady state γ values were corrected using a pore diffusion model. The relative O₂ product yield varies from 1.0 to 1.3 ± 0.05 for unheated and heated (450 K, 5 h under vacuum) samples, respectively. Release of water correlated with the ozone concentration. Passivated samples could be reactivated by evacuation overnight.
- (e) Static reaction cell (Pyrex) equipped with detection of O₃ using UV absorption at 254 nm resulting in a typical signal-to-noise ratio of 1 at $2 \times 10^{12} \text{ molecule cm}^{-3}$ and 1 s integration. The dust powder was coated onto the surface by applying a methanol slurry and drying without heating. The BET surface area of separate coatings was measured using Kr adsorption at 77 K ($2.2 \text{ m}^2/\text{g}$ for alumina and $14 \text{ m}^2/\text{g}$ for Saharan dust). The first-order decays of O₃ have been measured over the first 10 s and have been converted to the listed γ , considered as γ_0 , as a slightly decreased slope can be recognised at times later than 10 s. γ_0 seemed to be constant for O₃ concentrations between 10^{12} and 10^{13} cm^{-3} for alumina and was inversely proportional to the O₃ concentration above 10^{13} cm^{-3} for both alumina and Saharan dust. γ does not change with humidity in the range 0 to 75% rh. A significant degree of reactivation of exposed samples was detected ranging from a few to over 50% of the initial value of γ by storing the spent samples in a container purged with dry and CO₂-free air for a few days. No products were detected.
- (f) Steady state and pulsed uptake experiment on powder substrates using a Knudsen flow reactor equipped with molecular beam modulated MS detection. The γ values displayed were obtained using a pore diffusion model for the data on kaolinite and CaCO₃. For CaCO₃, also a sample of roughened marble was used to represent a flat CaCO₃ surface and to avoid corrections to the uptake coefficient. The uptake coefficient obtained was 3.5×10^{-5} , which is a factor 50 higher than the one obtained for the CaCO₃ powder sample after pore diffusion correction. Further experiments were performed with Saharan dust and Arizona test dust, for which only uptake coefficients referred to the geometric sample surface area are reported. The reactivity of the ATD was slightly lower than that of CaCO₃, while that of SD was slightly higher. The SD sample showed a factor of 2 decrease in reactivity with O₃ concentration increasing from 3.5×10^{12} to $1.0 \times 10^{13} \text{ cm}^{-3}$. In general, initial uptake coefficients were a factor of 3 to 10 higher than steady state values. The only gas phase product detected was O₂. The O₂ yield per O₃ consumed showed significant variation from 0.0 to 2.0.
- (g) Powder samples were evacuated prior to use and then injected into a 0.15 m^{-3} chamber. The aerosol was not further characterized. The surface to volume ratio of the aerosol used to calculate uptake coefficients was taken from the injected sample mass and the BET surface area of the sample measured separately. O₃ was detected using FTIR in the range of up to 40 ppm and with UV absorption below 10 ppm. Under dry conditions, for $\alpha\text{-Fe}_2\text{O}_3$, turnover numbers, defined as number of O₃ molecules lost divided by the number of available surface sites, were 2 and above, indicating catalytic reactivity. For $\alpha\text{-Al}_2\text{O}_3$, the turnover number remained smaller than 1, in spite of a large excess of O₃. The uptake coefficient was decreasing with increasing O₃ concentration and strongly decreasing by a factor of 50 with humidity increasing from dry to 58 % relative humidity.

- (h) Saharan dust samples were deposited on a sample holder in the form of an ethanol paste. The experiment was aimed at determining NO to NO₂ oxidation rates as a function of O₃ concentration. The rates were fitted assuming Langmuir adsorption of both NO and O₃ prior to reaction. The value of K_{linC} given in the table has been derived from $K_{\text{LangC}}=4\times 10^{-12}\text{ cm}^3$ reported by the authors and an assumed $N_{\text{max}}=4\times 10^{14}\text{ cm}^{-2}$.

Preferred values

Parameter	Value	T/K
γ	$1500 [\text{O}_3 (\text{cm}^{-3})]^{-0.7}$	298
<i>Reliability</i>		
$\Delta \log (\gamma)$	± 0.5	298

Comments on preferred values

Given the different techniques used to obtain kinetic data, the data agree fairly well, when considering the strong dependence of the steady state uptake coefficients on ozone concentration, which has also been discussed in most of the studies cited. The initial uptake coefficients are more difficult to compare as they seem to depend more on the way the samples were exposed, and possibly also on the treatment of the samples prior to the experiment (heating, evacuation). Also the time resolution of the experiments is different, which makes the interpretation of initial uptake coefficients difficult without explicit kinetic modelling of especially the static and aerosol experiments. Probably because of the small steady state reactivities, interpretation of the kinetic data using the BET surface area of the powder samples in the linear mass dependent regime or using pore diffusion theory led to fairly consistent results. We therefore use only uptake coefficients derived from steady state uptake data that are referred to the BET surface area in our evaluation. The earlier study by Alebic-Juretic et al. (1992) is in qualitative agreement with the studies cited here, but does not directly provide quantitative kinetic data.

Considering the steady state values only, the Saharan dust, kaolinite, Al₂O₃, Fe₂O₃ and CaCO₃ agree surprisingly well with each other. We used the available Saharan dust data to obtain a recommendation of the uptake coefficient as a function of ozone concentration in the range of 10¹⁰ to 10¹³ cm⁻³, for relative humidity below 5%.

All studies note the potential effects of humidity, which has a significant effect on spectroscopic signatures on alumina observed in DRIFTS experiments (Roscoe and Abbatt, 2005; see below). Sullivan et al. (2004), however, found no humidity dependence in their kinetic experiments using the same type of samples. On the other hand, Mogili et al. (2006) report a significant humidity dependence of the uptake coefficient, which was reduced by a factor of 50 from dry to 60% relative humidity for Fe₂O₃ and a factor of about 10 from dry to 20% relative humidity for Al₂O₃.

Given the consistent dependence of steady state uptake coefficients of the ozone concentration, the rate limiting step in the mechanism of the reaction of ozone with mineral dust seems to be common among the different materials investigated, even in the atmospherically relevant concentration range around 10¹² cm⁻³. This mechanism may be represented by the following reactions, which have been consistently proposed in most studies:



Therein, SS denotes a reactive surface site, which are likely Lewis acid sites as present on alumina or Fe₂O₃ that are susceptible to dissociative adsorption of O₃, a Lewis base. Whether this first dissociation reaction occurs as a Langmuir-Hinshelwood or Eley Rideal reaction is not clear. But since desorption of O₃ from a dust surface has never been observed, Langmuir type adsorption is unlikely, even though Hanisch and Crowley (2003b) reported a Langmuir constant for O₃ to explain the oxidation behaviour of NO on the dust surface. We therefore do not recommend a value for K_{linC} . It is more likely that complete oxidation of all available SS to SS-O, which is the reactive species towards NO and O₃, explains the saturation behaviour. It is likely that in the experiment by Hanisch and Crowley (2003a), the O₃ loss kinetics was driven by uptake due to Eq. (1) at the lower O₃ concentration. An oxidised surface species SS-O is consistent with IR spectroscopic features observed by Roscoe and Abbatt (2006). The formation of the second, peroxy species, by Eq. (2) has been suggested based on a study of O₃ decomposition on MnO (Li et al., 1998), but could not be observed by Roscoe and Abbatt (2006), because the IR signature was outside the wavelength region they probed.

Overall, Eqs. (1) and (2) can explain turnover rates of ozone of up to two, which have indeed been observed, along with the formation of O₂ as a product (Mogili et al., 2006; Karagulian et al., 2006). Slow decomposition of SS-O₂ and self reaction of SS-O have been suggested to release reactive SS again, which would establish a catalytic cycle for ozone destruction. The time scale of reactivation observed in the experiment was on the order of a day.

The role of humidity in the reaction mechanism is not clear. On one hand, hydroxylated surface sites seem to be involved in Eq. (1) (Hanisch and Crowley, 2003a), while water can be involved in removing oxygen from SS-O as observed by Roscoe and Abbatt (2006), which would also explain the strong humidity dependence observed by Mogili et al. (2006), though at very high O₃ concentrations. Therefore, humidity on one hand can competitively adsorb to reactive sites and therefore reduce the uptake coefficient, while on the other hand, it may lead to reactivation of oxidised surface sites.

In view of the significant uncertainties related to the mechanism (details of Eqs. (1) and (2), humidity dependence, reactivation processes), we have allowed for a relatively large uncertainty associated with the recommended steady uptake coefficients.

References

- Alebic-Juretic, A., Cvitas, T., and Klasinc, L.: *Ber. Bunsenges. Phys. Chem.*, 96, 493–495, 1992.
- Chang, R. Y. W., Sullivan, R. C., and Abbatt, J. P. D.: *Geophys. Res. Lett.*, 32, L14815, doi:10.1029/2005GL023317, 2005.
- Hanisch, F. and Crowley, J. N.: *Phys. Chem. Chem. Phys.*, 5, 883–887, 2003b.
- Hanisch, F. and Crowley, J. N.: *Atmos. Chem. Phys.*, 3, 119–130, 2003a.
- Ill'in, S. D., Selikhanovich, V. V., Gershenson, Y. M., and Rozenshtein, V. B.: *Sov. J. Chem. Phys.*, 8, 1858–1880, 1991.
- Karagulian, F. and Rossi, M. J.: *Int. J. Chem. Kin.*, 38, 407–419, 2006.
- Li, W., Gibbs, G. V., and Oyama, S. T.: *J. Am. Chem. Soc.*, 120, 9041–9046, 1998.
- Michel, A. E., Usher, C. R., and Grassian, V. H.: *Geophys. Res. Lett.*, 29, 1665, doi:10.1029/2002GL014896, 2002.
- Michel, A. E., Usher, C. R., and Grassian, V. H.: *Atmos. Environ.*, 37, 3201–3211, 2003.
- Mogili, P. K., Kleiber, P. D., Young, M. A., and Grassian, V. H.: *J. Phys. Chem. A.*, 110, 13799–13807, 2006.
- Roscoe, J. M. and Abbatt, J. P. D.: *J. Phys. Chem. A.*, 109, 9028–9034, 2005.
- Sullivan, R. C., Thornberry, T., and Abbatt, J. P. D.: *Atmos. Chem. Phys.*, 4, 1301–1310, 2004.
- Usher, C. R., Michel, A. E., Stec, D., and Grassian, V. H.: *Atmos. Environ.*, 37, 5337–5347, 2003.

V.A2.3

H₂O₂ + mineral oxide (dust) surfaces → products**Experimental data**

Parameter	Temp./K	Reference	Technique/Comments
γ 1.5 × 10 ⁻³ (TiO ₂ aerosol; 15% RH)	298	Pradhan et al., 2010a	AFT-CIMS (a)
5.0 × 10 ⁻⁴ (TiO ₂ aerosol; 70% RH)			
(6.03 ± 0.26) × 10 ⁻⁴ (Gobi sand, 15 % RH)	298	Pradhan et al., 2010b	AFT-CIMS (b)
(6.03 ± 0.42) × 10 ⁻⁴ (Gobi sand, 70 % RH)			
(6.20 ± 0.22) × 10 ⁻⁴ (Saharan dust, 15 % RH)			
(9.42 ± 0.41) × 10 ⁻⁴ (Saharan dust, 70 % RH)			

Comments

- (a) H₂O₂ (initial concentration ≈ 4.1 × 10¹² molecule cm⁻³) was detected by CIMS using CF₃O⁻ (*m/z*=85) as a reagent ion. A sub-micron aerosol was generated by nebulising an aqueous dispersion of TiO₂ particles followed by diffusion drying. Particle number and size distribution was analysed using a DMA, giving typically surface area of $S_a = 6 \times 10^{-3}$ cm² cm⁻³ and D_{\max} of 0.45 μm at 40% RH. The uptake coefficient was calculated using the time- and aerosol area dependent loss rate of H₂O₂, which was first order in all cases. Uptake coefficients ($\gamma_{\text{H}_2\text{O}_2}$) were measured at relative humidities (RH) of 15, 35 and 70% .
- (b) Experimental method as in comment (a). For Gobi sand the available surface area was mainly from particles of diameter ~0.4 μm; for Saharan dust ~0.2 μm. The relative humidity was varied between 15 and 70 % (not all uptake coefficients are listed in the table above).

Preferred values

Parameter	Value	T/K
γ (15–70 %RH)	6.24 × 10 ⁻⁴ - 1.87 × 10 ⁻⁶ RH + 9.37 × 10 ⁻⁸ (RH) ²	298
<i>Reliability</i>		
$\Delta \log(\gamma)$	0.5	

Comments on preferred values

The uptake kinetics of H₂O₂ on mineral dust has been reported in two publications from the same group (Pradhan et al., 2010a and 2010b). Pradhan et al. found irreversible uptake of H₂O₂ to sub micron Saharan dust, Gobi sand and TiO₂ aerosols, but no gas phase products were detected. For TiO₂ aerosol an increase of γ was observed as RH decreased below ~40%, but γ remained approximately constant above 50% RH. This was attributed to competition between water molecules and H₂O₂ for reactive surface sites. In contrast the uptake of H₂O₂ to both Gobi sand and Saharan dust became more efficient with increasing RH. No dependence of γ on H₂O₂ was observed. In this case the authors argue that the increasing uptake with RH is due to dissolution of H₂O₂ in surface adsorbed water.

Our preferred values are based on the data for Saharan dust, which is most likely to best represent atmospheric mineral aerosol. The parameters were derived by fitting a polynomial to data read from a graph and should not be extrapolated beyond the range given. The error limits are expanded to reflect this.

References

- Pradhan, M., Kalberer, M., Griffiths, P. T., Braban, C. F., Pope, F. D., Cox, R. A., and Lambert, R. M.: *Environ. Sci. Technol.*, 44, 1360–1365, 2010a.
- Pradhan, M., Kyriakou, G., Archibald, T., Papageorgiou, A. C., Kalberer, M., and Lambert, R. M.: *Atmos. Chem. Phys.*, 10, 7127–7136, 2010b.

V.A2.4

NO₂ + mineral oxide (dust) surfaces → products

Experimental data

Parameter	Temp./K	Reference	Technique/Comments
γ , γ_0 , γ_{ss}			
$\gamma_{0,PD}=2 \times 10^{-8}$ (γ -Al ₂ O ₃ powder, 10 ⁻⁵ –10 ⁻² mbar)	298	Underwood, et al., 1999	Knud-MS(a)
$\gamma_{0,PD}=7 \times 10^{-7}$ (α -Fe ₂ O ₃ powder, 10 ⁻⁵ –10 ⁻² mbar)	298		
$\gamma_{0,PD}=1 \times 10^{-7}$ (TiO ₂ powder, 10 ⁻⁵ –10 ⁻² mbar)			
$\gamma_{ss,BET}=1.3 \times 10^{-9}$ (γ -Al ₂ O ₃ , 5 × 10 ⁻⁴ mbar)	299	Börensén et al., 2000	DIFTS (b)
$\gamma_{ss,BET}=2.6 \times 10^{-8}$ (γ -Al ₂ O ₃ , 3.5 × 10 ⁻² mbar)	299		
$\gamma_{0,BET}=9.1 \times 10^{-6}$ (γ -Al ₂ O ₃ , 5.3 × 10 ⁻⁶ mbar)	298	Underwood et al., 2001	Knud-MS (c)
$\gamma_{0,BET}=2.0 \times 10^{-8}$ (γ -Al ₂ O ₃ , 5.3 × 10 ⁻⁶ mbar)			
$\gamma_{0,BET}=7.7 \times 10^{-6}$ (α -Fe ₂ O ₃ , 5.3 × 10 ⁻⁶ mbar)			
$\gamma_{0,BET}=4.0 \times 10^{-6}$ (γ -Fe ₂ O ₃ , 5.3 × 10 ⁻⁶ mbar)			
$\gamma_{0,BET}=1.3 \times 10^{-7}$ (TiO ₂ , 5.3 × 10 ⁻⁶ mbar)			
$\gamma_{0,BET}=1.2 \times 10^{-5}$ (MgO, 5.3 × 10 ⁻⁶ mbar)			
$\gamma_{0,BET}=2.2 \times 10^{-5}$ (CaO, 5.3 × 10 ⁻⁶ mbar)			
$\gamma_{0,BET}=2.1 \times 10^{-6}$ (China loess, 5.3 × 10 ⁻⁶ mbar)			
$\gamma_{0,BET}=1.2 \times 10^{-6}$ (Sahara sand, 5.3 × 10 ⁻⁶ mbar)			
$\gamma_{0,BET}=(6.2 \pm 3.4) \times 10^{-7}$ (Sahara sand, 4.1 × 10 ⁻⁴ mbar)	298	Ullerstam et al., 2003	Knud-MS/DRIFTS (d)
$\gamma=9.6 \times 10^{-4}$ (illuminated TiO ₂ , 15% RH, 1 × 10 ⁻⁴ mbar)	298	Gustafsson et al., 2006	AFT-CLD (e)
$\gamma=1.2 \times 10^{-4}$ (illuminated TiO ₂ , 80% RH, 1 × 10 ⁻⁴ mbar)			
$\gamma_{ss,BET}=(8.1 \pm 0.2) \times 10^{-8}$ (kaolinite, 2.3 × 10 ⁻⁴ mbar)	298	Angelini et al., 2007	DRIFTS (f)
$\gamma_{ss,BET}=(2.3 \pm 0.4) \times 10^{-8}$ (kaolinite, 3.6 × 10 ⁻³ mbar)	298		
$\gamma_{ss,BET}=(7 \pm 1) \times 10^{-9}$ (pyrophyllite, 1.2 × 10 ⁻² mbar)			
$\gamma_{ss,BET}=1 \times 10^{-9}$ (1% TiO ₂ /SiO ₂ , SiO ₂ , Saharan dust, Arizona Test dust)	295	Ndour et al., 2008	CWFT-CLD/LOPAP (g)
$\gamma_{ss,BET}=1 \times 10^{-6}$ (illuminated 1% TiO ₂ /SiO ₂)			
$\gamma_{ss,BET}=(8.9 \pm 5.2) \times 10^{-9}$ (Saharan sand, 25% RH, 6 × 10 ⁻⁸ mbar)	295	Ndour et al., 2009	CWFT-CLD (h)
$\gamma_{ss,BET}=(8.9 \pm 5.2) \times 10^{-9}$ (illuminated Saharan sand, 25% RH, 6 × 10 ⁻⁸ mbar)			
$\gamma_{0,BET}=(4.3 \pm 1.2) \times 10^{-9}$ (CaCO ₃ , 0.28–0.69 mbar, 0% RH)	296	Li et al., 2010	DRIFTS (i)
$\gamma_{0,BET}=(2.5 \pm 0.1) \times 10^{-9}$ (CaCO ₃ , 0.19–0.47 mbar, 60–71% RH)			

Comments

- (a) Uptake experiment in a Knudsen flow reactor equipped with residual gas MS detection covering a NO₂ concentration range of 10 ppb to 10 ppm. The powder samples (as is) were thick enough so that the uptake coefficient did not depend on mass. The mineral particle sizes were 18 nm, 690 nm, 25 nm for γ -Al₂O₃, α -Fe₂O₃, TiO₂ (80% anatase, 20% rutile). The observed uptake coefficient did not depend on the gas phase concentration. The tabulated γ values were corrected using the pore diffusion model. Gaseous NO was observed as product, with a delay after initial exposure to NO₂. Overall, the ratio of NO₂ to NO was 2:1. FTIR measurements at 5–350 mTorr of NO₂ showed nitrite and nitrate species on the surface. It is suggested that a bidentate nitrito species is the first intermediate that disproportionates into a nitrate species and gaseous NO. The suggested mechanism also indicates that saturation will occur, when the product nitrate species reaches monolayer capacity.

- (b) Samples were obtained from ball-milling γ -Al₂O₃ powder (100 mesh) and packed into the DRIFTS reactor. Nitrite and nitrate species were observed on the surface. The absorption was calibrated by performing offline analysis with ion chromatography. The suggested mechanism involves disproportionation of physisorbed NO₂ into surface coordinated nitrite and nitrate, followed by release of HONO to the gas phase. The tabulated uptake coefficients were normalized to the BET area of the samples. They increase linearly with increasing NO₂ concentration between 10⁻⁴ and 10⁻² mbar, confirming the second order character of the reaction.
- (c) Bulk dust samples were prepared by spraying an aqueous slurry onto the heated sample holder and kept under vacuum overnight prior to an experiment. Experiments were carried out in the linear mass dependent regime, and the tabulated γ_0 values were normalized to the BET surface area of the dust sample and were measured at about 5 × 10⁻⁶ mbar. A further correction to the uptake coefficient suggested to account for internal roughness of individual particles led to an increase of up to a factor of 2. The uptake coefficient decreased with time, while the surface became saturated (observed at 8 × 10⁻³ Torr). Gaseous NO was observed as a product, with a ratio of NO₂ lost to NO formed of 2:1. Based on earlier work of the same group, this confirmed that an initial surface species, presumably nitrite, reacts with gaseous or adsorbed NO₂ to NO and nitrate.
- (d) Combined Knudsen flow reactor and FTIR diffuse reflectance study in the presence of both SO₂ (5.3 × 10¹² molecule cm⁻³) and NO₂ ((1.7–10) × 10¹² molecule cm⁻³). Mineral dust samples from Cape Verde Islands with a BET area of 50 m² g⁻¹ were applied to the heated sample holder as an aqueous suspension. The sample was dried at 333 K under vacuum. The listed values are initial uptake coefficients of steady-state uptake experiments in absence of SO₂. The tabulated uptake coefficients were referred to the BET area of the sample. The sample masses were kept low to stay within the linear mass regime. Adsorbed nitrite and nitrate species were identified using FTIR. It is suggested that the primary reactive process (in absence of other reactants) is heterogeneous hydrolysis of NO₂ to yield adsorbed HONO and HNO₃.
- (e) TiO₂ (3:1 anatase to rutile) aerosol was generated by nebulizing an aqueous powder suspension. The surface area in the aerosol flow tube was quantified by an SMPS. NO₂ and HONO were measured using a chemiluminescence detector. The fluorescent lamps had a maximum at 365 nm. The light intensity in the reactor was 1.6 mW cm⁻². The HONO yield was about 75%. The uptake of NO₂ in the dark was below detection limits.
- (f) Kaolinite (Al₂Si₂O₅(OH)₄) and pyrophyllite (AlSi₂O₅OH) samples obtained from ball-milling clay powders were packed into a DRIFTS reaction chamber. Nitrate in different conformations was observed as products on kaolinite. The tabulated uptake coefficients are obtained from the rate of nitrate formation during the initial phase of reaction (before nitrate starts to deplete available surface sites) under dry conditions and referred to the BET area of the sample. Formation of HONO was observed over wetted kaolinite samples by UV-VIS spectroscopy in a separate cell.
- (g) Synthetic and authentic dust samples were coated onto the surface of a Duran glass flow tube, irradiated by UV in the wavelength region 300 to 420 nm with an irradiance of 0.069 mW cm⁻². The light induced uptake coefficient was inversely related to the NO₂ concentration within 10¹¹ to 10¹³ cm⁻³. HONO was observed as product with a yield of 30% from the TiO₂/SiO₂ mixtures and 80% from Saharan dust.
- (h) Ground Saharan sand samples from Mauritania, Tunisia, Morocco and Algeria were coated onto the surface of a Duran glass atmospheric pressure flow tube, irradiated by UV in the wavelength region 300 to 420 nm with an irradiance of 1.45 mW cm⁻². Uptake coefficients derived from the observed loss of NO₂ in the gas phase were corrected for gas phase diffusion and referred to the BET surface area. The tabulated values are the average of the values reported for the four individual samples. The variability associated with the different samples was attributed to the variability in mineralogy of the samples assessed through EDX measurements. No pressure dependence was investigated. The uptake coefficient reported for irradiated conditions were upscaled for solar irradiance at 48° zenith angle. As measured they were a factor of 8 to 15 above those measured in the dark.
- (i) CaCO₃ powder was obtained by grinding to particles with 5.6 μm diameter, with 0.19 m²/g external surface area and 4.91 m²/g BET surface area. 20 mg of the powder were pressed into the DRIFTS sample holder and dried using a desiccator. The tabulated uptake coefficients were obtained from the observed rate of nitrate formation. The nitrate formation rate showed complex behaviour under dry conditions, but apparent first order behaviour with respect to NO₂ under humid conditions (> 50 % RH). At low humidity, the humidity dependence indicated competitive adsorption of water and NO₂; at high humidity, the rate of nitrate formation increased linearly with humidity. Offline analysis with IC and X-ray photoelectron spectroscopy (XPS) confirmed the presence of nitrate under dry conditions, and the presence of nitrite and nitrate under wet conditions.

Preferred values

Parameter	Value	<i>T</i> /K
γ	1.2×10^{-8}	298
<i>Reliability</i>		
$\Delta \log(\gamma)$	1.0	

Comments on preferred values

Uptake of NO₂ to mineral oxides is relatively slow. The available studies agree comparatively well on the reported values for the uptake coefficient, when considering similar materials. Most studies report reactivity at or below the detection limit for silica. For γ -Al₂O₃ and pyrophyllite uptake coefficients are on the order of 10⁻⁸. In this case also the uptake coefficients obtained in a Knudsen cell by Underwood et al. (1999) using thick samples and applying a pore diffusion model agree with those of the later study of the same group using thin samples and normalization to the BET area. In addition, results obtained in the Knudsen cell agree with those derived from the appearance of absorption bands observed in a DRIFTS reactor by Börensen et al. (2000) and Angelini et al. (2007). For the most reactive basic oxides, uptake coefficients can get up to 10⁻⁵. For clay minerals and Saharan dust, the uptake coefficient is on the order of 10⁻⁶. The difference between the values observed by Ullerstam et al. (2003) and by Underwood et al. (2001) might be due to saturation effects at the higher pressures noted by Ullerstam et al. (2003). The same likely applies to the study of Li et al. (2010) on CaCO₃ performed at NO₂ pressures in the 0.1 mbar range. We therefore recommend the parameterisation obtained by Ndour et al. (2009) for Saharan dust, with a large uncertainty.

Distinctly different mechanisms are suggested for the different substrates and especially in the presence and absence of water. The reactive process driving uptake is an initial adsorption and reaction of NO₂ with the surface oxides followed by secondary processes, or heterogeneous hydrolysis of NO₂ to yield HONO and HNO₃. Given that Underwood et al. (1999) observed the predominant appearance of the nitrite species at the lowest pressures used on dry Al₂O₃, Fe₂O₃ and TiO₂, it is likely that nitrite formation and further oxidation by NO₂ is important under dry atmospheric conditions. For more humid conditions and the basic oxide (or carbonate) components of dust, it is likely that the heterogeneous hydrolysis of NO₂ and displacement reactions of the acids are the processes driving uptake. Given that mineralogy strongly affects the reactivity, we associate a large uncertainty with the uptake coefficient.

All studies indicate that the uptake coefficient is time dependent and decreases to zero after roughly a monolayer equivalent (based on BET area) has been reacted. This is less an issue for carbonates, for which the particle bulk may become accessible through the action of HNO₃ formed from NO₂.

Given the limited detailed kinetic information in the atmospherically relevant pressure range, no detailed parameterization of the uptake coefficient is given.

While the reactivity of TiO₂ is comparable to that of the other materials in the dark, under illumination in the range of 300 to 400 nm, it catalyses the reduction of NO₂ to HONO (Gustafsson et al., 2006, Ndour et al., 2008). Ndour et al. used a linear model to extrapolate the measured uptake coefficient to other irradiances: $\gamma = 1.48 \times 10^{-5} \times I$ [mW cm⁻²].

References

- Angelini, M. M., Garrard, R. J., Rosen, S. J., and Hinrichs, R. Z.: *J. Phys. Chem. A.*, 111, 3326–3335, 2007.
- Börensen, C., Kirchner, U., Scheer, V., Vogt, R., and Zellner, R.: *J. Phys. Chem. A.*, 104, 5036–5045, 2000.
- Gustafsson, R. J., Orlov, A., Griffiths, P. T., Cox, R. A., and Lambert, R. M.: *Chem. Commun.*, 3936–3938, 2006.
- Li, H. J., Zhu, T., Zhao, D. F., Zhang, Z. F., and Chen, Z. M.: *Atmos. Chem. Phys.*, 10, 463–474, 2010.
- Ma, Q., Liu, Y., and He, H.: *J. Phys. Chem. A.*, 112, 6630–6635, 2008.
- Ndour, M., D’Anna, B., George, C., Ka, O., Balkanski, Y., Kleffmann, J., Stemmler, K., and Ammann, M.: *Geophys. Res. Lett.*, 35, doi:10.1029/2008GL036662, 2008.
- Ndour, M., Nicolas, M., D’Anna, B., Ka, O., and George, C.: *Phys. Chem. Chem. Phys.*, 11, 1312–1319, 2009.
- Ullerstam, M., Johnson, M. S., Vogt, R., and Ljungström, E.: *Atmos. Chem. Phys.* 3, 2043, 2003.
- Underwood, G. M., Miller, T. M., and Grassian, V. H.: *J. Phys. Chem. A.*, 103, 6184, 1999.
- Underwood, G. M., Song, C. H., Phadnis, M., Carmichael, G. R., and Grassian, V. H.: *J. Geophys. Res.*, 106, 18055–18066, 2001.

V.A2.5

NO₃ + mineral oxide (dust) surfaces

Experimental data

Parameter	Temp./K	Reference	Technique/Comments
γ_0, γ_{ss} $\gamma_{ss}=(6.7\pm 4.0)\times 10^{-2}$ (CaCO ₃) $\gamma_0=(13\pm 10)\times 10^{-2}$ (CaCO ₃) $\gamma_{ss}=(14\pm 2)\times 10^{-2}$ (Kaolinite) $\gamma_0=(11\pm 8)\times 10^{-2}$ (Kaolinite) $\gamma_{ss}=(12\pm 8)\times 10^{-2}$ (Saharan dust) $\gamma_0=(23\pm 20)\times 10^{-2}$ (Saharan dust) $\gamma_{ss}=(10\pm 6)\times 10^{-2}$ (Arizona dust) $\gamma_0=(20\pm 10)\times 10^{-2}$ (Arizona dust)	298±2	Karagulian and Rossi, 2006	Knudsen-MS (a)
$\gamma=(12\pm 5)\times 10^{-3}$ (Saharan dust, 0–70%RH)	298	Tang et al., 2010	RR-CRD(b)

Comments

- (a) Continuous flow experiments using bulk samples (on a 19.6 cm² glass optical flat) prepared from a suspension in methanol or water (5–110 mg) or powder samples (up to 2000 mg) and pre-treated by drying under vacuum at 294 K until H₂O desorption ceased (~30 min). NO₃ (5–93 × 10¹¹ molecule cm⁻³) was generated by the thermal decomposition of N₂O₅. MS detection of NO₃ and HNO₃ was accompanied by REMPI detection of NO and NO₂ impurities/products. The uptake coefficients were calculated using the geometric surface area. A pore diffusion correction was rejected based on observations of NO₃ uptake to various molecular sieve substrates. A strong dependence of γ on [NO₃] was observed, the values given are for [NO₃]₀ = 7 × 10¹¹ molecule cm⁻³.
- (b) Relative rate approach in which the uptakes of NO₃ and N₂O₅ (at concentrations of < 10¹⁰ molecule cm³) to Saharan dust aerosol were measured simultaneously. The Saharan dust sample (1–2 mg) was supported on an inert Teflon membrane filter. No significant change in the relative uptake rate was observed when the relative humidity was varied from 0 to 70 %. The uptake coefficient ratio obtained, $\gamma(\text{NO}_3)/\gamma(\text{N}_2\text{O}_5) = 0.9\pm 0.4$, was combined with the preferred value of $\gamma(\text{N}_2\text{O}_5) = 1.3 \times 10^{-2}$ to give the value of $\gamma(\text{NO}_3)$ listed in the Table.

Preferred values

Parameter	Value	T/K
γ	1.2×10^{-2}	298
<i>Reliability</i>		
$\Delta \log(\gamma)$	0.5	

Comments on preferred values

Karagulian and Rossi (2005) found efficient and irreversible uptake of NO₃ to various mineral dust substrates. A strong dependence of γ on [NO₃] may imply that interaction of [NO₃] with the dust samples uptake is not simply defined by γ . With the exception of kaolinite, the ratio of γ_0/γ_{ss} was found to be \approx a factor of two. As the uptake coefficients was based on the projected geometric surface area of the dust sample, they represent an upper limit. Tang et al. (2010), used a relative rate approach, which allowed them to derive uptake coefficients relative to N₂O₅ on the same substrate. This eliminated the need for absolute surface area estimation. As Tang et al. used the same dust as in their absolute AFT experiments (Wagner et al., 2008) the relative rate measurement can be reliably converted to an absolute one. The much smaller uptake coefficient for NO₃

+ Saharan dust determined by Tang et al. compared to Karagulian et al. (despite use of the same dust sample) most probably reflects use of the geometric surface area to derive γ in the Knudsen reactor experiments. As Tang et al. point out, the two absolute studies of Karagulian et al. (2005, 2006) on N_2O_5 and NO_3 uptake to Saharan dust also result on an uptake coefficient ratio close to unity, supporting the dataset of Tang et al., which provides the basis of our recommendation.

References

- Karagulian, F. and Rossi, M. J.: *Phys. Chem. Chem. Phys.*, 7, 3150–3162, 2005.
Karagulian, F., Santschi, C., and Rossi, M. J.: *Atmos. Chem. Phys.*, 6, 1373–1388, 2006.
Tang, M. J., Thieser, J., Schuster, G., and Crowley, J. N.: *Atmos. Chem. Phys.* 10, 2965–2974, 2010.
Wagner, C., Hanisch, F., de Coninck, H. C., Holmes, N. S., Schuster, G., and Crowley, J. N.: *Atmos. Chem. Phys.* 8, 91–109, 2008.

V.A2.8

HNO₃ + mineral oxide (dust) surfaces

Experimental data

Parameter	Temp./K	Reference	Technique/Comments
γ, γ_0			
$\gamma_0=0.09$ (CaCO ₃ , dried)	298	Fenter et al., 1995	Knudsen-MS (a)
$\gamma_0=0.15\pm 0.03$ (CaCO ₃ , non-dried)			
$\gamma_0=1.4\times 10^{-5}$ (CaCO ₃ , dried)	298	Underwood et al., 2000	Knudsen-MS DRIFTS (b)
$\gamma_0=(2.5\pm 0.1)\times 10^{-4}$ (CaCO ₃ , dried)	295	Goodman et al., 2000	Knudsen-MS DRIFTS (c)
$\gamma_0=0.10\pm 0.025$ (CaCO ₃ , heated)	298	Hanisch and Crowley, 2001a	Knudsen-MS (d)
$\gamma_0=0.18\pm 0.045$ (CaCO ₃ , non-heated)			
$\gamma_0=0.13\pm 0.033$ (Al ₂ O ₃)			
$\gamma_0=0.11\pm 0.03$ (Saharan dust)			
$\gamma_0=0.06\pm 0.015$ (Arizona dust)			
$\gamma_0=0.14$ (Saharan dust)	296	Hanisch and Crowley, 2001b	Knudsen-MS (e)
$\gamma_0=0.17$ (Chinese dust)			
$\gamma_0=(9.7\pm 0.5)\times 10^{-5}$ (α -Al ₂ O ₃)	298, 295	Underwood et al., 2001a, b	Knudsen-MS (f)
$\gamma_0=5.2\times 10^{-5}$ (Gobi dust)			
$\gamma_0=(2.0\pm 0.1)\times 10^{-5}$ (Saharan sand)			
$\gamma_0=(5.3\pm 0.3)\times 10^{-5}$ (α -Fe ₂ O ₃)			
$\gamma_0=(2.9\pm 0.2)\times 10^{-5}$ (SiO ₂)			
$\gamma=(1.6\pm 0.3)\times 10^{-9}$ (SiO ₂)	296	Goodman et al., 2001	FTIR (g)
$\gamma=(4\pm 1)\times 10^{-8}$ (α -Al ₂ O ₃)			
$\gamma_0=(1.5\pm 1.0)\times 10^{-5}$ (γ -Fe ₂ O ₃)	297	Frinak et al., 2004	Knudsen-MS/FTIR (h)
$\gamma_0=2.9\times 10^{-5}$ (γ -Fe ₂ O ₃)	220		
$\gamma_0=0.13\pm 0.02$ (α -Al ₂ O ₃)	298	Seisel et al., 2004	Knudsen-MS/DRIFTS (i)
$\gamma_0=0.11\pm 0.02$ (Sahara)			
$\gamma_0=2\times 10^{-3}$ (CaCO ₃ , dried)	296	Johnson et al., 2005	Knudsen-MS (j)
$\gamma=0.11$ (Arizona dust, RH 33%)		Vlasenko et al., 2006	AFT (k)
$\gamma=0.11$ (CaCO ₃ , RH 33%)			
$\gamma < 5\times 10^{-4}$ (SiO ₂ , RH 33%)			
$\gamma_0=0.01$ (CaCO ₃ , polished marble)	300	Sanchi and Rossi, 2006	Knudsen-MS (l)
$\gamma_0=0.04$ (CaCO ₃ , cut marble)			
$\gamma_0=0.3$ (CaCO ₃ , powder)			
$\gamma_0 > 8\times 10^{-5}$ (Na-montmorillonite, RH 29%)	210–232	Mashburn et al., 2006	Knudsen-MS/FTIR (m)
$\gamma_0=4\times 10^{-4}$ (Na-montmorillonite, RH 44%)			
$\gamma \geq 0.06$ (40% RH)	298	Liu et al., 2008	(n)
$\gamma = 0.21$ (80% RH)			
α_s			
1.0 (Arizona dust, RH 33%)	298	Vlasenko et al., 2009	AFT (o)

Comments

- (a) Irreversible uptake observed with H₂O and CO₂ detected as gas-phase products of reaction of HNO₃ with bulk samples. Comparison of results using powder and pressed pellet samples revealed no dependence of the uptake coefficient on the internal surface area, hence the geometric surface area was used to derive the value listed in the Table. Under the experimental conditions employed ([HNO₃]=10¹⁰-10¹³ molecule cm⁻³) the uptake coefficient decreased slowly with time of exposure, and initial uptake coefficients (γ_0) are reported. Pellet samples that had been dried (under vacuum) for several hours were less reactive than non-dried samples.

- (b) The uptake coefficients were derived from experiments with $[\text{HNO}_3] \approx 1 \times 10^{11}$ molecule cm^{-3} . Linear dependence of uptake coefficient on mass observed and taken to justify use of the BET surface area to calculate the uptake coefficient. An uptake coefficient of 1×10^{-3} was derived when the geometric surface area was assumed.
- (c) Bulk dust samples were prepared by drying a water slurry. The uptake coefficients were derived from experiments with $[\text{HNO}_3] \approx 1 \times 10^{12}$ molecule cm^{-3} using a pore diffusion calculation to account for uptake to internal surfaces of the bulk samples. Heating and evacuating the samples overnight resulted in significantly lower values of γ .
- (d) Bulk dust samples were prepared by mixing the powder sample to a paste with ethanol or H_2O , and were usually treated by evacuation for 5 h at 363 K. Four different grain sizes of Al_2O_3 were used, all yielding the same initial uptake coefficient. The data were thus analysed using the geometric surface area, and ignoring the contribution of internal surfaces. The initial HNO_3 concentration was varied between 6.5×10^{10} and 1.5×10^{12} molecule cm^{-3} . For Saharan dust, the same value of γ was obtained whether the sample was heated or not.
- (e) Same methods as (d) but better sensitivity enabled lower HNO_3 concentrations to be used (10^9 molecule cm^{-3}). In contrast to (c), most of the samples were not heated after dispersion. In addition to those listed, initial uptake coefficients were also obtained for a series of clay minerals: Kaolinite (0.11), ripidolite (0.10), illite (0.11), illite/smectite (0.09), Ca-montmorillonite (0.11), Ca-montmorillonite (0.08), palygorskite (0.20), dolomite (0.14) and orthoclase (0.08). Three different grain sizes of Chinese dust were used, all yielding the same initial uptake coefficient, as did use of different sample depths. The data were thus analysed using the geometric surface area, and ignoring the contribution of internal surfaces. For Chinese dust, the same value of γ was obtained whether the sample was heated or not.
- (f) See (c). Bulk dust samples were prepared by spraying an aqueous slurry onto the heated sample holder and kept under vacuum overnight prior to an experiment. Experiments were carried out in the linear mass dependent regime, so that γ was calculated using the BET surface area of the dust sample. The effect of heating the sample was found to reduce the uptake coefficient by a factor of 10 for Gobi dust. A strong increase in the uptake coefficient with decreasing nitric acid was observed for $\alpha\text{-Al}_2\text{O}_3$. A kinetic model of surface saturation and diffusion through the surface layers showed that the uptake coefficient obtained this way may be underestimated by factors of between 5 and 60, depending on e.g. the initial HNO_3 .
- (g) Dry samples. The uptake coefficients were derived from time dependence of surface nitrate formation at high HNO_3 (10^{14} molecule cm^{-3}). The rate of HNO_3 uptake to $\alpha\text{-Al}_2\text{O}_3$ and CaO increased nearly 50-fold going from 0% to 20% humidity. The authors suggest that the results obtained are lower limits to γ due e.g. to the use of high HNO_3 . A value of $\gamma = (4 \pm 1) \times 10^{-7}$ was obtained for CaO.
- (h) Bulk dust samples were prepared from an aqueous (or CH_3OH) slurry and dried under vacuum. Initial $[\text{HNO}_3] \approx 3 \times 10^{11}$ molecule cm^{-3} . Specific surface area of sample (measured using H_2O adsorption) used to calculate the uptake coefficient. Surface nitrate was observed following exposure of $\gamma\text{-Fe}_2\text{O}_3$ to HNO_3 .
- (i) Bulk dust samples were prepared from an aqueous slurry and dried at room temperature under vacuum. $[\text{HNO}_3]$ was varied between 4×10^{11} and 1×10^{13} molecule cm^{-3} . The value of γ listed for Saharan dust is that obtained at low $[\text{HNO}_3]$. No dependence of γ on the mass of the substrate was observed, confirming that the geometric surface area was appropriate for calculating the uptake coefficient. For $\alpha\text{-Al}_2\text{O}_3$ the uptake coefficient decreased as $[\text{HNO}_3]$ was increased, and H_2O was released into the gas phase with a yield of unity.
- (j) Experiments used multiple, single or fractional layers of the sample. Initial $[\text{HNO}_3]$ was 6.5×10^{10} molecule cm^{-3} . The value of γ_0 is larger (factor of 10) than previously reported by the same group (Goodman et al., 2000) due to reduction of saturation effects. Results were also obtained for dolomite for which $\gamma = (6 \pm 4) \times 10^{-4}$ (average of multi-, single- and fractional layer experiments) was obtained. Geometric uptake coefficients for CaCO_3 were observed to show a dependence on sample mass, maximising at values of ≈ 0.03 .
- (k) HNO_3 (initial concentration $\approx 10^{11}$ – 10^{12} molecule cm^{-3}) detected using radioactive labelled (H^{13}NO_3). Sub-micron Arizona dust aerosol was introduced into reactor via dry dispersion from its powder, CaCO_3 aerosol was generated by nebulising a saturated aqueous solution of CaCO_3 and diffusion drying. Particle number and size distribution was analysed using SMPS. The uptake coefficient was calculated using the time- and aerosol area dependent change in aerosol phase ^{13}N . Uptake coefficient on Arizona dust was observed to show a dependence on relative humidity ($\gamma = 0.02$ at RH=12%, increasing to $\gamma = 0.11$ at 73% RH when $[\text{HNO}_3]$ was 10^{12} molecule cm^{-3}).

- (l) Samples were cut and sometimes polished marble disks or CaCO_3 powder. H_2O (but not CO_2) observed as reaction product. $[\text{HNO}_3]_0 \approx (3-7) \times 10^{11} \text{ molecule cm}^{-3}$. Partial HNO_3 desorption from marble surfaces was observed, suggesting that part of the initial uptake was due to physisorption.
- (m) Na-montmorillonite samples exposed to $[\text{HNO}_3] > 3 \times 10^{12} \text{ molecule cm}^{-3}$. Uptake coefficients were extracted from IR surface analysis of nitrate formation (providing lower limits) and MS analysis of the gas-phase. In both cases the BET surface area was used. A strong dependence (> factor of ten) of uptake coefficient on the relative humidity was observed.
- (n) Suspended CaCO_3 particles ($\approx 0.8 \mu\text{m}$) exposed to HNO_3 ($\approx 2-6 \times 10^{11} \text{ molecule cm}^{-3}$) in humidified air. Uptake coefficient derived from rates of change of CaCO_3 conversion to nitrate as monitored by ex-situ SEM-EDX analysis.
- (o) HNO_3 (initial concentration $\approx 10^{11}-10^{12} \text{ molecule cm}^{-3}$) detected using radioactive labelling (H^{13}NO_3). Arizona dust aerosol (diameter $< 800 \text{ nm}$) was introduced into reactor via dry dispersion from its powder. Both gas and particle phase HNO_3 was detected. The efficiency of uptake of HNO_3 and its time evolution was observed to depend on the relative humidity (6–60 %) and the HNO_3 concentration. An uptake mechanism involving Langmuir like adsorption and surface reaction was proposed to explain this and derive time dependent values of γ . Data were consistent with a surface accommodation coefficient of 1.

Preferred values

Parameter	Value	T/K
α_s	1	298
$\tau_{\text{des}}/\text{s}$	0.1	298
$[\text{Y}]/\text{molecule cm}^{-2}$ (RH \leq 60%)	$6.5 \times 10^{13} + 4.1 \times 10^{10} * \text{RH} + 4.0 \times 10^{11} * \text{RH}^2$	298
$k_s/\text{cm}^2 \text{ s}^{-1}$	4×10^{-15}	298
$K_{\text{LangC}}/\text{cm}^3 \text{ molec}^{-1}$	2.25×10^{-12}	298
<i>Reliability</i>	see comments on preferred values	

Comments on preferred values

The experimental investigations of the kinetics of HNO_3 uptake to substrates representing atmospheric mineral aerosol show a great variability in the values of γ that have been obtained. There are several reasons for this, which are outlined below:

The role of internal surfaces in bulk, powder substrates has been assessed in different ways. Experimental uptake coefficients in Knudsen reactors are initially analysed using the geometric surface area of the sample surface (γ_{geom}). Diffusion into the samples interstitial space on the time scale of the measurement necessitates a correction factor, which can be empirically derived from observations of a sample mass dependence of γ_{geom} . In some instances such a behaviour has been observed (Goodman et al., 2000, 2001; Underwood et al., 2001a, b; Frinak et al., 2004) and in other cases it was not observed (Fenter et al., 1995; Hanisch and Crowley, 2001a, b; Seisel et al., 2004). The uptake coefficients which use either a pore-diffusion correction or the BET surface area are orders of magnitude smaller than those relying on the geometric surface area, the correction factor depending (for pore diffusion) on the value of (γ_{geom}) obtained. In those cases where uncorrected values of γ_{geom} are available, comparison shows that even here substantial deviations exist. For example, the maximum value of γ_{geom} obtained by Johnson et al. (2004) for HNO_3 uptake to CaCO_3 is still a factor of 6 lower than that obtained by Hanisch and Crowley (2001a). The influence of saturation effects (requiring correction factors of between 5 and 60) is a possible explanation as discussed by Underwood et al. (2001b). Hanisch and Crowley (2001b) have also indicated how use of high HNO_3 concentrations and reactive sample supports can result in underestimation of γ_{geom} . As shown in the Table above, results within the same research group, and using the same method and sample type reveal variations of more than two orders of magnitude in the value of γ obtained (Underwood et al., 2000; Goodman et al., 2000; Johnson et al., 2005). Thus, whereas γ_{geom} must be considered an upper limit to the true value of γ , values based on pore diffusion corrections or BET surface areas are often lower limits.

Part of the variability in γ_{geom} for any given substrate is also related to the use of differently prepared (different water content due to different heating and vacuum treatments) and intrinsically different samples (e.g. Saharan sand has a very different mineralogy and alkalinity to Saharan loess). The Knudsen reactor experiments with which the majority of the kinetic data have been obtained are necessarily conducted at low humidity. For some substrates (e.g. CaCO_3) there is strong evidence that the availability of H_2O can influence the uptake coefficient (Goodman et al., 2000, 2001; Hanisch and Crowley 2001a; Vlasenko et al., 2005) whereas for others the effects of substrate heating are negligible, suggesting that sufficient strongly bound surface water is available to support high values of the initial uptake coefficient, even though the capacity may be reduced e.g. Hanisch and Crowley, 2001a,b for uptake to Saharan and Chinese dust; Seisel et al. (2004) for uptake to $\alpha\text{-Al}_2\text{O}_3$.

The aerosol flow tube experiments of Vlasenko et al. (2006, 2009) provide uptake coefficients that avoid the issues related to effective surface area calculations for bulk surfaces discussed above. They also allow variation of the relative humidity to regions found in the atmosphere. Their data indicate initial uptake coefficients of the order of 0.1, but also show that this value may change as reactive sites are consumed. Vlasenko et al. (2009) propose a parameterisation for the uptake of HNO_3 to the surface of Arizona dust, which breaks γ into the individual steps (accommodation, reversible desorption, surface reaction) and takes into account the role of RH. We have adopted their values (tabulated above) for use in the following expressions:

$$\frac{1}{\gamma} = \frac{1}{\alpha_s} + \frac{1}{\Gamma_s}$$

where

$$\begin{aligned} \Gamma_s &= \frac{4k_s[\text{Y}]_s K_{\text{LangC}}(\text{X}) N_{\text{max}}}{\bar{c}(1 + K_{\text{LangC}}(\text{X})[\text{X}]_g)} \\ &= \frac{k_s[\text{Y}]_s \alpha_s \tau_{\text{des}}}{(1 + K_{\text{LangC}}(\text{X})[\text{X}]_g)} \end{aligned}$$

and \bar{c} (mean thermal velocity of HNO_3) = 30000 cm s^{-1} . The RH dependence of $[\text{Y}]_s$ was derived by fitting a polynomial to their data at 6, 33 and 60% RH and should not be extrapolated above this range. This parameterisation results in values of γ that vary from 0.03 at 6% RH to 0.6 at 60% RH.

The Vlasenko et al. data appear to be the most reliable, however, when applying their numbers to atmospheric dust, some considerations must be made:

- (1) The Arizona test dust examined by Vlasenko et al. (2005) has been found to be less reactive than Saharan or Chinese dust (see Table above), which provide the bulk of emissions to the atmosphere.
- (2) We note that relative humidity will play a role, but this may be different for Saharan or Chinese dust, when compared with the CaCO_3 or Arizona dust samples investigated by Vlasenko et al. (2005). Mashburn et al. (2006) found a very strong dependence of the HNO_3 uptake to Na-montmorillonite (a clay mineral with a large capacity to adsorb water) on relative humidity. Liu et al. (2008) also found a pronounced increase in HNO_3 uptake to CaCO_3 when the RH was increased from 10 to 80%.
- (3) A time independent value of γ will not always be appropriate to model dust plumes that will age chemically during transport through the atmosphere (Vlasenko et al., 2009). This is especially the case if the uptake is limited to the surface of the particle.
- (4) For interactions where the uptake is not limited to the surface (i.e. when dealing with alkaline particles) the capacity of mineral dust to consume HNO_3 in the atmosphere will be constrained by the fraction of calcite and dolomite present. The kinetics of the uptake at long time scales may then be determined not by a surface uptake coefficient, but by the rate of dissolution of an alkaline core covered by a deliquesced, aqueous nitrate layer. There is strong laboratory evidence (Goodman et al., 2000; Mashburn et al., 2006; Prince et al., 2007) that the reaction of HNO_3 on mineral samples is not limited to the surface if sufficient H_2O is present. At exposure to high concentrations of HNO_3 at sufficient relative humidity morphological and phase changes in individual particles have been observed, with up to 40 % of particle mass converted to nitrate (Krueger et al., 2003, 2004; Laskin et al., 2005). At sufficient RH (greater than $\approx 10\text{--}20\%$) the large hygroscopicity of surface nitrate induces further HNO_3 and water uptake (Liu et al., 2008) until the particle alkalinity is neutralised. Liu et al. observed a jump in the reactive uptake between 10 and 20 % RH, which they ascribe to $\text{Ca}(\text{NO}_3)_2$ deliquescence. HNO_3 uptake to CaCO_3 particles at high RH therefore represents a situation where the uptake can be enhanced by a chemical and thermodynamic change in the surface state. At low $[\text{HNO}_3]$ and humidity, this is not observed (Hanisch and Crowley, 2001a) and the reaction is largely limited to the surface yet the H_2O -induced reactivation of chemically aged “dry” dust samples has been documented on several occasions (Hanisch and Crowley, 2001a; Seisel et al., 2004).

- (5) There are indications that dust samples from different source regions may also display different reactivity to HNO₃ (Krueger et al., 2004) so that a single value is not appropriate.

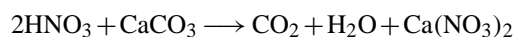
There is general agreement that the reaction of HNO₃ with mineral dust is essentially irreversible and that the products are surface and bulk nitrate species as observed spectroscopically (Goodmann et al., 2000, 2001; Börensens et al., 2000; Krueger et al., 2003, 2004; Seisel et al., 2004; Laskin et al., 2005; Mashburn et al. 2006) and also gas phase CO₂ and H₂O (Fenter et al., 1995, Goodmann et al., 2000; Hanisch and Crowley 2001a; Prince et al., 2007). Angelini et al. (2007) observed both molecularly adsorbed HNO₃ and nitrate on kaolinite and pyrophyllite samples. The reaction of HNO₃ with kaolinite was observed to generate surface adsorbed H₂O.

Mechanisms for the reaction of HNO₃ with CaCO₃ at low RH have been proposed (Al-Hosney and Grassian, 2005; Johnson et al., 2005; Santschi and Rossi, 2006) that invoke the intermediacy of Ca(OH)(CO₃H). The models attempt to explain the observed dependence of the CO₂ yield on available H₂O (Fenter, 1995, Hanisch and Crowley, 2001a, Santschi and Rossi, 2006), the differences in powdered CaCO₃ and marble samples (Santschi and Rossi, 2006), and the concurrent removal of surface OH groups and formation of nitrate groups during exposure (Börensens et al., 2000; Seisel et al., 2004).



The observation of Santschi and Rossi (2006) of no CO₂ release for marble samples, yet observation of 100 % yield of H₂O led them to propose that Eq. (3) dominates and that CO₂ is generated in a later step in the reaction of Ca(CO₃H)(NO₃) with a further molecule of HNO₃.

At large RH, the overall mechanism for calcite rich particles may resemble the acid-assisted, aqueous phase dissolution of carbonate, with the reaction proceeding until alkalinity is neutralised.



The uptake of HNO₃ to dust surfaces is not sensitive to chemical aging of the dust by atmospheric O₃ concentrations, at least at low RH (Hanisch and Crowley, 2003).

The time dependent γ formalism of Vlasenko et al. (2009) is appropriate for those time scales in which the processing of alkaline mineral dust particles by HNO₃ is restricted to the surface only. Both field observations of large nitrate content of mineral dust particles (e.g. Matsuki et al., 2005) and the laboratory observations made at high RH suggest that for the time scales associated with dust transport lifetimes (days), the uptake of HNO₃ will be controlled by rates of dissolution of alkaline components in an aqueous layer.

References

- Al-Hosney, H. A. and Grassian, V. H.: *Phys. Chem. Chem. Phys.*, **7**, 1266–1276, 2005.
- Angelini, M. M., Garrard, R. J., Rosen, S. J., and Hinrichs, R. Z.: *J. Phys. Chem. A*, **111**, 3326–3335, 2007.
- Börensens, C., Kirchner, U., Scheer, V., Vogt, R., and Zellner, R.: *J. Phys. Chem. A*, **104**, 5036–5045, 2000.
- Fenter, F. F., Caloz, F., and Rossi, M.: *Atmos. Environ.*, **29**, 3365–3372, 1995.
- Frinak, E. K., Wermeille, S. J., Mashburn, C. D., Tolbert, M. A., and Pursell, C. J.: *J. Phys. Chem. A*, **108**, 1560–1566, 2004.
- Goodman, A. L., Underwood, G. M., and Grassian, V. H.: *J. Geophys. Res.*, **105**, 29053–29064, 2000.
- Goodman, A. L., Bernard, E. T., and Grassian, V. H.: *J. Phys. Chem. A*, **105**, 6443–6457, 2001.
- Hanisch, F. and Crowley, J. N.: *J. Phys. Chem.*, **105**, 3096–3106, 2001.
- Hanisch, F. and Crowley, J. N.: *Phys. Chem. Chem. Phys.*, **3**, 2474–2482, 2001.
- Hanisch, F. and Crowley, J. N.: *Phys. Chem. Chem. Phys.*, **5**, 883–887, 2003.
- Johnson, E. R., Sciegienka, J., Carlos-Cuellar, S., and Grassian, V. H.: *J. Phys. Chem. A*, **109**, 6901–6911, 2005.
- Krueger, B. J., Grassian, V. H., Cowin, J. P., and Laskin, A.: *Atmos. Environ.*, **38**, 6253–6261, 2004.
- Krueger, B. J., Grassian, V. H., Laskin, A., and Cowin, J. P.: *Geophys. Res. Lett.*, **30**, 2003.
- Laskin, A., Wietsma, T. W., Krueger, B. J., and Grassian, V. H.: *J. Geophys. Res.*, **110**, 2005.
- Liu, Y., Gibson, E. R., Cain, J. P., Wang, H., Grassian, V. H., and Laskin, A.: *J. Phys. Chem. A*, **112**, 1561–1571, 2008.
- Mashburn, C. D., Frinak, E. K., and Tolbert, M. A.: *J. Geophys. Res.*, **111**, 2006.
- Matsuki, A., et. al: *Geophys. Res. Lett.*, **32**, L22806, doi:10.1029/2005GL0244176, 2005.
- Prince, A. P., Kleiber, P., Grassian, V. H., and Young, M. A.: *Phys. Chem. Chem. Phys.*, **9**, 3432–3439, 2007.
- Santschi, C. and Rossi, M. J.: *J. Phys. Chem. A*, **110**, 6789–6802, 2006.

- Seisel, S., Borensen, C., Vogt, R., and Zellner, R.: *Phys. Chem. Chem. Phys.*, 6, 5498–5508, 2004.
- Underwood, G. M., Li, P., Usher, C. R., and Grassian, V. H.: *J. Phys. Chem. A.*, 104, 819–829, 2000.
- Underwood, G. M., Song, C. H., Phadnis, M., Carmichael, G. R., and Grassian, V. H.: *J. Geophys. Res.*, 106, 18055–18066, 2001a.
- Underwood, G. M., Li, P., Al-Abadleh, H., and Grassian, V. H.: *J. Phys. Chem. A.*, 105, 6609–6620, 2001b.
- Vlasenko, A., Sjogren, S., Weingartner, E., Stemmler, K., Gäggeler, H. W., and Ammann, M.: *Atmos. Chem. Phys.*, 6, 2147–2160, 2006.
- Vlasenko, A., Huthwelker, T., Gäggeler, H. W., and Ammann, M.: *Phys. Chem. Chem. Phys.*, 36, 7921–7930, 2009.

V.A2.9

N₂O₅ + mineral oxide (dust) surfaces

Experimental data

Parameter	Temp./K	Reference	Technique/Comments
$\gamma, \gamma_{ss}, \gamma_0$ $\gamma_0=0.08\pm 0.003$ (Saharan dust) $\gamma_{ss}=0.013\pm 0.003$ (Saharan dust)	298	Seisal et al., 2005	Knudsen-MS/DRIFTS (a)
$\gamma_0=0.3\pm 0.08$ (Saharan dust) $\gamma_{ss}=0.2\pm 0.05$ (Saharan dust) $\gamma_0=0.2\pm 0.06$ (Arizona dust) $\gamma_{ss}=0.11\pm 0.03$ (Arizona dust) $\gamma_0=0.12\pm 0.04$ (CaCO ₃) $\gamma_{ss}=0.021\pm 0.006$ (CaCO ₃)	298±2	Karagulian et al., 2006	Knudsen-MS (b)
$\gamma=(1.9\pm 0.2)\times 10^{-4}$ (CaCO ₃)		Mogili et al., 2006	(c)
$\gamma=(13\pm 2)\times 10^{-3}$ (Saharan dust)	296±2	Wagner et al., 2007	AFT-CLD (d)
$\gamma=(37\pm 12)\times 10^{-3}$ (Saharan dust) $\gamma=(22\pm 8)\times 10^{-3}$ (Arizona dust) $\gamma=(50\pm 20)\times 10^{-3}$ (CaCO ₃ , unheated) $\gamma=(26\pm 8)\times 10^{-3}$ (CaCO ₃ , unheated)	296±2	Wagner et al., 2007	Knudsen-MS (e)
$\gamma=(4.8\pm 0.7)\times 10^{-3}$ (CaCO ₃ , RH=0%) $\gamma=(5.3\pm 1.0)\times 10^{-3}$ (CaCO ₃ , RH=29%) $\gamma=(11.3\pm 1.6)\times 10^{-3}$ (CaCO ₃ , RH=58%) $\gamma=(19.4\pm 2.2)\times 10^{-3}$ (CaCO ₃ , RH=71%) $\gamma=(9.8\pm 1.0)\times 10^{-3}$ (Arizona dust, RH=0%) $\gamma=(7.3\pm 0.7)\times 10^{-3}$ (Arizona dust, RH=29%) $\gamma=(8.6\pm 0.6)\times 10^{-3}$ (quartz, RH=0%) $\gamma=(4.5\pm 0.5)\times 10^{-3}$ (quartz, RH=29%)	296±2	Wagner et al., 2009	AFT-CLD (f)

Comments

- (a) Continuous flow and pulsed valve experiments using bulk samples (140–460 mg) which were prepared from an aqueous suspension of Saharan dust, and dried under vacuum before each experiment. The initial N₂O₅ concentration in Knudsen reactor experiments was 3–100×10¹⁰ molecule cm⁻³. No dependence of γ on sample mass was observed and the uptake coefficients given in the table were thus calculated using the geometric surface area of the sample. The rate of uptake was seen to decrease with exposure time, leading to the steady state value of γ listed. A lower value of $\gamma=(9.1\pm 0.7)\times 10^{-3}$ was calculated using DRIFTS measurements of the time dependence of surface nitrate formation.
- (b) Continuous flow experiments using bulk samples from a slurry in water which were pre-treated by drying under vacuum at 294 K until H₂O desorption ceased (≈30 min). Pulsed valve experiments were in good agreement. A dependence of γ on [N₂O₅] was observed, those listed were obtained at the lowest N₂O₅ concentrations used (circa 4×10¹¹ molecule cm⁻³). Data were also obtained for kaolinite and limestone.
- (c) 150 L environmental chamber with detection of N₂O₅ and HNO₃ by FTIR. CaCO₃ surface area was ≈0.25 m₂ (based on mass of CaCO₃ added and the known BET surface area of the sample). Uptake coefficients are cited as “apparent” and are a factor ≈160 less than a true value. This factor was derived from a comparison of N₂O₅ uptake in the chamber to literature values of its uptake coefficient for NaCl.
- (d) Atmospheric pressure aerosol flow tube (mean diameter of dust particles measured using aerodynamic sizer to be ≈1 μm) with detection of N₂O₅ (present at ≈10¹³ molecule cm⁻³) by modified CLD (N₂O₅ measured via thermal dissociation to NO₃ and modulation of NO signal). No dependence on the uptake coefficient on RH (0–30%) or [N₂O₅] was observed.
- (e) Bulk dust samples were prepared by mixing the powder to a paste with methanol and evenly spreading this onto a polished α-Al₂O₃ flat prior to drying under vacuum for ≈8 h at room temperature. Some CaCO₃ samples were heated to 400 K for several hours under vacuum. The data were analysed using the geometric surface area. The initial N₂O₅ concentration was varied between 3×10⁹ and 2×10¹⁰ molecule cm⁻³.

- (f) Atmospheric pressure aerosol flow tube (mean diameter of dust particles measured using aerodynamic sizer as ≈ 0.7 , 1.5 and 5 μm for quartz, CaCO_3 and ATD respectively. Detection of N_2O_5 (varied between 10^{12} and 10^{13} molecule cm^{-3}) was as described in comment (d). The CaCO_3 uptake coefficient increased with RH (0–71 %). No dependence on $[\text{N}_2\text{O}_5]$ was observed. Values listed in the table were corrected for diffusive effects and, as suggested by the authors, carry estimated uncertainties of > factor two, stemming mainly from assumptions about particle shape.

Preferred values

Parameter	Value	T/K
γ (Saharan dust)	1.3×10^{-2}	290–300
<i>Reliability</i>		
$\Delta \log(\gamma)$	0.5	

Comments on preferred values

Despite the use of very similar experimental methods, the common assumption that the geometric surface is appropriate for determination of γ and the use of similar surfaces, the agreement in the derived uptake coefficients returned by the three Knudsen reactor studies on Saharan dust, (Seisel et al., 2005; Karagulian et al., 2006 and Wagner et al., 2007) is poor, with the reported values of γ between 0.2 and 0.037.

Both Seisel et al. (2005) and Karagulian et al. (2006) report a decrease in reactivity with exposure time, with the ratio of γ_0 to $\gamma_{ss} \approx 6$ (Seisel et al.) and ≈ 2 (Karagulian et al.). In contrast, Wagner et al. (2007) report no surface deactivation on the time scales of their Knudsen reactor experiments with $\gamma_0 = \gamma_{ss}$. Part of this difference is certainly caused by the use of much lower concentrations of N_2O_5 by Wagner et al., but may also be caused by different rates of diffusion into the sample, as Seisel et al. (2005) and Karagulian et al. (2006) report very different average diameters for the particles comprising the bulk samples. It may also be related to different amounts of water associated with the substrates.

The AFT experiments of Wagner et al. (2007, 2009), report lower uptake coefficient than the Knudsen reactor experiments using similar samples. Note that, in Knudsen reactor experiments, the use of the projected surface area to calculate γ , should lead to upper limits for the uptake coefficient. No variation in γ with RH was observed by Wagner et al. (2007) for Saharan dust, though the reaction with calcite appears to become more efficient at relative humidities larger than about 60 %. The uncertainty associated with use of the geometric area of a porous, bulk sample in the Knudsen studies leads us to prefer the results of Wagner et al. (2007, 2009) obtained using dispersed aerosol.

The formation of NO_3^- , H_3O^+ and H_2O and the loss of surface OH groups during the reaction of N_2O_5 with Saharan dust has been observed using DRIFTS (Seisel et al., 2005). In Knudsen experiments using CaCO_3 , gas-phase HNO_3 , H_2O and CO_2 were observed (Karagulian et al., 2006; Wagner et al., 2007). Mogili et al. (2006) report stoichiometric conversion of N_2O_5 to HNO_3 .

A mechanism has been proposed (Seisel et al., 2005; Karagulian et al., 2006) whereby N_2O_5 can either react with initially present surface-OH groups (on CaCO_3 these are available as $\text{Ca}(\text{OH})(\text{HCO}_3)$) to form HNO_3 and surface-nitrate, or with adsorbed H_2O to form HNO_3 . The HNO_3 product can react with surface-OH to form H_2O and surface-nitrate, or with H_2O to form the observed H_3O^+ and NO_3^- ions. The removal of surface-OH groups (or $\text{Ca}(\text{OH})(\text{HCO}_3)$) explains the change in reactivity during exposure, whereas the steady state uptake coefficient will be dominated by the reaction of N_2O_5 with surface- H_2O . The yield of gas-phase HNO_3 depends on its reactivity with the dust substrate and is of the order of 4–5 % for reactive surfaces such as CaCO_3 and Saharan dust (Karagulian et al., 2006). The irreversible nature of the reaction could be confirmed by heating exposed samples to 470 K, with no loss of surface adsorbed nitrate (Seisel et al., 2005).

References

- Mogili, P. K., Kleiber, P. D., Young, M. A., and Grassian, V. H.: Atmos. Environ., 40, 7401–7408, 2006.
 Karagulian, F., Santschi, C., and Rossi, M. J.: Atmos. Chem. Phys., 6, 1373–1388, 2006.
 Seisel, S., Börensens, C., Vogt, R., and Zellner, R.: Atmos. Chem. Phys., 5, 3423–3432, 2005.
 Wagner, C., Hanisch, F., Holmes, N. S., de Coninck, H. C., Schuster, G., and Crowley, J. N.: Atmos. Chem. Phys., 8, 91–109, 2008.
 Wagner, C., Schuster, G., and Crowley, J. N.: Atmos. Env., 43, 5001–5008, 2009.

V.A2.10

SO₂ + mineral oxide (dust) surfaces

Experimental data

Parameter	Temp./K	Reference	Technique/Comments
$\gamma, \gamma_0, \gamma_{ss}$			
$\gamma_0 = (8.4 \pm 0.3) \times 10^{-5}$ (Adobe clay)	298*	Judeikis and Stewart, 1976	CRFT-MS (a)
$\gamma_0 = 1 \times 10^{-3}$ (MgO)	298*	Judeikis et al., 1978	CRFT-MS (b)
$\gamma_0 = 5.5 \times 10^{-4}$ (Fe ₂ O ₃)			
$\gamma_0 = 4.0 \times 10^{-4}$ (Al ₂ O ₃)			
$\gamma_0 = (9.5 \pm 0.3) \times 10^{-5}$ (α -Al ₂ O ₃)	296	Goodman et al., 2001	Knudsen-MS/FTIR (c)
$\gamma_0 = (2.6 \pm 0.2) \times 10^{-4}$ (MgO)			
$\gamma_0 = (1.0 \pm 0.2) \times 10^{-4}$ (TiO ₂)	298*	Usher et al., 2002	Knudsen-MS/FTIR (c)
$\gamma_0 = (1.4 \pm 0.7) \times 10^{-4}$ (CaCO ₃)			
$\gamma_0 = (7.0 \pm 2.0) \times 10^{-5}$ (α -Fe ₂ O ₃)			
$\gamma_0 = (5.1 \pm 0.5) \times 10^{-4}$ (MgO)			
$\gamma_0 = (1.6 \pm 0.5) \times 10^{-4}$ (α -Al ₂ O ₃)			
$\gamma_0 < 1 \times 10^{-7}$ (SiO ₂)			
$\gamma_0 = (3 \pm 1) \times 10^{-5}$ (Chinese dust)			
$\gamma = 5 \times 10^{-7}$ (Saharan dust, O ₃)	299	Ullerstam et al., 2003	DRIFTS (d)
$\gamma = (1.6 \pm 0.1) \times 10^{-5}$ (Saharan dust)	299	Ullerstam et al., 2003	Knudsen-DRIFTS (e)
$\gamma_0 = (6.6 \pm 0.8) \times 10^{-5}$ (Saharan dust)	298	Adams et al., 2005	CWFT-MS (f)
$\gamma_0 = (6.4 \pm 0.7) \times 10^{-5}$ (Saharan dust, RH \approx 0)	258		
$\gamma_0 = (6.0 \pm 1.0) \times 10^{-5}$ (Saharan dust, RH = 27 %)	258		
$\gamma_0 = 0.1$ (CaCO ₃ , powder)	300	Santschi and Rossi, 2006	Knudsen-MS (g)
$\gamma_0 = (7.7 \pm 1.6) \times 10^{-4}$ (CaCO ₃ , O ₃)	293	Li et al., 2006	DRIFTS (h)
$\gamma_{ss} = (8.1 \pm 2.6) \times 10^{-5}$ (CaCO ₃ , O ₃)			
K_{inc}/cm (1.2 \pm 0.4)		Adams et al., 2006	CWFT-MS (f)

* Room temperature assumed to be 298 K (not cited in manuscript).

Comments

- (a) Samples prepared by coating reactor with aqueous slurry before drying in vacuum. γ based on geometric surface area.
- (b) Samples prepared by coating reactor with H₂O/ethanol slurry before drying in vacuum. γ based on geometric surface area.
- (c) Bulk powder samples generated by spraying an aqueous slurry onto the heated sample support. A SO₂ concentration of 1×10^{11} molecule cm⁻³ was employed. The initial uptake coefficients (γ_0) given in the table were calculated using the BET surface area of the sample. Maximum surface coverages of reversibly adsorbed SO₂ of $(1.5 \pm 0.3) \times 10^{14}$ and $(3.5 \pm 0.6) \times 10^{14}$ molecule cm⁻² were obtained by surface spectroscopic methods for α -Al₂O₃ and MgO, respectively.
- (d) The initial SO₂ concentration was ≈ 2 – 20×10^{12} molecule cm⁻³. Dust samples made from aqueous suspension and were dried at 333 K before use. Uptake coefficient of SO₂ in the presence of O₃ (5.6×10^{12} molecule cm⁻³) was calculated from time dependent IR signals due to the sulphate product. The values of γ listed were obtained using the BET surface area. For comparison, a value of $\approx 10^{-3}$ was obtained using the geometric surface area.
- (e) Dust samples made from aqueous suspension deposited onto sample holder at 373 K (Knudsen reactor experiments) and dried at 333 K before use. The concentration of SO₂ was 5.4 – 15×10^{12} molecule cm⁻³. The value of γ listed was obtained in pulsed valve experiments using the BET surface area. For comparison, a value of $\approx 10^{-3}$ was obtained using the geometric surface area. Values obtained in continuous flow mode were a factor of three lower. No significant change in γ_0 was found when NO₂ was present at $[\text{NO}_2] \approx 1 \times 10^{-13}$ molecule cm⁻³.

- (f) Dust samples made from a suspension in ethanol. Initial SO₂ concentration was between 2 and 40 × 10¹⁰ molecule cm⁻³. Uptake coefficients were determined using the BET surface area of the sample. Experiments carried out at relative humidity of ≈0 (298 K) and 27% (258 K). No significant change in γ_0 was found when O₃ was added at ≈1 × 10¹³ molecule cm⁻³. The partition coefficient for reversibly adsorbed SO₂, K_{linC} , was determined from the area of desorption peaks at 298 K and was derived from the published values of $K_{\text{LangC}}=(6\pm 2)\times 10^{-14}$ molecule⁻¹ cm³ and $N_{\text{max}}=2\times 10^{13}$ molecules cm⁻².
- (g) Powder samples were evacuated for 30 min prior to use, which left the equivalent ≈3% of one monolayer H₂O on the surface. CO₂ formed promptly with 100% yield and detected in the gas-phase. The uptake coefficient listed in the Table was calculated using the geometric surface area of the powder sample. H₂O (but not CO₂) observed as reaction product. [HNO₃]₀ ≈(3–7) × 10¹¹ molecule cm⁻³. Partial HNO₃ desorption from marble surfaces was observed, suggesting that part of the initial uptake was due to physi-sorption.
- (h) The initial uptake coefficients listed were obtained in the presence of O₃ (4.9 × 10¹⁴ molecule cm⁻³) and water vapour (RH=40%) and are based on the geometric surface area of the sample. The initial uptake coefficient was independent of SO₂ concentration (0.6–9.8 × 10¹⁴ molecule cm⁻³), RH and O₃ concentration. The steady state uptake coefficient was observed to be dependent on RH and was in the range 1.0–10.7 × 10⁻⁵ for RH 5–60%. Use of the BET surface area resulted in uptake coefficients of $\gamma_0=(1.4\pm 0.3)\times 10^{-7}$ and $\gamma_{\text{ss}}=(1.5\pm 0.5)\times 10^{-8}$ at RH=40 %.

Preferred values

Parameter	Value	T/K
γ (RH 0–27%)*	4 × 10 ⁻⁵	260–300
<i>Reliability</i>		
$\Delta\log(\gamma)$	0.7	

Reliability

See below.

Comments on preferred values

Most of the uptake coefficients measured for SO₂ interaction with mineral surfaces obtained using SO_{2(g)} analysis (CWFT, Knudsen) indicate that the process is relatively inefficient, with values of γ_0 close to 10⁻⁴–10⁻⁵. The large variability in γ is due to the different mineral sample types used, due to different sample treatments and data analysis (i.e. use of BET or geometric surface area) and due to use of different SO₂ concentrations. The value of $\gamma=0.1$ on CaCO₃ of Santschi and Rossi (2006) is the exception and is likely due to the use of the geometric rather than BET surface area. Li et al. (2006) and Ullerstam et al. (2002) used DRIFTS to derive much lower uptake coefficients. Uptake coefficients measured using airborne aerosol and at atmospherically relevant conditions of [SO₂], [O₃] and RH are required to reduce the uncertainty.

In the absence of such data, for the purpose of atmospheric modelling, an average uptake coefficient of 4 × 10⁻⁵, independent of relative humidity and based on Saharan (Adams et al., 2006) and Chinese dust (Usher et al., 2002) is presently recommended. The errors associated with this uptake coefficient are likely to be large (> factor of 10) and it is not clear whether the initial or the steady state uptake coefficient is appropriate for atmospheric conditions. The initial uptake coefficient contains components from both reversible and irreversible uptake. The fraction of SO₂ taken up reversibly is however small and dependent on the O₃ concentration. Adams et al. (2005) determined that 86–98% was taken up irreversibly, the larger fraction obtained when O₃ was present.

Not only the uptake coefficient, but also the capacity of the mineral surface to convert SO₂ to sulphate depends on the mineral type and humidity. Although the initial uptake coefficient appears to be invariant with humidity on Saharan dust (Adams et al., 2005), CaCO₃ (Li et al., 2006) and clay surfaces (Judeikis and Stewart, 1976; Judeikis, 1978), the steady state uptake coefficient on CaCO₃ was not (Li et al., 2006). In addition, Ullerstam et al. (2002) found that the capacity of Saharan dust increased by ≈50 % following treatment with H₂O vapour at high humidity (22 mbar H₂O); Li et al. (2006) also found that the capacity (on CaCO₃) was enhanced by gas phase H₂O.

Adams et al. (2005) report a maximum amount of irreversibly taken up SO_2 as 8×10^{13} molecule cm^{-2} of Saharan dust; Al-Hosney et al. (2005) found that a CaCO_3 surface saturated at a coverage of 4×10^{13} molecules cm^{-2} . Santschi and Rossi report a lower capacity of CaCO_3 to take up SO_2 of 7×10^{12} molecules cm^{-2} , probably related to differences in humidity in their experiments (see above). Using dispersed aerosol samples of CaCO_3 , Prince et al. (2007) found that the amount of CO_2 generated and the amount of SO_2 lost both depended strongly on relative humidities between 30 and 90% but was not influenced by the presence of HNO_3 .

Judeikis and Stewart (1976) found that exposure of a pre-reacted clay surface to 95% RH recovered the reactivity completely. The capacity of MgO increased dramatically (factor 100) going from RH=0 to 95%, whereas those of Fe_2O_3 and Al_2O_3 were not substantially changed. Capacities of 25–150 mg of sulphate per gram of clay mineral for 0.86 ppm SO_2 and RH=86% (Mamane and Gottlieb, 1989) have been measured.

Surface spectroscopy (Goodman et al., 2001; Usher et al., 2002; Ullerstam et al., 2002) has shown that SO_2 can be oxidised to sulphite (SO_3^{2-}) and bisulphite (HSO_3^-) on the dry mineral oxide samples used, probably via reaction with surface-OH and surface-O groups. Contrasting results were found by Li et al. (2006), who found sulphite formation only in the presence of gas-phase water vapour. Baltrusaitis et al. (2007) found that the extent of reaction of SO_2 with CaCO_3 is enhanced ≈ 5 -fold for particulate CaCO_3 and ≈ 10 -fold for single crystal CaCO_3 in the presence of H_2O vapour at RH between 30 and 85%.

To explain their observations of prompt CO_2 formation, Santschi and Rossi, 2006 suggest that the reaction proceeds via the $\text{Ca}(\text{OH})(\text{HCO}_3)$ surface species (1). In contrast, Al-Hosney et al. (2005) propose reaction (2) to explain their 296 K surface spectroscopic observations of H_2CO_3 and non-observation of CO_2 :



There is clearly some uncertainty regarding the true mechanism and the role of surface water. In the presence of O_3 , (or NO_2 , Ullerstam et al., 1993) further oxidation of sulphite to SO_4^{2-} and HSO_4^- occurs (Li et al., 2006).

In O_3 -free experiments, Judeikis et al. (1978) found, by wet chemical analysis and x-ray photoelectron spectroscopy, that SO_2 was quantitatively (within a factor of two) converted to sulphate except on Al_2O_3 , for which the uptake was found to be reversible. Goodman et al. (2001) found spectroscopic evidence for reversibly adsorbed SO_2 , on both $\alpha\text{-Al}_2\text{O}_3$ and MgO , and, using calibrated FTIR signals derived adsorption isotherms with maximum coverages listed in the comments above. The reversible component of uptake was however much smaller than reactive uptake to form sulphite.

References

- Adams, J. W., Rodriguez, D., and Cox, R. A.: *Atmos. Chem. Phys.*, 5, 2679–2689, 2005.
Al-Hosney, H. A. and Grassian, V. H.: *Phys. Chem. Chem. Phys.*, 7, 1266–1276, 2005.
Baltrusaitis, J., Usher, C. R., and Grassian, V. H.: *Phys. Chem. Chem. Phys.*, 9, 3011–3024, 2007.
Goodman, A. L., Li, P., Usher, C. R., and Grassian, V. H.: *J. Phys. Chem. A.*, 105, 6109–6120, 2001.
Judeikis, H. S. and Stewart, T. B.: *Atmos. Env.*, 10, 769–776, 1976.
Judeikis, H. S., Stewart, T. B., and Wren, A. G.: *Atmos. Env.*, 12, 1633–1641, 1978.
Li, L., Chen, Z. M., Zhang, Y. H., Zhu, T., Li, J. L., and Ding, J.: *Atmos. Chem. Phys.*, 6, 2453–2464, 2006.
Mamane Y. and Gottlieb, J.: *J. Aerosol. Sci.*, 20, 303–311, 1989.
Prince, A. P., Kleiber, P., Grassian, V. H., and Young, M. A.: *Phys. Chem. Chem. Phys.*, 9, 3432–3439, 2007.
Santschi, C. and Rossi, M. J.: *J. Phys. Chem. A.*, 110, 6789–6802, 2006.
Ullerstam, M., Vogt, R., Langer, S., and Ljungström, E.: *Phys. Chem. Chem. Phys.*, 4, 4694–4699, 2002.
Ullerstam, M., Johnson, M. S., Vogt, R., and Ljungström, E.: *Atmos. Chem. Phys.*, 3, 2043–2051, 2003.
Usher, C. R., Al-Hosney, H., Carlos-Cuellar, S., and Grassian, V. H.: *J. Geophys. Res.*, 107, 4713, 2002.

V.A2.11**HC(O)OH + mineral oxide (dust) surfaces****Experimental data**

Parameter	Temp./K	Reference	Technique/Comments
γ_0			
0.3±0.1 (dry CaCO ₃)	298*	Al-Hosney et al., 2005	Knudsen-MS (a)
1.7×10 ⁻⁵ (Na-Montmorillonite, RH = 0 %)	212	Hatch et al., 2007	Knudsen-MS(b)
1.7×10 ⁻⁵ (Na-Montmorillonite, RH = 29 %)			
2.3×10 ⁻⁵ (Na-Montmorillonite, RH = 45 %)			

* Experimental temperature not given, presumably room temperature

Comments

- (a) Continuous flow Knudsen experiments using bulk samples of CaCO₃ prepared from an aqueous slurry by allowing H₂O to evaporate under vacuum overnight. The HC(O)OH concentration was 1.9×10¹¹ molecule cm⁻³. The mass of substrate was varied (≈2–70 mg) to enable a pore diffusion correction to be carried out (all uptake coefficients were derived in this manner). Transmission-FTIR and ATR-FTIR analysis of the substrate were used to obtain mechanistic information.
- (b) Bulk samples of Na-montmorillonite prepared from an aqueous slurry. Concentration of HC(O)OH was varied between ≈2–30 ×10¹¹ molecule cm⁻³. The initial uptake coefficient (based on the BET surface area) obtained in first two seconds of exposure was not influenced by slowly changing surface area due to swelling of the clay mineral at non-zero RH and was independent of the formic acid concentration. FTIR sample analysis indicated that the interaction is (at least in part) irreversible.

Preferred values

No recommendation.

Comments on preferred values

Al-Hosney et al. (2005) found largely (98%) irreversible uptake of HC(O)OH to calcite. Time and mass dependent uptake coefficients were observed and a pore diffusion correction was performed to derive the “true” uptake coefficient. The tortuosity coefficient (τ) derived from fitting to the mass dependence of the uptake coefficient was 4, somewhat larger than the maximum value of 3 suggested to be acceptable for powder samples (Boulter and Marschall, 2006).

Exposure of dry CaCO₃ to ≈8×10¹⁵ HC(O)OH resulted in formation of formates and carbonic acid via reaction with Ca(OH)(HCO₃) present on CaCO₃ surfaces. Carbonic acid was converted to CO₂ in the presence of moisture, which also results in an enhanced capacity for CaCO₃ to take up HC(O)OH and an enhanced rate of formate formation. This is explained in terms of surface reorganisation (reactivation) and involvement of underlying layers so that no surface saturation is observed at high relative humidity. Hatch et al. (2007) observed that the initial uptake of formic acid to Na-montmorillonite increased only slightly as RH increased and that the uptake HC(O)OH saturated at calculated coverages that varied between <0.1 and 0.5 ×10¹⁴ molecules cm⁻², which are sub-monolayer. Al Hosney et al. derived a saturation surface coverage of ~ 3 ×10¹⁴ molecules cm⁻² for CaCO₃. The initial uptake coefficients of formic acid to calcite and Na-montmorillonite are vastly different (factor 100), thus uptake to atmospheric dust would be dominated by the calcite fraction. As the uptake of HC(O)OH to calcite was observed to cease at coverages of ≈3×10¹⁴ molecules cm⁻² the initial uptake coefficient is not appropriate for modelling the interaction of HC(O)OH and mineral dust in the atmosphere. Assuming ≈3×10¹⁴ reactive sites per cm², and a HC(O)OH mixing ratio of 350 ppt, the initial uptake coefficient would be reduced by a factor of ~10 following one hour of exposure. This may be offset by reorganisation of the particle surface at high humidities, but until quantitative kinetic data are available at RH other than zero, we make no recommendation.

References

- Al-Hosney, H. A., Carlos-Cuellar, S., Baltrusaitis, J., and Grassian, V. H.: *Phys. Chem. Chem. Phys.*, 7, 3587–3595, 2005.
- Boulter, J. E. and Marschall, J.: *J. Phys. Chem. A*, 110, 10444–10455, 2006.
- Hatch, C. D., Gough, R. V. and Tolbert, M. A.: *Atmos. Chem. Phys.* 7, 4445–4458, 2007.

V.A2.12

CH₃C(O)CH₃ + mineral oxide (dust) surfaces

Experimental data

Parameter	Temp./K	Reference	Technique/Comments
γ, γ_0			
$\gamma=3.7 \times 10^{-4}$ Adobe clay soil, RH \approx 0	298	Judeikis, 1982	CRFT (a)
$\gamma > 5.4 \times 10^{-7}$ (Adobe clay soil, RH > 12%)			
$\gamma_0=6.2 \times 10^{-6}$ (SiO ₂)	298	Li et al., 2001	Knudsen -MS (b)
$\gamma_0=2.0 \times 10^{-5}$ (α -Al ₂ O ₃)	298		
$\gamma_0=1.6 \times 10^{-4}$ (α -Fe ₂ O ₃)	298		
$\gamma_0=3.6 \times 10^{-4}$ (TiO ₂)	298		
$\gamma_0=1.2 \times 10^{-4}$ (CaO)	298		
$K_{\text{linC}} / \text{cm}$			
$5.3 \times 10^{-11} \exp(6109/T)$ (Quartz, RH=30 %)	323–373	Goss, 1992	PC-GC (c)
$4.8 \times 10^{-11} \exp(5736/T)$ (Quartz, RH=50 %)			
$9.1 \times 10^{-12} \exp(5984/T)$ (Quartz, RH=70 %)			
$\exp(-0.0523 * \text{RH} - 4.37)$ (Quartz)			
$1.67 \times 10^{-4} \exp(100 - \text{RH} * 0.0106)$ (α -Al ₂ O ₃)	333.5	Goss and Eisenreich, 1996	PC-GC (c)
$1.93 \times 10^{-4} \exp(100 - \text{RH} * 0.0187)$ (α -Fe ₂ O ₃)			
$1.44 \times 10^{-4} \exp(100 - \text{RH} * 0.0484)$ (Quartz)			
2.36×10^{-2} (Quartz, RH=40 %)	288	Goss and Schwarzenbach, 2002	PC-GC (c)
6.45×10^{-2} (Quartz, RH=70 %)			
2.23×10^{-2} (Quartz, RH=90 %)			
5.29×10^{-3} (α -Al ₂ O ₃ , RH=40 %)			
2.74×10^{-3} (α -Al ₂ O ₃ , RH=70 %)			
2.09×10^{-3} (α -Al ₂ O ₃ , RH=70 %)			
3.76×10^{-3} (CaCO ₃ O, RH=40 %)			
2.51×10^{-3} (CaCO ₃ O, RH=70 %)			
2.27×10^{-3} (CaCO ₃ O, RH=70 %)			

Comments

- (a) Soil sample deposited onto outside of cylindrical flow tube insert from an aqueous slurry and dried under vacuum. Observation of acetone displacement by adding water vapour to previously exposed dry sample and lack of uptake at RH=12–90% suggest competitive adsorption between acetone and H₂O. Photosensitised desorption of acetone also observed.
- (b) Uptake to bulk samples (1–30 mg) investigated using a Knudsen reactor with pulsed gas inlet and MS analysis of acetone at an initial concentration of 6×10^{10} molecule cm⁻³. The initial uptake coefficients (γ_0) given in the table were calculated using the BET surface area of the sample. Uptake was seen to saturate with exposure time, and time dependent values of γ were obtained. FTIR and UV/Vis diffuse reflectance analysis of the sample exposed to higher acetone concentrations revealed the presence of reaction products resulting from dehydration reactions (e.g. mesityl oxide).
- (c) Packed column with mineral particles BET-N₂ surface areas used to calculate available surface). K_{linC} found to be decrease as temperature and RH increase. The parameterisation in the table is valid for RH > 30 % .

Preferred values

No recommendation.

Comments on preferred values

Goss and co-workers have shown that, at equilibrium, the amount of acetone associated with a mineral oxide surface depends on the availability of surface adsorbed water for relative humidity between 30 and 90% (Goss, 1992, 1994; Goss and Eisenreich, 1994; Goss and Schwarzenbach, 2002), and displays only weak dependence on the nature of the mineral. At RH close to 100% the partitioning is controlled by dissolution in an aqueous surface film. Goss (1994) presented an algorithm for calculating the equilibrium partitioning, K_{linC} for mineral surfaces such as quartz and kaolinite from given values of temperature and relative humidity: $\ln K = A - \Delta H/R (1/T - 1/323.15) - C(100 - \text{RH})$, where $A = -8.18$, $\Delta H = -48.7 \text{ kJ mol}^{-1}$ and $C = -0.0523$ with R in kJ mol^{-1} . Most data were obtained at non-ambient temperatures and no information is available for authentic dust samples. For these reasons, no recommendation for K_{linC} is given for the purpose of atmospheric modelling.

References

- Goss, K.-U.: *Env. Sci. Tech.*, 26, 2287–2294, 1992.
Goss, K.-U.: *Env. Sci. Tech.*, 28, 640–645, 1994.
Goss, K.-U. and Eisenreich, S. J.: *Env. Sci. Tech.*, 30, 2135–2142, 1996.
Goss, K.-U. and Schwarzenbach, R. P.: *J. Colloid. Interface Sci.*, 252, 31–42, 2002.
Judeikis, H. S.: Laboratory measurement of dry deposition of acetone over adobe clay soil, in: “Heterogeneous Atmospheric Chemistry”, edited by: Schryer, D. R., Geophysical Monograph 26, American Geophysical Union, Washington D. C., 1982.
Li, P., Perreau, K. A., Covington, E., Song, C. H., Carmichael, G. R., and Grassian, V. H.: *J. Geophys. Res.*, 106, 5517–5529, 2001.

Appendix A3**Uptake on soot surfaces**

We do not present any data sheets for uptake of trace gases on soot in this evaluation and therefore Appendix 3 contains no material. We include the header here as a requirement to keep the data sheet numbering on the IUPAC web-site and the publications in ACP consistent.

Appendix A4**Uptake on sulphuric acid hydrate surfaces (SAT, SAM)****HO₂ + SAT****V.A4.1**

No experimental data.

N₂O₅ + H₂O (SAT) → products**V.A4.2****Experimental data**

Parameter	Temp./K	Reference	Technique/Comments
γ			
0.6×10^{-3} (60 wt. % H ₂ SO ₄ , RH 40%)	192	Hanson and Ravishankara, 1993	CWFT-CIMS (a)
2.4×10^{-3} (60 wt. % H ₂ SO ₄ , RH 80%)	192		
5×10^{-3} (57.5 wt. % H ₂ SO ₄ , RH 44–100%)	195		
8×10^{-3} (57.5 wt. % H ₂ SO ₄ , RH 22–85%)	205		
5×10^{-3} (60 wt. % H ₂ SO ₄ , RH 24–87%)	205		

Comments

- (a) Sulphuric acid tetrahydrate was generated by freezing H₂SO₄ solutions (57.5 or 60 wt. %). The relative humidity above the film was varied by adjusting the temperature at fixed H₂O partial pressure or by adjusting the H₂O partial pressure at fixed temperature. The geometric surface area was used to calculate the uptake coefficient. Experiments were conducted with p(N₂O₅) at $\approx 10^{-7}$ Torr.

Preferred values

Parameter	Value	T/K
γ (RH 22–100 %)	6.5×10^{-3}	195–205
<i>Reliability</i>		
$\Delta \log \gamma$	0.4	195–205

Comments on preferred values

The hydrolysis of N₂O₅ on sulphuric acid tetrahydrate films is much less efficient (\approx factor 20) than on liquid H₂SO₄. For SAT formed from an acid of concentration 57.5 wt.%, no dependence on RH was observed, whereas at 60 wt. % larger RH resulted in larger γ , possibly due to the presence of other hydrates. At 205 K values of γ were larger than at 192 K and the authors speculated that this may have been due to formation of a liquid ternary mixture. Our preferred value uses the data obtained at 57.5 wt. % H₂SO₄, which corresponds to the composition of SAT. It takes a simple average value of the results at the two temperatures covered and is independent of RH from 22 to 100%.

References

Hanson, D. R. and Ravishankara, A. R.: J. Geophys. Res., 98, 22931–22936, 1993.

HCl + SAT**V.A4.3****Experimental data**

Parameter	Temp./K	Reference	Technique/Comments
K_{linC} (cm)			
6800 (RH=79.4 %)	195 K	Zhang et al., 1994	FT-MS (a)

Comments

- (a) Sulphuric acid tetrahydrate films (>0.1 mm thick) were generated by freezing H₂SO₄ solutions (57.7 wt %) at 200 K. The relative humidity above the film was varied by adjusting the temperature at fixed H₂O partial pressure or by adjusting the H₂O partial pressure at fixed temperature to form either H₂O-rich or H₂SO₄-rich forms of SAT. The geometric surface area was used to calculate the uptake coefficient.

Preferred values

Parameter	Value	<i>T</i> /K
K_{linC} /cm (RH=79.4% only)	6800	195
<i>F</i>	$(-2.47 \times 10^{11} + 3.28 \times 10^{11} \cdot \text{RH} + 3.27 \times 10^9 \cdot \text{RH}^2 + 2.43 \times 10^8 \cdot \text{RH}^3) / 1.7 \times 10^{14}$	
RH	$100 \times P_{\text{H}_2\text{O}} / P_{\text{ice}}$	
Reliability		
$\Delta \log N$	0.5	190–199

Comments on preferred values

The interaction of HCl with sulphuric acid tetrahydrate film shows a strong dependence on both temperature and the pressure of water vapour, with the H₂O-rich form of SAT accommodating more HCl at the surface than the H₂SO₄-rich form. Zhang et al. (1994) present three separate parameterisations of the HCl surface coverage (*N*) with either *T*, p(H₂O) or p(HCl) as variables. The value of K_{linC} listed in the Table was taken from a dataset in which p(HCl) was systematically varied at a fixed temperature and fixed p(H₂O). Only data taken at low p(HCl) (p(HCl) < 2 × 10⁻⁶ Torr) were considered as here the adsorption isotherm is approximately linear and this range of pressures is relevant for the atmosphere.

The dependence of surface coverage (*N*) on temperature is very large, with a change < 10 K resulting in a factor of 100 change in *N* indicating that the surface interaction is driven by the availability of H₂O. We have taken the observed dependence of the surface coverage on p(H₂O) at a fixed temperature to derive the dependence of *N* on the relative humidity (relative to pure ice as given in Marti and Mauersberger, 1993) and provide a parameterisation for the surface coverage (*N*) that requires only the relative humidity and the HCl concentration (in molecule cm⁻³) as input:

$$N = [\text{HCl}] \times 6800 \times F$$

over the temperature range 190–199 K. Note that the parameterisation assumes that the low partial pressure HCl isotherm is linear at all relative humidities and is probably not valid for high partial pressures of HCl (e.g. greater than 10⁻⁶ Torr). It does however reproduce the data of Zhang et al. (1994) between to within a factor of two for *T* < 200 K.

References

- Marti, J. and Mauersberger, K.: Geophys. Res. Lett., 20, 363–366, 1993.
 Zhang, R. Y., Jayne, J. T., and Molina, M. J.: J. Phys. Chem., 98, 867–874, 1994.

HBr + SAT → products**V.A4.4****Experimental data**

Parameter	Temp./K	Reference	Technique/Comments
γ, γ_0			
0.25 (10% H ₂ SO ₄ , frozen)	190	Seisel and Rossi, 1997	Knud-MS (a)
0.18 (60% H ₂ SO ₄ , frozen)	190		
$<1 \times 10^{-4}$ (95% H ₂ SO ₄ , frozen)	220		
K (cm)			
No reversible adsorption			

Comments

- (a) HBr $(2-8) \times 10^{11}$ molecule cm⁻³. Uptake of pure HBr on frozen bulk aqueous solutions of defined [H₂SO₄]. No saturation effects observed.

Preferred values

Parameter	Value	T/K
γ_{ss}	0.18	190
<i>Reliability</i>		
$\Delta \log(\gamma_{ss})$	0.3	190

Comments on preferred values

There appears to be only one experimental study of HBr interaction with specifically prepared H₂SO₄-hydrate surfaces at temperatures and concentrations corresponding to hydrate thermodynamically stability regions. Under these conditions uptake is continuous and irreversible. There is a strong decrease of γ with increasing concentration of H₂SO₄ in frozen as well as in liquid supercooled H₂SO₄-H₂O mixtures.

References

Seisel, S. and Rossi, M. J.: Ber. Bunsenges. Phys. Chem., 101, 943, 1997.

N₂O₅ + HCl**V.A4.5**

No data for this reaction.

N₂O₅ + HBr**V.A4.6**

No data for this reaction.

ClONO₂ + H₂O (SAT) → HNO₃ + HOCl**V.A4.7****Experimental data**

Parameter	Temp./K	Reference	Technique/Comments
γ			
2.0×10^{-3} (RH=90%)	191.5	Hanson and Ravishankara, 1993	CWFT-CIMS (a)
2.0×10^{-3} (RH=30%)	196		
5.0×10^{-4} (RH=16%)	200		
1.0×10^{-4} (RH=7%)	205		
0.016 ± 0.004 (RH=100%)	195	Zhang et al., 1994	CWFT-MS (b)
5.6×10^{-3} (RH=72%)*	195		
2×10^{-3} (RH=36%)*	195		
9×10^{-4} (RH=18%)*	195		
$(5.0 \pm 1.3) \times 10^{-4}$ 8%RH	195		
0.02 (RH=100%)*	192		
4.0×10^{-3} (RH=52%)*	196		
1.5×10^{-3} (RH=28%)*	200		
0.85×10^{-3} (RH=13%)*	205		
$< 1 \times 10^{-4}$	200–220	Zhang et al., 1995	CWFT-CIMS (c)

Data marked * were extracted from graphs.

Comments

- (a) Solid film of sulphuric acid ≥ 0.1 mm thickness made from freezing a liquid solution of composition corresponding to SAT (57.5% H₂SO₄/H₂O) on the inside of the flow tube wall to 195K. The cryogenic deposits were characterized by their vapour pressure of H₂O monitored by an ion-molecule reaction with F₂⁻. The results were obtained as a function of relative humidity in the range 10 to 90%, obtained by using a fixed p(H₂O) $\sim 3.3 \times 10^4$ mbar and varying the temperature from 192–205 K. p(ClONO₂) = (1.3 to 7×10^{-7}) mbar. Uptake slower than onto liquid sulphuric acid surfaces.
- (b) Solid film of sulphuric acid ≥ 0.1 mm thickness made from freezing a liquid solution of composition corresponding to SAT (57.5% H₂SO₄/H₂O) on the inside of the flow tube wall to < 200 K. The thermodynamic state of the SAT sample was controlled by setting the vapour pressure of H₂O, either H₂O-rich (approaching 100% RH) or H₂SO₄-rich at constant temperature or selecting the temperature at constant p(H₂O). The p(H₂O) for the cited data are given in terms of relative humidity expressed relative to p(H₂O) for pure ice at the experimental temperature. The dependence of γ on p(H₂O) (Torr) and on temperature (K) was expressed in parametric form: $\log \gamma = 10.12 + 5.75 \log P + 0.62 \log^2 P$ for $T = 195$ K, [$P = p(\text{H}_2\text{O})$]; p(ClONO₂) = 3 to 5×10^{-8} Torr, p(H₂O) = 4×10^{-5} to 5.6×10^{-4} Torr; $\log \gamma = 318.67 - 3.13 \log T + 0.0076 \log^2 T$ for T in the range 192–206 K, p(ClONO₂) = 2 to 4×10^{-8} Torr and p(H₂O) = 3.4×10^{-4} Torr.

- (c) Uptake experiment on solid sulphuric acid monohydrate ($\text{H}_2\text{SO}_4 \cdot \text{H}_2\text{O}$, SAM) using a fast flow tube reactor coupled either to MS (most data) or CIMS. The thickness of the crystalline SAM films was approximately 0.1 mm, $p(\text{H}_2\text{O}) = (1.3\text{--}5.2) \times 10^{-4}$ mbar at 220–240 K. ClONO_2 uptake was much slower than onto liquid sulphuric acid surfaces.

Preferred values

Parameter	Value	T/K
γ	$1 \times 10^{-4} + 4 \times 10^{-5} \text{RH} + 4.7 \times 10^{-7} \text{RH}^2$	195–205
Reliability		
$\Delta(\log \gamma)$	0.3	195–205

$$\text{RH} = p(\text{H}_2\text{O})/p(\text{ice})$$

Comments on preferred values

Uptake of ClONO_2 on solid sulphuric acid films is followed by rapid reaction with H_2O to form HOCl and HNO_3 in a surface reaction. HOCl partitions into the gas phase, but HNO_3 can remain on the surface. The two studies on SAT show that uptake is slower than on liquid sulphuric acid and is a strong function of relative humidity. Thus the uptake coefficient depends on the thermodynamic state of the surface. The γ values of Hanson and Ravishankara (1993) are significantly lower than the more extensive data of Zhang et al. (1994), especially at low RH. The γ value of Zhang et al. (1993) for H_2O -rich SAT (>90% RH) is intermediate between that observed for ice (0.08 ± 0.02) and H_2O -rich NAT (~ 0.002). At lower $p(\text{H}_2\text{O})$ and higher temperatures the reaction becomes very slow, although there is some indication that γ on H_2O -rich SAT increases with decreasing temperature. The origin of the apparent discrepancy in the two studies at low RH is unclear. Hanson and Ravishankara (1993) reported time-dependent γ , characteristic of inhibition of uptake by surface HNO_3 , whilst Zhang et al. (1994) report γ constant with exposure time.

The IUPAC recommended parameterisation for hydrolysis of ClONO_2 on ice surfaces used a Langmuir-Hinshelwood model. Application of this model to solid sulphuric acid films requires the surface concentration of water molecules $[\text{H}_2\text{O}]_s$ to be defined. If $[\text{H}_2\text{O}]_s$ is related directly to $p(\text{H}_2\text{O})$ (i.e., low coverage of available H_2O molecules) γ_{gs} should be linearly dependent on RH (or $p(\text{H}_2\text{O})$ at a fixed temperature). The experimental γ values of Zhang et al. (1994) 195 K show higher order dependence on RH, indicating a more complex model is needed. Note that if surface saturation at high RH occurs the opposite trend would result.

The recommended expression for γ_{ClONO_2} is a second order polynomial fit as a function of relative humidity to results of Zhang et al. (1994) over the temperature range 191.5 to 205 K. An alternate parameterisation based on the Langmuir-Hinshelwood model fit to the data for 195 K:

$$\frac{1}{\gamma} = \frac{1}{\alpha_s} + \frac{A}{\text{RH}(\%)}$$

where $\alpha_s = 1$ and $A = (1.68 \pm 0.22) \times 10^4$. This gives a reasonable representation of the uptake coefficient at $\text{RH} < 60\%$ but underestimates the uptake coefficient 100% RH. The factor A in the RH dependent part of the expression contains usual \bar{c} , k_s and K_{linC} terms for ClONO_2 , as well as the conversion between $[\text{H}_2\text{O}]_s$ (molecule cm^{-2}) and relative humidity (i.e., $p(\text{H}_2\text{O})/p(\text{ice})$) [$= 7.4 \times 10^{-4}$ mbar at 195 K]. The temperature dependence of these terms is needed if the expression is applied to other temperatures.

References

- Hanson, D. R. and Ravishankara, A. R.: J. Geophys. Res., 98, 22931, 1993.
 Leu, M.-T., Moore, S. B., and Keyser, L. F.: J. Phys. Chem., 95, 7763, 1991.
 Zhang, R., Jayne, J. T., and Molina, M. J.: J. Phys. Chem., 98, 867, 1994.



V.A4.8

Experimental data

Parameter	Temp./K	Reference	Technique/Comments
γ, γ_0			
0.125 100% RH	192	Hanson and Ravishankara, 1993	CWFT-CIMS (a)
2.4×10^{-4} 8% RH	205		
0.12±0.03 100% RH	195	Zhang et al., 1994	CWFT-EIMS (b)
0.06±0.03 72% RH*			
0.04±0.03 61% RH*			
0.01±0.03 36% RH*			
0.00350±03 18% RH*			
$(7.0 \pm 2.0) \times 10^{-4}$ 7% RH			
>0.2*	190		
0.02*	208		
$<1.0 \times 10^{-4}$	200–220	Zhang et al., 1995	CWFT-CIMS (c)

Comments

- (a) Solid film of sulphuric acid ≥ 0.1 mm thickness made from freezing a liquid solution of composition corresponding to SAT (57.5% $\text{H}_2\text{SO}_4/\text{H}_2\text{O}$) on the inside of the flow tube wall to 195K. The cryogenic deposits were characterized by their vapour pressure of H_2O monitored by an ion-molecule reaction with F_2^- . The results were obtained as a function of relative humidity in the range 10 to 90%, obtained by using a fixed $p(\text{H}_2\text{O})$ and varying the temperature from 192–205 K. $p(\text{ClONO}_2) = (1.3 \text{ to } 7 \times 10^{-7})$ mbar. $p(\text{HCl})$ was approximately held at 2×10^{-7} mbar (2–3 ppbv at 17 km) and $p(\text{H}_2\text{O})$ for the displayed γ values was 6.7×10^{-4} mbar. The uptake coefficients could be expressed as $\ln \gamma = -0.636 - 0.4802 \Delta T$, where $\Delta T = T - 189$. ΔT can be approximated by $T - T_{\text{ice}}$ where T_{ice} is the temperature of the ice point at a given partial pressure of water vapor and where $p(\text{H}_2\text{O}) < p(\text{ice})$.
- (b) Solid film of sulphuric acid ≥ 0.1 mm thickness made from freezing a liquid solution of composition corresponding to SAT (57.5% $\text{H}_2\text{SO}_4/\text{H}_2\text{O}$) on the inside of the flow tube wall to < 200 K. The thermodynamic state of the SAT sample was controlled by setting the vapour pressure of H_2O , either H_2O -rich (approaching 100% rh) or H_2SO_4 -rich at constant temperature or selecting the temperature at constant $p(\text{H}_2\text{O})$. The HCl was always in excess of ClONO_2 and no HOCl product was detected. γ strongly depends on the relative humidity over the SAT surface, a trend that reflects the partitioning of HCl to the surface; its value decreases by more than two orders of magnitude at 195 K, from 0.12 at 100% rh to 7×10^{-4} at low rh. The following expressions are provided for the uptake coefficient at typical stratospheric [HCl]: $\log \gamma = 5.25 + 1.91 \log p(\text{H}_2\text{O})$ for $T = 195$ K, $p(\text{ClONO}_2) = 4$ to 5.3×10^{-8} mbar, $p(\text{HCl}) = 5.3$ to 10.5×10^{-7} mbar, $p(\text{H}_2\text{O}) = 5.3 \times 10^{-5}$ to 7.4×10^{-5} mbar; $\log \gamma = 175.74 - 1.59 \log T + 0.0035 \log^2 T$ for T in the range 195–206 K, $p(\text{ClONO}_2) = 4$ to 6.7×10^{-8} mbar, $p(\text{HCl}) = 5.3$ to 10.6×10^{-7} mbar and $p(\text{H}_2\text{O}) = 7.4 \times 10^{-4}$ mbar.
- (c) Solid film of sulphuric acid ≥ 0.1 mm thickness made from freezing a liquid solution of composition corresponding to SAM (75–85% $\text{H}_2\text{SO}_4/\text{H}_2\text{O}$) on the inside of the flow tube wall at 220–230 K. $p(\text{HCl})$ and $p(\text{ClONO}_2)$ were in the range 2.7 to 10.6×10^{-7} mbar. The experiment was performed by first exposing SAM to HCl and subsequently measuring the uptake of ClONO_2 which was identical to hydrolysis on SAM with HCl absent.

Preferred values

Parameter	Value	T/K
γ_{gs}	0.12	190–199
F	$(-2.47 \times 10^{11} + 3.28 \times 10^{11} \text{RH} + 3.27 \times 10^9 \text{RH}^2 + 2.43 \times 10^9 \text{RH}^3) / 1.7 \times 10^{14}$	190–200
<i>Reliability</i>		
$\Delta\gamma_{\text{gs}}$	± 0.2	190–200

RH=p(H₂O)/p(ice)

Comments on preferred values

As with ice films the uptake of ClONO₂ on SAT films is followed by reaction with HCl to form Cl₂ and HNO₃ in a surface reaction. At stratospheric temperatures HOCl partitions into the gas phase. The two studies of Hanson and Ravishankara (1993) and Zhang et al. (1994) on SAT show that reactive uptake of ClONO₂ on HCl-doped SAT is a strong function of relative humidity, declining as RH reduced, as was also found for NAT surfaces. In the case of SAT, Zhang et al. (1994) showed that surface coverage resulting from a given p(HCl) also declined rapidly with decreasing RH, which accounts for the effect on the surface reaction rate and hence the reactive uptake coefficient of ClONO₂. The γ values of Hanson and Ravishankara (1993) are in good agreement with the more extensive data Zhang et al. (1994). For H₂O-rich SAT (>90% RH) at 195 K, $\gamma=0.12$ which is approximately a factor of 2 lower than observed for HCl doped ice (0.27 ± 0.02) for similar p(HCl) of 7×10^{-7} mbar. At lower p(H₂O) and higher temperatures γ reduces to $\sim 10^{-3}$, although there is some indication that γ on H₂O-rich SAT increases with decreasing temperature. Reactive uptake of ClONO₂ on HCl-doped SAM is very slow, $\gamma \sim 1 \times 10^{-4}$.

The IUPAC recommended uptake coefficient parameterisation for reaction of ClONO₂+HCl on ice surfaces used an Eley-Rideal model. Application of this model to solid sulphuric acid films requires the surface concentration [HCl]_s to be defined as a function of temperature and p(H₂O). The partitioning of HCl to SAT studied by Zhang et al. (1994) forms the basis of our recommendation for K_{linC} for HCl as a function of RH in the temperature range 190–199 K. The recommended reactive uptake coefficients for ClONO₂+HCl uses the IUPAC K_{linC} to evaluate surface coverage of HCl in the following expression:

$$\gamma(\text{ClONO}_2) = \gamma_{\text{gs}} \times [\text{HCl}] \times 6800 \times F$$

where [HCl] is in molecule cm⁻³. The uptake coefficients from this expression give a reasonable fit to results of Zhang et al. (1994) as a function of relative humidity and temperature over the temperature range 191.5 to 205 K.

References

- Hanson, D. R. and Ravishankara, A. R.: J. Geophys. Res., 98, 22931, 1993.
 Leu, M.-T., Moore, S. B., and Keyser, L. F.: J. Phys. Chem., 95, 7763, 1991.
 Zhang, R., Jayne, J. T., and Molina, M. J.: J. Phys. Chem., 98, 867, 1994.

HNO₃ + SAT → products**V.A4.9****Experimental data**

Parameter	Temp./K	Reference	Technique/Comments
γ, γ_0			
$\gamma_0 > 0.3$	191.5	Hanson, 1992	CWFT-CIMS (a)
$\gamma_0 > 0.2$	200		
$\gamma_0 = 0.20$ 10% H ₂ SO ₄	180	Aguzzi and Rossi, 1991	Knudsen (b)
$\gamma_0 = 0.05$ 98% H ₂ SO ₄	180		
$\gamma_0 = 0.10$ 10% H ₂ SO ₄	200		
$\gamma_0 = 0.03$ 98% H ₂ SO ₄	200		
K(cm)			
No reversible adsorption observed			

Comments

- (a) HNO₃ uptake on SAT film made by freezing aqueous sulphuric acid solutions of composition 57.5 or 59.6 wt.% on the flow tube wall at <200 K. γ corrected for gas diffusion using estimated diffusion coefficients. Pressure=0.6 mbar He. Rapid uptake observed, but with increasing surface coverage of HNO₃ the rate of uptake decreased. The steady-state partial pressure of HNO₃ over SAT surface at 191 K with a coverage of approximately 1 monolayer of HNO₃ was about a factor of ~ 3 higher than the vapor pressure over NAT, showing that new hydrate was not formed. At 200 K $p(\text{HNO}_3)$ was $\sim 3 \times$ lower than over pure NAT. This is attributed to the formation of metastable NAM at this temperature.
- (b) SAT film made by freezing aqueous sulphuric acid solutions of composition indicated in wt. %. Uptake was continuous and γ was time-independent except at the highest [H₂SO₄], when some decline with exposure time was noticed. The initial uptake coefficient decreased linearly with increasing [H₂SO₄] in the range given at both temperatures. If H₂O vapour was added to the flow into the Knudsen cell, the uptake coefficient was independent of [H₂SO₄] up to ~ 60 –70%, depending on temperature.

Preferred values

Parameter	Value	T/K
α_s	>0.2	190–240
<i>Reliability</i>		
$\Delta \log(\alpha_s)$	0.3	190–240

Comments on preferred values

The results of the two experimental studies of nitric acid interaction with specifically prepared solid H₂SO₄-hydrate surfaces at temperatures and concentrations relevant for the lower stratosphere are in good agreement. Under these conditions uptake is rapid, continuous and irreversible, but declined with increasing coverage of surface HNO₃. Evidence from measurements of the $p(\text{HNO}_3)$ over the surfaces indicated that the NAT-type solids formed on the surfaces were not in complete vapour-solid equilibrium. The data do not allow determination of the partition coefficient for adsorption, but the agreement between the results from different techniques allows us to recommend an accommodation coefficient.

References

- Aguzzi, A. and Rossi, M. J.: Phys. Chem. Chem. Phys., 3, 3707, 2001.
Hanson, D. R.: J. Geophys. Res. Lett., 19, 2063, 1992.

N₂O₅ + H₂O (SAM) → products**V.A4.10****Experimental data**

Parameter	Temp./K	Reference	Technique/Comments
γ			
$0.162+0.789 \times \log p(\text{H}_2\text{O})$	210	Zhang et al., 1995	CWFT-MS (a)
$4.78-0.0386 \times T$ ($p(\text{H}_2\text{O})=2 \times 10^{-5}$ Torr)	200–225		

Comments

- (a) Sulphuric acid monohydrate was generated by freezing a liquid film (≈ 0.1 mm thick, ≈ 85 wt. %). The relative humidity above the film was varied by adjusting the temperature at fixed H₂O partial pressure or vice-versa. The geometric surface area was used to calculate the uptake coefficient. Experiments were conducted with [N₂O₅] at $\approx 4-7 \times 10^{-7}$ Torr which was ionised by electron impact or CIMS. Note that the authors reported $\gamma=0.162-0.789 \times \log p(\text{H}_2\text{O})$, which appears to have a sign error.

Preferred values

Parameter	Value	T/K
γ	$\text{RH} * 4.63 \times 10^{-4} + 2.6 \times 10^{-4}$	200–225
<i>Reliability</i>		
$\Delta \log \gamma_{\text{net}}$	0.5	200–225

Comments on preferred values

The only study (Zhang et al., 1995) of the hydrolysis of N₂O₅ on sulphuric acid monohydrate showed that the process is much less efficient (\approx factor 50) than on liquid H₂SO₄ and displayed a strong dependence on the water vapour partial pressure and the temperature (see expressions given in the Table) with γ (210 K) increasing by a factor of 5 going from $p(\text{H}_2\text{O})=1 \times 10^{-5}$ Torr to $p(\text{H}_2\text{O})=1 \times 10^{-4}$ Torr. This represents a change in RH from ≈ 0.3 to 3%. Higher values of RH would have caused a phase change to SAT and were thus not possible. Similar results were obtained when the partial pressure of H₂O was held at 2×10^{-5} Torr and the temperature was varied (200–225 K). The preferred values of γ were obtained by combining these two data sets by plotting γ versus RH, defined as $\text{RH}=100 * p(\text{H}_2\text{O})/p(\text{ice})(T)$ with values of the vapour pressure of H₂O over ice taken from Marti and Mauersberger (1993). Note that RH is given in %.

References

- Marti, J. and Mauersberger, K.: Geophys. Res. Lett., 20, 363–366, 1993.
 Zhang, R. Y., Leu, M. T., and Keyser, L. F.: Geophys. Res. Lett., 22, 1493–1496, 1995.

N₂O₅ + HCl (SAM) → products**V.A4.11****Experimental data**

Parameter	Temp./K	Reference	Technique/Comments
γ 1×10^{-4} (p(HCl)= $2-8 \times 10^{-7}$ Torr)	200–220	Zhang et al., 1995	CWFT-MS (a)

Comments

- (a) Sulphuric acid monohydrate was generated by freezing a liquid film (≈ 0.1 mm thick, ≈ 85 wt. %). The surface was doped with p(HCl)=($2-8$) $\times 10^{-4}$ Torr. The geometric surface area was used to calculate the uptake coefficient. Experiments were conducted with p(N₂O₅) at $\approx (2-7) \times 10^{-7}$ Torr which was ionised by electron impact or CIMS. No enhancement in the uptake coefficient compared to the hydrolysis values (on pure SAM) were observed and a conservative upper limit of 10^{-4} was obtained for γ .

Preferred values

Parameter	Value	T/K
γ	$< 10^{-4}$	200–220
<i>Reliability</i>		
$\Delta \log(\gamma)$	undetermined	

Comments on preferred values

The low (net) uptake coefficient measured for reaction of N₂O₅ with HCl is consistent with the low water activity associated with the SAM surfaces, which results in low coverage by HCl.

References

Zhang, R. Y., Leu, M. T., and Keyser, L. F.: Geophys. Res. Lett., 22, 1493–1496, 1995.

Appendix A5

Uptake on nitric acid hydrate surfaces (NAT)

O₃ + NAT → products

V.A5.1

Experimental data

Parameter	Temp./K	Reference	Technique/Comments
γ			
$\gamma_{ss}=(1-5)\times 10^{-4}(1.0\times 10^{-8}\text{ mbar})$	195	Dlugokencky and Ravishankara, 1992	CWFT-CLD (a)
$\gamma_{ss}=(0.2-9)\times 10^{-5}(5.0\times 10^{-9}\text{ mbar})$	196		
$\gamma_{ss}<8\times 10^{-5}(1.6\times 10^{-4}\text{ mbar})$	193	Kenner et al., 1993	CWFT-MS (b)

Comments

- (a) Coated flow tube reactor using high sensitivity chemiluminescence detection of ozone. $[\text{O}_3]=10^8$ molecule cm^{-3} to 10^{12} molecule cm^{-3} with 1.3 mbar of He carrier gas. The flow tube was coated by freezing a 0.25 mole fraction solution at 196 K onto the flow tube walls, resulting in a coating of approx. 2 mm thickness. These films were not characterized. They presumably contain some NAT, but likely also remaining nitric acid solution. A measurable but not well reproducible uptake of O₃ was observed that decreased with time.
- (b) Fast flow reactor with electron-impact MS. A 4–7 μm thick NAT film was deposited from a 3:1 gas phase mixture of H₂O:HNO₃ on top of a previously deposited 2–3 μm thick ice film. No loss of O₃ could be observed, and the value given in the table is an upper limit based on the sensitivity. As ClO was the main target of this study, the O₃ detection by mass spectrometry was not calibrated, and the pressure given is only a rough estimate.

Preferred values

Parameter	Value	T/K
γ	$<1\times 10^{-6}$	180–200
<i>Reliability</i>		
$\Delta\log(\gamma)$	undetermined	

Comments on preferred values

Even though the study using the more sensitive method to detect O₃ at very low concentration detects a measurable loss of O₃, which decreases with time, the authors caution that they may have observed uptake of O₃ into cracks and remaining liquid nitric acid solution of the not well characterized NAT film. At higher O₃ concentration, the study by Kenner et al. could not detect any uptake. No products have been observed. We therefore use the lowest observed uptake coefficient of the experiment by Dlugokencky and Ravishankara (1992) to recommend an upper limit for γ .

References

- Dlugokencky, E. J. and Ravishankara, A. R.: Geophys. Res. Lett., 19, 41–44, 1992.
 Kenner, R. D., Plumb, I. C., and Ryan, K. R.: Geophys. Res. Lett., 20, 193–196, 1993.

H₂O + NAT**V.A5.2****Experimental data**

Parameter	Temp./K	Reference	Technique/Comments
γ			
$2.0 \times 10^{-3} \leq \gamma_{ss} \leq 1.0 \times 10^{-2}$	197	Middlebrook et al., 1992	Static reactor/FTIR (a)
α			
$(2.2-6.0) \times 10^{-2}$ (β -NAT))	192-202	Biermann et al., 1998	Slow-Flow reactor/FTIR (b)
0.32 ± 0.14 (α -NAT)	179-185	Delval and Rossi, 2005	SFR-FTIR (c)
0.15 ± 0.12 (β -NAT)			
0.38 ± 0.12 (α -NAT)	189-195		
0.069 ± 0.047 (β -NAT)			
0.56 ± 0.31 (α -NAT)	205-208		
0.0166 ± 0.001 (β -NAT)			

Comments

- (a) Isothermal film growth experiment in a static chamber with time-dependent FTIR monitoring of optical density at 3371 cm^{-1} during deposition of NAT film on Si support. $p_{\text{H}_2\text{O}} = (2.0-4.0) \times 10^{-4}$ mbar and $p(\text{HNO}_3) = (5.3-40) \times 10^{-7}$ mbar. The spread of the γ values given in the table corresponds to the range in the HNO_3 pressure. A doubling of H_2O at the upper limit of the HNO_3 pressure left the uptake coefficient unchanged.
- (b) Evaporation experiment performed in a 100 cm^3 slow-flow cell fed by a thermostatted bubbler containing a binary $\text{H}_2\text{O}/\text{HNO}_3$ solution ($[\text{H}_2\text{O}]/[\text{HNO}_3] = 68$) and using N_2 as a carrier gas at 0.85 mbar. Polished Au-coated support was used as a mirror for near-normal incidence FTIR absorption. The α values have been calculated from the thickness vs. time curves obtained from FTIR absorption and optical constants of ice and NAT. They and do not include corrections for mass transport or desorption and are therefore lower limiting values. No apparent temperature dependence was found. The vapour pressure of an ice film is altered neither by co-condensed NAT nor an ice-free NAT layer located on top of pure ice.
- (c) Measurement of H_2O evaporation rate using a multidagnostic stirred flow reactor using a quartz crystal microbalance (QCMB), FTIR absorption in transmission and residual gas MS. The ice sample was vapour-deposited on either a Au-coated SiO_2 crystal (QCMB) or a Si-window (FTIR) at 190K upon which typically between a few and 200 monolayers of HNO_3 were deposited, respectively. The evaporation rate of H_2O was recorded as a function of time and ranged from the rate of pure ice evaporation at the start of the experiment to decomposition of β -NAT at the end. FTIR absorption of thin ice films doped with HNO_3 pointed to the existence of pure ice, α - and β -NAT, in this sequence, upon evaporation.

Preferred values

Parameter	Value	T/K
α (α -NAT)	0.32	182
α (α -NAT)	0.38	192
α (α -NAT)	0.56	207
α (β -NAT)	0.15	182
α (β -NAT)	7.0×10^{-2}	192
α (β -NAT)	1.7×10^{-2}	207
Reliability		
$\Delta \log \alpha$	0.3	

Comments on preferred values

The kinetic uptake data of Middlebrook et al. (1992) have been obtained from a pressure measurement inside a static reactor and observation of the changes in optical density of the growing film using FTIR absorption, whereas Biermann et al. (1998) have measured the evaporation rates at small undersaturation of H₂O close to equilibrium. Delval and Rossi (2005) have measured $\alpha(\text{H}_2\text{O})$ from time-dependent evaporation rates under conditions that precluded adsorption processes (low partial pressure of H₂O, hence strong H₂O undersaturation owing to fast pumping conditions). The Middlebrook et al. (1992) and Biermann et al. (1998) values (γ_{ss}) are lower limits to H₂O accommodation on β -NAT, the stable crystalline modification of NAT. The results of Delval and Rossi (2005) approach those corresponding to the upper limit of Middlebrook et al. (1992) at the high temperature end, in agreement with the known trend of α to decrease with increasing temperature (negative temperature dependence) in analogy to the interaction of H₂O with pure ice in the same temperature range. The general agreement of $\alpha(\text{H}_2\text{O})$ for β -NAT in the narrow overlapping temperature range of Biermann et al. (1998) and Delval and Rossi. (2005) is satisfactory although the former do not report a specific temperature dependence. However, the positive temperature dependence of α of Delval and Rossi (2005) on α -NAT, a metastable form of crystalline NAT and a precursor during formation of β -NAT, is unexpected and not yet understood. The larger α value for amorphous compared to crystalline ice in the given temperature range is in agreement with the results of Speedy et al. (1996) if we identify the α -NAT phase with an amorphous state of the condensate. Although β -NAT was the stable species in the H₂O/HNO₃ system in the kinetic experiments of Delval and Rossi (2005) in agreement with the phase diagram, the IR-spectroscopic identification of both α - and β -NAT have been made using HNO₃ doses that were a factor of 30 to 50 larger to enable the spectroscopic detection of thin films of NAT in the mid-IR spectral region. The significant scatter in the α -values for α - and β -NAT of Delval and Rossi (2005) is perhaps due to the time scale of α to β -NAT conversion that is competitive with H₂O evaporation.

References

- Biermann, U. M., Crowley, J. N., Huthwelker, T., Moortgat, G. K., Crutzen, P. J., and Peter, T.: *Geophys. Res. Lett.*, 25, 3939, 1998.
- Delval, C. and Rossi, M. J.: *J. Phys. Chem. A.*, 109, 7151, 2005.
- Middlebrook, A. M., Koehler, B. G., McNeill, L. S., and Tolbert, M. A.: *Geophys. Res. Lett.*, 19, 2417, 1992.
- Speedy, R. J., Debenedetti, P. G., Smith, R. S., Huang, C., and Kay, B. D.: *J. Chem. Phys.*, 105, 240, 1996.

NO + NAT**V.A5.3**

No experimental data.

NO₂ + NAT**V.A5.4**

No experimental data.

N₂O₅ + NAT**V.A5.5****Experimental data**

Parameter	Temp./K	Reference	Technique/Comments
γ, γ_0			
$\gamma_0=0.13\pm 0.03$	188	Quinlan et al., 1990	Knud-MS (a)
$\gamma=(6\pm 3)\times 10^{-4}$	200	Hanson and Ravishankara, 1991	CWFT-CIMS (b)
$\gamma=6\times 10^{-4}$	191	Hanson and Ravishankara, 1992	CWFT-CIMS (c)
$\gamma=(3\pm 1)\times 10^{-4}$	191	Hanson and Ravishankara, 1993	CWFT-CIMS (d)

Comments

- (a) Ice condensed from the vapor phase and doped with HNO₃. Product HNO₃ observed when the ice phase was allowed to warm up after the reaction. γ drops from the maximum given in the Table to a value of 4×10^{-3} .
- (b) A NAT layer 1 to 2 monolayers thick (2 to 4×10^{14} HNO₃ cm⁻²) was prepared in situ by converting N₂O₅ into HNO₃ on the ice surface. No saturation of γ on NAT.
- (c) Influence of the thickness of the substrate on γ was investigated. γ varied by a factor of no more than three and 1.5 for NAT and pure ice, respectively, when the thickness was varied from 1 to 100 μ m. The conclusion is that there is no significant dependence of γ on thickness. Thus the relevant surface corresponded to the geometric area.
- (d) This study further confirmed the independence of the measured uptake coefficients on the substrate thickness.

Preferred values

Parameter	Value	T/K
γ	6×10^{-3}	190–200
<i>Reliability</i>		
$\Delta\log(\gamma)$	0.3	190–200

Comments on preferred values

N_2O_5 uptake on specifically prepared HNO_3 -hydrate surfaces at conditions corresponding to NAT stability regions, is irreversible and leads to formation of HNO_3 . The uptake rate does not saturate and the preferred value for the steady-state reactive uptake coefficient is based on the results of Hanson and Ravishankara (1991).

References

- Hanson, D. R. and Ravishankara, A. R.: J. Geophys. Res., 96, 5081, 1991.
Hanson, D. R. and Ravishankara, A. R.: J. Phys. Chem., 96, 2682, 1992.
Hanson, D. R. and Ravishankara, A. R.: J. Phys. Chem., 97, 2802, 1993.
Quinlan, M. A., Reihls, C. M., Golden, D. M., and Tolbert, M. A.: J. Phys. Chem., 94, 3255, 1990.

HNO₃ + NAT**V.A5.6****Experimental data**

Parameter	Temp./K	Reference	Technique/Comments
γ, γ_0			
$\gamma_0 > 0.3$	191.5	Hanson, 1992	CWFT-CIMS-MS (a)
$\gamma_0 > 0.2$	200		
$\gamma_0 > 0.4$	197	Middlebrook et al., 1992	Knudsen (b)
$\gamma = 0.165$ HNO ₃ ·3H ₂ O (NAT)	160–170	Reinhardt et al., 2003	(c)
0.145 HNO ₃ ·2H ₂ O (NAD)			
0.13 HNO ₃ ·H ₂ O (NAM)			
K_{inC} (cm)			
No reversible adsorption			

Comments

- (a) HNO₃ deposited on ice condensed from the vapor phase onto the cold flow tube. γ corrected for gas diffusion using estimated diffusion coefficients. Pressure=0.6 mbar He. Rapid uptake observed, but with increasing surface coverage of HNO₃ the rate of uptake decreased. The steady-state partial pressure of HNO₃ over an ice surface with a coverage of approximately 1 monolayer of HNO₃ was about a factor of five higher than the vapor pressure over NAT, showing that new hydrate was not formed.
- (b) Static chamber with time-dependent FTIR monitoring of depositing NAT film. The thickness of the deposited NAT film was measured by optical interference in the range 4000 cm⁻¹ to 7000 cm⁻¹ assuming a refractive index of 1.45 for NAT. $p(\text{H}_2\text{O}) = 2 \times 10^{-4}$ mbar and $p(\text{HNO}_3) = (5.3\text{--}13.3) \times 10^{-7}$ mbar. A doubling of the H₂O left the uptake coefficient unchanged.
- (c) Slow flow reaction cell with DRIFTS for detection of adsorbed species and downstream FTIR for gas phase HNO₃. Total pressure 10–30 mbar. At 170K and $[\text{HNO}_3] = (2\text{--}5) \times 10^{14}$ molecule cm⁻² continuous uptake was observed with formation of crystalline HNO₃·H₂O (NAT). Monohydrates and dihydrates formed at higher $p(\text{HNO}_3)$. Uptake coefficient independent of $p(\text{HNO}_3)$.

Preferred values

Parameter	Value	T/K
α_s	0.2	190–200
<i>Reliability</i>		
$\Delta \log(\alpha_s)$	0.3	190–200

Comments on preferred values

There have been few experimental studies of nitric acid interaction with specifically prepared HNO₃-hydrate surfaces at temperatures and concentrations corresponding to hydrate thermodynamically stability regions. Under these conditions at $T < 210$ K uptake is continuous and irreversible.

References

- Hanson, D. R.: J. Geophys. Res. Lett., 19, 2063 1992.
 Middlebrook, A. M., Koehler, B. G., McNeill, L. S., and Tolbert, M. A.: Geophys. Res. Lett., 19, 2417, 1992.
 Reinhardt, H., Fida, M., and Zellner, R.: J. Mol. Struct., 661–662, 567–577, 2003.

HCHO + NAT → products**V.A5.7**

No experimental data.

HCl + NAT → products**V.A5.8****Experimental data**

Parameter	Temp./K	Reference	Technique/Comments
γ, γ_0 $\gamma > 0.2$	202	Abbatt and Molina, 1992	CWFT-MS (a)
K_{linC} (cm) 27.5 (at $p(\text{H}_2\text{O})=6.7 \times 10^{-4}$ mbar) 534 (at $p(\text{H}_2\text{O})=16.6 \times 10^{-4}$ mbar)	202	Abbatt and Molina, 1992	CWFT-MS (a)
3×10^4 (at $p(\text{H}_2\text{O}) \sim 3 \times 10^{-4}$ mbar)	191	Hanson and Ravishankara, 1992	CWFT-CIMS (b)
2.57×10^4 (at $p(\text{H}_2\text{O})=1 \times 10^{-4}$ mbar)	199	Chu et al., 1993	CWFT-MS (c)

Comments

- (a) The NAT films were prepared from 10 μm thick ice films exposed to $\sim 1 \times 10^{-4}$ mbar HNO_3 to form a NAT layer a few μm thick on top of the ice film. $p(\text{H}_2\text{O})$ was varied to provide water-rich or HNO_3 -rich NAT films. At $p(\text{HCl})$. At higher $p(\text{HCl})$ ($> 2 \times 10^{-4}$ mbar) irreversible uptake occurs above a threshold value which depends on $p(\text{H}_2\text{O})$, suggested due to formation of a liquid surface by HCl. The cited uptake coefficient refers to these conditions. The surface coverage increased from 0.05 to 1.7×10^{14} molecules cm^{-2} in the reversible adsorption region depending on $p(\text{HCl})$ and $p(\text{H}_2\text{O})$. The value of K_{linC} at low $p(\text{H}_2\text{O})=6.7 \times 10^{-4}$ mbar was obtained from a linear plot of surface coverage against $[\text{HCl}]$. At higher $p(\text{H}_2\text{O})$ and fixed $[\text{HCl}]$ ($=2.3 \times 10^{10}$ molecules cm^{-3}) partition coefficients were calculated observed surface coverages assuming $N_{\text{max}}=3 \times 10^{14}$ molecules cm^{-2} .
- (b) The NAT films were prepared from 10 μm thick ice films exposed to HNO_3 . $p(\text{H}_2\text{O})$ was set at the ice pressure which provided water-rich NAT films. $[\text{HCl}] \sim 1 \times 10^{10}$ molecules cm^{-3} . The HCl uptake is reported to be reversible and saturates at a surface coverage of $(2-3) \times 10^{14}$ molecules cm^{-2} , which was $50 \pm 10\%$ of the coverage achieved on ice at the same $[\text{HCl}]$. No dependence on $p(\text{HCl})$ is given, but the partition constant is calculated assuming $N_{\text{max}}=3 \times 10^{14}$ molecules cm^{-2} and a fractional surface coverage of $\theta=0.5$ (1.5×10^{14} molecules cm^{-2} at $[\text{HCl}]=1 \times 10^{10}$ molecules cm^{-3}).
- (c) The NAT films were prepared by freezing vapours from 54% aqueous HNO_3 solutions at 188K. They consisted of a mixture of NAT and water ice and were $\sim 1.6 \mu\text{m}$ thick. $p(\text{H}_2\text{O})$ was set at the ice pressure which provided water-rich NAT films. Uptake was fully reversible at low $[\text{H}_2]/[\text{HNO}_3]$ and increased with $p(\text{H}_2\text{O})$. Partition coefficient calculated from the surface coverage of $\sim 2 \times 10^{14}$ molecules cm^{-2} at $[\text{HCl}]=2.33 \times 10^{10}$ molecules cm^{-3} assuming $N_{\text{max}}=3 \times 10^{14}$ molecules cm^{-2} .

Preferred values

Parameter	Value	T/K
α_s	0.3	190-210
$N_{\text{max}}/\text{molecule cm}^{-2}$	3×10^{14}	190-230
$K_{\text{linC}}/\text{cm}$	3×10^4	191
$K_{\text{linC}}/\text{cm}$	$9.5 \times 10^{-3} \exp(2858)$	190-210
<i>Reliability</i>		
$\Delta \log(\alpha_s)$	0.3	190-210
$\Delta(K_{\text{linC}})/\text{cm}$	0.3	191-210

Comments on preferred values

The three studies which addressed uptake of HCl on NAT surfaces show that uptake is strongly dependent on the state of the NAT surface, and in particular the water vapour partial pressure. At low [HCl] on HNO₃-rich NAT films (low p(H₂O)) uptake is reversible, saturates and is much weaker than on water ice surfaces. However H₂O-rich NAT films take up HCl in amounts similar to water ice surfaces. At high p(HCl) ($>1.33 \times 10^{-4}$ mbar) very much greater uptake by both H₂O-rich and HNO₃-rich NAT films is observed, which indicates surface melting occurs in these cases.

Only the study of Abbatt and Molina (1992) using HNO₃-rich NAT films showed an [HCl] dependence of uptake that could be used to derive partition coefficients at low coverage. Their data for (taken from Fig. 4 of Abbatt and Molina, 1992) was used to obtain the cited value of $K_{\text{linC}}=27.5$ cm. At higher surface coverages partition coefficients were calculated from observed surface coverages assuming $N_{\text{max}}=3 \times 10^{14}$ molecules cm⁻². The K_{linC} values as a function of p(H₂O) (obtained from data in Fig. 4 of Abbatt and Molina, 1992) were fitted to a power law function: $K_{\text{linC}}=3.75 \times 10^{12} \times (\text{p}(\text{H}_2\text{O}))^{3.73}$. The extrapolated value at p(H₂O)=0.0017 Torr (ice vapour pressure at 202 K) is $K_{\text{linC}}=1.75 \times 10^3$ cm, which is substantially lower than that for HCl uptake on water ice at this temperature, $\sim 3.0 \times 10^4$ cm. The K_{linC} values calculated from uptakes on H₂O-rich NAT films observed by Hanson and Ravishankara (1992) and Chu et al. (1993) at lower temperatures were in reasonable agreement, and are only a factor of 2 or so lower than they observed on ice at the same conditions. There appears to be some inconsistency in the results at this stage, which may arise from complications from the use of higher [HCl] by Abbatt and Molina (1992). The recommendation for K_{linC} at 191 K for H₂O-rich NAT films based on the results of Hanson and Ravishankara (1992). The temperature dependence for partition coefficients for HCl on H₂O-rich NAT is likely to be similar to that on ice and the recommend a temperature dependence is based on the 191 K value of K_{linC} and the recommended (E/R)=2858 K.

References

- Abbatt, J. P. D. and Molina, M. J.: J. Phys. Chem., 96, 7674, 1992.
Chu, L. T., Leu, M.-T., and Keyser, L. F.: J. Phys. Chem., 97, 7779, 1993.
Hanson, D. R. and Ravishankara, A. R.: J. Phys. Chem., 96, 2682, 1992.

ClO + NAT → products**V.A5.9****Experimental data**

Parameter	Temp./K	Reference	Technique/Comments
γ $\gamma_{ss}=(8\pm 4)\times 10^{-5}$	183	Kenner et al., 1993	CWFT-MS (b)

Comments

- (a) Fast flow reactor with electron-impact MS. A 4–7 μm thick NAT film was deposited from a 3:1 gas phase mixture of $\text{H}_2\text{O}:\text{HNO}_3$ on top of a previously deposited 2–3 μm thick ice film. ClO was passed through the flow tube either continuously or in pulses. ClO was produced by microwave discharge of O_2 and Cl_2 in He or by first producing Cl atoms by microwave discharge of Cl_2 in He and reacting Cl with O_3 . Both methods led to consistent observations of ClO uptake. The ClO pressure was about 6.3×10^{-6} mbar. Cl_2 could not be measured as product because of excess of Cl_2 present from the source. HCl could also not be measured due to a large background in the MS.

Preferred values

Parameter	Value	T/K
γ	$<1\times 10^{-4}$	180–200
<i>Reliability</i> undetermined		

Comments on preferred values

The most likely reactive fate of ClO on solid surfaces is surface recombination and secondary chemistry (Abbatt, 1996; McKeachie et al., 2004). The NAT films prepared by Kenner et al. (1993) were likely porous and possibly did not cover the entire ice surface area on which they were deposited, as cautioned by the authors. We therefore only recommend an upper limit to the uptake coefficient.

References

- Abbatt, J. P. D.: Geophys. Res. Lett., 23, 1681–1684, 1996.
 Kenner, R. D., Plumb, I. C., and Ryan, K. R.: Geophys. Res. Lett., 20, 193–196, 1993.
 McKeachie, J. R., Appel, M. F., Kirchner, U., Schindler, R. N., and Benter, T.: J. Phys. Chem. B, 108, 16786–16797, 2004.

HBr + NAT → products**V.A5.10****Experimental data**

Parameter	Temp./K	Reference	Technique/Comments
γ, γ_0 $\gamma^{ss} > 0.3$	201	Hanson and Ravishankara, 1992	CWFT-CIMS (a)

Comments

- (a) HNO₃ deposited on ice condensed from the vapor phase onto the cold flow tube. γ corrected for gas diffusion using estimated diffusion coefficients. Pressure=0.6 mbar He. Rapid uptake observed with no signs of saturation suggests the formation of new fluid binary phase HBr–H₂O.

Preferred values

Parameter	Value	T/K
α_s	0.3	190–200
<i>Reliability</i>		
$\Delta \log(\alpha_s)$	0.5	190–200

Comments on preferred values

There appears to be only one experimental study of HBr interaction with specifically prepared HNO₃-hydrate surfaces at temperatures and concentrations corresponding to hydrate thermodynamically stability regions. Under these conditions uptake is rapid, continuous and irreversible.

References

Hanson, D. R. and Ravishankara, A. R.: J. Phys. Chem., 96, 9441, 1992.



V.A5.12

Experimental data

Parameter	Temp./K	Reference	Technique/Comments
γ^{ss} (HOCl)			
0.10±0.025 (HCl=2.6×10 ⁻⁷ mbar; 100% RH)	191	Hanson and Ravishankara, 1992	CWFT-CIMS (a)
0.17±0.1 (HCl=1.3×10 ⁻⁵ mbar, p(H ₂ O)=2.2×10 ³ mbar)	202	Abbatt and Molina, 1992	CWFT-MS (b)
0.07±0.1 (HCl=1.3×10 ⁻⁵ mbar, p(H ₂ O)>1.07×10 ³ mbar; 45%RH)	202		
0.002±0.001 (HCl=1.3×10 ⁻⁵ mbar, p(H ₂ O)>0.4×10 ³ mbar; 18% RH)	202		
0.18±0.10 (HCl=1.3×10 ⁻⁶ mbar, p(H ₂ O) >2.6×10 ⁴ mbar)	195		

Comments

- (a) NAT film prepared by doping ice film deposited from vapour with HNO₃. The decay of HCl and HOCl resulted in identical decay rates for [HOCl] and [HCl] of $\approx 1 \times 10^{10}$ molecule cm⁻³. Gas phase Cl₂ observed as product. Uptake coefficient significantly lower than observed on pure ice ($\gamma > 0.3$).
- (b) NAT film (~1 mm thick) prepared by exposing ice film deposited from vapour to 10⁻⁴ mbar HNO₃ for up to 1 h. H₂O was added upstream during experiments to change RH (relative to pure ice) above surface layers of NAT. The uptake of HOCl in the presence of HCl (in excess by a factor of two or so) is time-independent, and Cl₂ was detected as product with a yield of 0.87±0.20 and therefore not saturable. Weak dependence on p(HCl). As p(H₂O) drops from 2.3×10⁻³ at 202 K (equilibrium vapor pressure for pure H₂O ice) to 1.1×10⁻³ mbar, γ drops from 0.17 to 0.07; for HNO₃-rich NAT at p(H₂O)=4×10⁻⁴ mbar $\gamma=0.002$.

Preferred values

Parameter	Value	T/K
$\gamma_{\text{gs}}(\text{HOCl})$	0.18	180–205
$K_{\text{linC}}(\text{HCl})$	$9.5 \times 10^{-3} \exp(2858/T)$	180–205
<i>Reliability</i>		
$\Delta \log(\gamma_{\text{gs}})$	0.2	298

Comments on preferred values

Both studies report rapid uptake of HOCl onto NAT films doped with HCl. Cl₂ is the sole product with a yield of 100%. The reported uptake coefficients on H₂O-rich NAT films agree but are lower by a factor of ~2 compared to water ice surfaces at the same conditions. The more comprehensive study by Abbatt and Molina (1992) found that γ values depend weakly on [HCl] and are strongly dependent on the state of the NAT surface, as determined by the water vapour partial pressure, decreasing rapidly as p(H₂O) decreased. This is consistent with observations of surface adsorption of HCl on NAT.

There are insufficient data to distinguish between Eley-Rideal and Langmuir-Hinshelwood mechanisms. The surface coverage of HCl was estimated from the temperature dependent expression for $K_{\text{linC}}(\text{HCl})$ on ice (see data sheet V.A1.27), modified to match the value of for $K_{\text{linC}}(\text{HCl})$ on NAT derived from the data of Hanson and Ravishankara (1992) at 191 K ($=3 \times 10^4$ cm). A plot of the uptake coefficient using an Eley-Rideal formalism with $\gamma(\text{HOCl}) = \gamma_{\text{gs}} \times \theta(\text{HCl})$ calculated as a function of $\theta(\text{HCl})$, gives a reasonable fit to the experimental values at 100% RH from Hanson and Ravishankara (1992) and from Abbatt and Molina (1992). The slope gives $\gamma_{\text{gs}} = 0.18$. This is the basis of our recommendation for H₂O-rich NAT surfaces over the limited range of 180–205 K.

Although the fall off in uptake coefficient at lower p(H₂O) undoubtedly results from reduced surface coverage of HCl, no quantitative parameterisation of this effect on HCl uptake on NAT can be recommended.

References

- Abbatt, J. P. D. and Molina, M. J.: *Geophys. Res. Lett.*, 19, 461, 1992.
Hanson, D. R. and Ravishankara, A. R.: *J. Phys. Chem.*, 96, 2682, 1992.



V.A5.13

Experimental data

Parameter	Temp./K	Reference	Technique/Comments
$\gamma(\text{ClONO}_2)$			
0.3 (+0.7, -0.1)	210	Hanson and Ravishankara, 1991	CWFT-CIMS(a)
0.27±0.04	196	Leu et al., 1991	CWFT-MS(b)
0.3 (+0.7, -0.1)	191	Hanson and Ravishankara, 1992	CWFT-CIMS(c)
$\gamma_{\text{ss}} \geq 0.20$ 100%RH	202	Abbatt and Molina, 1992	CWFT-MS(d)
$\gamma_{\text{ss}} = (3.0 \pm 1.0) \times 10^{-3}$ 25% RH			
$\gamma_{\text{ss}} = 0.23$ (p(HCl) = 6.7×10^{-8} mbar) 90% RH	190	Hanson and Ravishankara, 1993	CWFT-CIMS(e)
$\gamma_{\text{ss}} = 0.20$ (p(HCl) $\sim 4.6 \times 10^{-7}$ mbar) 90% RH	190		
$\gamma_{\text{ss}} = 0.03$ (p(HCl) $\sim 4.6 \times 10^{-7}$ mbar) 30% RH	197		

Comments

- (a) Vapour deposited ice; NAT was prepared in situ by converting N_2O_5 into HNO_3 on the ice surface well past saturation. The HNO_3 vapor detected at the downstream end of the flow tube was consistent within a factor of two with the expected vapor pressure over NAT/ HNO_3 in ice solid solution near 201K. $[\text{HCl}]_0 = 2 \times [\text{ClONO}_2]_0$, i.e. $\sim 0.4\text{--}1.2 \times 10^{10}$ molecule cm^{-3} .
- (b) The films, typically 70 μm thick, were prepared in situ by vapour condensation of HNO_3 and H_2O at 196K. Initial $p(\text{HCl}) = 0.27$ to 2.7×10^{-3} mbar, $p(\text{ClONO}_2) = 10.6 \times 10^{-5}$ mbar. The measured values of γ were independent of the composition of HNO_3/NAT in the range 41.8 to 60.4% and of the HCl content (0.0375% to 3.91% HCl). The authors give a corrected value of $\gamma = 0.10 \pm 0.02$ if pore diffusion is taken into account.
- (c) Details under (a). The uptake of ClONO_2 , HCl and the formation of the reaction product Cl_2 were studied at constant HCl concentration (10^{10} molecule cm^{-3}) and varying ClONO_2 concentration ranging from $0.6\text{--}3.0 \times 10^{10}$ molecule cm^{-3} . The authors argue in favor of a direct reaction between ClONO_2 and HCl rather than a reaction via the intermediate HOCl in view of the high value for γ .
- (d) The NAT films were prepared starting from 10 μm thick ice films exposed to small pressures of HNO_3 over long periods of time resulting in a 0.1 μm thick NAT layer on top of the ice film. pressure of ClONO_2 ranging from 1.3 to 12×10^{-6} mbar and HCl ranging from 5.3 to 13.3×10^{-6} mbar. A factor of four increase in γ (from 0.01 to 0.04) was noted when $p(\text{HCl})$ increased from 2 to 10.6×10^{-6} mbar.
- (e) Details under (a and c). A 0.05 mm thick NAT film was grown on a 0.5 mm thick H_2O ice undercoat by flowing HNO_3 at 1.3×10^{-6} mbar. Subsequently the ice undercoat was evaporated. $p(\text{H}_2\text{O})$ added to He flow to adjust relative humidity over the film. γ decreased strongly with decreasing relative humidity which was varied by adjusting the temperature of the frozen phase at a constant H_2O flow rate of 3.3×10^{-4} mbar. γ given by the expression: $1/\gamma = 1/\gamma_{\text{max}} + 1/A \exp(B\Delta T)$ where Δ is $(T - 190)$, the difference between the temperature of interest and the ice point temperature at which RH is 100% at the chosen flow rate of H_2O ($\text{RH} = 100 \times p(\text{H}_2\text{O})/p(\text{ice})(T)$). For $p(\text{HCl}) \approx 6.7 \times 10^{-8}$ mbar and $\approx 4.6 \times 10^{-7}$ mbar ($[\text{HCl}]$ (2.5 and 17.5×10^{-9} molecule cm^{-3} at 195 K)), $\gamma_{\text{max}} = 0.23$ and 0.20, $A = 0.7022$ and 2.2543, $b = -0.518$ and -0.558 respectively.

Preferred values

Parameter	Value	<i>T</i> /K
$\gamma_{\text{gs}}(\text{p}(\text{HCl})=6.7 \times 10^{-8} \text{ mbar})$	0.25	190–200
$\gamma_{\text{gs}}(\text{p}(\text{HCl})=4.6 \times 10^{-8} \text{ mbar})$	0.20	190–200
A ($\text{p}(\text{HCl})=6.7 \times 10^{-8} \text{ mbar}$)	0.7022	190–200
A ($\text{p}(\text{HCl})=4.6 \times 10^{-8} \text{ mbar}$)	2.2543	190–200
B ($\text{p}(\text{HCl})=6.7 \times 10^{-8} \text{ mbar}$)	−0.518	190–200
B ($\text{p}(\text{HCl})=4.6 \times 10^{-8} \text{ mbar}$)	−0.558	190–200
<i>Reliability</i>		
$\Delta \log(\gamma)$	0.3	190–200

Comments on preferred values

As with ice films the uptake of ClONO₂ on NAT films in the presence of HCl is followed by reaction to form Cl₂ and HNO₃ in a surface reaction. At stratospheric temperatures Cl₂ partitions into the gas phase, but HNO₃ remains at the surface with formation of hydrates. The uptake coefficients of ClONO₂ in the presence of HCl on H₂O-rich NAT substrates are similar to those on pure ice, but show a strong dependence on relative humidity. Thus γ decreases with decreasing p(H₂O) and decreases with increasing temperature at fixed p(H₂O). This reflects the amounts of surface-adsorbed water and reactants, and leads to a complex dependence of γ with conditions.

Uptake coefficients measured on water-rich NAT (100% RH) from the different studies agree quite well. At lower RH there is more variability. Only Hanson and Ravishankara and Abbatt and Molina (1992) did a systematic study of the water dependence; in the former study RH was varied by changing *T* at constant p(H₂O) and they observed less dependence of γ compared to Abbatt and Molina who varied p(H₂O) at constant *T*; the latter used higher reactant concentrations which could have led to more influence of HNO₃ product, reducing surface water availability. On H₂O-rich NAT substrates Hanson and Ravishankara observed that γ increases slowly with p(HCl) in the range (0.5–5) × 10^{−7} mbar, which is consistent with the high fractional surface coverage for HCl ($\theta \approx 0.33$) for these conditions. At lower RH and higher [HCl], Abbatt and Molina (1992) observed much stronger dependence of p(HCl) in the range $\approx (2–10) \times 10^{-6}$.

The preferred values for the reactive uptake coefficient on NAT under stratospheric conditions are given by the parameterisation of Hanson and Ravishankara (1993):

$$\frac{1}{\gamma} = \frac{1}{\gamma_{\text{gs}}} + \frac{1}{A \exp(B \Delta T)}$$

where $\Delta T = (T(\text{K}) - 190)$. This expression gives the reactive uptake coefficient for specified p(HCl) and fixed p(H₂O) = 3.3 × 10^{−4} mbar, as a function of temperature in the range 190–200 K. This corresponds to RH in the range 20–100%.

In view of the complex dependence of the uptake coefficient on the state of the HNO₃-rich surfaces, and the lack of consistency in the reported data for these conditions, no recommendation is made for γ at lower [HCl] and absolute humidity. For uptake on NAT surfaces at lower [HCl] and absolute humidity in the NAT stability region, a parameterisation for γ using a Langmuir-Hinshelwood model such as used for ClONO₂+HCl on ice (IUPAC, 2009), would require a better definition of the surface concentration of water and HCl on NAT than is available at present.

References

- Abbatt, J. P. D. and Molina, M. J.: J. Phys. Chem., 96, 7674, 1992.
 Hanson, D. R. and Ravishankara, A. R.: J. Geophys. Res., 96, 5081, 1991.
 Hanson, D. R. and Ravishankara, A. R.: J. Geophys. Res., 98, 22931, 1993.
 Hanson, D. R. and Ravishankara, A. R.: J. Phys. Chem., 96, 2682, 1992.
 Leu, M.-T., Moore, S. B., and Keyser, L. F.: J. Phys. Chem., 95, 7763, 1991.

ClONO₂ + HBr(NAT) → BrCl + products**V.A5.14****Experimental data**

Parameter	Temp./K	Reference	Technique/Comments
γ >0.3	200	Hanson and Ravishankara, 1992	CWFT-CIMS (a)

Comments

(a) Ice surfaces (2–10 μm thick) were made by vapour deposition and doped with HNO₃ (the amount of HNO₃ was not given). The geometric surface area was used to calculate the uptake coefficient. Experiments were conducted with either HBr (5×10^9 – 10^{11} molecule cm^{-3}) or ClONO₂ (10^{10} – 10^{11} molecule cm^{-3}) in excess to give the same value of γ . BrCl was observed as primary gas-phase product, but not quantified. When HBr was in excess, some BrCl was converted to Br₂. Note that the same value of γ (and the same product) was also obtained for pure ice.

Preferred values

Parameter	Value	T/K
$\gamma_{\text{gs}}(\text{ClONO}_2)$	0.56	180–200
θ_{HBr}	$4.14 \times 10^{-10} [\text{HBr}]^{0.88}$	188
<i>Reliability</i>		
$\Delta \log \gamma_{\text{gs}}$	0.3	200

Comments on preferred values

The single study (Hanson and Ravishankara, 1992) of the reaction of ClONO₂ and HBr on a NAT-like (or HNO₃ doped) surface shows that the reaction proceeds very efficiently and that BrCl escapes to the gas-phase at low HBr concentrations. There is no difference in the uptake coefficient if pure ice or NAT-like surfaces are used and we adopt the same parameterisation for γ as for pure ice, which relies on a parameterisation for the HBr surface coverage (see datasheet on HBr+ice).

$$\gamma = \gamma_{\text{gs}}(\text{ClONO}_2)\theta_{\text{HBr}} \quad \text{with } [\text{HBr}] \text{ in molecule cm}^{-3}.$$

Note that the parameterisation, which is only valid for $\theta_{\text{HBr}} \leq 1$ and assumes that the maximum coverage is 1×10^{15} molecule cm^{-2} , generates uptake coefficients that are in close to or greater than 0.3 for $[\text{HBr}] \geq 10^{10}$ molecule cm^{-3} , as observed by Hanson and Ravishankara, 1992.

References

Hanson, D. R. and Ravishankara, A. R.: J. Phys. Chem., 96, 9441–9446, 1992.

N₂O₅ + HCl (NAT) → products**V.A5.15****Experimental data**

Parameter	Temp./K	Reference	Technique/Comments
γ 3.2×10^{-3}	200	Hanson and Ravishankara, 1991	CWFT-CIMS (a)

Comments

- (a) Ice surfaces (7–15 μm thick) were made by vapour deposition and doped with HNO₃ formed during the N₂O₅ uptake (the amount of HNO₃ was not given). The geometric surface area was used to calculate the uptake coefficient. Experiments were conducted with [N₂O₅] and [HCl] at $\approx 10^9$ – 10^{10} molecule cm³. HCl was generally in excess, but first order loss of N₂O₅ was still observed when [N₂O₅]/[HCl]=2. Variation of [N₂O₅] over a factor of 10 did not change the uptake coefficient, a dependence of γ on [HCl] was not reported.

Preferred values

Parameter	Value	T/K
γ_{gs}	4×10^{-3}	190–210
θ_{HCl}	$7.3 \times 10^{-17} \exp(2858/T)$ [HCl] / $(7.3 \times 10^{-17} \exp(2858/T)$ [HCl]+1)	190–210
<i>Reliability</i>		
$\Delta \log \gamma$	0.5	190–210

Comments on preferred values

The single study (Hanson and Ravishankara, 1991) of the reaction of N₂O₅ and HCl on a NAT surface shows that the N₂O₅ uptake proceeds more efficiently than on NAT alone (for which a value of $\gamma=6 \times 10^{-4}$ was obtained), indicating that a surface reaction takes place presumably to form HNO₃ and ClNO₂, though these products were not seen. Application of the reported value of γ to the atmosphere requires parameterisation of the HCl surface coverage on NAT. We assume that this is the same as for pure ice to derive the expression for θ_{HCl} (see HCl+ice data sheet), which can be combined with a value of γ_{gs} of 4×10^{-3} to give net uptake coefficients in line with those observed by Hanson and Ravishankara, 1991.

$$\gamma = \gamma_{\text{gs}} \theta_{\text{HCl}} + 6 \times 10^{-4}$$

This expression assumes that the reaction is driven by the availability of surface HCl and the temperature dependence is controlled only by HCl coverage. As HCl→0, the uptake coefficient should approach that on pure NAT (i.e. 6×10^{-4}). The ratio of ClNO₂ formation to the overall uptake is given by $(\gamma - 6 \times 10^{-4})/\gamma$.

References

Hanson, D. R. and Ravishankara, A. R.: J. Geophys. Res., 96, 5081–5090, 1991.

N₂O₅ + HBr(NAT) → products**V.A5.16****Experimental data**

Parameter	Temp./K	Reference	Technique/Comments
γ 5×10^{-3}	200	Hanson and Ravishankara, 1992	CWFT-CIMS (a)

Comments

(a) Ice surfaces (2–10 μm thick) were made by vapour deposition and doped with HNO₃ (the amount of HNO₃ was not given). The geometric surface area was used to calculate the uptake coefficient. Experiments were conducted with 5×10^9 – 10^{11} molecule cm⁻³ HBr and 10^{11} – 10^{12} molecule cm³ N₂O₅. Values of the uptake coefficient varied between a high value of $\approx 4 \times 10^{-2}$ and a low value of 5×10^{-3} , the latter being obtained at the lower HBr concentrations.

Preferred values

Parameter	Value	T/K
γ_{gs}	2×10^{-2}	
θ_{HBr}	$4.14 \times 10^{-10} [\text{HBr}]^{0.88}$	
<i>Reliability</i>		
$\Delta \log \gamma$	0.5	200

Comments on preferred values

There is a single study (Hanson and Ravishankara, 1992) of the reaction of N₂O₅ and HBr on a NAT-like (or HNO₃ doped) surface. The uptake coefficient was found to be enhanced compared to N₂O₅ uptake to pure NAT ($\gamma \leq 1 \times 10^{-3}$), indicative of surface reaction with possible products BrONO and HNO₃ (not observed). To parameterise the uptake coefficient, γ_{net} , we have assumed an Eley-Rideal type mechanism with the surface coverage of HBr the same as that for pure ice.

$$\gamma = \gamma_{\text{gs}} \theta_{\text{HBr}}, \text{ with } [\text{HBr}] \text{ in molecule cm}^{-3}.$$

The parameterisation above yields a value of $\gamma_{\text{net}} = 5 \times 10^{-3}$ at concentrations of HBr close to 10^{10} molecule cm⁻³, increasing to $\gamma = 4 \times 10^{-2}$ at HBr close to 10^{11} molecule cm³, which are consistent with the experimental observations.

References

Hanson, D. R. and Ravishankara, A. R.: J. Phys. Chem., 96, 9441–9446, 1992.



V.A5.17

Experimental data

Parameter	Temp./K	Reference	Technique/Comments
$\gamma_{\text{ss}}, \gamma_0$			
$\gamma_{\text{ss}}=(6.0\pm 2.0)\times 10^{-3}$	201	Hanson and Ravishankara, 1992	CWFT-CIMS (a)
$\gamma_{\text{ss}}=1.0\times 10^{-5}$	196	Leu et al., 1991	CWFT-MS (b)
$\gamma_{\text{ss}}=(2.0\pm 0.8)\times 10^{-3}$	191	Hanson and Ravishankara, 1992	CWFT-CIMS (c)
$\gamma_{\text{ss}}=(4.0\pm 1.6)\times 10^{-3}$	201		
$\gamma_{\text{ss}}=(8.0\pm 3.2)\times 10^{-3}$	211		
$\gamma_{\text{ss}}=(2.0\pm 0.8)\times 10^{-3}$ 100% RH	202	Abbatt and Molina, 1992	CWFT-MS (d)
$\gamma_{\text{ss}}=(5.0\pm 2.5)\times 10^{-5}$ 25% RH			
$\gamma_{\text{ss}}=(1.0\pm 0.3)\times 10^{-3}$	191	Hanson and Ravishankara, 1993b	CWFT-CIMS (e)
$\gamma_{\text{ss}}=2.0\times 10^{-3}$ 90% RH	191	Hanson and Ravishankara, 1993a	CWFT-CIMS (f)
$\gamma_{\text{ss}}=0.5\times 10^{-3}$ 50% RH	194		
$\gamma_{\text{ss}}=0.3\times 10^{-3}$ 25% RH	198		
$\gamma_{\text{ss}}=(2.0\pm 0.3)\times 10^{-3}$ 100%RH	195	Zhang et al., 1994	CWFT-MS (g)
$\gamma_0=(5\pm 3)\times 10^{-4}$ NAD, β -NAT	185	Barone et al., 1997	Knud-MS (h)
$\gamma_0=(4\pm 2)\times 10^{-4}$ α -NAT			
$\gamma_0=(7\pm 3.5)\times 10^{-3}$ NAD, α -NAT, β -NAT			

Comments

- (a) Vapour deposited ice; NAT was prepared in situ by converting N_2O_5 into HNO_3 on the ice surface well past saturation. The HNO_3 vapor detected at the downstream end of the flow tube was consistent within a factor of two with the expected vapor pressure over NAT/ HNO_3 -in-ice solid solution near 201 K. $[\text{ClONO}_2] \sim 0.5\text{--}3\times 10^{10}$ molecule cm^{-3} .
- (b) The films, typically 70 μm thick, were prepared in situ by vapour condensation of HNO_3 and H_2O at 196K. The film surface areas and bulk densities were measured ex situ in addition to their FTIR absorption spectra. γ on samples of varying HNO_3/NAT composition was in the range 10^{-5} to 10^{-3} and was observed to saturate within a few minutes. No added water vapour (low RH).
- (c) Details under (a). The values for γ given in the Table correspond to a vapour deposited film of 10 μm thickness. $p(\text{H}_2\text{O})$ added to He flow from upstream ice film to prevent evaporation of film, i.e. high RH. γ varied by a factor of ≤ 3 when the thickness was varied from 2 to 20 μm , showing reaction occurred on external surface of film. $[\text{ClONO}_2] \sim 0.5\text{--}3\times 10^{10}$ molecule cm^{-3} .
- (d) Uptake of ClONO_2 on NAT with $p(\text{ClONO}_2)$ ranging from 2.7 to 26.7×10^{-6} mbar. The NAT films were prepared starting from 10 μm thick ice films exposed to small pressures of HNO_3 over long periods of time resulting in a 0.1 μm thick NAT layer on top of the ice film. The steady-state uptake coefficient γ increases exponentially with $p(\text{H}_2\text{O})$ over the NAT surface, reaching a similar value to that on ice at the ice vapour pressure of pure ice; $p(\text{ClONO}_2)=(0.27\text{--}2.67)\times 10^{-5}$ mbar ($\sim 1\text{--}10\times 10^{11}$ molecule cm^{-3}).
- (e) Details under (a and c). $p(\text{H}_2\text{O})$ added to He flow from upstream ice film to prevent evaporation of film. This study was undertaken to supplement the original work on ice and HNO_3 -doped (NAT) surfaces to further confirm the independence of γ on the substrate thickness.

- (f) A 0.05 μm thick NAT film was grown on a 0.5 μm thick H_2O ice undercoat by flowing HNO_3 at 1.3×10^{-6} mbar. Subsequently the ice undercoat was evaporated. $p(\text{H}_2\text{O})$ added to He flow to adjust relative humidity over the film. The uptake coefficients were strongly dependent on RH.
- (g) Ice films were deposited from the vapour phase at 195K, attained a thickness of between 15–25 μm , and were subsequently exposed to gas phase HNO_3 in order to generate NAT. $[\text{ClONO}_2] \sim 1.5\text{--}2.5 \times 10^9$ molecule cm^{-3} ; mean of 11 experiments at $p(\text{H}_2\text{O}) = 6.4 \times 10^{-4}$ mbar.
- (h) Uptake study performed in a Knudsen flow reactor interfaced with MS and FTIR-RAS. Total pressure ranged between 0.67 to 27×10^{-5} mbar. Smooth films of NAD, α - and β -NAT were grown by co-deposition of ClONO_2 and H_2O at 150K and annealing the resulting films at 185K at a rate of 10 K min^{-1} . Crystallization of the deposits to NAT and NAD was observed to occur between 170 and 185 K. The reactant films were in the range 5 to 50 nm thick.

Preferred values

Parameter	Value	T/K
γ	$7.1 \times 10^{-3} \exp(-2940/T)$	185–210
Reliability		
$\Delta \log \gamma$	± 0.20	185–210

Comments on preferred values

As with ice films, the uptake of ClONO_2 on NAT films is followed by reaction with H_2O to form HOCl and HNO_3 in a surface reaction. At stratospheric temperatures HOCl partitions into the gas phase, but HNO_3 remains at the surface with formation of hydrates (NAT). The uptake coefficients on NAD and NAT substrates are substantially lower than on pure ice and show a strong dependence on relative humidity, which is reflected in an increase in γ with $p(\text{H}_2\text{O})$ and temperature. This is believed to reflect the decreasing amounts of available surface-adsorbed water.

Uptake coefficients measured on water-rich NAT (100% RH) from the different studies agree quite well. At lower RH there is more variability. Only Hanson and Ravishankara (1992) and Abbatt and Molina (1992) did a systematic study of the water dependence; in the former study RH was varied by changing T at constant $p(\text{H}_2\text{O})$ and they observed less dependence of γ compared to Abbatt and Molina who varied $p(\text{H}_2\text{O})$ at constant T ; the latter used higher $[\text{ClONO}_2]$ which could have led to more influence of HNO_3 product, reducing surface water availability.

The preferred values for the reactive uptake coefficient on water rich NAT are given by an Arrhenius fit of the uptake coefficients measured near 100% RH in the studies of Hanson and Ravishankara (1992), Abbatt and Molina (1992), and Zhang et al. (1994), which are in reasonable agreement for these conditions, considering the uncertainties arising from sensitivity of γ to the $p(\text{H}_2\text{O})$, and the state of the surface.

In view of the complex dependence of the uptake coefficient on the state of the HNO_3 -rich surfaces, and the lack of consistency in the reported data for these conditions, no recommendation is made for γ at low RH. For uptake on surfaces with HNO_3 present in the NAT stability region a parameterisation for γ using a Langmuir-Hinshelwood model such as used for ice (e.g A1.43), would require a better definition of the surface water concentration than is available at present.

References

- Abbatt, J. P. D. and Molina, M. J.: J. Phys. Chem., 96, 7674, 1992.
- Barone, S. B., Zondlo, M. A. and Tolbert, M. A.: J. Phys. Chem. A., 101, 8643, 1997.
- Hanson, D. R. and Ravishankara, A. R.: J. Geophys. Res., 96, 5081, 1991.
- Hanson, D. R. and Ravishankara, A. R.: J. Geophys. Res., 98, 22931, 1993a.
- Hanson, D. R. and Ravishankara, A. R.: J. Phys. Chem., 96, 2682, 1992.
- Hanson, D. R. and Ravishankara, A. R.: J. Phys. Chem., 97, 2802, 1993b.
- Leu, M.-T., Moore, S.B., and Keyser, L. F.: J. Phys. Chem., 95, 7763, 1991.
- Zhang, R., Jayne, J. T., and Molina, M. J.: J. Phys. Chem., 98, 867, 1994.